

Fundamental Discoveries in Heterogeneous Catalysis Focus Topic

Room A212 - Session HC+SS-MoM

Utilization of Theoretical Models, Machine Learning, and Artificial Intelligence for Heterogeneously-Catalyzed Reactions

Moderators: Liney Arnadottir, Oregon State University, Sharani Roy, University of Tennessee Knoxville

8:40am HC+SS-MoM2 Theoretical Study of Acetic Acid Decomposition on Pd (111) using Density Functional Theory, *Kingsley Chukwu, L. Arnadottir, Oregon State University*

Acetic acid decomposition on Pd (111) and the effects of water on the decomposition are good model systems for the study of solvent effects on small oxygenates. Numerous studies have found that solvents influence the selectivity and rate of heterogeneous catalytic reactions, so fundamental understanding of how water affects OC-O, C-OH, CO-H, C-H and C-C bond cleavages will give us valuable insight into how water influences selectivity of oxygenates decomposition, further enabling bottom up design of effective catalyst and catalyst system. Here we present density functional theory calculations of the decomposition of acetic acid on Pd (111) and the effects of water on the reaction mechanism. Our results suggest that the most favorable decarboxylation (DCX) and decarbonylation (DCN) mechanisms in vacuum proceed through dehydrogenation of acetic acid (CH_3COOH) to acetate (CH_3COO), followed by dehydrogenation of CH_3COO to CH_2COO . The competition between the most favorable DCN and DCX pathway depends on two endothermic elementary steps, the deoxygenation of CH_2COO to ketene (CH_2CO) and dehydrogenation of the carboxylmethylidene (CH_2COO) to carboxylmethylidyne (CHCOO). Water can affect the different elementary steps by changing the stability of the initial, transition and/or final state or by providing new reaction paths such as through hydrogen shuttling, which can lead to changes in the selectivity of a complex reaction network as presented herein. Here we will discuss how water influences different critical reaction steps and how that effects the overall reaction network.

9:00am HC+SS-MoM3 Towards a Chemically Accurate Description of Reactions of Molecules with Transition Metal Surfaces, *Geert-Jan Kroes, Leiden University, Netherlands*

INVITED

Heterogeneously catalyzed processes consist of several elementary reactions. Accurately calculating their rates requires the availability of accurate barriers for the rate controlling steps. Unfortunately, currently no first principles methods can be relied upon to deliver the required accuracy. To solve this problem, in 2009 we came up with a novel implementation of the specific reaction parameter approach to density functional theory (SRP-DFT). This allowed us to reproduce experiments for H_2 reacting on copper surfaces, and to determine barrier heights for H_2 -Cu systems, with chemical accuracy. The original procedure used was not extendable to reactions of molecules heavier than H_2 with surfaces, because the metal surface was treated as static. This problem has been solved by combining SRP-DFT with Ab Initio Molecular Dynamics (AIMD). This method was applied to the dissociative chemisorption of methane on a Ni surface, a rate-limiting step in the steam reforming reaction. We were able to reproduce experiments on $\text{CHD}_3 + \text{Ni}(111)$ with chemical accuracy, and have predicted a value of the reaction barrier height that we claim to be chemically accurate. We have new results for $\text{CHD}_3 + \text{Pt}(111)$ that are even better, and which show that the SRP density functional for methane interacting with Ni(111) is transferable to methane interacting with another group X metal surface, i.e., Pt(111). Even more interestingly for applications to catalysis, the SRP functional derived for methane reacting with Ni(111) also gives a very accurate description of molecular beam sticking experiments on $\text{CHD}_3 + \text{Pt}(211)$. Finally, thanks to a collaboration with Jörg Behler (University of Göttingen) we are now able to develop potential energy surfaces also depending on the degrees of freedom associated with the surface phonons, for polyatomic molecules interacting with metals. This has enabled us to compute statistically accurate reaction probabilities for highly activated reactions not open to investigation with AIMD, for which reaction probabilities are less than 0.01.

9:40am HC+SS-MoM5 The Apparent Activation Energy for Complex Mechanisms: A Simple Relationship via Degrees of Rate Control, *Zhongtian Mao^{1,2}, C.T. Campbell, University of Washington*

Reactions on surface usually consists of several elementary steps. It is known that the observed reaction kinetics often represents a composite of the contribution from each of these elementary steps. The “rate-determining step” (RDS) assumption is a common approach for dealing with multistep mechanisms, where a single step is assumed to dominate the reaction kinetic behaviors and the kinetic parameters of this RDS (e.g., net rate, activation energy) are good estimation for those of the overall reaction. However, RDS is not a rigorous concept in mathematics and there is no universal definition for RDS. Efforts have been made to clarify the actual physical meaning behind RDS, and the “Degree of Rate Control” (DRC) was raised as a rigorous mathematical approach to quantify to what extent the change of the Gibbs free energy of a species in the reaction scheme can affect the rate of the overall reaction. DRC analysis to reaction kinetics elucidates that there are only rate-determining species with non-negligible DRCs instead of rate-determining steps.

The apparent activation energy E_{app} is determined by fitting the temperature dependence of the reaction rate to the Arrhenius law. It is believed that E_{app} is a direct measurement of energy information in the RDS, which has been challenged by DRC analysis. A general and accurate elaboration of the microscopic origin of E_{app} has not been reported except in cases where there is an analytical rate expression. Here a simple but general mathematical expression of E_{app} in terms of the enthalpies of species in the reaction and their DRCs is derived. To verify the accuracy of this equation, microkinetic modelling of methanol synthesis through CO_2 hydrogenation on Cu-based model catalysts under three different conditions was carried out based on previously-published DFT energetics. On pure Cu(211) at 450 K, there are only one transition state and only one intermediate with non-negligible DRCs, and E_{app} estimated using our equation is within 1 kJ/mol of the true value. When the temperature is raised to 570 K, the surface sites are mostly unoccupied; and, when the model catalyst is promoted by Zn, there are four transition states with non-negligible DRCs, which means the single RDS assumption is not true. In both these complicated cases, the error of the estimated value for E_{app} is still <1 kJ/mol.

10:00am HC+SS-MoM6 First-Principles Kinetic Monte Carlo Simulation of CO Oxidation on PdO(101): Role of Oxygen Vacancies, *Minkyu Kim, A. Asthagiri, The Ohio State University*

CO oxidation on transition metal (TM) oxide surfaces has been widely studied both experimentally and theoretically; however, a healthy debate continues on the coupling between changes in oxide phase and surface reactivity. In this study, we investigated CO oxidation over PdO(101) surface, which has been proposed to be important in Pd oxidation catalysis. In contrast to earlier studies of CO oxidation on TM oxide surfaces, we incorporate neighbor effects of oxygen vacancies on all the elementary surface processes. We employ density functional theory (DFT) to map out the kinetics of 50 elementary surface processes. We find that barriers for elementary steps such as O vacancy, O_2 dissociation, and CO_2 formation can be decreased by 20-40% in the presence of O vacancies, while O_2 desorption is increased by 70%. Using the DFT-derived rate constants, we have developed a lattice-based kinetic Monte Carlo (kMC) framework that can simulate CO oxidation under both ultra-high vacuum (UHV) and reaction conditions.

Initially, the kMC simulations were performed under UHV conditions (low CO partial pressure, no O_2 pressure) as a function of increasing surface temperature. As the CO oxidation proceeds and the surface lattice O atom coverage is depleted, the CO oxidation rate decreases rapidly at 400 K; however, the rate sharply increases at temperatures above 450 K. At 450 K, we find a new complex pathway to CO_2 formation that is activated in the presence of O vacancies and is the source of the increased CO oxidation rate despite the depletion of surface oxygen atoms. These kMC results match UHV isothermal experiments under similar conditions. kMC simulations at steady state conditions of low CO and O_2 pressures ($P_{\text{CO}}: 5 \times 10^{-9}$ Torr / $P_{\text{O}_2}: 1.5 \times 10^{-8}$ Torr), show that the rate-limiting step is O_2 dissociation and this elementary step requires the presence of adjacent oxygen vacancies to be activated at temperatures below 500 K. Without the addition of O vacancy neighbor effects to the kMC model, the PdO(101) surface would be inactive to CO oxidation because surface oxygens cannot

¹ Morton S. Traum Award Finalist

² Heterogeneous Catalysis Graduate Student Presentation Award Finalist

Monday Morning, October 21, 2019

be healed by gaseous O_2 . In addition, we will discuss kMC simulations under reaction conditions at varying CO/O_2 partial pressures.

11:20am **HC+SS-MoM10 Knowledge-Based Approaches in Catalysis and Energy Modelling**, *Karsten Reuter*, Technical University of Munich, Germany **INVITED**

Reflecting the general data revolution, knowledge-based methods are now also entering theoretical catalysis and energy related research with full might. Automatized workflows and the training of machine learning approaches with first-principles data generate predictive-quality insight into elementary processes and process energetics at undreamed-of pace. Computational screening and data mining allows to explore these data bases for promising materials and extract correlations like structure-property relationships. At present, these efforts are still largely based on highly reductionist models that break down the complex interdependencies of working catalysts and energy conversion systems into a tractable number of so-called descriptors, i.e. microscopic parameters that are believed to govern the macroscopic function. For certain classes of materials like transition metal catalysts, corresponding human-designed models have indeed established trend understanding and spurred a targeted materials design. Future efforts will concentrate on using artificial intelligence also in the actual generation and reinforced improvement of the reductionist models. This is expected to better capture complexities like incomplete understanding or operando changes of interfacial morphology, to provide access to structured and compound materials classes, or ultimately to even fulfill the dream of an inverse (de novo) design from function to structure. In this talk, I will briefly survey these developments, providing examples from our own research, in particular on adsorption energetics at bimetallic catalysts and data mining for the design of organic semiconductors.

Plasma Science and Technology Division Room B130 - Session PS+AS+EM+SS+TF-MoA

Plasma-Surface Interactions

Moderators: Sebastian Engemann, IBM T.J. Watson Research Center, Sumit Agarwal, Colorado School of Mines

2:00pm **PS+AS+EM+SS+TF-MoA2 Plasma Resistance of Sintered Yttrium Oxyfluoride (YOF) with Various Y, O, and F Composition Ratios**, *Tetsuya Goto*, *Y. Shiba*, *A. Teramoto*, Tohoku University, Japan; *Y. Kishi*, Nippon Yttrium Co., Ltd, Japan; *S. Sugawa*, Tohoku University, Japan

Yttrium oxyfluoride (YOF) has been received much attention as the material for various functional components used in the plasma process chamber for semiconductor manufacturing. This is because, as compared to the widely used Y_2O_3 , YOF is stable against various corrosive plasmas using halogen gases which is frequently used in the etching processes and/or chamber cleaning processes. We have reported that YOF (1:1:1) film has the higher resistance to various plasma conditions (N_2/Ar , H_2/Ar , NH_3/Ar , NF_3/Ar , O_2/Ar) than the Y_2O_3 and YF_3 films^{1,2}. In this presentation, we report the effect of ion bombardment on the surface structure of sintered yttrium oxyfluoride (YOF) with various Y, O, and F composition ratios. By combining the starting materials of YOF, $Y_5O_4F_7$, and YF_3 in sintering, the YOF samples with different Y, O, and F composition ratios were prepared. In these samples, the oxygen composition ratio was changed from 33 at% to 7at%. According to this, the fluorine composition ratio was changed from 33at% to 66at%, and thus, the samples became from Y_2O_3 rich to YF_3 rich. Ar ion beam with 500 eV was irradiated to these YOF samples. It was found that the sputtering etching rate was monotonically decreased as the oxygen composition ratio was decreased. It was also found that the surface roughness was relatively smaller for the samples with the composition ratios of Y:O:F=1:1:1 and 5:4:7 (both correspond to the stable composition) than those with other composition ratios. The results indicated that the atomic composition ratio is an important parameter to obtain YOF with good stability against plasmas.

Acknowledgement

The plasma irradiation and inspection were carried out in Fluctuation-Free-Facility in Tohoku University.

1. Y. Shiba, A. Teramoto, T. Goto, Y. Kishi, Y. Shirai and S. Sugawa, *J. Vac. Sci. Technol. A*, 35 (2), 021405 (2017).
2. A. Teramoto, Y. Shiba, T. Goto, Y. Kishi and S. Sugawa p. 16, AVS 65th International Symp., Long Beach, 2019.

2:20pm **PS+AS+EM+SS+TF-MoA3 Understanding Atomic Layer Etching: Thermodynamics, Kinetics and Surface Chemistry**, *Jane P. Chang*¹, University of California, Los Angeles **INVITED**

The introduction of new and functionally improved materials into silicon based integrated circuits is a major driver to enable the continued down-scaling of circuit density and performance enhancement in analog, logic, and memory devices. The top-down plasma enhanced reactive ion etching has enabled the advances in integrated circuits over the past five decades; however, as more etch-resistive materials are being introduced into these devices with more complex structures and smaller features, atomic level control and precision is needed in selective removal of these materials. These challenges point to the growing needs of identifying and developing viable etch chemicals and processes that are more effective in patterning complex materials and material systems such as multiferroics, magnetic materials and phase change materials, with tailored anisotropy and selectivity.

In this talk, a universal chemical approach is presented, combining thermodynamic assessment and kinetic validation to identify and validate the efficacy of various plasma chemistries. Specifically, potential reactions between the dominant vapor phase/condensed species at the surface are considered at various temperatures and reactant partial pressures. The volatility of etch product was determined to aid the selection of viable etch chemistry leading to improved etch rate of reactive ion etching process. Based on the thermodynamic screening, viable chemistries are tested experimentally to corroborate the theoretical prediction. Some of the above mentioned material systems such as complex oxides and metallic material systems used in logic and memory devices are used as examples to demonstrate the broad applicability of this approach.

¹ PSTD Plasma Prize Winner

3:00pm **PS+AS+EM+SS+TF-MoA5 Comparison of Silicon Surface Chemistry between Photo-Assisted Etching and Ion-Assisted Etching**, *Emilia Hirsch*, *L. Du*, *V.M. Donnelly*, *D.J. Economou*, University of Houston

Etching of p-Si in 60 mTorr Cl_2/Ar Faraday-shielded inductively coupled plasmas was investigated under both ion-assisted etching (IAE) and photo-assisted etching (PAE) conditions. Real-time etching rate and after-etch Si surface chemical composition were characterized by laser interferometry and vacuum-transfer X-ray photoelectron spectroscopy (XPS), respectively. By varying the duty cycle of a pulsed negative DC bias applied to the sample stage, it was found that the IAE rate scaled with the ion current integrated over the bias period, and the total etching rate was simply the sum of PAE and IAE rates. Consequently, little or no synergism occurred between VUV photon- and ion-bombardment stimulated etching. The PAE rate was ~ 210 nm/min at 60 mTorr. Above the 25 eV threshold, the IAE etching rate increased with the square root of the ion energy. Compared to RF bias, a more monoenergetic IED was obtained by applying pulsed DC bias, allowing precise control of ion energy near the low-energy IAE threshold. XPS spectra showed that, when compared to IAE, the chlorinated layer on the surface of samples etched under PAE conditions had significantly lower chlorine content, and it was composed of SiCl only. Under IAE conditions, however, Si· dangling bonds, $SiCl_2$, and $SiCl_3$ were found, in addition to SiCl, with relative abundance of $SiCl > SiCl_2 > SiCl_3$. The absence of higher chlorides and Si· dangling bonds under PAE conditions suggested that VUV photons and ions are interacting with the Si surface very differently. When PAE and IAE occurred simultaneously, energetic ion bombardment dictated the surface chemistry that resulted in the formation of higher chlorides.

3:20pm **PS+AS+EM+SS+TF-MoA6 Chemical Reaction Probabilities in the Etching of Si by Fluorine Atoms Produced in a Mixture of NF_3/SF_6 Plasma**, *Priyanka Arora*², *T. Nguyen*, University of Houston; *S. Nam*, Samsung Electronic Company, Republic of Korea; *V.M. Donnelly*, University of Houston

Reaction probabilities in the absence of ion bombardment, defined as the number of silicon atoms removed per incident fluorine atom, have been investigated in mixtures of NF_3 and SF_6 plasmas in an inductively-coupled plasma reactor. Fluorine atom densities were measured by optical emission actinometry, and isotropic etching rates were measured by the degree of undercutting of SiO_2 -masked silicon, using cross-sectional scanning electron microscopy (SEM). In addition, atomic force microscopy (AFM) was used to examine surface roughness after etching. The F atom reaction probabilities derived from these measurements indicate ~ 30 -fold higher reaction probability in SF_6 plasma compared with values in NF_3 plasma. Surfaces etched in SF_6 plasma were much smoother than those etched in NF_3 plasma. Addition of only 10% SF_6 to an NF_3 plasma produced a much higher reaction probability (~ 10 -fold) than in a pure NF_3 plasma. This surprising enhancement of reaction probabilities for F with Si in SF_6 plasma will be shown to be due to adsorbed sulfur acting as a catalyst to greatly enhance the etching rate of Si. By allowing sulfur in isopropyl alcohol to evaporate on the masked Si samples, sulfur could be preferentially deposited in relatively high concentrations near mask edges in ~ 2 mm diameter periodic "strings of beads". When this sample is placed side by side with one not exposed to sulfur, the sulfur dosed sample etched several times faster at the center of each bead, while sulfur-free surface exhibited the expected slower rate.

4:00pm **PS+AS+EM+SS+TF-MoA8 John Thornton Memorial Award Lecture: Low Temperature Plasma-Materials Interactions: Foundations of Nanofabrication And Emerging Novel Applications At Atmospheric Pressure**, *Gottlieb S. Oehrlein*³, University of Maryland, College Park **INVITED**

Our ability to understand and control the interactions of non-equilibrium plasma with surfaces of materials has been an exciting frontline and enabled the realization of new applications and technologies. The plasma-surface interactions (PSI) field has grown rapidly because of a number of reasons. First, plasma-assisted etching (PE) is one of the foundations of micro- and nanofabrication where increasingly atomistic precision in materials processing is required. By enabling the realization of intricate material features that semiconductor circuits and microstructures consist of, PE makes possible our technological tools that form modern society. This exceedingly complex procedure begins with the transfer of a resist mask in a directional and chemically selective fashion into various

² Coburn & Winters Student Award Finalist

³ John A. Thornton Memorial Award Winner

Monday Afternoon, October 21, 2019

materials. Controlling profile shape, critical dimensions, surface roughness, and electrical integrity are crucial, and determined by PSI. Second, development of novel low temperature plasma sources operating at atmospheric pressure has enabled advances in areas where use of PSI has historically been limited, e.g. biology. In this talk I will present a brief review of contributions that I and my collaborators have been honored to make to our understanding of PSI, in particular in the areas of surface processes that are essential for achieving the objectives of plasma etching processes in current semiconductor fabrication that are approaching the atomic scale, and interaction of low temperature atmospheric pressure plasma sources with model polymers and biomolecules aimed at disinfection and sanitation of biological materials.

4:40pm PS+AS+EM+SS+TF-MoA10 Determining Surface Recombination Probabilities during Plasma-enhanced ALD using Lateral High Aspect Ratio Structures, Karsten Arts, Eindhoven University of Technology, The Netherlands, Netherlands; *M. Utriainen*, VTT Technical Research Centre of Finland, Finland; *R.L. Puurunen*, Aalto University School of Chemical Engineering, Finland; *W.M.M. Kessels*, Eindhoven University of Technology, The Netherlands, Netherlands; *H.C.M. Knoops*, Eindhoven University of Technology, The Netherlands

In this work we measure surface recombination probabilities r of plasma radicals, which is essential for the modeling and understanding of radical-driven plasma processes. Such quantitative information on r is scarcely reported in the literature and typically obtained by difficult and indirect measurement techniques. Here, we determine r using plasma-enhanced atomic layer deposition (ALD) on high aspect ratio (AR) structures, where the AR up to which film growth is obtained gives direct insight into r corresponding to the growth surface. This is demonstrated by measuring the recombination probabilities of O atoms on SiO₂, TiO₂, Al₂O₃ and HfO₂, revealing a surprisingly strong material-dependence. Aside from studying different materials, our method can for instance be used to investigate the impact of pressure and temperature on r . This can provide valuable information for e.g., device fabrication, plasma source design and simulations, in the context of plasma-enhanced ALD but also relevant outside this field.

For this study, we use microscopic lateral-high-aspect-ratio (LHAR) structures¹ supplied by VTT (PillarHall[®] LHAR4). These chips have extremely high AR trenches (AR<10000) such that film growth is limited up to a certain penetration depth for even the most conformal processes. In the case of plasma ALD, where the film conformality is typically limited by surface recombination,² we show that the achieved penetration depth can be used to determine r . Furthermore, the LHAR structures allow for comparison of growth behavior with and without an ion component.

These opportunities are demonstrated by plasma ALD of SiO₂, TiO₂, Al₂O₃ and HfO₂, using an O₂/Ar plasma and SiH₂(N(C₂H₅)₂)₂, Ti(N(CH₃)₂)₄, Al(CH₃)₃ and HfCp(N(CH₃)₂)₃, respectively, as precursors. It is observed that an exponential increase in plasma exposure time is required to linearly increase the film penetration depth. This relation, which solely depends on r , has been used to determine $r=(6\pm 2)\cdot 10^{-5}$, $(6\pm 3)\cdot 10^{-5}$, $(1-10)\cdot 10^{-3}$ and $(0.1-10)\cdot 10^{-2}$ for oxygen radicals on SiO₂, TiO₂, Al₂O₃ and HfO₂, respectively. Corresponding to these large differences in r , growth of SiO₂ and TiO₂ penetrated extremely deep up to AR~900, while deposition of Al₂O₃ and HfO₂ was achieved up to AR~90 and AR~40, respectively. This strong material-dependence illustrates the importance of our quantitative research on surface recombination of plasma radicals.

1. Arts, Vandalon, Puurunen, Utriainen, Gao, Kessels and Knoops, *J. Vac. Sci. Technol. A* **37**, 030908 (2019)
2. Knoops, Langereis, van de Sanden and Kessels, *J. Electrochem. Soc.* **157**, G241 (2010)

5:00pm PS+AS+EM+SS+TF-MoA11 Study of Plasma-Photoresist Interactions for Atomic Layer Etching Processes, Adam Pranda¹, K.-Y. Lin, G.S. Oehrlein, University of Maryland, College Park

The emergence of atomic layer etching (ALE) processes has enabled improved control of surface profiles. Whereas the implementation of ALE processes on hard mask materials has been well established, the effects of these processes on photoresist materials is not well known. With the advent of next generation extreme ultraviolet (EUV) photoresists, there is the potential to utilize ALE processes with photoresist materials for fabrication of sub-10 nm feature sizes.

The plasma processing of photoresist materials induces several key physical and chemical modifications which affect material properties such as the etching behavior and surface roughness. In this work, we utilize in-situ ellipsometry, atomic force microscopy (AFM), x-ray photoelectron spectroscopy (XPS), and Fourier transform infrared (FTIR) spectroscopy to interpret the relationships between the aforementioned material properties, the photoresist chemical composition, and plasma ALE parameters such as ion energy and precursor gas type. By comparing these relationships between baseline continuous plasma etching processes and ALE processes, which include the introduction of chemically reactive surface passivation, we elucidate the intrinsic photoresist behaviors under plasma exposure and how an ALE process specifically impacts these behaviors.

Under nonreactive plasma chemistries, a universal response among photoresist materials is the development of a surface dense amorphous carbon (DAC) layer due to energetic ion bombardment. We have found that the photoresist etch rate is inversely proportional to the DAC layer thickness.¹ However, photoresists with UV sensitive pendant groups, such as 193 nm photoresists, develop a greater surface roughness due to the stresses in the surface generated by synergistic ion and UV photon interactions.

With depositing fluorocarbon (FC)-based ALE gas chemistries, the deposited FC layer reacts with the DAC layer and converts it into a mixed layer. This incorporation of FC into the DAC layer reduces the surface roughness without impacting the etch rate of the underlying photoresist as long as a sufficient DAC layer thickness remains.² This behavior is potentially advantageous for maximizing the photoresist to SiO₂ selectivity while maintaining an adequate surface roughness.

The authors acknowledge S.A. Gutierrez Razo, J.T. Fourkas, R.L. Bruce, S. Engelmann, and E.A. Joseph for collaborations on aspects of this work, and financial support by the National Science Foundation (NSF CMMI-1449309) and Semiconductor Research Corporation (2017-NM-2726).

¹ A. Pranda et al., *J. Vac. Sci. Technol. A* **36**, 021304 (2018).

² A. Pranda et al., *Plasma Process. Polym.* e1900026 (2019).

New Challenges to Reproducible Data and Analysis Focus Topic

Room A211 - Session RA+AS+NS+SS-MoA

Quantitative Surface Analysis II/Big Data, Theory and Reproducibility

Moderators: Kateryna Artyushkova, Physical Electronics, Donald Baer, Pacific Northwest National Laboratory

1:40pm RA+AS+NS+SS-MoA1 A Data-Centric View of Reproducibility, Anne Plant, National Institute of Standards and Technology (NIST); *J. Elliott*, NIST; *R. Hanisch*, National Institute of Standards and Technology (NIST)

INVITED

Ideally, data should be shareable, interpretable, and understandable within the scientific community. There are many challenges to achieving this, including the need for high quality documentation and a shared vocabulary. In addition, there is a push for rigor and reproducibility that is driven by a desire for confidence in research results. We suggest a framework for a systematic process, based on consensus principles of measurement science, to guide researchers and reviewers in assessing, documenting, and mitigating the sources of uncertainty in a study. All study results have associated ambiguities that are not always clarified by simply establishing reproducibility. By explicitly considering sources of uncertainty, noting aspects of the experimental system that are difficult to characterize quantitatively, and proposing alternative interpretations, the researcher provides information that enhances comparability and reproducibility.

2:20pm RA+AS+NS+SS-MoA3 Enhancing Data Reliability, Accessibility and Sharing using Stealthy Approaches for Metadata Capture, Steven Wiley, Pacific Northwest National Laboratory

INVITED

Science is entering a data-driven era that promises to accelerate scientific advances to meet pressing societal needs in medicine, manufacturing, clean energy and environmental management. However, to be usable in big data applications, scientific data must be linked to sufficient metadata (data about the data) to establish its identity, source, quality and reliability. This has also driven funding agencies to require projects to use community-based data standards that support the FAIR principles: Findable, Accessible,

¹ Coburn & Winters Student Award Finalist

Interoperable, and Reusable. Current concerns about data reproducibility and reliability have further reinforced these requirements. Truly reusable data, however, requires an enormous amount of associated metadata, some which is very discipline and sample-specific. In addition, this metadata is typically distributed across multiple data storage modalities (e.g. lab notebooks, electronic spreadsheets, instrumentation software) and is frequently generated by different people. Assessing and consolidating all of the relevant metadata has traditionally been extremely complex and laborious, requiring highly trained and motivated investigators as well as specialized curators and data management systems. This high price has led to poorly documented datasets that can rarely be reused. To simplify metadata capture and thus increase the probability it will indeed be captured, EMSL (Environmental Molecular Sciences Laboratory) has developed a general-purpose metadata capture and management system built around the popular ISA-Tab standard (Investigation-Study-Assay Tables). We have modified this framework by mapping it onto the EMSL workflow, organized as a series of “transactions”. These transactions are natural points where metadata is generated, include specifying how samples will be generated and shipped, instrument scheduling, sample storage, and data analysis. Software tools have been built to facilitate these transactions, automatically capture the associated metadata and link it to the relevant primary data. This metadata capture system works in concert with automated instrument data downloaders and is compatible with commercial sample tracking and inventory management systems. By creating value-added tools that are naturally integrated into the normal scientific workflow, our system enhances scientific productivity, thus incentivizing adoption and use. The entire system is designed to be general purpose and extensible and thus should be a useful paradigm for other scientific projects that can be organized around a transactional model.

3:00pm RA+AS+NS+SS-MoA5 From Electrons to X-rays: Tackling Big Data Problems through AI, Mathew Cherukara, Y. Liu, M.V. Holt, H. Liu, T.E. Gage, J.G. Wen, I. Arslan, Argonne National Laboratory **INVITED**

As microscopy methods and detectors have advanced, the rates of data acquisition and the complexity of the acquired data have increased, and these are projected to increase several hundred-fold in the near future. The unique electron and X-ray imaging capabilities at the Center for Nanoscale Materials (CNM) are in a position to shed light on some of the most challenging and pressing scientific problems we face today. To fully leverage the capability of these advanced instruments, we need to design and develop effective strategies to tackle the problem of analyzing the data generated by these imaging tools, especially following facility upgrades such as the upgrade to the Advanced Photon Source (APS-U) and the commissioning of the ultrafast electron microscope (UEM).

The data problem is especially acute in the context of coherent imaging methods, ultra-fast imaging and multi-modal imaging techniques. However, analysis methods have not kept pace. It is infeasible for a human to sort through the large, complex data sets being generated from imaging experiments today. At the CNM, we apply machine learning algorithms to our suite of electron and X-ray microscopy tools. Machine learning workflows are being developed to sort through data in real-time to retain only relevant information, to invert coherently scattered data to real-space structure and strain, to automatically identify features of interest such as the presence of defects, and even to automate decision making during an imaging experiment. Such methods have the potential not only to decrease the analysis burden on the scientist, but to also increase the effectiveness of the instruments, for instance by providing real-time experimental feedback to help guide the experiment.

4:00pm RA+AS+NS+SS-MoA8 Quantifying Shell Thicknesses of Core-Shell Nanoparticles by means of X-ray Photoelectron Spectroscopy, Wolfgang Werner, Vienna University of Technology, Austria **INVITED**

Determining shell thicknesses and chemistry of Core-Shell Nanoparticles (CSNPs) presently constitutes one of the most important challenges related to characterisation of nanoparticles. While for particulae number concentration various routine analysis techniques as well as methods providing reference measurements have been or are in the process of being developed, one of the most promising candidates for shell thickness determination is x-ray photoelectron spectroscopy (XPS).

Different approaches to quantify shell thicknesses will be presented and compared. These comprise: (1) The infinitesimal columns model (IC), (2) Shard's empirical formula (TNP-model) and (3) SESSA (Simulation of Electron Spectra for Surface Analysis) simulations with and (4) without elastic scattering.

CSNP XPS intensities simulated with SESSA for different combinations of core/shell-material combinations for a wide range of core and shell thicknesses have been evaluated with the TNP-model and the retrieved thicknesses are in good agreement with the nominal thickness, even when elastic scattering is turned on during the simulation, except for pathological cases. For organic shell materials these simulations fully confirm the validity of the (much simpler) TNP-method, which also coincides with the IC model.

Experimental data on of a round robin experiment of PMMA@PTFE CSNPs involving three research institutions were analysed with the aforementioned approaches and show a good consistency in that evaluations of the shell thicknesses among the institutions agree within 10% (and are in good agreement with the nominal shell thickness). This consistency is promising since it suggests that the error due to sample preparation can be controlled by following a strict protocol.

Use of the F1s signal leads to significant deviations in the retrieved shell thickness. Independent measurements using Transmission Electron Microscopy were also performed, which revealed that the core-shell structure is non-ideal, i.e. the particles are aspherical and the cores are acentric within the particles. SESSA simulations were employed to estimate the effect of various types of deviations of ideal NPs on the outcome of shell thickness determination.

The usefulness and importance of different kind of electron beam techniques for CSNP analysis and in particular shell thickness determination is discussed.

4:40pm RA+AS+NS+SS-MoA10 Modeling the Inelastic Background in X-ray Photoemission Spectra for Finite Thickness Films, Alberto Herrera-Gomez, CINVESTAV-Unidad Queretaro, México

The background signal in photoemission spectra caused by inelastic scattering is usually calculated by convolving the total signal with the electron-energy loss-function. This method, which was proposed by Tougaard and Sigmund in their classic 1982 paper [1], only works (as clearly indicated in [1]) for homogeneous materials. However, the method is commonly applied to finite thickness films. In this paper it is going to be described the proper way to remove the inelastic background signal of spectra from thin-conformal layers including buried layers and delta-doping [2]. The method is based on the straight-line inelastic scattering path, which is expected to be a very good approximation for low energy losses (near-peak regime). It is also a common practice to use the parametric Tougaard Universal Cross Section [3] with the provision that, instead of using the theoretical values for the parameters valid for homogeneous materials, the B-parameter is allowed to vary until the experimental background signal ~ 50 to 100 eV below the peak is reproduced. This is equivalent to scale the loss-function, which partially compensates the error from using the convolution method [1]. The error compensation on the modeling of the background of finite-thickness layers by scaling the loss-function will be quantitatively described.

[1] S. Tougaard, P. Sigmund, Influence of elastic and inelastic scattering on energy spectra of electrons emitted from solids, Phys. Rev. B. 25 (1982) 4452–4466. doi:10.1103/PhysRevB.25.4452.

[2] A. Herrera-Gomez, The photoemission background signal due to inelastic scattering in conformal thin layers (Internal Report), 2019. http://www.qro.cinvestav.mx/~aherrera/reportesInternos/inelastic_background_thin_film.pdf.

[3] S. Tougaard, Universality Classes of Inelastic Electron Scattering Cross-sections, Surf. Interface Anal. 25 (1997) 137–154. doi:10.1002/(SICI)1096-9918(199703)25:3<137::AID-SIA230>3.0.CO;2-L.

5:00pm RA+AS+NS+SS-MoA11 R2R(Raw-to-Repository) Characterization Data Conversion for Reproducible and Repeatable Measurements, Mineharu Suzuki, H. Nagao, H. Shinotsuka, National Institute for Materials Science (NIMS), Japan; K. Watanabe, ULVAC-PHI Inc., Japan; A. Sasaki, Rigaku Corp., Japan; A. Matsuda, K. Kimoto, H. Yoshikawa, National Institute for Materials Science (NIMS), Japan

NIMS, Japan, has been developing a materials data platform linked with a materials data repository system for rapid new material searching by materials informatics. The data conversion from raw data to human-legible/machine-readable data file is one of the key preparation techniques prior to data analysis, where the converted data file should include meta-information. Our tools can convert raw data to a structured data package that consists of (1) characterization measurement metadata, (2) primary parameters which we will not call “metadata” to distinguish from (1), (3) raw parameters as written in original raw data, and (4) formatted

numerical data. The formatted numerical data are expressed as matrix type with robust flexibility, not obeying a rigid definition. This flexibility can be realized by applying the data conversion style of Schema-on-Read type, not Schema-on-Write type based on *de jure* standards such as ISO documents. The primary parameters are carefully selected from raw parameters and their vocabularies are replaced from instrument-dependent terms to general ones that everyone can readily understand. These primary parameters with linked specimen information are useful for reproducible and repeatable instrument setup. By this R2R conversion flow, we have verified that we can generate and store interoperable data files of XPS spectra and depth profiles, powder XRD patterns, (S)TEM images, TED patterns, EELS spectra, AES spectra, EPMA spectra and elemental mapping, and theoretical electron IMFP data. We have also developed a system to allow semi-automatic data transfer from an instrument-controlling PC isolated from the network, by adopting a Wi-Fi-capable SD card's scripting capability, while keeping the PC offline. We are working on further software development for on-demand data manipulation after R2R data conversion. So far it has been possible to perform XPS peak separation using automated information compression technique. Using these components, high-throughput data conversion/accumulation and data analyses are realized, where human interaction is minimized. Using metadata extracted from raw data, other users can reproduce or repeat measurements even if they did not carry out the original measurement. Human-legible and machine-readable numerical data is utilized for statistical analyses in informatics.

Surface Science Division

Room A220-221 - Session SS+HC-MoA

CO₂, CO, Water, and Small Molecule Chemistry at Surfaces

Moderators: Donna Chen, University of South Carolina, Omur E. Dagdeviren, Yale University

1:40pm SS+HC-MoA1 Calculations of the Electrochemical Reduction of CO₂ and the Competing Hydrogen Evolution Reaction, *Hannes Jónsson*, University of Iceland, Iceland

INVITED

Calculations of electrochemical CO₂ reduction to formate, alcohols and hydrocarbons will be presented. The mechanism for the formation of the various products is established, the rate evaluated and comparison made with experimental measurements. The rate of the main side reaction, the hydrogen evolution reaction, is also estimated. The calculations are based on a detailed atomistic model of the electrical double layer (metal slab and water layer) and density functional theory calculations to evaluate not only the free energy of intermediates as a function of applied voltage but also the activation energy for each elementary step, both Heyrovsky and Tafel reactions [1]. Comparison is also made with calculations using an implicit solvation model [2]. A range of close packed metal surfaces are compared, including Cu, Ag, Au, Ni, Fe, Rh, Ir and Pt. The results are in remarkably good agreement with the reported experimental measurements. A two parameter descriptor is established that can help identify improved catalysts for CO₂ electrochemical reduction.

[1] J. Hussain, H. Jónsson and E. Skúlason, ACS Catalysis 8, 5240 (2018).

[2] M. Van den Bossche, E. Skúlason, C. Rose-Petruck and H. Jónsson, J. Phys. Chem. C 123, 4116 (2019).

2:20pm SS+HC-MoA3 CO₂ Adsorption on the O-Cu(100) Surface Studied by STM and DFT, *S.J. Tjung, Q. Zhang, J.J. Repicky, S. Yuk*, The Ohio State University; *X. Nie*, Dalian University of Technology; *Seth Shields*, The Ohio State University; *N. Santagata*, University of Memphis; *A. Asthagiri, J.A. Gupta*, The Ohio State University

Copper oxide catalysts are promising candidates for reducing CO₂ into useful fuels, such as ethanol, but the mechanism remains obscure. Studying the O-Cu(100) surface, which represents the initial transition of the oxidation of copper to copper oxide, and the adsorption process of CO₂ has the potential to elucidate the CO₂ reduction mechanism.

We performed a DFT/STM theoretical and experimental probe of the properties of CO₂ adsorption on the O-Cu(100) surface. The Cu(100) surface was repeatedly sputtered with Ar⁺ and annealed at 550°C in an ultra-high vacuum chamber, and subsequent Auger spectroscopy revealed the lack of surface contamination. The O-Cu(100) surface was obtained by exposing the Cu(100) face to 10⁻⁶ mbar of oxygen for 5 minutes at 300°C. The sample was then cooled and transferred into an attached low temperature (5K) ultra-high vacuum (10⁻¹¹ mbar) STM chamber.

The atomic resolution STM revealed the (2√2 × √2) R45°O-Cu(100) reconstruction, in good agreement with the DFT calculations. The reconstruction consists of an O-Cu-O row structure separated by missing Cu rows. Additionally, there are two equivalent domains which result from nucleation along the [001] and [010] directions of the Cu(100). Differential conductance spectroscopy reveals an increase in the work function of the O-Cu(100) surface, and two additional unoccupied states generated by the oxygen atoms, in agreement with the DFT calculations.

CO₂ was adsorbed onto the O-Cu(100) surface via *in situ* dosing in the STM. The CO₂ adsorbed exclusively between two oxygen atoms in the missing row reconstruction, which has the largest predicted adsorption energy. The lack of point defects on the surface indicates that the CO₂ does not dissociate, and the CO₂ molecules are easily disturbed by the tip under all tunneling conditions, which is consistent with the theoretically predicted low diffusion barrier.

This work acknowledges funding from the NSF (1809837).

2:40pm SS+HC-MoA4 Employing Carbon Monoxide and Carbon Dioxide Plasmas to Improve the Gas Sensing Performance of Tin(IV) Oxide, *Kimberly Hiyoto, E.R. Fisher*, Colorado State University

Metal oxide semiconductors are commonly researched materials for solid-state gas sensors; however, several limitations (i.e., operating temperatures of ≥300 °C and poor selectivity) impede wide-spread commercialization of these devices. Plasma processing offers a desirable alternative route to traditional methods, such as doping, because of the tunability of treatment parameters and the ability to modify the surface of the material while maintaining bulk properties. Previous work using plasma modification to enhance tin dioxide (SnO₂) gas sensor performance has mainly focused on oxygen or oxygen/argon plasma systems because these systems are thought to etch oxygen from the SnO₂ lattice creating oxygen vacancies that can lead to lower operating temperatures and improved sensor selectivity. Thus, further work needs to be done with other precursor gases to determine an effective strategy for fabricating improved gas sensors.

Here, we present carbon monoxide (CO) and carbon dioxide (CO₂) plasma-treated SnO₂ nanoparticle gas sensors treated at various applied rf powers. After plasma processing, the sensors demonstrate higher response to CO, ethanol, and benzene at lower operating temperatures compared to untreated SnO₂. In addition, the response and recovery behavior of the treated and untreated sensors were also evaluated as a metric for improved performance. To elucidate how plasma modification resulted in these changes, optical emission spectroscopy measured during plasma treatment and material characterization post plasma processing (X-ray photoelectron spectroscopy and X-ray powder diffraction) will also be discussed. All of these data work toward better understanding the relationship between surface chemistry and gas sensing performance, ultimately to develop a targeted approach to designing improved gas sensors.

3:00pm SS+HC-MoA5 The Role of Steps in the Dissociation of CO₂ on Cu, *Johan Gustafson, B. Hagman*, Lund University, Sweden; *A. Posada-Borbón, A. Schaefer*, Chalmers University of Technology, Sweden; *M. Shipilin*, Stockholm University, Sweden; *C. Zhang*, Lund University, Sweden; *L.R. Merte*, Malmö University, Sweden; *A. Hellman*, Chalmers University of Technology, Sweden; *E. Lundgren*, Lund University, Sweden; *H. Grönbeck*, Chalmers University of Technology, Sweden

INVITED

CO₂ chemistry has received significant attention recently, due to the greenhouse effect of CO₂ emissions and the resulting climate change. CO₂ reduction reactions, such as methanol synthesis and reverse water-gas shift, provide routes for recycling of CO₂ and thus limiting the CO₂ emissions. These reactions are commonly performed over Cu-based catalysts, making the interaction of CO₂ and Cu, on the atomic scale, of importance for a fundamental understanding and the development of new and more efficient catalysts.

We have previously studied the dissociative adsorption of CO₂ on Cu(100) using APXPS and DFT. In summary, exposure of the Cu surface to CO₂ in the mbar range at temperatures above room temperature results in dissociation of CO₂ into CO, that desorbs, and O that stays on the surface. The rate of the increase in O coverage, however, was not consistent with what one would expect from adsorption on the flat Cu(100) surface. Instead, we propose a model where the dissociation happens at atomic steps. The steps were found to both lower the activation barrier for the dissociation and separate the products, such that the probability of recombination is lowered.

Monday Afternoon, October 21, 2019

As an obvious follow-up of this study, we have studied the dissociative adsorption of CO₂ on Cu(911), which exposes five atoms wide (100) terraces separated by monatomic steps. In contrast to what we expected, the O coverage did not increase significantly faster on this stepped surface. Our preliminary analysis suggests that diffusion of O from one step to another reduces the effect of the steps separating O and CO, but also that the steps facilitate O diffusion to the subsurface region and possibly stabilisation of CO₂ or CO₃ species on the surface.

In this presentation we will report how we conclude that the steps control the dissociation and, especially, the present status of the studies of Cu(911).

4:00pm **SS+HC-MoA8 Surface Temperature Dependence of Methane Dissociation on Ni(997)**, *Daniel Tinney, E.A. High, L. Joseph, A.L. Utz*, Tufts University

Commercial steam reforming reactors operate at temperatures of 1000K or higher, and methane dissociation on the Ni catalyst is generally believed to be the rate-limiting step in this industrially important process. Despite the commercial importance of this reaction, nearly all studies probing the dynamics of methane dissociation have focused on surface temperatures of 600K or lower. Here, we use energy and vibrationally state selected methane molecules in a supersonic molecular beam to quantify the impact of surface temperature on methane activation over a wide range of surface temperatures. Our use of methane molecules with a precisely defined energy highlights provides a clear view of how surface temperature impacts reactivity.

Vibrationally state-resolved reactivity measurements reveal details of fundamental processes that impact reactivity in the field of heterogeneous catalysis. Non-statistical, mode-specific, and bond-selective enhancements observed for methane and its isotopologues on transition metal surfaces provide insights into energy flow during reactions. Reactive gas molecules with strictly-defined energy in well-defined energetic coordinates used in state-selective experiments have also proven to be valuable probes of how surface atom motion affects overall reactivity. For this work, vibrationally state-resolved data was collected via infrared (IR) laser excitation of the anti-symmetric stretch of supersonically-expanded methane (CH₄) gas molecules impinging on a lightly-stepped Ni(997) surface. Measurements on the single crystal were investigated over a broad range of surface temperatures (82 K ≤ T_s ≤ 1000 K) while utilizing varying incident energies (E_i = 20 kJ/mol to >140 kJ/mol). A comparison with prior data on Ni(111) surface reveals the role that steps may play in methane activation.

4:20pm **SS+HC-MoA9 Promotion and Inhibition of Methane Dissociation by Carbon on Ni Single Crystal Surfaces**, *Arthur Utz, E.A. High, D.G. Tinney*, Tufts University

State-resolved beam-surface scattering measurements, when coupled with molecular beam reactivity modulation measurements, permit real-time measurement of methane dissociation on Ni(111) and Ni(997) surfaces. At surface temperatures above 550K, methyl reaction products dehydrogenate to C atoms, and H atoms recombine and desorb, leaving C atoms behind. At higher surface temperatures, C atoms begin to aggregate on the surface and also absorb into the Ni subsurface region. We monitor how the presence of these C atoms on and beneath the surface impacts methane dissociation probability.

4:40pm **SS+HC-MoA10 Two-Dimensional Polymorphism as a Result of Non-Equilibrium Self-Assembly**, *Angela Silski¹, J. Petersen*, University of Notre Dame; *R.D. Brown*, Clarkson University; *S.A. Kandel*, University of Notre Dame

The challenge in the field of molecular self-assembly is that the outcome of these processes is not easily predicted a priori, rather, results of self-assembly processes are often rationalized after the fact. In this study, a systemic approach to self-assembly is taken; the chemical structure of the starting molecule is iteratively changed (adding, removing or substituting particular functional groups) and the resulting self-assembled structure is observed via scanning tunneling microscopy. The focus of this study is on the functional groups that can form directional interactions (hydrogen- and halogen-bonds). We observe a metastable cyclic pentamer for isatin (1H-indole-2,3-dione) with density functional theory providing support for a cyclic structure stabilized by both NH \cdots O and CH \cdots O hydrogen bonds between neighboring molecules. The CH \cdots O hydrogen bond is made between the 7-position proton acting as the hydrogen bond donor and the 3-position carbonyl as the hydrogen bond acceptor, and calculations

indicate that the isatin pentamer structure is 17 kJ/mol more stable than the dimer on the per molecule basis. To probe the importance of the CH \cdots O hydrogen bond in stabilizing the isatin pentamer, we compare to isatin derivatives: we replace the 3-position carbonyl with a methyl group (3-methyl 2-oxindole), the 7-position proton with a fluorine (7-fluoroisatin), systematically move the location of the hydrogen bond donor/acceptor by one position, (phthalimide), and remove of the primary hydrogen bond donor (1,2-indandione and 1,3-indandione). We show that cyclic pentamer formation is either altered or precluded as a result of these substitutions. To our surprise, substituting the 6-position with a bromine (6-bromoisatin) which is a position remote to the positions of the hydrogen-bond contacts, does not result in the formation of cyclic pentamers on the surface. A monolayer of 6-bromoisatin consists of almost entirely "zipper" dimer structures. Additionally, the importance of CH \cdots O bonding in forming isatin pentamers is supported by electrospray ionization mass spectrometry (ESI-MS) measurements, which include a magic-number isatin pentamer peak. A mass spectrum of 6-bromoisatin also shows a relatively intense pentamer peak, whereas the other derivative molecules show little clustering under the same conditions. This work is significant in understanding the role that the position of the hydrogen- and halogen-bond donor/acceptor groups has on the resulting 2D supramolecular assemblies.

Thin Films Division

Room A124-125 - Session TF+2D+AP+EL+SS-MoA

ALD and CVD: Nucleation, Surface Reactions, Mechanisms, and Kinetics

Moderators: *Adrie Mackus*, Eindhoven University of Technology, The Netherlands, *Qing Peng*, University of Alabama

1:40pm **TF+2D+AP+EL+SS-MoA1 ALD on Particles: What is Different from Wafers?**, *Ruud van Ommen*, Delft University of Technology, Netherlands
INVITED

Advanced materials, often relying on nanostructured particles as building blocks, are crucial in meeting grand challenges in energy and health. Atomic layer deposition (ALD) is an excellent technique to make such nanostructured particles: particles of which the surface is either covered by an ultrathin film or by nanoclusters. Although the underlying mechanisms are similar, there are quite some differences between ALD processing of wafers and ALD processing of particles. This presentation will discuss recent developments and insights in the field of applying ALD to particles, with an emphasis on reactor technology, precursor utilization, operating conditions, and scaling up. I will show that ALD is suited to produce nanostructured particles with very high precision. Moreover, it is scalable such that large amounts of such particles can be produced.

2:20pm **TF+2D+AP+EL+SS-MoA3 Insights into Particle ALD Peculiarities from In- and Ex-Situ Characterization**, *Benjamin Greenberg*, American Society for Engineering Education; *J.A. Wollmershauser, B. Feygelson*, U.S. Naval Research Laboratory

Particle atomic layer deposition (pALD) is an increasingly popular technique for mass production of core/shell nanoparticles (NPs). In a typical pALD process, NP powders are agitated in a fluidized bed or rotary reactor, and conformal coating of the entire powder surface—often > 100 m² in lab-scale reactors—is attempted via prolonged precursor exposures and purges. Over the past 2+ decades there have been many reports of highly encouraging results, including TEM images of NPs individually encapsulated by shells of uniform thickness. Nevertheless, several fundamental questions about pALD mechanisms and behavior remain challenging to answer. For example, how does the pALD growth per cycle (GPC) deviate from the corresponding ALD GPC on a flat substrate, and why? Or more importantly, what conditions are required to maximize the fraction of powder that attains an ideal core/shell structure (individual NP encapsulation) rather than a coated-agglomerate structure in which cores are glued together? In this work, using a commercial rotary pALD reactor to coat various NPs with oxide shells, we employ a wide array of characterization techniques to shed light on these issues and inform process optimization. In situ, we experiment with relatively uncommon techniques such as high-speed video analysis and pyrometry of the agitated NP powder, as well as conventional techniques such as mass spectrometry

¹ Morton S. Traum Award Finalist

Monday Afternoon, October 21, 2019

(RGA). High-speed videos in particular reveal aspects of the process often undiscussed (and sometimes difficult to convey) in the pALD literature, including changes in the powder motion as surface chemistry evolves. *Ex situ*, we characterize the coated NPs via TEM, XRD, SAXS, XPS, and N_2 -adsorption surface area measurements (BET method).

3:00pm TF+2D+AP+EL+SS-MoA5 Controlling the Nucleation of CVD Cobalt Films on SiO₂: Combining an Amido-based Nucleation Promotor with an Amine-based Growth Inhibitor to Afford Atomically-smooth Surfaces, Zhejun Zhang, G.S. Girolami, J.R. Abelson, University of Illinois at Urbana-Champaign

Cobalt films are of interest for the back-end metallization and transistor contact in microelectronics because cobalt has a greater electromigration resistance and a lower diffusion rate in dielectrics compared with copper. However, few-nanometer thick Co films deposited by CVD on dielectrics are usually non-continuous – they consist of islands with pinholes and significant roughness – which renders them unsuitable for nanoscale device fabrication. A nucleation layer, such as TiN, can be pre-deposited to improve the area density of Co nuclei; this approach eliminates the problem of islanding, but it subtracts cross-sectional area from the plug or line, thus increasing the electrical resistance.

Here, we solve the Co nucleation problem in CVD using a two-pronged approach. First we expose the SiO₂ surface to a tetrakis(dimethylamido)(transition metal) precursor at low temperature. This affords a self-limiting, submonolayer coverage of an intermediate, similar to the behavior of such molecules in ALD processes. The adsorbate layer then enhances the nucleation of cobalt from the Co₂(CO)₈ precursor, such that a large area density of nanoscale islands forms with essentially no nucleation delay. Using this approach, the rms surface roughness for a 1.5-nm-thick Co film decreases from 2.5 to 1.0 nm.

Second, we further improve the surface morphology by adding a co-flow of ammonia together with the carbonyl precursor; this serves as a growth inhibitor that reduces the steady-state growth rate of Co films by 50%. The presence of the inhibitor does not alter the nucleation rate, however, the rms roughness of a 1.5-nm-thick film is further reduced to only 0.4 nm. We suggest that the roughness is due to a better valley-filling at low precursor reaction probability, consistent with the literature. In summary, our approach enables the use of CVD to afford excellent Co films for nanofabrication.

3:20pm TF+2D+AP+EL+SS-MoA6 Plasma-assisted Atomic Layer Epitaxy of Indium Aluminum Nitride Studied Using *in situ* Grazing Incidence Small-angle X-ray Scattering, Jeffrey M. Woodward, ASEE (residing at US Naval Research Laboratory); S.G. Rosenberg, American Society for Engineering Education (residing at US Naval Research Laboratory); S.D. Johnson, N. Nepal, U.S. Naval Research Laboratory; Z.R. Robinson, SUNY Brockport; K.F. Ludwig, Boston University; C.R. Eddy, U.S. Naval Research Laboratory

Indium aluminum nitride (InAlN) is an attractive material for power electronic applications. However, conventional methods of epitaxial growth of InAlN are challenged by a large miscibility gap and the significant differences in optimal growth conditions for the constituent aluminum nitride (AlN) and indium nitride (InN) binary compounds. Despite these challenges, the epitaxial growth of InAlN alloys throughout the entire compositional range has been demonstrated using plasma-assisted atomic layer epitaxy (ALEp)¹, a variant of atomic layer deposition in which relatively higher temperatures are utilized. In the ALEp growth of InAlN, the desired alloy compositions are achieved by forming ultra-short period superlattices of alternating InN and AlN layers, referred to as digital alloys (DA). In order to further advance these empirical efforts, significant research is needed to better understand the nucleation and growth kinetics of ALEp DA growth. To this end, we employ *in situ* grazing incidence small angle X-ray scattering (GISAXS) for the real-time study of the evolving ternary InAlN surfaces as has been done previously for binary InN² and AlN³.

Here we present *in situ* GISAXS studies of ALEp growth of InN, AlN, and a range of InAlN DAs on GaN (0001) substrates, which were performed at Brookhaven National Laboratory's NSLS-II using a custom reactor. The InAlN DAs studied include In_{0.19}Al_{0.81}N (3 AlN cycles and 2 InN cycles per supercycle), In_{0.5}Al_{0.5}N (1 AlN cycle and 3 InN cycles per supercycle), In_{0.64}Al_{0.36}N (1 AlN cycle and 5 InN cycles per supercycle) and In_{0.83}Al_{0.17}N (1 AlN cycle and 14 InN cycles per supercycle). Preliminary analysis of the data suggests that while the pure InN and AlN grew in 3D and 2D modes, respectively, the InAlN growth mode did not follow a simple trend as the nominal composition was tuned from InN to AlN. Instead, select compositions (50% and 83% In) exhibited predominantly 3D growth, while

others (19% and 64% In) exhibited 2D growth. We also present complementary ALEp growth studies using a commercial Ultratech/Cambridge Nano Tech Fiji 200 and *ex situ* characterization methods, including high resolution X-ray diffraction, X-ray reflectivity, and atomic force microscopy.

¹ N. Nepal, V.R. Anderson, J.K. Hite, and C.R. Eddy, *Thin Solid Films* **589**, 47 (2015)

² J.M. Woodward, S.G. Rosenberg, A.C. Kozen, N. Nepal, S.D. Johnson, C. Wagenbach, A.H. Rowley, Z.R. Robinson, H. Joress, K.F. Ludwig Jr, C.R. Eddy Jr, *J. Vac. Sci. Technol. A* **37**, 030901 (2019)

³ V.R. Anderson, N. Nepal, S.D. Johnson, Z.R. Robinson, A. Nath, A.C. Kozen, S.B. Qadri, A. DeMasi, J.K. Hite, K.F. Ludwig, and C.R. Eddy, *J. Vac. Sci. Technol. A* **35**, 031508 (2017)

4:00pm TF+2D+AP+EL+SS-MoA8 Real-time Monitoring of the Surface Chemistry of Atomic Layer Deposition by Ambient Pressure X-ray Photoelectron Spectroscopy, Joachim Schnadt, P. Shayesteh, Lund University, Sweden; R. Tsyshkevskiy, University of Maryland; J.-J. Jean-Jacques, F. Bournel, Sorbonne Université, France; R. Timm, Lund University, Sweden; A.R. Head, Brookhaven National Laboratory; G. D'Acunto, F. Rehman, S. Chaudhary, Lund University, Sweden; R. Sánchez-de-Armas, Uppsala University, Sweden; F. Rochet, Sorbonne Université, France; B. Brena, Uppsala University, Sweden; A. Mikkelsen, S. Urpelainen, A. Troian, S. Yngman, J. Knudsen, Lund University, Sweden

INVITED

Atomic layer deposition (ALD) and chemical vapour deposition (CVD) are very important methods that enable a highly controlled growth of thin films [1]. The surface chemistry of the underlying processes remains, however, little understood. While idealised reaction mechanisms have been developed, they represent postulates rather than models based on the factual identification of surface species and kinetics [2]. New *in situ* and *operando* methods offer the prospect of gaining a much more thorough understanding of the involved molecular and atomic surface processes and (dynamic) structures, which, in turn, means that a much better knowledge basis can be achieved for the future improvement of materials and growth recipes (see, e.g. [3,4]). One such *operando* method, which can be applied to the investigation of ALD and CVD, is synchrotron-based ambient pressure x-ray photoelectron spectroscopy (APXPS). While conventional x-ray photoelectron spectroscopy (XPS) is limited to vacuum pressures of 10⁻⁵ mbar and below, APXPS can be carried out at realistic pressure. Today, most APXPS machines can operate at pressures up to the 10 mbar regime, which is an ideal match to the pressure regime used in standard ALD reactors.

Here, I will report on our recent efforts to apply density functional theory (DFT)-assisted synchrotron-based APXPS to the ALD/CVD of oxides (TiO₂, SiO₂, and HfO₂) on semiconductor (InAs and Si) and oxide surfaces (TiO₂, RuO₂) [3-5]. I will show that APXPS allows the identification of the surface species occurring during thin film growth and the real-time monitoring of their evolution with a time resolution of down into the millisecond regime. Here, DFT is an important tool for pinpointing the nature of the chemical species and for providing deeper insight in the surface chemical processes. I will also report on our efforts to further improve instrumentation with the goal of achieving a much closer match of the APXPS sample environment with the geometries used in conventional ALD reactors. The development will also open for the use of a wider range of precursors and growth protocols.

[1] V. Miikkulainen et al., *J. Appl. Phys.* **113** (2013) 021301.

[2] F. Zaera, *Coord. Chem. Rev.* **257** (2013) 3177.

[3] B. A. Sperling et al. *Appl. Spectrosc.* **67** (2013) 1003.

[4] K. Devloo-Casier et al., *J. Vac. Sci. Technol.* **32** (2014) 010801.

[3] S. Chaudhary et al., *J. Phys. Chem. C* **119** (2015) 19149.

[4] A. R. Head et al., *J. Phys. Chem. C* **120** (2016) 243.

[5] R. Timm et al., *Nature Commun.* **9** (2018) 412.

4:40pm TF+2D+AP+EL+SS-MoA10 Kinetics during TMA-H₂O ALD: The Possible Role of Cooperative Surface Reactions, Brent Sperling, B. Kalanyan, J.E. Maslar, National Institute of Standards and Technology (NIST)

Until recently, the CH₃ groups produced by surface reactions of trimethylaluminum (TMA) during atomic layer deposition were widely believed to always be highly reactive toward H₂O, but *in situ* measurements have shown this is not the case below about 200 °C.[1] At these temperatures, some CH₃ groups react slowly, and a significant amount

Monday Afternoon, October 21, 2019

persists from cycle to cycle under typical growth conditions. Interestingly, these persistent CH₃ groups are not incorporated as carbon impurities. We have observed these CH₃ groups using *in situ* reflection infrared spectroscopy and have confirmed low carbon concentrations in our films using *ex situ* XPS. Furthermore, we have measured the kinetics of the reaction with H₂O and have found them to be well-described by a double-exponential decay function. A simple Monte Carlo simulation that incorporates cooperative effects by clustered surface reactants (as suggested by DFT calculations[2]) reveals that a double-exponential decay of coverage can result even when only one species of reactant is present. Furthermore, the short-range distributions of coverage that result in the simulation differ from purely random ones. This difference implies that measurements sensitive to dipole-dipole interactions when combined with an independent measurement of surface coverage could be used to confirm or disprove the cooperative reaction model.

[1] V. Vandalon and W. M. M. Kessels, *J. Vac. Sci. Technol. A* **35** (2017) 05C313

[2] M. Shirazi and S. D. Elliott, *Nanoscale* **7** (2015) 6311.

5:00pm **TF+2D+AP+EL+SS-MoA11 Atomic Layer Deposition of Metal Sulfides: Growth and Surface Chemistry**, *Xinwei Wang*, Shenzhen Graduate School, Peking University, China

Atomic layer deposition (ALD) of metal sulfides has recently aroused great interest, and many new sulfide ALD processes have emerged during the past several years. Surface chemistry plays a key role in ALD, but it remains yet to be investigated for many recently developed sulfide ALD processes. In this representation, I will report our study on the growth and surface chemistry of the ALD of nickel, iron, and cobalt sulfides, using various *in situ* characterization techniques of X-ray photoelectron spectroscopy (XPS), low-energy ion scattering (LEIS), quartz crystal microbalance (QCM), and quadrupole mass spectrometry (QMS). For instance, nickel sulfide (NiS) can be deposited from a Ni amidinate precursor (Ni(amd)₂) and H₂S by ALD (*Chem. Mater.* (2016) **28**, 1155), but the surface chemistry of this process is found to deviate from the conventional ligand-exchange ALD scheme, and a formation of a nonvolatile acid-base complex from acidic surface sulfhydryl and basic amidine is suggested during the H₂S half-cycle (*J. Phys. Chem. C* (2018) **122**, 21514). The initial ALD growth of NiS on a SiO_x surface is also intriguing, as the initial growth mechanism is found to be rather different from that in the later steady film growth. In the initial ALD cycles, the XPS results show a drastic cyclic variation of the signals for the Ni–O bonds, with prominently observable Ni–O signals after each Ni(amd)₂ dose but almost negligible after the subsequent H₂S dose. These results suggest that the Ni–O bonds are first formed on the surface in the Ni(amd)₂ half-cycles and then mostly converted to NiS in the following H₂S half-cycles. To describe this initial ALD growth process, a reaction-agglomeration mechanistic scheme is proposed (*Chem. Mater.* (2019) **31**, 445). Surface thermolysis study of the Ni amidinate precursor further reveals the temperature-dependent behavior of the film growth.

Energy Transition Focus Topic

Room A212 - Session TL+2D+HC+SS-MoA

Surface Reaction Mechanisms in Energy Conversion (ALL INVITED SESSION)

Moderators: Marie Turano, Loyola University Chicago, Sarah Zaccarine, Colorado School of Mines

1:40pm **TL+2D+HC+SS-MoA1 Selective Photo-driven Organic Reactions on the Surfaces of Colloidal Quantum Dots**, *Y. Jiang, K. McClelland, C. Rogers, Emily Weiss*, Northwestern University **INVITED**

Colloidal quantum dots present a unique opportunity not only to power chemical reactions with sunlight but to control those chemical reactions through various templating strategies. This talk will explore demonstrations of chemo-, regio-, and stereoselective reactions photocatalyzed by quantum dots.

2:20pm **TL+2D+HC+SS-MoA3 Single-Atom Alloy Catalysts: Born in a Vacuum, Tested in Reactors, and Understood In Silico**, *Charles Sykes*, Tufts University **INVITED**

In this talk I will discuss a new class of metallic alloy catalysts called *Single Atom Alloys* in which precious, reactive metals are utilized at the ultimate limit of efficiency.¹⁻⁵ These catalysts were discovered by combining atomic-scale scanning probes with more traditional approaches to study surface-catalyzed chemical reactions. This research provided links between the

atomic scale surface structure and reactivity which are key to understanding and ultimately controlling important catalytic processes. Over the last five years the concepts derived from our surface science and theoretical calculations have been used to design *Single Atom Alloy* nanoparticle catalysts that can perform industrially relevant reactions at realistic reaction conditions in collaboration with Maria Flytzani-Stephanopoulos at Tufts. For example, alloying elements like platinum and palladium with cheaper, less reactive host metals like copper enables 1) dramatic cost savings in catalyst manufacture, 2) more selective chemical reactions, 3) reduced susceptibility to CO poisoning, and 4) higher resistance to deactivation by coking. I go on to describe very recent theory work by collaborators Stamatakis and Michaelides at UCL that predicts reactivity trends of 16 different *Single Atom Alloy* combinations for important reaction steps like activation of H-H, C-H, N-H, O-H and C=O bonds. This project illustrates that the field of surface science is now at the point where it plays a critical role in the design of new heterogeneous catalysts.

References:

[1] Kyriakou et al. *Science* **335**, 1209 (2012).

[2] Marcinkowski et al. *Nature Materials* **12**, 523 (2013).

[3] Lucci et al. *Nature Communications* **6**, 8550 (2015).

[4] Liu et al. *JACS* **138**, 6396 (2016).

[5] Marcinkowski et al. *Nature Chemistry* **10**, 325 (2018).

3:00pm **TL+2D+HC+SS-MoA5 Understanding Fundamental Energy Conversion Mechanisms: How Surface Science Can Help**, *Ulrike Diebold*, Institute of Applied Physics, TU Wien, Austria **INVITED**

As we move to a more sustainable society, current energy conversion schemes need to be improved and novel ones designed. The relevant charge transfer processes and chemical transformations all occur at interfaces, so insights into fundamental mechanisms are needed to provide a scientific basis for these developments.

Using the frontier tools of surface science, I will discuss how we can directly inspect charge transfer to molecules, investigate the influence of the local environment on the reactivity of active sites, or probe the acidity of individual hydroxyls. Together with first-principles computations such experiments give crisp and clear insights into surface processes. I will also discuss the steps that are necessary to transfer the knowledge gained from model systems to more complex environments.

4:00pm **TL+2D+HC+SS-MoA8 Atomically-defined Model Interfaces in Energy-related Catalysis, Electrochemistry, and Photoelectrochemistry**, *Jörg Libuda*, University Erlangen-Nuremberg, Germany **INVITED**

The transformation between chemical energy, solar energy, and electrical energy occurs at interfaces. Therefore, functional interfaces are the key to the development of new materials in energy technology and energy-related catalysis. In our work, we explore model systems, which provide detailed insight into the chemistry and physics at such functional interfaces. Complex, yet atomically-defined model systems are studied both under 'ideal' surface science conditions and under 'real' conditions, i.e., in contact with gases, liquids, in electrochemical, and in photoelectrochemical environments. We illustrate the approach in three examples from our recent research.[1-5]

First, we consider new noble-metal-efficient catalysts for fuel cell applications.[1] We show that precious noble metals such as Pt can be anchored to nanostructured oxide supports. The resulting materials show very high noble metal efficiency and high stability. Surface science studies on model catalysts provide insight into the functionality of these systems. Electronic metal support interactions modify the reactivity of the catalytic surfaces but also stabilize sub-nanometer-sized Pt nanoparticles against sintering and deactivation.

Secondly, we report on the development of atomically defined model systems for oxide-based electrocatalysts, which can be studied under true operation conditions, i.e., in liquid environments and under potential control. We describe how such model electrodes are prepared by surface science methods and, subsequently, are studied in liquid electrolytes preserving their atomic structure. We investigate the role of particle size effects and identify the origin of metal-support interactions.

In the third part, we scrutinize the role of organic-oxide hybrid interfaces in energy transformation. Particularly fascinating are organic layers of molecular photoswitches, which provide an extremely simple solution for solar energy conversion and storage. We show that it is possible to assemble fully operational solar-energy-storing hybrid interfaces by

Monday Afternoon, October 21, 2019

anchoring tailor-made norbornadiene photoswitches to atomically defined oxides. Interestingly, the activation barrier for energy release in these systems is not affected by the anchoring reaction. Finally, we demonstrate that solar energy storage and release in such systems can also be controlled electrochemically with high reversibility.

[1] A. Bruix, et al., *Angew. Chem. Int. Ed.*, 53, 10525 (2014)

[2] Y. Lykhach, et al., *Nat. Mater.* 15, 284 (2016)

[3] O. Brummel et al., *ChemSusChem* 9, 1424 (2016)

[4] O. Brummel et al., *J. Phys. Chem. Lett.*, 8, 2819 (2017)

[5] F. Faisal et al., *Nat. Mater.*, 17 592 (2018)

4:40pm **TL+2D+HC+SS-MoA10 Controlling Ultrafast Photochemical Reactions in Photocatalysis, Annemarie Huijser**, University of Twente, The Netherlands, The Netherlands **INVITED**

The transition from fossil to renewable energy is one of the most important challenges of our society. Solar devices are widely considered as a highly promising option, as the energy provided by the sun to the earth by far exceeds global needs. We are investigating the use of nanostructured materials for application in solar energy conversion. The overall efficiency relies on the complex interplay of many elementary processes, occurring at different time scales and also dependent on the nanostructure. In this presentation I will show how a combination of methods for ultrafast spectroscopy can shed light on the nature of photoinduced processes and provide mechanistic information valuable for the design of novel materials.

Surface Science Division

Room A220-221 - Session SS+2D+HC-TuM

Atom Manipulation and Synthesis/Oxide Surface Reactions & Flash Session

Moderators: Liney Arnadottir, Oregon State University, Stephen McDonnell, University of Virginia, Martin Setvin, TU Wien, Austria

8:00am **SS+2D+HC-TuM1 Angstrom Scale Chemical Analysis of Metal Supported *Trans*- and *Cis*-Regioisomers by Ultrahigh Vacuum Tip-Enhanced Raman Mapping.** S. Mahapatra, J. Schultz, L. Li, Nan Jiang, University of Illinois at Chicago

Real space chemical analysis of two structurally very similar components i.e. regioisomers lies at the heart of heterogeneous catalysis reactions, modern-age electronic devices and various other surface related problems in surface science and nanotechnology. One of the big challenges in surface chemistry is to identify different surface adsorbed molecules and analyze their chemical properties individually. Herein, we report a topological and chemical analysis of two regioisomers, *trans*- and *cis*-tetrakis(pentafluorophenyl)porphodilactone (*trans*- and *cis*-H₂F₂₀TPPDL) molecules by high resolution scanning tunneling microscopy (STM), and ultrahigh vacuum tip-enhanced Raman spectroscopy (UHV-TERS). Both isomeric structures are investigated individually on Ag(100) at liquid nitrogen temperature. Following that, we have successfully distinguished these two regioisomeric molecules simultaneously through TERS with an angstrom scale (8 Å) spatial resolution. Also, the two-component organic heterojunction has been characterized at large scale using high resolution two-dimensional (2D) mapping. Combined with time-dependent density functional theory (TDDFT) simulations, we explain the TERS spectral discrepancies for both isomers in the fingerprint region.

8:40am **SS+2D+HC-TuM3 On-surface Synthesis by Atom Manipulation Studied with Atomic Force Microscopy.** Leo Gross, IBM Research - Zurich, Switzerland

INVITED

Elusive molecules are created using atomic manipulation with a combined atomic force/scanning tunneling microscope (AFM/STM). Employing high-resolution AFM with functionalized tips provides insights into the structure, geometry, aromaticity, charge states and bond-order relations of the molecules created and into the reactions performed [1].

We created radicals, diradicals [2], non-Kekulé molecules [3] and polyynes [4] and studied their structural and electronic properties. We recently showed that the reorganization energy of a molecule on an insulator can be determined [5]. In addition, we expanded the toolbox for the synthesis of molecules by atomic manipulation, demonstrating reversible cyclisation reactions [2], skeletal rearrangements [4] and controlled reactions on insulating substrates by electron attachment/detachment [6].

On insulating substrates we can control the charge state of molecules and resolve changes within molecular geometry, adsorption and aromaticity related to the oxidation state.

References:

- [1] L. Gross *et al.* *Angew. Chem Int. Ed* **57**, 3888(2018)
- [2] B. Schuler *et al.* *Nat. Chem.* **8**, 220 (2016)
- [3] N. Pavliček *et al.* *Nat. Nano.* **12**, 308 (2017)
- [4] N. Pavliček *et al.* *Nat. Chem.* **10**, 853 (2018)
- [5] S. Fatayer *et al.* *Nat. Nano.* **13**, 376 (2018)
- [6] S. Fatayer *et al.* *Phys. Rev. Lett.* **121**, 226101 (2018)

9:20am **SS+2D+HC-TuM5 The Large Effect of Solvents on Heats of Adsorption versus Gas Phase Explained with a Simple Bond-additivity Model: A Case Study with Phenol on Pt(111) in Water.** Charles T. Campbell, University of Washington; N. Singh, University of Michigan; J.R. Rumpitz, University of Washington

The low-coverage heat of adsorption of phenol on Pt(111) facets of a Pt wire in aqueous phase is approximately 21 kJ/mol (relative to aqueous phenol)¹, much smaller than the heat for gas phase phenol adsorption at this same low coverage on single-crystal Pt(111) in ultrahigh vacuum (200 kJ/mol from adsorption calorimetry²). Here we quantitatively analyze the individual contributions that give rise to this large solvent effect using a simple pairwise bond-additivity model, taking advantage of experimental data from the literature to estimate the bond energies. The dominant contribution to the lowering in heat when adsorbing phenol in water is the

energy cost to break the strong bond of liquid water to Pt(111) ($E_{\text{adhesion}} = \sim 116$ kJ per mole of phenol area). The water-phenol bonding is lost on one face of the phenol and this costs ~ 50 kJ/mol, but this is nearly compensated by the new water-water bonding (~ 53 kJ/mol of phenol area). The results indicate that the intrinsic bond energy between phenol and Pt(111) is not very different when in gas versus aqueous phase, provided one takes into consideration the expectation that water forces phenol into 2D islands of high local coverage even at low average coverage (for the same reason that oil and water don't mix). This also explains the lack of a strong coverage dependence in the heat of adsorption when measured in aqueous phase, whereas it decreases by ~ 60 kJ/mol with coverage when measured in gas phase. This bond-additivity analysis can be extended to other surfaces and solvents for any flat adsorbate. It clarifies why catalysis with molecules like phenol which have very strong bonding to Pt group metals can proceed rapidly at room temperature in liquid solvents like water, but would never proceed in the gas phase at room temperature due to irreversible site poisoning. We also present many new measurements of solvent / metal adhesion energies that will aid future analyses of solvent effects in adsorption.

(1) Singh, N.; Sanyal, U.; Fulton, J. L.; Gutiérrez, O. Y.; Lercher, J. A.; Campbell, C. T. Quantifying Adsorption of Organic Molecules on Platinum in Aqueous Phase by Hydrogen Site Blocking and in Situ X-Ray Absorption Spectroscopy. *Submitted 2019*.

(2) Carey, S.; Zhao, W.; Mao, Z.; Campbell, C. T. Energetics of Adsorbed Phenol on Ni(111) and Pt(111) by Calorimetry. *J. Phys. Chem. C* **2019**, *123*, 7627–7632.

9:40am **SS+2D+HC-TuM6 Atomic-Scale Growth Mechanisms of Niobium Hydrides on Hydrogen Infused Nb(100).** Rachael Farber, D.R. Veit, S.J. Sibener, The University of Chicago

Particle accelerator technology and science, while commonly associated with fundamental high-energy physics applications, is also a crucial component in biological, chemical, and industrial scientific technologies. In order to increase the accessibility and applicability of accelerator-based technologies in multiple sectors, it is imperative to develop technologies that will enable the production of a more intense particle beam at a lower price point. As such, it is essential to identify structural and chemical features that inhibit beam intensity and develop methods to suppress such surface features.

Niobium (Nb) is the current standard for superconducting radio frequency (SRF) accelerator cavities due to its ultra-low surface resistance (R_s) and high cavity quality factor (Q) at operating temperatures of ~ 2 K. It is known that SRF cavity surface composition and contaminant incorporation is directly related to Q , and much work has been done to understand factors influencing SRF cavity performance for the clean and oxidized Nb surface. Hydrogen incorporation, which results in the formation of Nb hydrides, has been identified as a major source of decreased Q . There is not, however, a fundamental understanding of the growth mechanism for Nb hydrides. In this work, we have investigated the atomic-scale growth mechanism of Nb hydrides on oxidized Nb(100) under ultra-high vacuum (UHV) conditions using temperature programmed desorption (TPD), low-temperature scanning tunneling spectroscopy (LT-STM), and scanning tunneling spectroscopy (STS). The incorporation of relevant concentrations of hydrogen into the Nb(100) crystal was confirmed using TPD, LT-STM experiments revealed novel, real space information regarding the atomic-scale growth mechanism of Nb hydrides, and STS was used to elucidate the relationship between Nb hydride formation and the surface density of states.

11:00am **SS+2D+HC-TuM10 Water induced restructuring of Vanadium oxide clusters.** Kræn Christoffer Adamsen, J.V. Lauritsen, S. Chiriki, B. Hammer, Aarhus University, Denmark

Fundamental knowledge of catalytic processes for NO_x removal (Selective Catalytic reaction, SCR) is important for improving existing catalysts and developing new. In the SCR cycle, NO_x is known to react from gas-phase on adsorbed ammonia on a VO_x/TiO₂ based catalysts. It is well established that vanadium in the V⁵⁺-state is most catalytic active state, though is still debated whether it is a hydroxylated- or an unhydroxylated- species that is most active species. Here we investigate the structure of vanadium oxide (V₂O₅) before, under and after exposure of water.

By evaporation of Vanadium in an oxygen-rich atmosphere (10⁻⁶ mBar) on an anatase-TiO₂ (101) substrate, we can create well-dispersed single V₂O₅-clusters. Confirm the oxidation state of vanadium with X-ray Photoelectron Spectroscopy (XPS) and image the size and structure with high resolution Scanning Tunneling Microscopy (STM). Prior to water exposure V₂O₅ -

clusters appear predominately as elongated features extending across two bridging oxygen rows of the anatase-TiO₂ (101) substrate. Utilizing the high scanning speed of the Aarhus STM we can follow the water induced restructuring of the clusters in situ. We observe a clear change in appearance of the vanadium oxide cluster, where a vanadium atom moves across one of the bridging oxygen rows of the anatase-TiO₂ substrate. Removal of water causes another change in appearance, but re-exposure of water the previous appearance is restored. We therefore observe a reversible reaction with exposure and removal of water, however with several hours of pumping we cannot return to the initial state directly after evaporation.

Together with Theoreticians, we are able to suggest structure models of the interactions between the vanadium oxide and water. We are able to explain both the irreversible restructuring in the first water exposure and the reversible restructuring with re-exposure of water. Understanding the structure and its dynamical behavior under water exposure brings us closer to understanding the catalyst under working conditions.

11:20am **SS+2D+HC-TuM11 Hydrogenation of Titanium Dioxide with Low-energy Hydrogen Ions and Atomic Hydrogen**, *N. Nagatsuka, Y. Ohashi*, Institute of Industrial Science, The University of Tokyo, Japan; *M. Fujimoto, M. Matsumoto*, Tokyo Gakugei University, Japan; *Katsuyuki Fukutani*, Institute of Industrial Science, The University of Tokyo, Japan

Interaction of hydrogen with TiO₂ surfaces is of interest and importance in view of photocatalytic H₂ generation and hydrogen sensors. Furthermore, hydrogenated TiO₂ has recently acquired much attention due to its excellent photocatalytic activity [1]. In our previous study, we have investigated the interaction of hydrogen with the rutile TiO₂(110) surface with nuclear reaction analysis (NRA) and ultraviolet photoemission (UPS) [2]. Whereas the former allows us to quantify hydrogen in the sample in a depth-resolved manner [3], the latter provides us with the information on the electronic states. In the present study, we have studied interaction of low-energy hydrogen ions with TiO₂ single-crystal surfaces, where the hydrogen ion penetrates the surface being distributed in the near-surface region [4]. We also report atomic hydrogen interaction with TiO₂ nanoparticles in relation with hydrogenation of TiO₂.

When the rutile TiO₂(110) and anatase TiO₂(101) surfaces are exposed to atomic hydrogen, NRA shows adsorption of hydrogen on the surfaces with a coverage of about 0.5 monolayer [2]. When the rutile TiO₂(110) surface is exposed to a hydrogen ion beam at 500 eV, on the other hand, NRA reveals a maximum at a depth of about 1 nm extending to ~30 nm with an average concentration of 5.6 at. % and UPS shows an in-gap state (IGS) at ~0.8 eV below the Fermi level with a downward band-bending by 0.5 eV. The IGS intensity is about ten times as large as that of the H-adsorbed surface. Upon annealing at 673 K, the IGS intensity is reduced by about 40 % and H with a coverage of 1.4 monolayer remains in the near-surface region, which suggests stable H occupation of subsurface sites. When the H-ion-irradiated surface is exposed to oxygen molecules, on the other hand, the hydrogen distribution remains unchanged although the IGS intensity is substantially reduced. The effect of hydrogen in the near-surface region on the surface electronic state is discussed.

[1] Z. Wang et al., *Adv. Func. Mater.* 23, 5444 (2013).

[2] K. Fukada et al., *J. Phys. Soc. Jpn.* 84, 064716 (2015); N. Nagatsuka et al., in preparation.

[3] M. Wilde, K. Fukutani, *Surf. Sci. Rep.* 69, 196 (2014).

[4] Y. Ohashi et al., *J. Phys. Chem. C* in press.

11:40am **SS+2D+HC-TuM12 Direct Observation of Atomic Exchange during Surface Self-diffusion**, *Matthew Koppa, P.R. Schwoebel, D.H. Dunlap*, University of New Mexico

The growth of crystals from the vapor phase is widely used in many technological applications, ranging from the microfabrication of microprocessors to the development of biological sensors. The dynamics of processes such as the surface diffusion of adatoms are key phenomena governing mass transport and the resulting crystal growth. Atomic exchange with substrate atoms during surface self-diffusion has been inferred from previous field ion microscope (FIM)-based experiments by mapping adatom visitation sites. Here iridium enriched to >93% ¹⁹¹Ir was deposited onto an atomically clean and smooth *Ir(100)* plane as observed in an atom-probe field ion microscope. Following thermally activated surface self-diffusion the adatom was field desorbed and mass analyzed. Observation of the ¹⁹³Ir isotope in one-half of the cases demonstrates conclusively that atomic exchange can occur during surface self-diffusion.

Atomic Scale Processing Focus Topic

Room B130 - Session AP+EL+MS+PS+SS+TF-TuA

Advancing Metrology and Characterization to enable Atomic Layer Processing

Moderators: Eric A. Joseph, IBM T.J. Watson Research Center, Jessica Kachian, Intel Corporation

2:20pm **AP+EL+MS+PS+SS+TF-TuA1 In Situ Ellipsometry Characterization Of Atomic Layer Processes: A Review, James Hilfiker, G.K. Pribil, J. VanDerslice, J.A. Woollam Co., Inc.** **INVITED**

Atomic layer processes such as atomic layer deposition (ALD) and atomic layer etch (ALE) provide monolayer-level thin film deposition or etch. Spectroscopic ellipsometry (SE) is ideally suited for the characterization requirements of such very thin layers. In situ SE provides real-time feedback, which is invaluable for establishing new atomic layer processes. In situ SE characterization has been adopted by many researchers due to its versatility. SE measurements are sensitive to deposition or etch at the (sub)monolayer level. The real-time evolution of film thickness provides details on nucleation periods or delays, the growth or etch rates per cycle, and verifies the self-limiting nature of a process. Multiple experiments can be performed within a single run by modifying the process conditions, allowing quick qualification of deposition temperatures, chemical exposure times, plasma influences, and purge times. In this paper, we will review the areas where in situ SE has been applied to both atomic layer deposition and etch.

We will also discuss the applications of in situ SE that benefit from a broad wavelength range. SE is best known for determining film thickness and optical constants. This characterization can be accomplished for many types of materials – dielectrics, semiconductors, organics, and even metals – provided the layer remains semi-transparent. Other material properties affect the optical constants and can be determined via this relationship. In situ SE has been used to estimate the crystal structure, composition, and even conductivity of thin films. We will discuss the advantages and limitations of in situ SE, which in many ways has proven to be an ideal partner for atomic layer processes.

3:00pm **AP+EL+MS+PS+SS+TF-TuA3 Elucidating the Mechanisms for Atomic Layer Growth through In Situ Studies, Jeffrey Elam, Argonne National Laboratory** **INVITED**

Atomic Layer Deposition (ALD) provides exquisite control over film thickness and composition and yields excellent conformality over large areas and within nanostructures. These desirable attributes derive from self-limiting surface chemistry, and can disappear if the self-limitation is removed. Understanding the surface chemical reactions, i.e. the ALD mechanism, can provide insight into the limits of self-limitation allowing better control, successful scale up, and the invention of new processes. In situ measurements are very effective for elucidating ALD growth mechanisms. In this presentation, I will describe our recent investigations into the growth mechanisms of ALD nanocomposite films comprised of conducting (e.g. W, Mo and Re) and insulating (e.g. Al₂O₃, ZrO₂ and TiO₂) components using in situ measurements. These ALD nanocomposites have applications in particle detection, energy storage, and solar power. We have performed extensive in situ studies using quartz crystal microbalance (QCM), quadrupole mass spectrometry (QMS), Fourier transform infrared (FTIR) absorption spectroscopy, and current-voltage measurements. These measurements reveal unusual ALD chemistry occurring upon transitioning between the ALD processes for the two components. This results in unique reaction products that affect the properties of the films in beneficial ways. The knowledge gained from our in situ studies of the ALD nanocomposite films has helped us to solve problems encountered when we scaled up the ALD processes to large area substrates.

4:20pm **AP+EL+MS+PS+SS+TF-TuA7 Surface, Interface, or Film: A Discussion of the Metrology of ALD Materials in Semiconductor Applications, G. Andrew Antonelli, N. Keller, Nanometrics** **INVITED**

Atomic layer deposition, etching, and interface engineering are enabling technologies for semiconductor manufacturing. These processes have led to an explosion in the use of laboratory techniques such as transmission electron microscopy and the need to bring such instruments closer to or into the fab itself. However, there remains a need for in-line, non-destructive, non-contact metrology capable of quickly characterizing and monitoring these extremely thin films on test structures, on product, or in

device as these data are the only meaningful method for monitoring of ultimate device performance. Indeed, in cases such as the use of selective deposition or etching, no test vehicle other than the ultimate product may be relevant. A variety of measurement techniques with a focus on x-ray and optical probes as applied to this class of problems will be reviewed. Examples will be provided on relevant logic such as the Gat-All-Around FET and memory devices such as 3D NAND.

5:00pm **AP+EL+MS+PS+SS+TF-TuA9 In Line and Ex Situ Metrology and Characterization to Enable Area Selective Deposition, Christophe Vallee, M. Bonvalot, B. Pelissier, J-H. Tartai, S. David, S. belahcen, V. Pesce, M. Jaffal, A. Bsiesy, LTM, Univ. Grenoble Alpes, CEA-LETI, France; R. Gassilloud, N. Posseme, CEA-LETI, France; T. Grehl, P. Bruner, IONTOF GmbH, Germany; A. Uedono, University of Tsukuba, Japan**

Innovation in materials, architectures (3D), gap filling technologies, lithography and etch processes are mandatory at every node of CMOS or memory devices. These challenging integration issues can be facilitated by the use of an integration scheme currently being intensively investigated known as area selective deposition (ASD). Criteria for an adequate area selective deposition process are: growth only on specific regions, high throughput compatible with industrial demands, no so-called mushroom profiles into adjacent features as well as no nuclei defectivity on undesired sites. Several routes can be developed to achieve an ASD process with ALD. The one discussed here concerns the deposition/etch approach which takes benefit from an *in situ* etching step inserted in a standard ALD cycle [1]. By incorporation of anisotropic or isotropic etching steps in the ALD process, “surface” selective deposition, as well as topographically selective deposition (TSD) have been obtained [2, 3]. The major current shortcoming of this approach lies in the deep insight which is required regarding elementary atomic-scale reaction mechanisms. Indeed, in the case of an ALD/ALE Area Selective Deposition process, a highly precise control of etching and its selectivity at the atomic scale is needed. Controlling the nature and density of defects induced by etching or passivation steps and understanding their impact on the physical and electrical properties of selectively deposited films are of course also required. Moreover, in order to optimize these processes, an accurate understanding of the underlying reasons why passivation after a low number of ALD cycles, is no more effective. Thus, *in situ* as well as *ex situ* monitoring and metrology are mandatory.

In this presentation, we will discuss how to optimize and understand atomic-scale reaction mechanisms in an ALD/ALE ASD process using combined *in situ* or *ex situ* measurements, such as ellipsometry, XPS, XRR, LEIS, FIB-STEM, and positron annihilation. We will show that when crosslinked, these technics are very effective to perform atomic scale metrology and characterization. As an example, we will discuss F atom localization and density in selectively deposited oxides thanks to a F-based ALE chemistry incorporated in the ALD process. In the case of a topographically selective deposition (TSD) process attempts will be presented to understand ion/surface interactions when low energetic ions are extracted from the plasma of the PEALD reactor both during deposition and plasma-ALE steps.

[1] R. Vallat et al, JVSTA **35** (2017) 01B104

[2] R. Vallat et al, JVSTA **37** (2019) 020918

[3] A. Chacker et al, APL **114** (2019)

5:20pm **AP+EL+MS+PS+SS+TF-TuA10 Recent Progress in Thin Film Conformality Analysis with Microscopic Lateral High-aspect-ratio Test Structures, Riikka Puurunen, Aalto University, Finland** **INVITED**

Conformal thin films which cover complex 3D shapes with a film of uniform properties (thickness, composition, etc.) are increasingly demanded applications such as semiconductor devices, microelectromechanical systems, energy conversion/storage and catalysis. Atomic layer deposition (ALD) and its counterpart atomic layer etching (ALE) [together known as atomic layer processing (ALP)], are increasing in usage largely thanks to their known conformal character.

A question that needs to be asked in the R&D of 3D applications using conformal ALD/ALE processes is: how conformal is conformal; is the conformality sufficient to meet the specs? In semicon industry, vertical vias and cross-sectional transmission electron microscopy (TEM) are standardly used for conformality analysis. Recently, microscopic lateral high-aspect-ratio (LHAR) test structures have been developed to improve the conformality analytics capabilities. LHAR structures e.g. enable detailed conformality analysis at arbitrarily high aspect ratios (e.g., >5000:1), where no film can coat the 3D structure fully, thereby exposing the saturation

Tuesday Afternoon, October 22, 2019

profile characteristic for the process. This, in turn enables the kinetic analysis of the process and e.g. extraction of the sticking coefficients related to the growth reactions.

This invited talk will address recent progress related to the fabrication and the use of microscopic LHAR conformality test structures. After the breakthrough with the first prototypes (PillarHall LHAR1; Gao et al. 2015, Mattinen et al. 2016; reviewed in Cremers et al., 2019), third and fourth generation prototypes have been developed (PillarHall LHAR3 and LHAR4). This work will review the conformality analysis progress enabled by the microscopic LHAR structures and discuss the benefits and challenges of this approach. Recent published progress includes the conformality modelling by Ylilammi et al. (2018) and experimental extraction of sticking coefficient by Arts et al. (2019). In addition, several other ongoing conformality analysis cases will be presented.

References

Arts, Vandalon, Puurunen, Utriainen, Gao, Kessels, Knoops, J. Vac. Sci. Technol. A 37, 030908 (2019); <https://doi.org/10.1116/1.5093620>

Cremers, Puurunen, Dendooven, Appl. Phys. Rev. 6, 021302 (2019); <https://doi.org/10.1063/1.5060967>

Gao, Arpiainen, Puurunen, J. Vac. Sci. Technol. A 33, 010601 (2015); <https://doi.org/10.1116/1.4903941>

Mattinen, Hämäläinen, Gao, Jalkanen, Mizohata, Räisänen, Puurunen, Ritala, Leskelä, Langmuir, 32, 10559 (2016); <http://doi.org/10.1021/acs.langmuir.6b03007>

Ylilammi, Ylivaara, Puurunen, J. Appl. Phys. 123, 205301 (2018); <https://doi.org/10.1063/1.5028178>

6:00pm **AP+EL+MS+PS+SS+TF-TuA12 In operando XPS Study on Atomic Layer Etching of Fe and Co Using Cl₂ and Acetylacetone or Hexafluoroacetylacetone, Zijian Wang, O. Melton, D. Angel, B. Yuan, R.L. Opila**, University of Delaware

Etching of transition metals is one of the major challenges in magnetoresistive random-access memory (MRAM) device fabrication. In this work, atomic layer etching of iron and cobalt surfaces with halogen and an organic molecule was studied. We successfully performed etching of Fe and Co thin films via forming volatile metal complexes at low temperature with cyclic sequential reactions of Cl₂ and acetylacetone (acac) or hexafluoroacetylacetone (hfac). The etching reaction mechanism of acac and hfac reacting with Chlorine-modified Fe and Co surfaces was investigated: the surface was first activated with Cl₂ gas, and subsequently, the top layer of chlorinated metal was removed by reaction with a diketone (acac/hfac). The extent of Cl₂ reaction determines the etching rate of the metal. At substrate temperatures lower than 135°C, acac could remove the chlorinated Fe metal layer from Fe surfaces, but not chlorinated Co from Co surfaces. *In-operando* x-ray photoelectron spectroscopy (XPS) and density functional theory (DFT) simulation shows that the reaction of acac or hfac with Chlorinated Fe or Co surfaces is likely following a complex reaction pathway instead of simple diketone substitution for the metal chloride. Diketone decomposition may play an important role in the etching process.

Complex Oxides: Fundamental Properties and Applications Focus Topic

Room A220-221 - Session OX+EM+HC+MI+NS+SS+TF-TuA

Complex Oxides: Catalysis, Dielectric Properties and Memory Applications

Moderators: Alexander Demkov, University of Texas at Austin, Jeffrey Kelber, University of North Texas

2:20pm **OX+EM+HC+MI+NS+SS+TF-TuA1 Novel Multiferroic and Ferroelectric Ferrite Thin Films, Peter A. Dowben, C. Binek, X. Xu**, University of Nebraska-Lincoln **INVITED**

Ferroelectricity and ferromagnetism are foundational to numerous technologies, yet the combination of ferroelectricity and ferromagnetism, namely multiferroicity, may be even more desirable. Multiferroic materials are believed to be a route to voltage controlled spintronic devices. Yet very few single phase materials are known to be ferroelectric and ferromagnetic at the same time, i.e. multiferroic. Even fewer materials are fewer materials are magneto-electric, that is to say materials with magneto-electric coupling, i.e. voltage control of magnetization, but without separate order parameters for magnetism (or antiferromagnetism) and ferroelectricity. This talk will review the electronic structure of the tri-rutile

magneto-electric antiferromagnets, like Fe₂TeO₆, as well as rare earth ferrites like ReFeO₃ (Re = rare earth) stabilized in the hexagonal phase. Both types of materials are frequently antiferromagnetic, and, in principle, both can exhibit magneto-electric coupling. The surface termination affects the measured spin polarization of the surface and the interface with other materials. This will have a significant influence on the voltage control of magnetization. We have investigated the structural and electronic properties at the surface of these more unusual multiferroic materials using angle-resolved x-ray photoemission spectroscopy (ARXPS), complemented by x-ray diffraction (XRD), x-ray photoemission electron microscopy (X-PEEM), and X-ray circular dichroism. We find that the low local symmetry, especially at surfaces, will split the electronic states, via spin-orbit coupling. In some cases, the result is a net spin polarization at the surface, under electric field cooling. Because of the strongly preferential surface termination of these types of materials, the boundary polarization is roughness insensitive, in some cases making spintronic device applications plausible.

3:00pm **OX+EM+HC+MI+NS+SS+TF-TuA3 Potential Applications and Challenges for Complex Oxides in Advanced Memory and Computing Applications, Sebastian Engelmann, T. Ando, V. Narayanan, IBM T.J. Watson Research Center** **INVITED**

As the semiconductor industry continues to push for and develop higher performance computing systems, there is also a growing trend of redeveloping or optimizing fundamental computing approaches to be more energy efficient. The development of hardware for novel AI systems is no exception. New integration schemes, novel materials, multi-component materials or even nanoscale materials and the ability to integrate all of these approaches together becomes the compounded challenge. Deposition and etch technologies that offer differentiating solutions to these issues therefore need to meet somewhat conflicting demands, such as low damage processing as well as high rate processing beside many other issues.

Novel thin films, thin film laminates and alloys promising unprecedented performance are very interesting candidates to enable such computing paradigm shifts. In particular the class of complex oxides is a very interesting area of research as they offer new phenomena such as ferroelectricity, ferromagnetism or high temperature conductivity. While new phenomena are being discovered, unraveling the fundamental physics behind these properties is a critical element for an industrial exploitation of these properties.

In addition, these new and complex materials are growing the need for the ultimate process solution: atomic layer precision processing. Atomic layer etching is a promising path to answer the processing demands of new devices at the Angstrom scale. Self-limiting reactions, discrete reaction and activation steps or extremely low ion energy plasmas are some of the pathways being pursued for precise material removal control and maintaining the original film performance. Depending on the nature of the material, the etch response may be either too much or not enough chemical modifications of the material. Resulting modifications of the films is an important variable to consider in the readiness of material systems. In particular synergy to deposition approaches such as atomic layer deposition has been proposed as a solution, but more work is needed.

4:20pm **OX+EM+HC+MI+NS+SS+TF-TuA7 Epitaxial Design of Complex Oxides for Catalysis and Electrocatalysis, Yingge Du**, Pacific Northwest National Laboratory **INVITED**

Predictive synthesis of highly active and cost-effective catalysts and electrocatalysts for energy conversion and storage is critical for leveraging intermittently available energy sources. Transition metal oxides with perovskite (ABO₃) and perovskite-related structures (e.g., Brownmillerite and Ruddlesden-Popper) have been identified as robust catalysts with high oxygen reduction reaction (ORR) and/or oxygen evolution reaction (OER) activities that rival the performance of noble metals and their compounds. The study of perovskites as epitaxial thin films enables measurement of their intrinsic catalytic activity, deconvolved from the effects of surface roughness and polycrystalline defects (e.g., grain boundaries and edges between facets). In addition, epitaxial growth facilitates accurate control over the composition, crystallographic orientation, and strain in thin films.

In this talk, our recent efforts in the design of epitaxial complex oxides for catalysis and electrocatalysis will be highlighted. Using LaNiO₃, a bi-functional electrocatalyst, as an example, I will show how isovalent substitution, aliovalent substitution, and interfacial strain can be used to tune the structural, electronic, and optical properties of the resultant films, and how these observed changes correlate with their (electro)catalytic

Tuesday Afternoon, October 22, 2019

performance. The use of complex oxide thin films as support or anti-corrosion layers during catalytic reactions will also be discussed.

5:20pm **OX+EM+HC+MI+NS+SS+TF-TuA10 Vanadia/Tungsten Oxide on Anatase TiO₂(101): a Model Catalyst Study by STM and XPS**, *Tao Xu, J.V. Lauritsen, K.C. Adamsen*, Aarhus University, Denmark; *S. Wendt*, iNANO, Aarhus University, Denmark

Nitrogen oxides (NO_x) from flue gas are in concern as major sources of air pollution. Increasingly stricter NO_x emission control policies (e.g. Euro VI) demand innovation and better performance of NO_x reduction technology. The Selective Catalytic Reduction (SCR) of NO_x by vanadia supported on anatase titania, with tungsten oxide (WO₃) as promoter, has been widely used for this service and attracted much research attention. However, many aspects of the SCR catalysis process remain poorly understood at the atomic level. Particularly, the synergistic effect of tungsten oxide and vanadia remain elusive in literature, despite intensive RAMAN and infrared spectroscopy studies.

In this work, we use mineral α -TiO₂ single crystals exposing the (101) facets as the model surface and deposit V₂O₅ and WO₃ in our ultrahigh vacuum chamber (UHV) chamber by e-beam evaporation in oxygen. Combining Scanning Tunneling Microscope (STM) and X-ray photon-electron Spectroscopy (XPS), we systematically investigated the morphology and oxidation state changes of the model catalyst upon heating and reactant adsorption.

The STM results illustrate the distribution of V₂O₅ and WO₃ on anatase TiO₂(101) at the atomic level. It is found that both species are highly dispersed in the sub-monolayer region. For the deposition of surface oxide species, we explored different methods to achieve the highest oxidation state of vanadium (5+) and tungsten (6+). The thermal stability of the as-deposited V₂O₅ and WO₃ are investigated by XPS and STM systematically. We found that when V₂O₅ and WO₃ co-exist on the α -TiO₂ surface the stability of V₂O₅ is improved. This work provides atomic level understanding on the V₂O₅/WO₃/TiO₂ SCR catalyst and new insights into the synergistic interactions between vanadia and tungsten oxide on the α -TiO₂ surface.

5:40pm **OX+EM+HC+MI+NS+SS+TF-TuA11 Observation of Memory Effect and Fractal Surface in SrRuO₃ Epitaxial Thin Films**, *Ratnakar Palai*, University of Puerto Rico; *H. Huhtinen*, University of Turku, Finland

Integration of multifunctional oxide materials (ferroelectrics and multiferroics) into silicon technology is of great technological and scientific interests. The current interest in functional oxides is largely based on engineered epitaxial thin films because of their superior properties compared to the bulk and polycrystalline thin films and their technological applications in dynamic random access memories, magnetic recording, spintronics, and sensors. Most of these applications require bottom and top electrodes to exploit the electronic properties of the functional materials.

SrRuO₃ (SRO) has been found to be very useful for electrodes and junctions in microelectronic devices because of its good electrical and thermal conductivities, better surface stability, and high resistance to chemical corrosion, which could minimize interface electrochemical reactions, charge injection in oxide, and other detrimental processes, thus improving retention, fatigue resistance, and imprint. It also has good work function to produce the required large Schottky barrier on most ferroelectric oxide capacitors.

The bulk SRO exhibits several useful properties, such as extraordinary Hall effect, strong magnetocrystalline anisotropy, itinerant ferromagnetism, and spin-glass behavior. Spin-glass materials are currently frontier field of research and the most complex kind of condensed state of matter encountered so far in solid-state physics. Despite of the enormous importance of spin-glass models in neural networks, our knowledge of the underlying mechanistic processes involved is extremely limited. Although memory effect has been reported in bulk SRO, to our knowledge, the behavior is not well understood and there was no such report in thin films.

In this work, we report on the observation of memory effect and strong magnetic anisotropy in extremely smooth 1–3 Å roughness epitaxial (110) and (010) SrRuO₃ thin films. The observation of non-zero imaginary susceptibility and frequency dependent cusp at freezing temperatures confirms the spin-glass behavior, which agrees well with the dc magnetization measurement. The origin of memory effect can be attributed to the magnetic frustration and random interaction, which is affected by dynamics of cooling and will be discussed in details.

6:00pm **OX+EM+HC+MI+NS+SS+TF-TuA12 In situ Auger Electron Spectroscopy of Complex Oxide Thin Film Surfaces Grown by Pulsed Laser Deposition**, *Thomas Orvis, M. Surendran, Y. Liu, A. Cunniff, J. Ravichandran*, University of Southern California

Complex oxides can enhance the functionality of electronic and photonic devices by supplementing them with interesting properties such as ferroelectricity, superconductivity, and magnetoresistivity. Furthermore, low dimensionality in these materials can result in additional useful properties, inspiring the continued study of complex oxides in thin film form. However, the deposition of these materials is typically governed by notoriously complex growth mechanisms, revealing the need for *in situ* probes to observe and understand their precise nature. To this end, we report the *in situ* observation of chemical composition of complex oxide thin film surfaces with Auger electron microscopy during growth by pulsed laser deposition. Our implementation of real-time monitoring techniques for complex oxide thin films sheds an important light on the intricacies of the relationships between processing conditions and resulting composition.

Energy Transition Focus Topic

Room A226 - Session TL+AS+SS+TF-TuA

Breakthroughs and Challenges in Applied Materials for Energy Transition (ALL INVITED SESSION) & Panel Discussion

Moderators: Jason Avila, U.S. Naval Research Laboratory, Devika Choudhury, Argonne National Laboratory

2:20pm **TL+AS+SS+TF-TuA1 Interface Science and Engineering for Energy-Water Systems**, *Seth Darling*, Argonne National Laboratory **INVITED**

Driven by climate change, population growth, development, urbanization, and other factors, water crises represent the greatest global risk in the coming decades. Advances in materials represent a powerful tool to address many of these challenges. Understanding—and ultimately controlling—interfaces between materials and water are pivotal [1]. In this presentation, we will lay out the challenges and present several examples based on materials science strategies for addressing applications in water. In each instance, manipulation of interfacial properties provides novel functionality, ranging from selective transport to energy transduction to pollution mitigation.

[1] J. Appl. Phys. 124 (2018) 030901

3:00pm **TL+AS+SS+TF-TuA3 Atomic Dynamics of Noble Metal Surface in Gases Revealed by Time Resolved Environmental Transmission Electron Microscopy**, *Seiji Takeda, N. Kamiuchi, R. Aso, H. Yoshida, T. Tamaoka*, Osaka University, Japan **INVITED**

The surface of noble metals in gas has been extensively studied in the field of surface science. The surface has been investigated in both ultra high vacuum and various gases of high pressure and under various stimuli, for instance the illumination of intense light, the electric and/or magnetic field and the irradiation of charged particles. A microscopy study is potentially useful to provide us with the imaging data on the surface in real space and time at the resolution that is available in a microscopy apparatus to use. Among various methodologies for microscopy, atomic resolution environmental transmission electron microscopy has advanced greatly in the time resolution recently, allowing us to explore the dynamic surface and to elucidate the mechanism of the dynamic phenomena that are related to various energy transition processes. We show recent our studies, including the self-activated surface dynamics of gold catalysts in reaction environments [1] and the unexpected gas (nitrogen) -solid (palladium) transition [2] that is occurring on the surface under a strong electrostatic field. We demonstrate that the surface dynamics that is associated with the energy transition processes needs to be visualized at atomic scale for understanding the electronic excitations behind the surface dynamics.

References

[1] N. Kamiuchi et al., Nat. Commun. **9** (2018) 2060.

[2] T. Tamaoka, R. Aso et al., Nanoscale (2019) .

Tuesday Afternoon, October 22, 2019

4:20pm **TL+AS+SS+TF-TuA7 Totally Organic and Organic-Inorganic Hybrid Batteries**, **Burak Esat**¹, Fatih University, Turkey, Rutgers University; *S. Bahceci*, *S. Akay*, Fatih University, Turkey; *A. Momchilov*, Bulgarian Academy of Science, Bulgaria

We hereby represent novel polymers and reduced graphene oxide with pendant electro-active groups such as TEMPO and quinones.

The first example of polymers with pendant anode-active groups studied in our group is a polymethacrylate derivative carrying anthraquinone moieties (pMANtrq). This anthraquinone based anode-active material has proven to show a quite good reversible electrochemical reduction behavior in both aqueous and non-aqueous electrolytes in our studies. pMANtrq|1M LiClO₄ in EC:DEC=1:1|Li battery system has been constructed. The initial discharge capacity of the cell obtained was 151 mAh/g when cycled between 4.2 and 1.2V at 0.25C rate and 79.2 mAh/g when cycled between 4.0 and 1.5V at 0.3C rate during subsequent cycles.

This material was also used in an aqueous battery, pMANtrq |5M KOH aq. |LiMn₂O₄. Although an initial discharge capacity of 37.7 mAh/g was obtained, it deteriorated quickly due to the solubility of the reduced form of the polymer in this electrolyte system. This is the first reported example of such organic-inorganic hybrid battery.

An anode material based on reduced graphene oxide (RGO) functionalized with anthraquinone is also investigated and a battery against Li metal revealed a quite reversible capacity of 200 mAh/g based on the weight of electro-active anthraquinone moieties when cycled between 3.2 and 1.8 V at 0.3C rate. The energy density was found to be around 450 mWh/g.

We have also synthesized and characterized polyacetylene polymers with pendant TEMPO radicals which are electrochemically oxidizable in a reversible manner at around 3.5-3.6V vs. Li. These materials have been proven to be cathode-active materials for rechargeable batteries. We have demonstrated that a mixture of Tempo radical polymer with LiMn₂O₄ (1:1) can be used as a hybrid cathode material. Typically, this polymer may be expected to act as a polymeric electro-active binder and a stability improver for the inorganic cathode-active material.

Studies toward construction of all organic batteries using these anode and cathode materials are currently in progress.

4:40pm **TL+AS+SS+TF-TuA8 Electrochemical Strategies for Designing Interfaces of Battery Materials**, **Betar Gallant**, Massachusetts Institute of Technology

INVITED

Future generations of energy-storage devices require advances beyond state-of-the-art materials and redox systems. Rechargeable batteries, specifically today's Li-ion batteries, have largely been dominated by transition metal oxide cathodes; advanced conversion systems with higher theoretical energy densities, such as Li-S and Li-O₂, have received significant attention as "beyond Li-ion" batteries, but have their own challenges and limitations. Looking at the periodic table invites one to wonder, "Is there more beyond sulfur and O₂?" This talk will focus on challenges and opportunities related to a different chemical family: fluorine, or more specifically, active fluoride. Fluoride-containing additives, electrolytes, solid electrolyte interphases (SEI), and intercalation materials represent a recurring motif in many proposed next-generation battery chemistries, but current understanding of the behavior of fluorinated interfaces and materials remains largely phenomenological. In addition, controlling the incorporation of fluoride into materials still remains a major challenge owing to safety issues of fluorine and the intransigence of fluoride-containing precursors, hindering design in this space.

In this talk, I describe our group's exploration of several applications where fluoride-forming reactions can be harnessed and tailored for benefit in advanced batteries. First, I describe our efforts to develop high-energy density redox systems based on the electrochemical reduction of fluorinated gases. We show that fundamental knowledge and the experimental framework developed in the field of Li-O₂ batteries in recent years can be successfully translated to the development of new gas-to-solid conversion reactions with high energy densities. Next, I will discuss the opportunities presented by the ability to generate fluoride *in situ* in working batteries from these reactions, creating new possibilities to fluorinate interfaces in tailorable and precise ways. I will present our findings relevant to two examples where fluoride has been suggested to play a critical and enabling role: Li anode interfaces, and oxyfluoride-based intercalation cathodes. Using our gas-based fluoridation architecture, we explore the fundamental role that fluoride plays in each of these

applications. Finally, I will highlight future challenges and opportunities in the characterization of fluoridated materials.

¹ Scholar Rescue Fund Fellow

Tuesday Evening Poster Sessions, October 22, 2019

Surface Science Division

Room Union Station B - Session SS-TuP

Surface Science Poster Session

SS-TuP1 Mechanistic Studies of Thermal Dry Etching of Cobalt and Iron Thin Films, *Mahsa Konh, A.V. Teplyakov*, University of Delaware

Thermal dry etching of cobalt and iron thin films were investigated using diketones. Two diketones (1,1,1,5,5,5-hexafluoro-2,4-pentanedione (hfach) and 2,4-pentanedione (acach)) were used to show their reactivity toward cobalt and iron thin films with the results being relevant to etching of CoFe alloys. To understand the mechanism of etching process, possible surface reaction pathways were followed with temperature programmed desorption (TPD). Resulting surfaces were characterized using X-ray photoelectron spectroscopy (XPS) supplemented with microscopic investigations. Starting with oxidized or halogenated surfaces was found to be necessary to form volatile products that would make etching possible. However, halogenation makes the mechanism more complicated. It was shown that several products were desorbing from the halogenated metal surfaces containing M^{2+} and M^{3+} . These products may also contain both the organic ligands and halogens. The effect of dosing temperature on the etching process was also investigated.

SS-TuP2 Reaction of ZnO Nanomaterial with a Mixture of Gas-phase Prop-2-yneic acid and Acetic Acid to Control Surface Coverage of Reactive Functional Groups, *Dhamelyz Silva-Quinones, A.V. Teplyakov*, University of Delaware

Sensitization of oxide nanomaterials with a two-step process involving the reaction with gas-phase prop-2-yneic acid followed by "click" attachment of functionalized azides to the resulting alkyne functionality has been recently reported by our group. One advantage of the first modification step being a gas phase reaction with a nanomaterial is in the ability to control surface concentration of alkyne functionality by dosing predetermined mixtures of prop-2-yneic acid with another compound (in this case acetic acid) that reacts with the oxide surface in exactly the same way as prop-2-yneic acid but does not lead to the formation of a reactive functionality to be utilized in the second step of sensitization. This approach is demonstrated for the mixture of these acids reacting with ZnO nanomaterial, and the concentration of surface alkyne functional groups is determined by the concentration of the prop-2-yneic acid in the mixture with acetic acid. The resulting functionalized surface is interrogated by infrared spectroscopy to demonstrate that both acids co-adsorb on ZnO. Vibrational signatures of the CH_3 group at 1453 cm^{-1} and that of the alkyne group at 2110 cm^{-1} allow for quantification of the co-adsorbed species. This assessment is confirmed by the XPS investigation utilizing different ratios of the C 1s features corresponding to carboxylates compared to the methyl/alkyne carbon atoms in mixtures of prop-2-yneic and acetic acids. Solid state NMR spectroscopy is used to further confirm the formation and to quantify the concentration of two components in the mixed monolayer.

SS-TuP4 Barium Adsorption and De-wetting on W(112), *Michael Mroz*, Ohio University; *S.A. Tenney, C. Eads*, Brookhaven National Laboratory; *E. Kordesch*, Ohio University

The tungsten (112) surface has been observed with adsorbed barium in emission microscopy. The barium metal is deposited from a filament filled with a piece of metallic barium. When the barium layer on the W(112) surface is heated, the barium de-wets, forming a "wetting layer" and droplets of barium. The de-wetting is solid-solid de-wetting, because the rupture of the film into droplets occurs at about 1/3 of the barium melting temperature (727 C). At low coverage, about 20 nm barium, the droplets are sparse, and the wetting layer uses most of the available barium. Two 2x1 domains and weak centered 2x2 low energy electron diffraction (LEED) pattern are observed. At high coverage, about 200 nm, in addition to the wetting layer, and a dense coverage of droplets (250 nm diameter), there are also larger scale networks of barium drops spread over micron scale distances.

SS-TuP5 Self-Catalyzed Gas-Phase Cycloaddition on "Clickable" Nanostructured CuO Surface, *Chuan He, A.V. Teplyakov*, University of Delaware

The surface functionalization of nanostructured metal oxides (CuO, ZnO, TiO₂, CeO₂) has attracted substantial attention due to their extensive applications in sensing, photo-catalysis, electronics, and energy conversion. A number of studies have been reported to achieve the surface

sensitization of these metal oxides with organic or organometallic compounds in order to expand their versatile properties by introducing designated functionality. However, the most common approach to achieve this functionality utilizes sensitizer molecules reacting with oxide surfaces via carboxylic (COOH) or phosphonic (P(O)(OH)₂) anchor groups or by silylation (such as with R-Si(X)₃, where the X could be Cl or -OCH₃), which potentially leads to agglomeration, multilayer growth, or surface etching. Our recent research developed a two-step functionalization approach utilizing exposure of the oxide materials to prop-2-yneic acid (HC≡C-COOH, prop-2-yneic acid) in the gas phase as a first step, followed by second step of post-modification exploiting the created C≡C to introduce any pre-designed functionality to the surface via Cu(I)-catalyzed "click" chemistry with azides (R-N₃). More importantly, this approach requires no additional presence of the copper catalyst for nanostructured CuO due to the reduction of surface copper from prop-2-yneic acid modification. As a result, the second step of this functionalization can be achieved through self-catalyzed cycloaddition with gas-phase species. The morphology preservation and selective covalent attachment of the carboxylic acid onto the metal oxide surfaces have been confirmed by the combination of microscopic and spectroscopic investigations including scanning electron microscopy (SEM), X-ray photoelectron spectroscopy (XPS), and solid-state nuclear magnetic resonance spectroscopy (ss-NMR) that were used to follow the process and to compare with the traditional liquid-phase modification schemes. Vienna Ab Initio Simulation Package (VASP) calculations were used to explore the reaction mechanism and key intermediates.

SS-TuP6 XPS Study of the Gas Cluster Ion Beam Sputtering of PTFE and Oxygen-treated PTFE, *Bing Luo*, University of Minnesota

The XPS depth profiling results of polytetrafluoroethylene (PTFE) and oxygen-treated PTFE using monoatomic argon sputtering and gas cluster ion beam (GCIB) sputtering are reported. We evaluated the degrees of surface damage using these two sputtering methods. We found a mild surface damage under GCIB sputtering. On the non-sputtered PTFE surface, only CF₂ was present. After GCIB sputtering, CF₃ and CF groups were detected. Consistent with the results in the literature, monoatomic Ar sputtering induced a higher degree of damage; the CF₃ and CF levels were much higher than those obtained in the GCIB sputtering. The GCIB sputtering of the oxygen-treated PTFE samples revealed that the oxidation layer was mainly located in the top 10 nm. Below 10 nm, the oxygen content became insignificant. Analyzing the distribution of various carbon-fluorine species and comparing to the untreated samples indicated that in the layer from 10 to 60 nm, the PTFE composition or structure was altered by the oxygen treatment, and even at the depth of 120 nm, the property of the PTFE was affected by the oxygen treatment.

SS-TuP7 Ultra-high Resolution Imaging of Polymers using Atomic Force Microscopy: Structure and Property at Nanoscale, *V.V. Korolkov*, Oxford Instruments-Asylum Research; *A. Summerfield*, University of Manchester, UK; *A. Murphy, D. Amabilino*, University of Nottingham, UK; *P.H. Beton*, The University of Nottingham, UK; *M. Kocun, Roger Proksch*, Oxford Instruments-Asylum Research

Polymers, both synthetic and natural, are ubiquitous materials whose properties are strongly influenced by packing, conformation, and monomer composition of individual macromolecules. The ability to acquire real-space images of the microstructure of these materials with molecular-scale resolution is required to advance the understanding and control of their local ordering, a key element in the precise engineering of polymer properties. Real-space images of polymers with sub-molecular resolution could provide valuable insights into the relationship between morphology and functionality of polymers, but their acquisition is problematic due to perceived limitations in atomic force microscopy (AFM).

Here we show that individual polymer chains and sub-molecular resolution may be achieved using AFM under ambient conditions through the low-amplitude ($\leq 1\text{ nm}$) excitation of higher eigenmodes¹ of a cantilever on a range of commercial polymers (polythiophenes (PTs), polytetrafluoroethylene (PTFE), polyethylene(PE)). We have used this new approach to characterize both single strands of polymers adsorbed on surfaces as well as bulk semi-crystalline samples with Angstrom resolution. For example, on the surface of a spin-coated PT thin film, in which the thiophene groups are perpendicular to the interface, we resolve terminal CH₃-groups in a square arrangement with a lattice constant 5.5Å from which we can identify abrupt boundaries and also regions with more slowly varying disorder, which allow comparison with proposed models of PT domains. At the same time, bimodal tapping or AM-FM imaging² enables

Tuesday Evening Poster Sessions, October 22, 2019

modulus mapping on a wide range of polymer materials. Furthermore, molecular-level spatial resolution was achieved with AM-FM imaging on polymer chains in ambient conditions and revealed chain spacing and conformation predicted by theory and other experimental methods.

Our results highlight the important role for high-resolution AFM in determining the properties of polymer strands and thin films of technological relevance, and we anticipate future progress in correlating device performance with structural properties at the sub-molecular scale based on this technique.

¹Korolkov et al., Nat. Comm., 2019

²Kocun et al., ACS Nano, 2017

SS-TuP9 Determining the Surface Electrical Potential at the Air/Water Interface, *Tehseen Adel, S. Baumlner, H.C. Allen*, The Ohio State University

Several biological and chemical processes directly relate to the organization of molecules at the liquid surface. The surface electric potential across the air/liquid interface provides insight into the molecular organization and propagation of electrical fields by these surface molecules. Using a homemade Air Ionizing Surface Electrical Potential instrument, we measure the surface electrical potential of water, several pure solvents, and inorganic electrolyte solutions without disruption to the liquid surface. Alpha particle radiation from an ionizing source reduces the resistivity of the air gap above the liquid sample, establishing a closed electrical circuit for voltage measurements. From the measured surface potential, we show (i) the orientation of interfacial solvent molecules in pure solvents, and (ii) ascertain the propensity of specific aqueous ions with respect to the air/solution boundary.

SS-TuP10 Surface Photovoltage Studies of UV-driven Hydrophilic Flipping in Polysulfone Thin Films, *John Reeks, N. Posinski*, Texas Christian University; *T. Haun*, Home School High School Student; *H. Hilton*, Texas Christian University; *A. Dorward*, Washington and Lee University; *E. Bormashenko*, Ariel University, Israel; *Y.M. Strzhemechny*, Texas Christian University

It has been shown in previous studies that hydrophobic surfaces of polysulfone flip to become hydrophilic upon exposure to UV radiation. The exact mechanisms driving this phenomenon are not completely understood. We suggest that elucidation of the surface charge transport phenomena of the as-deposited and UV-irradiated polysulfone could explicate the conversion mechanism and thus contribute to the improved applications of polysulfone on the micro- and nanoscale for novel applications in microfluidics and biophysics. To investigate the UV-driven hydrophilic flipping we performed surface photovoltage (SPV) studies on thin polysulfone films spin-cast on silicon substrates. Since SPV is sensitive to buried interfaces, the resulting spectra are expected to be comprised of features originating not only from the polysulfone films, but also from the silicon wafer and the silicon oxide layer beneath the polymer films. Thereby, to identify the signal germane to polysulfone proper, we employed in our studies polysulfone films of varying and controllable thicknesses to be probed with SPV spectroscopy as well as SPV transient experiments. SPV measurements on Si substrates acted as a control for comparison. Our experiments revealed that SPV yield is significantly affected by the polysulfone films. In particular, we observed significant polarity reversal in the SPV transients in the samples with polysulfone films, whereas SPV spectra indicated transitions at 1.1-1.5 eV appearing in the polysulfone layers. We also report on the comparison of the SPV response in the as-deposited and UV-irradiated polysulfone samples.

SS-TuP11 Tuning Spontaneous Supramolecular Assembly via Manipulation of Intermolecular Forces and Growth Environment, *Ryan Brown*, Clarkson University

This poster will detail the initial experiments attempting to exploit non-equilibrium growth conditions to manipulate the spontaneous assembly of functionalized porphyrin molecules at the solid interface. Rapid evaporation of a solution can be considered a non-equilibrium growth environment, one in which a supersaturated thin film is produced and which can result in the formation of metastable supramolecular structures. Our research program seeks to manipulate the frequency and nature of the metastable structures produced in this process by varying the chemical functional groups on a porphyrin ring (and thus intermolecular interactions), the solid substrate (and thus molecule-substrate interactions), and the deposition conditions (varying the rpm and solvent during spin coating deposition). This research is achieved by imaging molecule-decorated surfaces with scanning tunneling microscopy to locally probe the supramolecular structures produced under a given deposition

condition. Structural models are then confirmed using electronic structure theory and then applied to understand how the combination of intermolecular forces, molecule-substrate interactions, and conditions in the evaporating solvent influence spontaneous assembly behavior.

SS-TuP12 State-Resolved Dissociative Chemisorption Dynamics with RAIRS Product Detection, *Laurin Joseph, S. Shepardson-Fungairino, A.L. Utz*, Tufts University

State-Resolved Dissociative Chemisorption Dynamics with RAIRS Product Detection

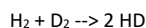
Laurin Joseph, Sally Shepardson-Fungairino, and Arthur Utz

State-resolved molecular beam molecular beam experiments use energy and quantum-state selected reactants to understand how specific molecular motions (molecular vibration, rotation, and translation) promote transition state access and chemical reactivity. They also generate experimental data that serve as rigorous benchmarks for DFT-based predictions of reaction barriers and dynamics.

We are currently updating one of our differentially pumped molecular beam reaction chambers to incorporate Reflection Absorption Infrared Spectroscopy (RAIRS) detection of surface-bound reaction products. This capability will allow for real-time, coverage-dependent studies of the reactions occurring on metal surfaces, will provide structural fingerprints of reaction products, and will open the door to the study of larger, more chemically complex, reactant molecules. This poster will survey our progress to date and present preliminary reactivity data for methanol dissociation on a Ru(0001) surface.

SS-TuP13 The Two-faced Role of Steps in the Isotopic Scrambling of Hydrogen on Pt, *Richard van Lent, L.B.F. Juurlink*, Leiden University, Netherlands

The simplest heterogeneously catalyzed reaction possible is isotopic scrambling of hydrogen:



On Pt, this reaction occurs by dissociative adsorption of H_2 and D_2 , mixing of H and D atoms on the surface, and recombination to form the three isotopologues, H_2 , D_2 , and HD. Full isotopic scrambling would lead to a product ratio of 1:1:2.

Step edges are well-known to enhance dissociative adsorption, especially at low impact energies. However, it is unknown whether subsequent diffusion and desorption only occur along the steps or involves diffusion onto terraces. We study this by combining supersonic molecular beam techniques with a curved Pt single crystal surface with straight A and B type step edges, c-Pt(111)[1-10]31⁰. At a high surface temperature, we probe HD formation, spatially resolved, along the curved surface by impinging a 50:50 mixture of low energy H_2 and D_2 . HD formation tracks the trend in dissociation: higher step densities yield higher HD formation. However, relatively, HD formation does not increase as rapidly as the dissociation probability. We explain why the (111) terraces are more selective toward HD formation and show that anisotropic diffusion affects isotopic scrambling.

SS-TuP14 It's Not just the Defects - How Terrace Symmetry Impacts H₂O Adsorption at Ag Step Edges, *S.V. Auras, Ludo Juurlink*, Leiden University, Netherlands

We investigate water desorption from hydrophobic surfaces using two curved Ag single crystals centered at (111) and (001) apices. On these types of crystals the step density gradually increases along the curvature, allowing us to probe large ranges of surface structures in between the (001), (111) and (110) planes. Subtle differences in desorption of submonolayer water coverages point toward structure dependencies in water cluster nucleation. The B-type step on hydrophobic Ag binds water structures more strongly than adjacent (111) planes, causing preferred nucleation at steps. This driving force for step-induced nucleation is smaller for A-type steps on (111) terraces. The A'-type step flanked by (001) terraces shows no indication of preferred adsorption to steps. Extrapolation to the (311) surface, not contained within either curved surface, demonstrates that both A- and A'-type steps can be regarded chemically identical for water desorption. The different trends in desorption temperature on the two crystals can thus be attributed to stronger water adsorption at (001) planes than at (111) planes and identical to adsorption at the step. These results show that our approach to studying the structure dependence of water desorption is sensitive to variations in desorption energy smaller than 'chemical accuracy', i.e. 1 kcal/mol.

Tuesday Evening Poster Sessions, October 22, 2019

SS-TuP15 Hydration Lubrication Between Hydrophobic and Hydrophilic Surfaces, Nir Kampf, I. Rosenhek-Goldian, W. Lin, J. Klein, Weizmann Institute of Science, Israel

How water rearrange above large stable, smooth, highly hydrophobic surface? We addressed this question by directly measure normal forces and sliding friction under aqueous environment between a negatively-charged hydrophilic mica surface and a fluoropolymer (AF) hydrophobic film, using a surface force balance. The roughness of the AF film was 0.3 nm determined under water by AFM. Normal-force vs. surface-separation profiles indicate that the hydrophobic surface is highly negatively-charge, in line with previous studies and attributed to adsorbed OH^- ions. Sliding of the compressed surfaces under water or salt solution reveals remarkably low friction (friction coefficient $\mu \approx 0.003 - 0.009$) up to applied pressures of at least 50 atm. Hydration lubrication by trapped hydrated counterions between the surfaces is well explained this efficient lubrication, exist in systems like artificial implants, contact lenses, etc. Moreover, molecules that are present in the biological systems were found to adsorb on the charged hydrophobic surface, contributing to reduced friction.

Reference:

Irit Rosenhek-Goldian*; Nir Kampf*; Jacob Klein (2018). Trapped Aqueous Films Lubricate Highly Hydrophobic Surfaces. *ACS Nano*. 12:(10)10075-10083.

*equally contributors

SS-TuP17 Common Errors in XPS Peak Fitting, George H. Major, Brigham Young University; C. Easton, CSIRO Manufacturing; W. Skinner, Future Industries Institute; D.R. Baer, Pacific Northwest National Laboratory; M.R. Linford, Brigham Young University

X-ray photoelectron spectroscopy (XPS) is the most popular method for chemically analyzing surfaces, being used in many areas of research and technology. XPS spectra have layers of information that can be extracted with proper analysis. Information ranges from a basic understanding of components (elements) present in a material to advanced peak fitting and background analysis that reveal chemical states and sample morphologies. There are many examples of good XPS peak fitting in the scientific literature. However, the process of peak fitting XPS spectra is still a mixture of art and science and in many cases have no absolutely correct fits. The peak fitting process can be affected by the instrument design and components, experimental settings, and the sample. Here, we discuss a series of common errors that regularly appear in XPS peak fitting in the literature and how to avoid them. These include: (i) not plotting the data according to the international convention with binding energy increasing to the left, (ii) presenting and interpreting data that are far too noisy to be interpretable, (iii) labeling noise as chemical components, (iv) not showing the original data -- only showing the synthetic (fit) peaks and their sum, (v) not showing any background in a fit, (vi) not providing the sum of the fit components, which makes it difficult for the future reader to determine the quality of a fit, (vii) having widely varying peak widths in a fit, e.g., using extremely broad and extremely narrow peaks when there is no chemical reason for doing so, (viii) having a baseline completely miss the noise/background on either side of the peak, (ix) not collecting data over a wide enough energy window to see a reasonable amount of baseline on both sides of the peak envelope, i.e., truncating the peak, (x) in a fit to a C 1s spectrum, reversing the labeling of the C-O and C=O fit components, and other mislabeling of the components in this envelope (fitting the C 1s peak envelope is well understood so these types of errors should not be made), (xi) for the most part, higher oxidation states of elements correlate with higher binding energies; unfortunately, fit components at higher binding energies are sometimes incorrectly labeled as coming from lower oxidation states, (xii) not taking spin-orbit splitting into account when it is necessary, and/or using inappropriate ratios for these pairs of peaks, and (xiii) in a comparison of related spectra, employing widely different peak widths and positions for components that are supposed to represent the same chemical state and/or using different background types or obviously different types of synthetic peaks in these spectra.

SS-TuP18 Exploring the Extent of Hydrogen/Deuterium Exchange on Au(111) between Molecularly-bound Surface Species, Hasan Kaleem, E. Maxwell, M. DePonte, J. Baker, M. Gillum, D.T. Boyle, A.E. Baber, James Madison University

The exchange between hydrogen and deuterium atoms in molecularly-bound surface species can occur at low temperatures on Au(111). The hypothesized mechanism for the hydrogen/deuterium exchange in ethanol-OD and water is by the Grotthuss mechanism facilitated by hydrogen-bonded molecular networks on Au(111). Therefore, the

molecular orientation and packing is central to this exchange. In an effort to rationalize the hypothesized mechanism and realize the extent of hydrogen/deuterium exchange at low temperatures, the co-adsorption of fully deuterated ethanol (EtOD_6) and water were investigated. The fragmentation pattern for EtOD_6 was first monitored using temperature programmed desorption (TPD), before increasing amounts of water were added to Au(111). A broad range of masses distinct to EtOD_6 were monitored using a mass spectrometer and desorption areas were quantified from TPD spectra. Comparing fractional coverages for hydrogen-exchanged EtOD_6 products suggest that hydrogen/deuterium exchange predominantly occurs through the hydrogen-bonded network.

SS-TuP19 First-Principles Study of on-surface and Sub-surface Oxygen in Rh(111), Kate Fanning, W. Walkosz, Lake Forest College; J. Garcia, H. Iddir, Argonne National Laboratory; D.R. Killelea, Loyola University Chicago

The interaction of oxygen with metal surfaces can directly alter their properties. On-surface and sub-surface O was shown to be a precursor for oxide formation and greatly affect the reactivity of catalytic surfaces [1-4]. Using Density Functional Theory calculations, we investigate various structures of O on the (111) surface of Rh as well as the competition between oxide formation and dissolution of oxygen into Rh to form subsurface oxygen. In particular, the work focuses on identifying pathways for surface diffusion of low-coverage adsorbed atomic O between different sites on Rh(111) as well as the surface to subsurface diffusion. The obtained results are expected to further our understanding of the chemistry of transition metal surfaces.

[1] Rose, M. K.; Borg, A.; Mitsui, T.; Ogletree, D. F.; Salmeron, M. J. *Chem. Phys.* 2001, 115, 10927-10934.

[2] Monine, M.; Pismen, L.; Bar, M.; Or-Guil, M. *J. Chem. Phys.* 2002, 117, 4473-4478.

[3] Xu, Y.; Greeley, J.; Mavrikakis, M. *J. Am. Chem. Soc.* 2005, 127, 12823-12827.

[4] Rotermund, H. H.; Pollmann, M.; Kevrekidis, I. G. *Chaos* 2002, 12, 157-163.

SS-TuP20 STM/S Study of Domain Walls and Atomic Defects on the Surface of Iron-based Superconductors, Zhuozhi Ge, Q. Zou, M. Fu, L. Sanjeewa, A. Sefat, Z. Gai, Oak Ridge National Laboratory

Surface defects, including domain walls and individual atomic defects, can dramatically modify the properties of iron-based superconductors. However, the nature of domain walls and atomic defects on the surface of in-situ cleaved iron-based superconductors has yet to be identified. Here, we systematically investigated the surface defects on low-temperature cleaved parent and doped BaFe_2As_2 superconductors by scanning tunneling microscopy/spectroscopy (STM/S). STM imaging reveals two types of domain walls on parent and Ni/Co doped BaFe_2As_2 , one as dark trench with missing atoms and the other as straightly aligned bright blobs. Two types of point defects are also identified, one intrinsically from growth or cleaving and the other induced by scanning of the STM tip. Tunneling spectroscopy shows similar surface states at about -200 meV on domain walls and the intrinsic point defects, while on the tip-induced defects there is only one peak at about -120 meV.

Fundamental Discoveries in Heterogeneous Catalysis Focus Topic

Room A213 - Session HC+2D+SS-WeM

Exotic Nanostructured Surfaces for Heterogeneously-Catalyzed Reactions

Moderators: Ashleigh Baber, James Madison University, Erin Iski, University of Tulsa

8:20am **HC+2D+SS-WeM2 Selective Alkane Chemistry on IrO₂(110) Surfaces, Aravind Asthagiri, M. Kim, The Ohio State University; J.F. Weaver, University of Florida**

Selective conversion of alkanes to higher value species using heterogeneous catalysts is of great interest with the increasing availability of light alkanes from shale fracking. We have used a combination of temperature programmed reaction spectroscopy (TPRS) and density functional theory (DFT) to demonstrate that the stoichiometric terminated IrO₂(110) surface can activate methane and ethane below room temperatures, and furthermore, that this surface can be selective towards ethane dehydrogenation to ethylene. For ethane, DFT shows that adsorption and initial C-H bond cleavage to surface bound C₂H₄* is facile and the selectivity step occurs between further C-H bond breaking leading to complete oxidation versus ethylene desorption. The reactivity of this surface is mediated by the presence of undercoordinated Ir (Ir_{cus}) and adjacent bridge O atoms (O_{br}). Using the combination of TPRS and DFT we find that pre-hydrogenating the IrO₂(110) surface results in the formation of HO_{br} sites that increases the selectivity towards ethylene by increasing the barrier to C-H bond cleavage for C₂H₄* and decreasing the desorption energy of C₂H₄*. We will discuss efforts to use DFT and microkinetic modeling to explore doping strategies of both the Ir_{cus} and O_{br} sites to promote selectivity towards ethylene formation.

8:40am **HC+2D+SS-WeM3 Design of Nanostructured Catalysts for Better Performance, Francisco Zaera, University of California, Riverside INVITED**

One of the major challenges in heterogeneous catalysis is the preparation of highly selective and robust catalysts. The goal is to be able to synthesize solids with stable surfaces containing a large number of specific surface sites designed for the promotion of a particular reaction. New synergies between surface-science studies and novel nanosynthesis methodology promise to afford new ways to design such highly selective catalysts in a controlled way. In this presentation we will provide a progress report on a couple of projects ongoing in our laboratory based on this approach. Platinum-based catalysts have been prepared for the selective trans-to-cis conversion of olefins, with a design based on early surface-science work with model surfaces and quantum mechanical calculations that indicated a particular preference for (111) facets in promoting the formation of the cis isomers. We are currently extending this research by using the concept of "single-site catalysis" with Pt-Cu bimetallics for the selective hydrogenation of unsaturated aldehydes. In a second example, new metal@TiO₂ yolk-shell nanomaterials conceived for both regular and photo-induced catalytic applications have been used to promote CO oxidation at cryogenic temperatures and to suggest that in photocatalysis the role of the metal may not be to scavenge the excited electrons produced in the semiconductor upon absorption of light, as commonly believed, but rather to promote the recombination of the adsorbed atomic hydrogen initially produced by reduction of H⁺ on the surface of that semiconductor. New mixed-oxide surfaces are being designed using atomic layer deposition (ALD) as well.

9:20am **HC+2D+SS-WeM5 Characterization of a Pd/Ag(111) Single Atom Alloy Surface Using CO as a Probing Molecule for H₂ Dissociation, Mark Muir, M. Trenary, University of Illinois at Chicago**

Tuning catalysts for selective hydrogenation reactions is ultimately determined by the nature of the active site for H₂ dissociation and the adsorption of atomic hydrogen on the surface. Several single atom alloys (SAAs) consisting of small amounts of Pd deposited onto surfaces of metals that do not activate H₂ dissociation, such as Cu(111) and Au(111), have been previously studied. In the present study, we characterize Pd/Ag(111), a possible new single atom alloy surface using reflection absorption infrared spectroscopy (RAIRS) of adsorbed CO as a probe. From 0.01 to 0.04 ML Pd/Ag(111), a ν(CO) stretching peak was seen at 2050 cm⁻¹ corresponding to CO adsorbed on palladium atoms at the on-top site, indicating a single atom alloy surface. By increasing the palladium coverage

to approximately 0.05 ML and above, a second ν(CO) stretching peak was seen at 1950 cm⁻¹ corresponding to CO adsorbed on a palladium bridge site, indicating palladium dimer formation. The surface palladium coverage was determined using temperature programmed desorption (TPD) of CO and Auger electron spectroscopy (AES). By annealing these surfaces to 500 K, the palladium atoms diffuse into the subsurface, and a ν(CO) stretching peak at 2150 cm⁻¹ (CO adsorbed on silver atoms) is greatly enhanced in intensity due to subsurface palladium. The subsurface to surface palladium ratios on the single atom alloy surfaces were varied from capped Ag/Pd/Ag(111), to a 50:50 ratio, to approximately a 60:40 ratio. The ability of subsurface palladium on the Pd/Ag(111) SAA surfaces to facilitate hydrogen dissociation was explored using H₂ and D₂ TPD.

9:40am **HC+2D+SS-WeM6 Propyne Hydrogenation over a Pd/Cu(111) Single Atom Alloy Catalyst Studied with Infrared Spectroscopy, Mohammed Abdel-Rahman, M. Trenary, University of Illinois at Chicago**

The hydrogenation of propyne (C₃H₄) to propylene (C₃H₆) using a Pd/Cu(111) single atom alloy (SAA) has been studied using polarization dependent-reflection absorption infrared spectroscopy. This method allows for simultaneous monitoring of reactants and products in the gas-phase and species adsorbed on the surface during the reaction. The results were compared with the hydrogenation of propyne using Pd-free Cu(111) as well as previous studies on Pd/Cu SAA alumina-supported metal catalysts. Propylene production first occurs at 383 K as indicated by the presence of an infrared peak at 912 cm⁻¹, which is a uniquely characteristic of gas-phase propylene. The presence of propyne oligomers on the surface is indicated by a dramatic increase in the peak intensity at 2968 cm⁻¹ at temperatures above 400 K. The progression of the peaks at 912 and 3322 cm⁻¹ was used to calculate the rate of production of propylene and the rate of consumption of propyne, respectively. This reaction rate was used to determine a turnover frequency (TOF) for the reaction on the Pd/Cu SAA catalyst.

11:00am **HC+2D+SS-WeM10 "Single-Atom" Catalysis: How Structure Influences Reactivity, Gareth S. Parkinson, TU Wien, Austria INVITED**

The field of „single-atom“ catalysis (SAC) [1-2] emerged as the ultimate limit of attempts to minimize the amount of precious metal used in heterogeneous catalysis. Over time, it has become clear that metal adatoms behave differently to supported nanoparticles [3-4], primarily because they form chemical bonds with the support and become charged. In this sense, SAC systems resemble the mononuclear coordination complexes used in homogeneous catalysis, and there is much excitement that SAC could achieve similar levels of selectivity, and even heterogenize problematic reactions currently performed in solution. It is important to note, however, that homogeneous catalysts are designed for purpose based on well-understood structure-function relationships, but the complexity of real SAC systems means that the structure of the active site is difficult to determine, never mind design. In this talk, I will describe how we are using precisely-defined model supports [5] to unravel the fundamentals of SAC. I will show a selection of our latest results in this area, including scanning probe microscopy, x-ray photoelectron spectroscopy (XPS) and temperature programmed desorption (TPD) data to show how the local structure of Ir₁/Fe₃O₄(001) and Rh₁/Fe₃O₄(001) single atom catalysts changes based on preparation and adsorption of reactants, and how the structures obtained can be rationalised by analogy to Ir(I) and Ir(IV) complexes, respectively. If time permits, I will also show that CO oxidation activity in the Pt₁/Fe₃O₄(001) system is promoted by water.

[1] Qiao, B., et al., Single-atom catalysis of CO oxidation using Pt₁/FeOx. *Nature Chemistry* **3** (2011) 634-41.

[2] Liu, J., Catalysis by supported single metal atoms. *ACS Catalysis* **7** (2016) 34-59.

[3] Gates, B.C., et al., Atomically dispersed supported metal catalysts: perspectives and suggestions for future research. *Catalysis Science & Technology* **7** (2017) 4259-4275.

[4] Parkinson GS, *Catalysis Letters* **149** (2019), 1137-1146

[5] Bliem, R., et al., Subsurface cation vacancy stabilization of the magnetite (001) surface. *Science*, **346** (2014) 1215-8.

11:40am **HC+2D+SS-WeM12 Oxidation Reactions on Rh(111), Marie Turano, G. Hildebrandt, Loyola University Chicago; R.G. Farber, The University of Chicago; D.R. Killelea, Loyola University Chicago**

The uptake and subsequent surface structures of oxygen on transition metal surfaces reveal much about the reactivity of the metal catalyst. On clean Rh(111) at room temperatures in ultra high vacuum (UHV), oxygen molecules (O₂) readily dissociate into two adsorbed oxygen atoms,

Wednesday Morning, October 23, 2019

asymptotically approaching a saturation coverage of 0.5 monolayers (ML, 1 ML = 1.5×10^{15} O atoms cm^{-2}). However, exposing Rh(111) to gas-phase oxygen atoms (atomic oxygen, AO) generated by thermally cracking molecular oxygen over a hot Ir filament, allows for higher oxygen coverages. In addition, oxygen not only adsorbs to the surface, but it may also penetrate into the subsurface region of the crystal. After atomic oxygen exposures at elevated temperatures, the Rh(111) surface is covered in a combination of oxides, adsorbed surface oxygen, and subsurface oxygen (O_{sub}). The coexistence of a variety of structures allows for the determination of which species is reactive to the oxidation of carbon monoxide (CO) on highly oxidized Rh(111) surfaces. Using scanning tunneling microscopy (STM), we have determined that CO oxidation occurs mainly at the interface between the metallic and oxidic surface phases on Rh(111) where the O_{sub} , upon emergence from the bulk, replenishes the surface oxygen. Once O_{sub} is depleted, CO consumes the oxide and the surface quickly degrades into the (2x2)-O+CO adlayer.

12:00pm HC+2D+SS-WeM13 Adsorption and Motion of Atomic Oxygen on the Surface and Subsurface of Ag(111) and Ag(110), S.B. Isbill, C.J. Mize, L.D. Crosby, Sharani Roy, University of Tennessee Knoxville

Silver surfaces act as important industrial catalysts for the partial oxidation of ethylene to ethylene oxide and methane to methanol. While significant strides have been taken towards understanding the mechanism of heterogeneous catalytic oxidation by silver, the role of subsurface oxygen in such catalysis has yet to be elucidated. Subsurface oxygen is adsorbed just beneath the surface of the metal and is believed to play an important role in surface reconstruction and oxidation catalysis. In the present study, density functional theory (DFT) was used to study the interactions of atomic oxygen with the surface and subsurface of the Ag(111) and Ag(110) surfaces. The goal was to investigate the adsorption of atomic oxygen at different coverages and examine its effects on the structural and catalytic properties of silver. Our study of O/Ag(111) showed that adsorption of atomic oxygen was strong at low coverage but became weaker with an increase in coverage, much more so for surface oxygen than for subsurface oxygen. Therefore, at higher and industrially relevant oxygen coverages, oxygen preferred to bind to the subsurface than to the surface. In contrast, atomic oxygen bound more strongly to the surface than to the subsurface at all studied coverages. Based on the results from DFT, we constructed analytic models for adsorption in O/Ag(111) and O/Ag(110) as well as performed kinetic Monte Carlo simulations to explain the differences in coverage dependence of surface adsorption versus subsurface adsorption on the two surfaces. The results provide qualitative insight on why surface and subsurface oxygen might have qualitatively different effects on the electronic, geometric, and catalytic properties of silver.

Complex Oxides: Fundamental Properties and Applications Focus Topic

Room A220-221 - Session OX+EM+MI+SS-WeM

Electronic and Magnetic Properties of Complex Oxide Surfaces and Interfaces

Moderators: Yingge Du, Pacific Northwest National Laboratory, Vincent Smentkowski, GE-Research

8:00am OX+EM+MI+SS-WeM1 Charge Transfer in Lanthanum Ferrite-Strontium Nickelate Superlattices, Le Wang, Z. Yang, M.E. Bowden, Pacific Northwest National Laboratory; J.W. Freeland, Argonne National Laboratory; Y. Du, S.A. Chambers, Pacific Northwest National Laboratory

Charge transfer at oxide interfaces can drive emergent phenomena that do not occur in the bulk, thereby significantly enriching our fundamental understanding of these material systems and their applications. Designing oxide heterostructures and seeking new and novel interfacial phenomena has been an active area of research for some time. We have synthesized a series of $[(\text{LaFeO}_3)_m(\text{SrNiO}_{3-d})_n]_z$ ($[(\text{LFO})_m(\text{SNO})_n]_z$) superlattices (SLs) ($z = 7$ to 21) by oxide molecular beam epitaxy on $(\text{LaAlO}_3)_{0.3}(\text{Sr}_2\text{AlTaO}_6)_{0.7}$ (LSAT) (001) substrates. *In situ* RHEED patterns and x-ray diffraction measurements reveal a high degree of structural quality in the SLs. X-ray photoemission spectroscopy (XPS) shows that the Fe is Fe^{4+} in the $(\text{LFO}_z/\text{SNO}_z)_{21}$ SL. However, the Fe 2p binding energy shifts to lower values with increasing LFO layer thickness in $(\text{LFO}_m/\text{SNO}_1)_z$ SLs, suggesting that the volume averaged Fe valence decreases. Fe L-edge X-ray absorption spectroscopy (XAS) measurements corroborate the XPS results, indicating that Fe is 4+ for the $(\text{LFO}_z/\text{SNO}_z)_{21}$ SL and mostly 3+ for the $(\text{LFO}_5/\text{SNO}_1)_{10}$ SL. On the other hand, Ni L-edge XAS shows that Ni valence is Ni^{3+} for the

$(\text{LFO}_z/\text{SNO}_z)_{21}$ SL as is also true for insulating NdNiO_3 , suggesting that the Ni layers in this SL are insulating, which is consistent with our in-plane transport measurements. However, for the $(\text{LFO}_5/\text{SNO}_1)_{10}$ SL, the Ni valence is larger than 3+. The measured energy shifts suggest that Ni is close to 4+. The thicker LFO layer in the $(\text{LFO}_5/\text{SNO}_1)_{10}$ SL may result in a larger band offset and create a potential well to trap the holes in the Ni layer, inducing the formation of Ni^{4+} . Our ongoing studies are probing the impact of the SNO layer thickness on material structure as well as the evolution of the Fe and Ni valences in $(\text{LFO}_5/\text{SNO}_n)_z$ SLs. Additional planned experimental and theoretical investigations will address how charge transfer from Fe to Ni occurs at the LFO/SNO interface, and how to stabilize the unusual high 4+ valence in Fe^{4+} and Ni^{4+} by means of interfacial engineering.

8:20am OX+EM+MI+SS-WeM2 Self-healing Growth of LaNiO_3 on Mixed-terminated $(\text{LaAlO}_3)_{0.3}(\text{Sr}_2\text{AlTaO}_6)_{0.7}$, Friederike Wrobel, H. Hong, S. Cook, T.K. Andersen, D. Hong, C. Liu, A. Bhattacharya, D.D. Fong, Argonne National Laboratory

Epitaxial LaNiO_3 (LNO) thin films and superlattices are known to be antiferromagnetic and weakly insulating for LNO thicknesses of 2 unit cells but paramagnetic and metallic for higher LNO thicknesses [1]. The quality of the single-crystal substrate surface, and in particular the chemical composition of the surface, is known to be a key factor governing the quality of the deposited thin film. For SrTiO_3 (001) substrates, there are well-established preparation methods to ensure that the surface is TiO_2 -terminated and atomically smooth; the only features that appear with atomic force microscopy are the regular steps and terraces associated with crystal miscut. SrTiO_3 is therefore often preferred as a substrate over other materials like $(\text{LaAlO}_3)_{0.3}(\text{Sr}_2\text{AlTaO}_6)_{0.7}$ (LSAT), whose surface composition is harder to control. Interestingly, for unknown reasons, the highest quality LaNiO_3 thin films have been grown on mixed-terminated, untreated LSAT (001) substrates [2, 3]. At present, very few detailed studies have been conducted regarding the precise influence of the substrate on thin film growth behavior due to the need for an in-situ, atomic-scale characterization technique. Exploiting an in-situ, oxide molecular beam epitaxy (MBE) chamber at the Advanced Photon Source, we were able to monitor the deposition of thin films of LNO on LSAT (001) substrates with different surface compositions. Both non-resonant and resonant (Sr K-edge) X-ray scattering measurements were conducted at several points during the growth process. We observed the formation of atomically smooth, high-quality LNO films regardless of the initial substrate surface composition, suggesting that any excess, non-stoichiometric material on the initial LSAT substrate rises to the surface during deposition. With atomic layer-by-atomic layer MBE under the right conditions, we can therefore achieve self-healing growth behavior of complex oxides on top of mixed-terminated substrates. We will discuss details of the in-situ growth measurements and the methods used to determine the atomic and chemical structures.

1. Frano, A., et al., *Orbital Control of Noncollinear Magnetic Order in Nickel Oxide Heterostructures*. Physical Review Letters, 2013. **111**(10): p. 106804.

2. Liu, C., et al., *Counter-thermal flow of holes in high-mobility LaNiO_3 thin films*. Physical Review B, 2019. **99**(4): p. 041114.

3. Wrobel, F., et al., *Comparative study of $\text{LaNiO}_3/\text{LaAlO}_3$ heterostructures grown by pulsed laser deposition and oxide molecular beam epitaxy*. Applied Physics Letters, 2017. **110**(4): p. 041606.

8:40am OX+EM+MI+SS-WeM3 Optoelectronics with Oxides and Oxide Heterostructures, Alexander Demkov, University of Texas at Austin

INVITED

Si photonics is a hybrid technology combining semiconductor logic with fast broadband optical communications and optical information technologies. With the increasing bandwidth requirement in computing and signal processing, the inherent limitations in metallic interconnection are seriously threatening the future of traditional IC industry. Silicon photonics can provide a low-cost approach to overcome the bottleneck of the high data rate transmission by replacing the original electronic integrated circuits with photonic integrated circuits. The development has proceeded along several avenues including mounting optical devices based on III-V semiconductors and/or LiNbO_3 (LNO) on Si chips, incorporation of active optical impurities into Si, and utilization of stimulated Raman scattering in Si. All these approaches have had limited success. Recently, another path to Si photonics through epitaxial integration of transition metal oxide films was demonstrated when an effective electro-optic (Pockels) coefficient of BaTiO_3 (BTO) films epitaxially grown on Si via an SrTiO_3 buffer was reported to be an order of magnitude larger than that in commercially-available LNO modulators. More generally, epitaxial growth of SrTiO_3 on

Wednesday Morning, October 23, 2019

Si(001) enables monolithic integration of many functional perovskite oxides on Si, including ferroelectric BTO, ferromagnetic LaCoO₃, photocatalytic TiO₂ and CoO, and many others.

In this talk, I will focus on two materials systems integrated on Si (001) and well-suited for implementation in the next-generation optical technologies: SrTiO₃/LaAlO₃ quantum wells and Pockels-active BTO thin film heterostructures. Both materials systems are promising for use in a wide variety of optical and electro-optical devices central to integrated photonic technologies, including quantum cascade lasers, photodetectors, electro-optic modulators and switches. The resulting devices achieve refractive index tuning with power consumption many orders of magnitude less than previously reported. Taken together, these two approaches will hopefully open the door for the development of new kinds of optical and electro-optical devices for use in integrated photonics technologies.

9:20am **OX+EM+MI+SS-WeM5 Medard W. Welch Award Lecture: Defect-Mediated Coupling of Built-in Potentials at Buried Interfaces Involving Epitaxial Complex Oxides, Scott. A Chambers¹**, Pacific Northwest National Laboratory **INVITED**

Semiconductor-based devices are of broad importance, not only in electronics, but also in energy technology. Internal electric fields dictate the flow of charge that occurs both laterally and vertically. The associated potential profiles can be approximated from electronic transport data, and also calculated via Poisson-Schrodinger modeling, provided the properties of the constituent materials and interface structures are sufficiently well understood. These approaches work well for heterostructures involving, for instance, III-V semiconductors. However, when complex oxides are involved, they become unreliable because of poorly understood defects that can be present. There is, therefore, a critical need for new methods to enable the determination of band-edge profiles in heterostructures involving these materials.

The SrTiO₃/Si(001) interface has been a prototypical system for understanding the materials physics and electronic structure of crystalline oxides on semiconductors. Thinner films (a few unit cells, u.c.) are known to result in flat-band heterojunctions in which the valence (conduction) band offset is large (small). However, we have recently found that thicker films (~30 u.c.) of SrNb_xTi_{1-x}O₃ (0 ≤ x ≤ 0.2) on intrinsic Si(001) result in completely different electronic structures. Transport data suggest sharp upward band bending in the Si, leading to hole gas formation at the interface, and a large (~2 eV) built-in potential in the SNT0, along with surface depletion. We have probed these buried interfaces using hard x-ray photoelectron spectroscopy (HAXPES). The resulting core-level spectra exhibit unusual features not seen in thinner films, and not credibly ascribed to secondary phases or many-body effects. In order to interpret these line shapes, we hypothesize that they result from large built-in potentials within the system. We have developed an algorithm to extract these potential profiles by fitting heterojunction spectra to linear combinations of spectra from phase-pure, flat-band materials, summed over layers within the probe depth, each with a binding energy characteristic of the potential at each depth. This approach leads to excellent agreement with experiment and band-edge profiles completely consistent with those from transport data. Moreover, we find that the built-in potentials extracted from HAXPES on the Si side of the interface are in quantitative agreement with those resulting from solving Poisson's equation using the SIMS profile for in-diffused oxygen from the STO. Oxygen is a shallow donor in Si, and assuming 100% donor ionization, along with the ¹⁸O SIMS depth profile, leads to near-perfect agreement with HAXPES.

11:20am **OX+EM+MI+SS-WeM11 Structural and Dielectric Characterization of Epitaxial Entropy-Stabilized Oxide Thin Films, George Kotsonis, J.-P. Maria**, Pennsylvania State University

The emergence of entropy-stabilized oxides (ESOs) represents a new paradigm for complex oxide engineering. The large configurational entropy of ESOs facilitates mixing of chemically dissimilar cations in significant proportions. ESO research continues to intensify as the oxide community works toward a thorough understanding of structure-property-synthesis relationships. Due to inherent metastability, high energy, non-equilibrium synthesis techniques are well suited for ESO fabrication. In particular, laser ablation has excelled at producing high quality epitaxial ESO thin films, which provide a platform for fundamental characterization.

We present the growth and characterization of Ba(Ti_{0.2}Sn_{0.2}Zr_{0.2}Hf_{0.2}Nb_{0.2})O₃ and similar Barium-based perovskite structured ESO thin films grown by laser ablation. Crystal structure, surface morphology, and optical properties

are characterized by X-ray diffraction, atomic force microscopy, and ellipsometry respectively. Epitaxial thin film capacitor structures were fabricated to characterize the frequency, voltage, and temperature dependence of electrical properties.

By exploiting the entropy-stabilized nature of ESOs, we demonstrate the incorporation of significant amounts of aliovalent cation pairs (*e.g.* Sc³⁺Ta⁵⁺) in hopes of producing nano-polar regions supporting a dispersive dielectric response similar to relaxor ferroelectrics. Additionally, we explore compositional space in search of a phase boundary between a high-symmetry ESO phase and a lower symmetry end-member. Compositions at such a boundary may exhibit phase instability and enhanced dielectric functionality similar to compositions at or near a morphotropic phase boundary. The compositional degrees of freedom available in ESO systems provide new avenues for property tuning and studying the effects of extreme chemical disorder on dielectric properties.

11:40am **OX+EM+MI+SS-WeM12 Oxygen Vacancy-Mediated Epitaxy: TiO₂(111)/Al₂O₃(0001) and Ferromagnetic Cr₂O₃(0001)/TiO₂(111), C. Ladewig, F. Anwar, Jeffry Kelber**, University of North Texas; S.Q.A. Shah, P.A. Dowben, University of Nebraska-Lincoln

The formation of all-oxide heterostructures comprising multiferroic oxides interfaced with appropriate semiconducting substrates is a promising path towards low power, voltage-switchable spintronics, including non-volatile memory and multi-functional logic devices. At the same time, the necessary scaling of film thicknesses to the nm range can induce structures and properties sharply different than those of the bulk. We report here in situ XPS, LEED, EELS and ex-situ MOKE data on the growth and properties of Cr₂O₃(0001) on TiO_{1.7}(111) on Al₂O₃(0001). The data indicate that the presence of O vacancies during film growth can mediate the further growth of oxides with unusual structures and properties. These data show that (a) O vacancies during initial stages of film growth yield a TiO₂ film of an unusual crystallographic orientation and structure; and that (b) this leads to growth of an epitaxial Cr₂O₃ layer exhibiting magnetic ordering above the expected Néel temperature of thin film chromia - indicative of a strained chromia lattice due to epitaxial growth on a substrate with a lattice constant of 5.1 Å, compared to the bulk chromia lattice constant of 4.9 Å. Molecular beam epitaxy (MBE) of Ti at 500 K in 10⁻⁶ Torr O₂ on Al₂O₃(0001) initially yields TiO_{1.7}(111) with the structure of corundum phase Ti₂O₃ (a = b = 5.1 Å). Further deposition and annealing in O₂ results in stoichiometric TiO₂(111), but with the same lattice structure and orientation as Ti₂O₃(111), and with a total thickness of 5 nm. This is sharply different from the generally observed growth of TiO₂(001) on Al₂O₃(0001). MBE of ~ 1 monolayer of Cr on TiO₂(111) yields hexagonally-ordered Cr₂O₃ and the formation of titania oxygen vacancies. MOKE measurements confirm that this chromia layer is magnetically ordered at 280 to 315 K, likely antiferromagnetically ordered, with exchange bias coupling to the TiO_{1.7}(111) substrate. O vacancies in the TiO₂(111) lattice exhibit weak ferromagnetic behavior, as is evident in the In-plane MOKE, enhancing the canting of the magnetism away from the thin film normal, which is expected for the Cr₂O₃(0001) alone. These data demonstrate that careful control of initial growth conditions and film stoichiometry during oxide MBE can template the subsequent growth of stoichiometric oxide heterostructures with non-bulk like structures and properties.

Acknowledgement: Work at UNL was supported in part by the Semiconductor Research Corporation (SRC) as task 2760.002 and NSF through ECCS 1740136.

12:00pm **OX+EM+MI+SS-WeM13 Incorporation of Ti into Epitaxial Films of Magnetite, Tiffany Kaspar, S.R. Spurgeon, D.K. Schreiber, S.D. Taylor, M.E. Bowden, S.A. Chambers**, Pacific Northwest National Laboratory

Magnetite, Fe₃O₄, exhibits metallic conductivity via electron hopping between Fe²⁺ and Fe³⁺ occupying octahedral sites in the spinel lattice. As Ti⁴⁺ is doped into the octahedral sites of magnetite (the titanomagnetite series), an equal fraction of Fe³⁺ is reduced to Fe²⁺ to maintain charge neutrality. The site occupancies of Fe²⁺ and Fe³⁺ determine the transport properties of the titanomagnetite series; the end-member ulvöspinel, Fe₂TiO₄, exhibits *p*-type semiconducting transport properties. The Fe²⁺/Fe³⁺ site occupancy remains controversial, but is likely in part a function of the lattice strain induced by doping smaller Ti⁴⁺ into the lattice. Here, we have deposited titanomagnetites and ulvöspinel as well-defined epitaxial thin films on MgO, MgAl₂O₄, and Al₂O₃ substrates by oxygen-plasma-assisted molecular beam epitaxy. The incorporation of Ti into the magnetite lattice is found to depend strongly on deposition conditions and substrate orientation. We have characterized the crystalline structure, phase segregation, and surface morphology with XRD, STEM/EDS, APT, and AFM,

Wednesday Morning, October 23, 2019

and related these to the kinetic and thermodynamic factors determined by the deposition conditions. The Fe valence state is evaluated with *in situ* XPS. The impact of film structure and Fe oxidation state on the electrical transport properties of the films will be discussed.

Chemical Analysis and Imaging Interfaces Focus Topic Room A120-121 - Session CA+NS+SS+VT-WeA

Chemical Analysis and Imaging of Liquid/Vapor/Solid Interfaces I

Moderators: Juan Yao, Pacific Northwest National Laboratory, Andrei Kolmakov, National Institute of Standards and Technology (NIST)

2:20pm **CA+NS+SS+VT-WeA1 Chemical Analysis and Imaging of Environmental Interfaces, Vicki Grassian**, University of California at San Diego **INVITED**

Environmental interfaces, defined as any surface in equilibrium with its surrounding environment, are ubiquitous. From this broad definition, there are a myriad of different types of environmental interfaces that include atmospheric aerosols, nanomaterials and indoor surfaces. This talk will focus on the use of different molecular probes including various spectroscopic and imaging techniques to investigate interfaces relevant to outdoor and indoor environments.

3:00pm **CA+NS+SS+VT-WeA3 Liquid/Vapor Interfaces Investigated with Photoelectron Spectroscopy, Hendrik Bluhm**, Fritz Haber Institute of the MPG, Germany **INVITED**

Aqueous solution/vapor interfaces govern important phenomena in the environment and atmosphere, including the uptake and release of trace gases by aerosols and CO₂ sequestration by the oceans.[1] A detailed understanding of these processes requires the investigation of liquid/vapor interfaces with chemical sensitivity and interface specificity under ambient conditions, *i.e.*, temperatures above 200 K and water vapour pressures in the millibar to tens of millibar pressure range. This talk will discuss opportunities and challenges for investigations of liquid/vapor interfaces using X-ray photoelectron spectroscopy and describe some recent experiments that have focused on the propensity of certain ions and the role of surfactants at the liquid/vapor interface.

[1] O. Björneholm et al., Chem. Rev. **116**, 7698 (2016).

4:20pm **CA+NS+SS+VT-WeA7 Methanol Hydration Studied by Liquid μ -jet XPS and DFT Simulations, Jordi Fraxedas**, Catalan Institute of Nanoscience and Nanotechnology (ICN2), CSIC and BIST, Spain; *E. Pellegrin, V. Perez-Dieste, C. Escudero*, CELLS-ALBA, Spain; *P. Rejmak*, Institute of Physics PAS, Poland; *N. Gonzalez, A. Fontseré, J. Prat, S. Ferrer*, CELLS-ALBA, Spain

The advent of liquid μ -jet setups, in conjunction with X-ray Photoemission Spectroscopy (XPS), has opened up a plethora of experimental possibilities in the field of atomic and molecular physics [1]. Here, we present a combined experimental and theoretical study of the hydration of methanol at the aqueous solution/vapor interface. These are first experimental results obtained from the new liquid μ -jet setup at the Near Ambient Pressure Photoemission (NAPP) endstation of the CIRCE helical undulator beamline (100–2000 eV photon energy range) at the CELLS-ALBA synchrotron light source, using a differentially pumped SPECS PHOIBOS 150 hemispherical electron energy analyzer [2]. The experimental results are compared with simulations from density functional theory (DFT) regarding the electronic structure of single molecules and cluster configurations as well as with previous experimental studies.

Methanol is the simplest amphiphilic molecule capable of hydrogen bonding due to its apolar methyl and polar hydroxyl groups. The results obtained from pure water at 600 eV photon energy emphasize the short range tetrahedral distribution as previously observed for crystalline and amorphous ice. We also find indications for ordering phenomena in water/methanol mixtures by the reduced O1s XPS liquid line width (as compared to pure water), which could be ascribed to the amphiphilic character of the methanol molecule. Regarding the C1s XPS lines, the vapor/liquid peak ratios allow for a quantitative determination of the methanol volume concentrations in both the vapor as well as in the liquid phase, that are corroborated by an analogue analysis of the valence band (VB) spectra. A detailed quantitative analysis of the water/methanol liquid VB XPS spectrum accounting for the photon energy dependence of photoemission cross sections confirms the atomic/orbital characteristics of the methanol molecular orbitals involved in the transitions and their pertinent intensities. From the decomposition of the liquid VB spectrum of the water/methanol mixture together with finite XPS probing depth we derive a methanol volume fraction of 43% for the outer liquid layers as compared to the nominal bulk liquid value of 37.5%. Finally, from the different binding energy (BE) shifts of the water/methanol liquid VB

spectrum with respect to that of pure methanol, we develop a CH₃OH-(H₂O)₃ cluster-based model that relates these different BE shifts to the different MO hybridizations within that cluster.

[1] B. Winter, M. Faubel, Chem. Rev. **106** (2006) 1176.

[2] V. Pérez-Dieste, L. Aballe, S. Ferrer, J. Nicolàs, C. Escudero, A. Milán, E. Pellegrin, J. Phys. Conf. Ser. **425** (2013) 072023.

4:40pm **CA+NS+SS+VT-WeA8 Survey of Ionic Liquid Interfaces under Vacuum and Ambient Conditions: An XPS Perspective, Yehia Khalifa**, Ohio State University; *A. Broderick, J.T. Newberg*, University of Delaware; *Y. Zhang, E. Maginn*, University of Notre Dame

Properties and behavior of Ionic Liquid interfaces tend to behave differently from their bulk counterparts. In this study the preferential enhancement of the lower molar concentration anion [TFSI] in a mixture of [C2MIM][OAc] and [C2MIM][TFSI] is shown in the top 17 Å via angle-resolved X-ray photoemission spectroscopy under ultra high vacuum conditions. This is supported by molecular simulations where a quantitative relationship is also established between the two techniques. This interfacial enhancement is not only unique to mixtures but is also displayed in a pure ionic liquid with a hydrophilic anion such as [HMIM][Cl] studied via ambient pressure X-ray photoemission spectroscopy. The surface of [HMIM][Cl] under vacuum and increasing pressures of water vapor was evaluated (maximum of 5 Torr, 27% relative humidity). Our quantitative results indicate a significantly larger mole fraction of water at the interface compared to the bulk with increasing pressures when compared to previously published tandem differential mobility analysis results on [HMIM][Cl] nanodroplets. Furthermore the reverse isotherms has shown that the water uptake on the interface is a reversible process. These results highlight the unique behavior of ionic liquid interfaces that can be exploited for smart materials design and application.

5:00pm **CA+NS+SS+VT-WeA9 Ambient Pressure XPS Study of Gallium-Indium Eutectic (EGaIn) Surface under Oxygen and Water Vapor, Meng Jia**, J.T. Newberg, University of Delaware

Liquid metals (LMs) have a combination of high thermal/electrical conductivity and excellent deformability. The application of LMs in the field of electronics has identified many opportunities for their use as stretchable electronics, self-healing conductors and interconnects. Gallium-Indium eutectic (EGaIn) is one of the leading alternatives to toxic liquid mercury because of its low vapor pressure, low viscosity, low toxicity and high conductivity. A surface oxide layer is known to form when EGaIn is exposed to ambient conditions. However, surface sensitive measurements of this chemistry occurring under ambient conditions are strongly lacking. Herein we present results from the interaction of oxygen and water vapor with the liquid-gas interface of an EGaIn droplet deposited on an W foil using ambient pressure X-ray photoelectron spectroscopy (AP-XPS). EGaIn was examined up to a maximum of 1 Torr pressure at 550 K. Results reveal that under ambient conditions both oxygen and water vapor form a Ga(3+) oxide (Ga₂O₃) as an outer layer, while a thin layer of Ga(1+) oxide (Ga₂O) resides between metallic EGaIn and the outer Ga(3+) oxide. Both gases were unreactive towards Indium under our experimental conditions. The oxidation kinetics in the presence of water vapor were much faster compared oxygen. Proposed reaction mechanisms will be discussed.

5:20pm **CA+NS+SS+VT-WeA10 Laboratory-based Hard X-ray Photoelectron System for the study of Interfaces, S. Eriksson**, Scienta Omicron; *Henrik Bergersen*, Scienta Omicron, Sweden

Hard X-ray photoelectron spectroscopy (HAXPES) has traditionally found its application in the core topics of condensed matter physics, but the slowly growing number of beamlines worldwide has widened its appeal to other interest groups. HAXPES uses X-rays in the 2-10 keV range to excite photoelectrons, which are used to non-destructively study the chemical environment and electronic structure of materials.

In contrast to the very surface-sensitive XPS, HAXPES is much more bulk sensitive. This makes it applicable to bulk materials and structured samples, e.g. layered samples and heterostructures. In addition, its bulk sensitivity means that realistic samples can be investigated without the need of prior surface preparation. However, the number of existing HAXPES systems is very small and they are predominantly located at synchrotrons (approx. 20 beamlines worldwide) due to low photoionization cross sections necessitating high X-ray intensities, limiting their availability to users and applications.

This work presents a new laboratory-based instrument capable of delivering monochromated hard X-rays with an energy of 9.25 keV and a focused 30x45 μ m² X-ray spot, giving excellent energy resolution of <0.5

Wednesday Afternoon, October 23, 2019

eV. Systematic reference measurements are presented outlining the systems capability as well as the latest results from various application fields including energy related materials such as batteries.

Ultimately, this spectrometer presents an alternative to synchrotron-based endstations and will help to expand the number and range of HAXPES experiments performed in the future. HAXPES is a cutting edge characterisation method and the advancement of this technique will tremendously increase the potential to study an ever increasing range of inorganic materials and beyond.

Fundamental Discoveries in Heterogeneous Catalysis Focus Topic

Room A213 - Session HC+OX+SS-WeA

Metal-Support Interactions Driving Heterogeneously-Catalyzed Reactions

Moderators: Aravind Asthagiri, The Ohio State University, Jason Weaver, University of Florida

2:20pm **HC+OX+SS-WeA1 Yttria-stabilized Zirconia (YSZ) Supports for Low Temperature Ammonia Synthesis**, Z. Zhang, S. Livingston, Colorado School of Mines; L. Fitzgerald, University College Dublin; J.D. Way, Colin Wolden, Colorado School of Mines

The use of renewable hydrogen for distributed synthesis of ammonia requires the development of efficient catalysts and processes that operate under mild conditions. Here we introduce yttria stabilized zirconia (YSZ) as a more active Ru catalyst support for NH₃ synthesis than traditionally used supports such as Al₂O₃. The addition of Cs promoter increased rates an order of magnitude higher by reducing the apparent activation energy from 103 kJ/mol to 65 kJ/mol. The rate enhancement is largely insensitive to the amount of promoter addition, with Cs outperforming Ba and K by a factor of 2. At 400°C under 1.0 MPa, the synthesis rate was comparable with that of most active oxide-supported Ru catalysts. The rate becomes inhibited by H₂ absorption at low temperature (< 350°C), but the use of lower H₂:N₂ ratios enables the rate to remain comparable to what is observed in stoichiometric mixtures at temperatures > 400°C. A detailed microkinetic model was developed that successfully captures the observed behavior, revealing that adsorption is coverage dependent. These results provide insight and direction into developing alternatives to Haber-Bosch for distributed synthesis of green ammonia.

2:40pm **HC+OX+SS-WeA2 Operando PTRF-XAFS Technique for 3D Structure Determination of Active Metal Sites on a Model Catalyst Surface under Working Conditions**, Satoru Takakusagi, L. Bang, D. Kido, Y. Sato, K. Asakura, Hokkaido University, Japan

Polarization-dependent total reflection fluorescence (PTRF)-XAFS is a powerful technique which can determine 3D structure of highly dispersed metal species on a single-crystal surface by measuring polarization-dependent XAFS of the metal species. To obtain atomic-level understanding of metal/oxide-support interaction in heterogeneous catalysis, we have determined the precise 3D structures of single metal atoms and metal clusters deposited on single-crystal oxide surfaces such as TiO₂(110) and Al₂O₃(0001) by UHV PTRF-XAFS apparatus.^[1]

Recently we have constructed a new apparatus which enables us to measure PTRF-XAFS of active metal species dispersed on a single-crystal oxide surface under working condition. A compact vacuum chamber which works both as PTRF-XAFS cell and batch-type reactor was designed and constructed. The sample can be transferred without exposure to air from another UHV chamber where the sample preparation (ion sputtering, annealing and metal deposition) and its surface characterization (LEED, XPS) are carried out. The sample in the compact chamber can be heated at high temperatures (< 700 °C) in the presence of reactant gases (typically 10~100 Pa), which makes the operando PTRF-XAFS measurements possible. Thus 3D structure-activity relationship of the active metal species on an oxide surface in heterogeneous catalysis can be obtained. We will show the details of the operando PTRF-XAFS technique and its application to CO oxidation on a Pt/Al₂O₃(0001) surface.

(References)

[1] S. Takakusagi et al., *Chem. Rec.* **18** (2018) 1, *J. Phys. Chem. C* **120** (2016) 15785, *Top. Catal.* **56**(2013) 1477, *Phys. Chem. Chem. Phys.* **15**(2013) 14080.

3:00pm **HC+OX+SS-WeA3 Understanding and Tuning Catalytic Materials Using Nanocrystal Precursors**, Matteo Cargnello, Stanford University
INVITED

Catalytic processes are central to the goal of a sustainable future. A promising approach in developing catalytic materials is represented by the design of catalytic sites based on the knowledge of reaction mechanisms and structure-property relationships and aided by computation, and in the precise synthesis of these sites at the atomic and molecular level. The materials-pressure gap, however, still hinders the full realization of this strategy. Nanocrystal precursors, with tunable active sites and compositions, can help bridge this gap. The goal of this talk is to show how this approach can provide not only fundamental understanding of catalytic reactions, but also represents a way to precisely engineer catalytic sites and metal-support interactions to produce efficient catalysts that are active, stable and selective for several important catalytic transformations. Examples of the use of these building blocks as supported systems or in combination with hybrid organic materials will be shown, both to understand trends in methane and CO₂ activation, and in the preparation of optimized catalytic systems combining multiple active phases. In all these examples, important efforts to obtain useful structure-property relationships will be highlighted, with this knowledge used to prepare more efficient catalysts for sustainable production of fuels and chemicals.

4:20pm **HC+OX+SS-WeA7 CO₂ Hydrogenation on Supported Zirconium Oxide Clusters**, Yilin Ma¹, Stony Brook University; M.G. White, Brookhaven National Laboratory

In this work, zirconium atoms and zirconium oxide clusters are deposited onto metal/metal oxide surfaces as model "inverse" catalysts for the study of CO₂ hydrogenation. The control over the stoichiometry of clusters and the oxidation state of the metal centers enables the study of atomic level details such as identification of active sites, interfacial electron transfer and the role of sulfur vacancies. Recent AP-XPS, AP-IR and STM results of supported zirconium oxide on Cu₂O/Cu(111) surface will be presented. Reactivity studies over Zr/Cu₂O/Cu(111) show that the formation of CO₂⁻(ad) and HCOO⁻ can be seen on regions with the presence of Zr on Cu₂O surface during the reaction condition (CO₂/H₂=1, total pressure=0.5 torr), however CO₂ only binds weakly on bare Cu₂O/Cu(111) surface. Moreover, the change of zirconium oxidation state indicates the adsorption of CO₂ happens on metal or metal-support interface, where the zirconium gets oxidized when exposing to CO₂. Some DFT studies of above systems will also be shown, including the electronic structures of clusters, binding sites of CO₂ molecules, etc.

4:40pm **HC+OX+SS-WeA8 Tuning Surface Hydrophobicity to Enhance Reaction Rate of the Lewis Acid Zeolite Nano Sn Beta for Alcohol Ring Opening of Epoxides**, Nicholas Brunelli, A.P. Spanos, A. Parulkar, N. Deshpande, The Ohio State University

Ring opening epoxides produces compounds that are valuable in the production of fine chemicals and pharmaceuticals. Recent work¹ has demonstrated that the bulky reactants typically involved in fine chemical synthesis benefit from reducing the length scale of the materials to produce nano-zeolites (nano-Sn-Beta), which requires using a custom-synthesized structure directing agent in hydroxide conditions. While the nanozeolites can achieve higher overall conversion than Sn-Beta synthesized using fluoride conditions, the initial reaction rate is higher for Sn-Beta that tends to be hydrophobic compared to nano-Sn-Beta that is demonstrated to be hydrophilic. These results suggest that the alcohol ring opening reaction is sensitive to the reaction environment. The surface of nano-Sn-Beta can be treated to reduce the amount of defects and correspondingly increase the hydrophobicity. Interestingly, the treatment of nano-Sn-Beta materials more than doubles the observed reaction rate. Overall, this demonstrates a valuable method to tune the reaction environment that could be widely applicable to many chemical reactions.

References

(1) Parulkar, A.; Spanos, A. P.; Deshpande, N.; Brunelli, N. A. Synthesis and catalytic testing of Lewis acidic nano zeolite Beta for epoxide ring opening with alcohols. *Applied Catalysis A: General*, **2019**, *577*, 28–34.

Wednesday Afternoon, October 23, 2019

5:00pm **HC+OX+SS-WeA9 Understanding Metal-Metal and Metal-Support Interactions in Bimetallic Catalysts**, *Donna Chen*, University of South Carolina; *S. Farzandh, D.M. Shkaya, A.J. Brandt, T.D. Maddumapatabandi*, University of South Carolina

INVITED

Bimetallic catalysts are known to exhibit superior properties compared to their individual pure metal components, but in many cases the nature of these improved properties is not well understood. The main goal of this work is to understand how oxidation states, metal-support interactions, and metal-metal interactions in supported bimetallic clusters can be used to control catalytic activity. Specific catalytic reactions investigated are the water gas shift reaction (WGS) on Pt-Re and selective hydrogenation of unsaturated aldehydes on Pt-Sn. Model catalyst surfaces are prepared via vapor-deposition of metal clusters on single-crystal oxide and carbon supports. These surfaces are fully characterized by a variety of ultrahigh vacuum (UHV) surface science techniques and their activities are studied in a microreactor ($P \sim 1$ atm) coupled to the UHV chamber. Scanning tunneling microscopy investigations indicate that exclusively bimetallic clusters can be prepared by sequential deposition of metals. For the WGS reaction, the active site is determined to be Pt with subsurface Re, while Re oxide does not play a role. Density functional theory studies show that the presence of subsurface Re decreases the adsorption energy of CO on Pt, thus preventing Pt active sites from being poisoned by CO. WGS activity increases with increasing perimeter for Pt/TiO₂ clusters, and the turnover frequency is also lower in the absence of the TiO₂ support. For hydrogenation on furfural, the Pt-Sn alloy surface exhibits high selectivity to furfuryl alcohol compared to pure Pt, whereas furan and tetrahydrofuran are the main products on Pt.

Surface Science Division

Room A220-221 - Session SS+AS+HC+OX-WeA

Reactions at Alloy Surfaces and Single Atom Catalysis

Moderators: Erin Iski, University of Tulsa, Bruce E. Koel, Princeton University

2:20pm **SS+AS+HC+OX-WeA1 Correlating Structure and Function for Nanoparticle Catalysts**, *Graeme Henkelman*, University of Texas at Austin

INVITED

Metal nanoparticles of only 100-200 atoms are synthesized using a dendrimer encapsulation technique to facilitate a direct comparison with density functional theory (DFT) calculations in terms of both structure and catalytic function. Structural characterization is done using electron microscopy, x-ray scattering, and electrochemical methods. Combining these tools with DFT calculations is found to improve the quality of the structural models. DFT is also successfully used to predict trends between structure and composition of the nanoparticles and their catalytic function for reactions including the reduction of oxygen and selective hydrogenation. This investigation demonstrates some remarkable properties of the nanoparticles, including facile structural rearrangements and nanoscale tuning parameters which can be used to optimize catalytic rates. In this presentation I will focus on a pair of random alloy bimetallic nanoparticles which have complete different trends in hydrogenation activity as a function of composition. Pd/Au is found to be tunable as a function of composition whereas Pt/Au is not. The reason behind these different behaviors will be discussed.

3:00pm **SS+AS+HC+OX-WeA3 Surface Reactivity of PtAg and PdAg: From Single-Atom Alloys to Supported Nanoparticles**, *Dipna Patel*^{1,2}, Tufts University; *C.R. O'Connor, R.J. Madix, C.M. Friend*, Harvard University; *E.C.H. Sykes*, Tufts University

Catalytic hydrogenation reactions are important in many industrial applications. While Pt and Pd are catalytically active towards hydrogenation, they are often costly, and can suffer from poisoning by CO and coke. Previously, Ag based catalysts have been modified by alloying Pt or Pd for applications in highly selective heterogeneous catalysis. This has shown promise for catalyst design since Ag is cheaper and more resilient to poisoning. It is well known that ensemble size can dramatically change the catalytic pathway, however the atomic-scale structure of PtAg and PdAg alloys and their relation to catalytic activity is still unknown. Using scanning tunneling microscopy (STM) and STM-based spectroscopies, we characterized the surface structure and local geometry of Pt deposited on Ag(111) as a function of alloying temperature. At low temperatures,

intermixing of PtAg is driven by a negative mixing enthalpy, resulting in different metastable states such as isolated Pt atoms in, and islands on, Ag terraces, as well as Pt rich brims located along Ag step edges. Increasing the alloying temperature results in an increased concentration of Pt atoms along Ag steps edges as well as direct exchange of Pt atoms into Ag terraces. At higher temperatures, there is sufficient thermal energy for Pt atoms to fully disperse in the Ag(111) surface layer as isolated atoms, forming single-atom alloys. STM characterization of the surface structure of PdAg alloys reveals the formation of large Pd islands on Ag(111). Using STM, we investigated H₂ activation on active Pd sites and spillover on to Ag(111). The characterization of PtAg and PdAg surface alloys enables us to correlate reaction activity and selectivity to the atomic-scale structure of the alloy and to inform catalyst design that optimizes catalytic selectivity.

3:20pm **SS+AS+HC+OX-WeA4 Single-site Catalysts by Metal-ligand Complexation at Surfaces: From Model Systems in Vacuum to High-pressure Catalysis on Oxide Supports**, *Steven L. Tait*, Indiana University

A grand challenge in heterogeneous catalysis is to achieve high levels of selectivity by controlling the chemical uniformity of metal catalyst sites at surfaces. Our group is working to apply principles of on-surface metal-organic redox assembly to develop a new approach to this problem. Metal-organic coordination networks at surfaces hold promise for selective chemical function, but there is a limited understanding of the chemical reactivity of these systems. Studies of model systems in ultra-high vacuum allow for detailed characterization of the structure and chemistry of these systems. We tested chemical activity of vanadium single-site complexes that are stabilized by tetrazine-based ligands and found activity toward dioxygen activation with a high degree of selectivity compared to vanadium nanoparticles. Reaction with O₂ causes an increase in V oxidation state from V^{II} to V^{IV}, resulting in a single strongly bonded V-oxo product and spillover of O to the Au surface [1]. The metal centers are stabilized in extended, ordered metal-organic complexes that self-assemble through an on-surface redox process on the Au(100) surface and are characterized by X-ray photoelectron spectroscopy, scanning tunneling microscopy, high-resolution electron energy loss spectroscopy, and density functional theory. New results extend these chemical studies to more complex systems that include bimetallic sites and redox isomer systems [2-3], which will also be highlighted in this presentation.

We have also developed synthesis schemes to assemble quasi-square planar metal-organic complexes on high surface area powdered oxides under ambient conditions through a modified wet-impregnation method. X-ray photoelectron spectroscopy measurements demonstrate loading of metal and ligand on the surface and synchrotron-based X-ray absorption spectroscopy measurements of the coordination shell of the metal centers demonstrates single site formation rather than nanoparticle assembly [4-5]. These systems are shown to be active for the catalysis of hydrosilylation reactions at a level that is competitive with current homogeneous catalysts. They also show excellent activity for hydrogenation in flow reactor experiment.

1. Tempas, Morris, Wisman, *et al.*, *Chem. Sci.*, **9**, 1674-1685 (2018). DOI: 10.1039/C7SC04752E

2. Tempas, Skomski, Cook, *et al.*, *Chem. Eur. J.*, **24**, 15852-15858 (2018). DOI: 10.1002/chem.201802943

3. Morris, Huerfano, Wang, *et al.*, *Chem. Eur. J.*, **25**, 5565-5573 (2019). DOI: 10.1002/chem.201900002

4. Chen, Sterbinsky, and Tait, *J. Catal.*, **365**, 303-312 (2018). DOI: 10.1016/j.jcat.2018.07.004

5. Chen, Ali, Sterbinsky, *et al.*, *ChemCatChem*, *in press* (2019). DOI: 10.1002/cctc.201900530

4:20pm **SS+AS+HC+OX-WeA7 Controlling the Local Coordination and Reactivity of Oxide-supported Atomically Dispersed Pt-group Species**, *Phillip Christopher*, University of California at Santa Barbara

INVITED

The synthesis of oxide supported Pt-group catalysts typically produces metal particles with dimensions of a few nanometers. Recent work has shown that Pt-group species can co-exist as nanoparticles and single atoms, and that careful synthetic approaches can produce exclusively single atoms. Interest in the reactivity of supported isolated Pt-group metal atoms stems from the maximized metal utilization efficiency, unique reactivity or selectivity, connection to organometallic catalysis, and the potential for making well-defined active sites. It has proven challenging to characterize the intrinsic catalytic activity of these dispersed active sites on oxide supports at a level that relates local electronic and geometric structure to function. The difficulty arises from their atomic dispersion,

¹ Morton S. Traum Award Finalist

² National Student Award Finalist

Wednesday Afternoon, October 23, 2019

heterogeneity in the local coordination of active sites on most catalysts (i.e. isolated species sit at different sites on the support), dynamic changes in local coordination under reactive environments, and often the low loading of metal that is required to achieve site isolation.

In this talk I will describe a synthetic approach to produce isolated Pt-group atoms that exhibit uniformity in their bonding environment on an oxide support and show how a combination of microscopy, spectroscopy and theory can be used to describe the local coordination of these species. Then I will describe two different approaches to control the local environment of Pt-group atoms: (1) through varied pre-treatment that tunes the local coordination and oxidation state of the single atom, and (2) through the site selective deposition of single atoms near well-defined acid sites on oxide supports. Detailed characterization by a combination of spectroscopy and microscopy is used to develop structure-function relationships for these well-defined single atom active sites in the context of CO oxidation, methanol carbonylation and ethylene hydroformylation. This work highlights the ability to tune the local environment of single Pt-group atom active sites on oxide supports in analogous ways to the engineering of organometallic catalysts.

5:00pm **SS+AS+HC+OX-WeA9 Coordination Defines Reactivity of a Model Single-atom Catalyst: Ir₁/Fe₃O₄(001), Zdenek Jakub¹, J. Hulva, M. Meier, U. Diebold, G.S. Parkinson, TU Wien, Austria**

The development of single-atom catalysts (SACs) was originally motivated by saving of the precious metal, but an equally intriguing characteristic of the ideal SAC is potentially high selectivity due to the high number of identical active sites. The coordination of the active metal center is known to play a crucial role in homogeneous catalysis, and in this talk, I will demonstrate that similar effects can be observed on a model single atom catalyst: Ir₁/Fe₃O₄(001). Using scanning tunneling microscopy (STM), noncontact atomic force microscopy (nc-AFM), temperature programmed desorption (TPD), x-ray photoemission spectroscopy (XPS) and DFT calculations, I will show that the coordination of single Ir₁ adatoms can vary depending on preparation, and that the local environment has dramatic consequences for the ability of the catalyst to adsorb CO. As deposited at room temperature, Ir atoms take 2-fold coordination to the surface oxygen atoms. Upon annealing, they incorporate into the first surface layer (5-fold coordinated Ir₁), and then into the first subsurface layer (6-fold coordinated Ir₁). The 2-fold adatoms can form both monocarbonyls and dicarbonyls, but the 5-fold Ir only binds a single CO. The structures are understood by analogy to square planar Ir(I) and octahedral Ir(III) complexes, respectively. The 6-fold Ir is coordinatively saturated, and thus deactivated for CO adsorption. These results show that control of the local coordination environment is critical to design so-called single-atom catalysts, and that incorporation into the support can be as critical a deactivation mechanism as thermal sintering.

5:20pm **SS+AS+HC+OX-WeA10 Capturing the Early Stages of Oxidation on Low-Index Ni and Ni-Cr Surfaces, William H. Blades, P. Reinke, University of Virginia**

The early stages of oxidation and corrosion of alloys control the structure and development of the oxide layer and therefore decisively influence its protective function. To this end, we have studied the nanoscale evolution of surface oxides prior to the formation of a complete layer. The oxidation of Ni(100), Ni(111), and Ni-Cr(100), Ni-Cr(111) surfaces was captured by sequential oxidization and measured with scanning tunneling microscopy/spectroscopy (STM/STS). The early-stage oxidation, and the influence of alloy composition and crystallographic orientation on surface reactivity, was studied by comparing pure Ni(100/111) and Ni-Cr(100/111) surfaces. Alloy thin films (8-18 wt.% Cr) were prepared on MgO(100/111) and exposed to oxygen up to 400 L at 773 K. Under these conditions, oxide nucleation is predicated by the development of oxygen adlayers on both the pure Ni(100/111) surfaces. The formation of a c(2x2)-O chemisorbed phase on the Ni(100) surface causes the step edges to facet into {100} segments, kinetically limiting NiO growth. However, no such faceting is observed on the Ni(111) surface and the nucleation and growth of NiO begins after only 300 L of O₂. Our experiments demonstrate that the addition of small amounts of Cr completely change the oxidation pathways. On the Ni-Cr(100) surface, the nucleation and growth of NiO initiates along the step edges, forming low-angle NiO wedges with a NiO-Ni(7x8) superstructure. Terrace oxide growth commences with the nucleation of small oxide particles, driven by the presence of Cr, which grow into large oxide nodules after further oxidation. NiO growth extends into the terraces

and takes a NiO-Ni(6x7) cube-on-cube interfacial relationship. Several novel surface reconstructions are observed and are tentatively attributed to Cr(100)-O reconstructions, suggesting surface segregation and phase separation of BCC Cr. Similarly, nano-sized oxide particles nucleate on the Ni-Cr(111) terrace and step edges, while single atomic NiO rows extend across the surface. Oxide nodules, similar to those found on the Ni-Cr(100) surface are observed and grow laterally along the terraces. Each of these aforementioned surface oxides present unique electronic signatures, and STS maps are used to quantify the spatial variations in their density of states and band gaps. The electronic heterogeneity of the surface underscores that the use of a homogenous electric field to capture oxidation kinetics at the alloy-oxide interface should be revisited.

5:40pm **SS+AS+HC+OX-WeA11 Evolution of Steady-state Material Properties during Catalysis: Oxidative Coupling of Methanol over Nanoporous Ag_{0.03}Au_{0.97}, Matthijs van Spronsen, Lawrence Berkeley National Laboratory; B. Zugic, Harvard University; M.B. Salmeron, Lawrence Berkeley National Laboratory; C.M. Friend, Harvard University**

Activating pretreatments can be used to tune both surface composition and surface structure of bimetallic alloy catalysts. Careful selection of both gas mixtures and reaction temperatures can lead to surfaces that are able to achieve optimum selectivity and activity under steady-state reaction conditions. The activation-induced changes in material properties of a nanoporous (np) Ag_{0.03}Au_{0.97} alloy and their subsequent evolution under steady-state conditions for CH₃OH oxidation are presented. Initial activation by oxidation in O₃ at 423 K leads to the formation of AgO and Au₂O₃ driving a strong Ag enrichment in the near-surface region, based on ambient-pressure X-ray photoelectron spectroscopy (AP XPS) and extended X-ray absorption fine structure (EXAFS) analysis. Exposing this oxidized np Ag_{0.03}Au_{0.97} to the O₂/CH₃OH reaction mixture reduces both Ag and Au oxides and results in a surface alloy locally highly enriched in Ag. Both the oxides and the highly Ag enriched alloy unselectively oxidize methanol to CO₂. However, at the reaction temperature of 423 K, the Ag slowly realloys with Au. Although decreasing, the composition remains enriched in Ag in the top few nanometers under steady-state conditions. The Ag content in the surface is 29 at.% in steady state and the desired product, methyl formate, is selectively produced without significant deactivation. The activation and evolution of the active phase is not uniform: nanometer-scale patches of AgO, leading locally to Ag-rich alloys, were observed with environmental transmission electron microscopy (E TEM). These local Ag-rich AgAu alloy regions are critical for initiation of the catalytic cycle through O₂ dissociation. Calculations based on density-functional theory (DFT) indicate that the O on the surface assist in stabilizing the Ag. Moreover, an essential factor for retaining this local enrichment in Ag is the modest reaction temperature of 423 K. At higher temperatures, bulk diffusion induces sintering and redistribution of the Ag, leading to a loss of activity. These findings demonstrate that material properties determining catalytic activity are *dynamic* and that metastable (kinetically trapped) forms of the material may be responsible for catalysis. Hence, catalytic activity and selectivity depend on the pretreatment, reaction temperature and gas composition. These observations provide guiding principles concerning the activation of heterogeneous catalysts for selective oxidation.

6:00pm **SS+AS+HC+OX-WeA12 Reduction and Oxidation of Transition Metal Oxides: From Tailoring the Surface and Interface Properties to the New Crystalline Phases Formation, Dominik Wrana, Jagiellonian University, Poland; C. Rodenbücher, Forschungszentrum Jülich GmbH, Germany; K. Cieřlik, B.R. Jany, Jagiellonian University, Poland; K. Szoł, Forschungszentrum Jülich GmbH, Germany; F. Krok, Jagiellonian University, Poland**

In the recent years transition metal oxides have attracted tremendous interest, mostly due to the manifold real applications, ranging from (photo)catalysis, through memristive and neuromorphic device development, to energy storage and production. A specific quality which makes them so versatile is the ease by which their electronic and structural properties can be controlled by changing a cation's reduction state.

In this presentation we will present an overview of the impact that thermal reduction and oxidation have on the surface properties, which enable a precise control over the valence state of prototypical binary and ternary oxide representatives: TiO₂ and SrTiO₃. We will focus on the preparation methods under regular UHV conditions and upon additionally reduced oxygen partial pressure.

Reduction of both crystals results in the formation of oxygen vacancies and therefore d-electrons, which leads to changes in the work function and a

¹ Morton S. Traum Award Finalist

Wednesday Afternoon, October 23, 2019

corresponding rise in electrical conductivity, which could be tuned over many orders of magnitude [1]. A newly developed SPM-based technique, combining LC-AFM and KPFM, allows both measurements to probe the same area of the reduced $\text{TiO}_2(110)$ surface [2], helping understanding of the nanoscale resistive switching. Besides the change in electrical properties, the surface structure evolves towards nonstoichiometric reconstructions [1], due to the increased oxygen deficiency. Surprisingly, not only is oxygen flow possible during UHV annealing of the oxide crystal, but also incongruent cation sublimation can be triggered, as demonstrated for the perovskite oxides like SrTiO_3 [3]. Extremely low oxygen partial pressure (ELOP), achieved by the use of an oxygen-getter, initiates SrTiO_3 crystal decomposition and the formation of stable monocrystalline cubic TiO nanowires with a $c(4 \times 4)$ reconstructed surface [4]. Such bottom-up growth of conductive TiO nanostructures could be an alternative to other costly methods, resulting in the creation of the $\text{TiO}/\text{SrTiO}_3$ interface, with a sharp transition between Ti^{2+} and Ti^{4+} states, proven by atomically-resolved electron microscopy. This oxide heterostructure provides an interesting metal/insulator junction with a 0.6 eV work function difference [5], opening many new possibilities for (photo)catalysis and aiding in the search for exotic interface states.

[1] Wrana, D. et al. (2018) *Applied Surface Science*, 432, 46-52.

[2] Rodenbücher, C. et al. (2018) *APL Materials*, 6(6), 066105.

[3] Rodenbücher, C. et al. (2017) *physica status solidi (RRL)—Rapid Research Letters*, 11(9), 1700222.

[4] Wrana, D. et al. (2019) *Nanoscale*, 11(1), 89-97.

[5] Wrana, D. et al. (2019) *Beilstein Arch.*, 201912.

2D Materials

Room A216 - Session 2D+EM+MI+NS+QS+SS-ThM

Dopants, Defects, and Interfaces in 2D Materials

Moderator: Evan Reed, Stanford University

8:00am **2D+EM+MI+NS+QS+SS-ThM1 Interfacial Engineering of Chemically Reactive Two-Dimensional Materials, Mark Hersam, Northwestern University** **INVITED**

Following the success of ambient-stable two-dimensional (2D) materials such as graphene and hexagonal boron nitride, new classes of chemically reactive layered solids are being explored since their unique properties hold promise for improved device performance [1]. For example, chemically reactive 2D semiconductors (e.g., black phosphorus (BP) and indium selenide (InSe)) have shown enhanced field-effect mobilities under controlled conditions that minimize ambient degradation [2]. In addition, 2D boron (i.e., borophene) is an anisotropic metal with a diverse range of theoretically predicted phenomena including confined plasmons, charge density waves, and superconductivity [3], although its high chemical reactivity has limited experimental studies to inert ultrahigh vacuum conditions [4-7]. Therefore, to fully study and exploit the vast majority of 2D materials, methods for mitigating or exploiting their relatively high chemical reactivity are required [8]. In particular, covalent organic functionalization of BP minimizes ambient degradation, provides charge transfer doping, and enhances field-effect mobility [9]. In contrast, noncovalent organic functionalization of borophene leads to the spontaneous formation of electronically abrupt lateral organic-borophene heterostructures [10]. By combining organic and inorganic encapsulation strategies, even highly chemically reactive 2D materials (e.g., InSe) can be studied and utilized in ambient conditions [11].

[1] A. J. Mannix, *et al.*, *Nature Reviews Chemistry*, **1**, 0014 (2017).

[2] D. Jariwala, *et al.*, *Nature Materials*, **16**, 170 (2017).

[3] A. J. Mannix, *et al.*, *Nature Nanotechnology*, **13**, 444 (2018).

[4] A. J. Mannix, *et al.*, *Science*, **350**, 1513 (2015).

[5] G. P. Campbell, *et al.*, *Nano Letters*, **18**, 2816 (2018).

[6] X. Liu, *et al.*, *Nature Materials*, **17**, 783 (2018).

[7] X. Liu, *et al.*, *Nature Communications*, **10**, 1642 (2019).

[8] C. R. Ryder, *et al.*, *ACS Nano*, **10**, 3900 (2016).

[9] C. R. Ryder, *et al.*, *Nature Chemistry*, **8**, 597 (2016).

[10] X. Liu, *et al.*, *Science Advances*, **3**, e1602356 (2017).

[11] S. A. Wells, *et al.*, *Nano Letters*, **18**, 7876 (2018).

8:40am **2D+EM+MI+NS+QS+SS-ThM3 Effects of Mn Doping on the Surface Electronic Band Structure and Bulk Magnetic Properties of ZnS and CdS Quantum Dot Thin Films, Thilini K. Ekanayaka¹, G. Gurung, University of Nebraska-Lincoln; G. Rimal, Rutgers University; S. Horoz, Siirt University, Turkey; J. Tang, T. Chien, University of Wyoming; T. Paudel, A.J. Yost, University of Nebraska-Lincoln**

Semiconducting quantum dots (QDs) are desirable for solar cells due to the ability to tune the band gap by changing the QD size without changing the underlying material or synthesis technique. Doping QDs with a transition metal is one way of further tailoring the electronic band structure and magnetic properties of QDs in order to improve overall device performance. Understanding the mechanisms causing the change in the electronic band structure and magnetic properties due to transition metal doping is important to device-by-design schemes. In this study, we measure the effects of Mn dopants on the surface electronic band structure of ZnS and CdS QDs using scanning tunneling microscopy/spectroscopy and photoemission spectroscopy. In both the ZnS and CdS systems, a decrease in band gap upon introduction of Mn is observed. Additionally, a rigid band shift was observed in ZnS upon Mn doping. It is argued, using X-ray photoemission spectroscopy, that the rigid band shift is due to a hole-doping mechanism caused by the formation of Zn vacancies accompanied by a Mn³⁺ oxidation state which leads to the reduction in total S vacancies as compared to the undoped ZnS system. No band shift was observed in CdS upon Mn doping, but a strong sp-d hybridization takes place which results in a significant band gap reduction. Furthermore, induced midgap states originating from the Mn dopant appear in the surface electronic band structure of Mn: CdS. Measurements of the magnetization of Mn doped and undoped ZnS and CdS confirms the

presence of d⁰ ferromagnetism. The magnetization is reduced and the coercive field is increased post Mn doping which suggests the anti-ferromagnetic alignment of Mn dopant atoms. Density Functional Theory calculations support the Mn anti-ferromagnetic alignment hypothesis and a ground state with Mn in the 3⁺ valence. This study provides important information on the role of dopants and vacancies in dilute magnetic semiconductor quantum dot materials for applications in photovoltaics and spintronics.

9:00am **2D+EM+MI+NS+QS+SS-ThM4 Interaction of Molecular O₂ with Organolead Halide Nanorods by Single-Particle Fluorescence Microscopy, Juvinch Vicente, J. Chen, Ohio University**

The photoluminescence (PL) of organolead halide perovskites (OHPs) is sensitive to its surface conditions, especially surface defect states, making the PL of small OHP crystals an effective way to report their surface states. At the ensemble level, when averaging a lot of nanocrystals, the photoexcitation of OHP nanorods under inert nitrogen (N₂) atmosphere leads to PL decline, while subsequent exposure to oxygen (O₂) results to reversible PL recovery. At the single-particle level, individual OHP nanorods photoblinks, whose probability is dependent on both the excitation intensity and the O₂ concentration. Combining the two sets of information, we are able to quantitatively evaluate the interaction between a single surface defect and a single O₂ molecule using a kinetic model. This model provides fundamental insights that could help reconcile the contradicting views on the interactions of molecular O₂ with OHP materials and help design a suitable OHP interface for a variety of applications in photovoltaics and optoelectronics.

9:20am **2D+EM+MI+NS+QS+SS-ThM5 Complementary Growth of 2D Transition Metal Dichalcogenide Semiconductors on Metal Oxide Interfaces, T.E. Wickramasinghe, Gregory Jensen, R. Thorat, Nanoscale and Quantum Phenomena Institute; S.H. Aleithan, Nanoscale and Quantum Phenomena Institute, Saudi Arabia; S. Khadka, E. Stinaff, Nanoscale and Quantum Phenomena Institute**

A chemical vapor deposition (CVD) growth model will be presented for a technique resulting in naturally formed 2D transition metal dichalcogenide (TMD) based metal-oxide-semiconductor structures. The process is based on a standard CVD reaction involving a chalcogen and transition metal oxide-based precursor. Here however, a thin metal oxide layer, formed on lithographically defined regions of a pure bulk transition metal, serves as the precursor. X-ray diffraction and cross-sectional SEM studies show insight into the type and thickness of the metal oxide created during optimal growth conditions. The chalcogen reacts with the metal oxide, forming TMD material which migrates outward along the substrate, leading to lateral growth of highly-crystalline, mono-to-few layer, films. In addition to displaying strong luminescence, monolayer Raman signatures, and relatively large crystal domains, the material grows deterministically and selectively over large regions and remains connected to the bulk metallic patterns, offering a scalable path for producing as-grown two-dimensional materials-based devices.

9:40am **2D+EM+MI+NS+QS+SS-ThM6 Kagome-type Lattice Instability and Insulator-metal Transition in an Alkali-doped Mott Insulator on Si(111), Tyler Smith, H. Weitering, University of Tennessee Knoxville**

The 1/3 ML monolayer (ML) 'alpha phase' of Sn on Si(111) is a remarkable platform for the study of strong correlations in a spin 1/2 triangular adatom lattice. In this work, we employ an adatom doping scheme by depositing potassium onto the triangular Sn lattice. The K-atoms destabilize the parent Mott insulating phase and produce a charge-ordered insulator, revealing a rare Kagome lattice at the surface. Scanning Tunneling Microscopy and Spectroscopy reveal a phase transition from an insulating kagome lattice to a metallic triangular lattice at about 200 K. DFT band structure calculations for this kagome system [J. Ortega et al., unpublished] reveal the presence of a flat-band just below the Fermi level, making this novel system a compelling platform for hole-doping studies of magnetic and/or superconducting instabilities.

11:00am **2D+EM+MI+NS+QS+SS-ThM10 Chemical Migration and Dipole Formation at TMD/TI Interfaces, Brenton Noesges, T. Zhu, The Ohio State University; D. O'Hara, University of California, Riverside; R. Kawakami, L.J. Brillson, The Ohio State University**

Proximity effects at the interface between two materials can induce physical properties not present in either material alone. Topological insulators (TIs) such as Bi₂Se₃ with non-trivial surface states are sensitive to interface proximity effects where overlayers and adsorbates can act as a dopant source, chemically interact with the TI surface, or couple across the

¹ National Student Award Finalist

Tl surface states leading to novel quantum phases. Transition metal dichalcogenides (TMDs), a class of 2D van der Waals materials, are a promising candidate to control this interface given the shared general hexagonal symmetry and wide range of TMD properties. However, the interface between TMDs and Bi₂Se₃ can be more complex than the ideal van der Waals interface. Chemical species exchange like metal cation exchange and selenium migration from substrate to growing film can impact the structure and properties of either layer. Self-assembly mechanisms have also been observed where complete metal monolayers form inside the Bi₂Se₃ quintuple layer [1]. We used x-ray photoelectron spectroscopy (XPS) connected in vacuo via UHV suitcase to a molecular beam epitaxy (MBE) system to investigate chemical interaction at the interface between selenide TMDs and Bi₂Se₃. Air-free transferring is crucial to minimize contamination at the interface and prevent oxidation in the air-sensitive TMDs. We compare the effects of ultrathin pure Mn metal overlayers and monolayer MnSe_x on Bi₂Se₃ to pristine Bi₂Se₃. In the case of pure Mn metal on Bi₂Se₃, Bi core levels exhibit a 1.7 eV shift toward lower binding energies while the Mn core levels also show signs of Mn-Se bonding. These core level changes indicate that, in the absence of excess Se during growth, Mn pulls Se from the substrate leaving behind Bi₂ bilayers near the surface. Depositing a monolayer of MnSe_x produces very different results than the pure metal case. Bi₂Se₃ core levels measured below the monolayer MnSe_x film exhibit a rigid 0.8 eV chemical shift toward higher binding energies indicative of surface/interface dipole formation. The presence of this dipole is likely due to growth of primarily α -MnSe instead of the 1T-MnSe₂ 2D phase [2]. Scanning tunneling microscopy (STM) height maps and spectroscopy data provide further evidence of majority α -MnSe formation. XPS core level analysis combined with controlled depositions, air-free transfers and surface analysis can provide a consistent explanation of chemical diffusion and dipole formation at a TMD/Tl interface. This work is supported by NSF MRSEC under award number DMR-1420451.

[1] J. A. Hagmann et al., *New J. Phys.* 19, 085002 (2017).

[2] D.J. O'Hara et al. *Nano Lett.*, 18(5), 3125-3131 (2018).

11:20am **2D+EM+MI+NS+QS+SS-ThM11 Atomically Resolved Electronic Properties of Defects in the in-plane Anisotropic Lattice of ReS₂**, *Adina Luican-Mayer*, University of Ottawa, Canada

Among the layered transition metal dichalcogenides, the compounds that exhibit in-plane anisotropy are of particular interest as they offer an additional tuning knob for their novel properties. In this talk, we present experimental evidence of the lattice structure and properties of semiconducting ReS₂ by using scanning tunneling microscopy and spectroscopy (STM/STS). We demonstrate that rhenium atoms form diamond-shaped clusters, organized in disjointed chains and characterize the semiconducting electronic band gap by STS. When imaging the surface of ReS₂, we encounter "bright" or "dark" regions indicating the presence of charged defects that will electrostatically interact with their environment. By spatially mapping the local density of states around these defects, we explore their origin and electrostatic nature. Experimental results are compared with ab-initio theory.

12:00pm **2D+EM+MI+NS+QS+SS-ThM13 Size-independent "Squeezed" Shape of Metal Clusters Embedded Beneath Layered Materials**, *A. Lii-Rosales*, Ames Laboratory and Iowa State University; *S. Julien, K.-T. Wan*, Northeastern University; *Y. Han*, Ames Laboratory and Iowa State University; *K.C. Lai*, Iowa State University; *M.C. Tringides, J.W. Evans, Patricia A. Thiel*, Ames Laboratory and Iowa State University

We have developed a continuum elasticity model for metals embedded beneath the surfaces of layered materials. The model predicts that the equilibrated cluster shape is invariant with size, manifest both by constant side slope and by constant aspect ratio (width:height ratio). This prediction is rationalized by dimensional analysis of the relevant energetic contributions. The model is consistent with experimental data for Cu and Fe clusters embedded in graphite, especially in the limit of large clusters. For comparison, we have performed a Winterbottom analysis of the equilibrium shape of an uncovered Cu cluster supported on top of graphite. The aspect ratio of the embedded cluster is about an order of magnitude higher than that of the supported cluster. Analysis of key energetics indicates that this is due to the strain energy (resistance to deformation) of the top graphene membrane, which effectively squeezes the metal cluster and forces it to adopt a relatively low, flattened shape. These insights may be useful for developing components such as metallic heat sinks or electrodes in electronic devices that use two-dimensional or layered materials.

Fundamental Aspects of Material Degradation Focus Topic Room A212 - Session DM+BI+SS-ThM

Material Stabilities and Technology for Degradation Protection

Moderators: Markus Valtiner, Vienna University of Technology, Austria, Gareth S. Parkinson, TU Wien, Austria

8:00am **DM+BI+SS-ThM1 Extremely Thin Protective Oxide Layer for Reflective Silver Thin Films**, *Midori Kawamura, E. Kudo, Y. Sasaki, T. Kiba, Y. Abe, K.H. Kim*, Kitami Institute of Technology, Japan; *H. Murotani*, Tokai University, Japan

Silver (Ag) thin films possess high electrical and optical properties, but their low stability should be resolved. We have developed a highly stable Ag thin film where thermal agglomeration can be suppressed, by utilizing nanometer thick surface Al layers. Then we have confirmed that Al surface nanolayer deposited Ag films show a high optical reflectance as well as Ag single film. Here, the Al nanolayer was oxidized to be Al oxide nanolayer, being transparent in visible region, by natural oxidation in air. In the present study, we investigate durability of the Ag films with surface nanolayers under high humidity condition.

We prepared Ag single layer (150 nm), Ti (1, 3 -nm) / Ag films and Al (1, 3 -nm) / Ag films on glass substrate by rf magnetron sputtering in Ar discharge. In addition, vacuum evaporation method was also used for the preparation of Al (1, 3 -nm) / Ag films. A difference on degradation of the films by different fabrication methods was investigated. The samples were kept for 16 hrs in a chamber where temperature and humidity was set to 55°C and 90%RH, respectively.

After the test, agglomeration occurred in Ag single layer and optical reflectance was decreased. On the other hand, Ti or Al nanolayer covered Ag films kept smooth surface even after the test. The surface roughness observed using AFM was as small as 1.0 nm. As a result, we have found that both Al and Ti surface nanolayers can play significant role as protective layer under high humidity condition. However, Ti / Ag films showed a lower reflectance due to light absorption by TiO₂ layer formed on the surface, and the samples with Al surface nanolayer showed a higher optical reflectance.

By XPS analysis, very thin Ag sulfide formation was observed in Ag single film after the humidity test, but not in Ti or Al covered Ag films. This suggests very thin Al oxide or Ti oxide nanolayer prevented contact of Ag atoms and SO₂ gas in air. However, Ag signal was detected in the surface oxide layers, which indicates onset of outward diffusion of Ag atoms.

8:20am **DM+BI+SS-ThM2 Influence of the Electric Double Layer on Degradation of Materials**, *Dominik Dworschak, M. Valtiner*, Vienna University of Technology, Austria

Corrosion and adhesion science usually focuses on the solid side of a liquid/solid or solid/adhesive interface. However, the only some nanometer thick interface itself is the complex transition region which drives many important processes in corrosion and delamination. The electric double layer (EDL) is a key part of the interfacial region but remains mostly neglected as a potential key player in degradation processes. Here, we will demonstrate that the EDL has an important influence on the corrosion mechanism of passivating materials in the transpassive region (material dissolution at potentials where the passive film breaks down).

We utilize an electrochemical flow cell combined with an inductively coupled mass spectrometer (ICP-MS) to enable the in-situ study of the time-resolved release of elements into solution. This provides detailed insights into the nature of the passive and transpassive condition. As model systems, we use nickel based alloys. These are essential to modern industry and uniquely tailored for a wide range of applications, which rely on high corrosion and heat resistance. In particular, we polarized a series of Ni₇₅Cr₁₆Fe₉, Ni₈₆Cr₅Fe₉ as well as Ni₇₄Cr₁₆Fe₉Mo₁ model alloys in order to understand the effect of chromium concentration and molybdenum on transpassive dissolution

In the transpassive regime we can detect the presence of protective species of chromium and molybdenum on the surface. Unexpectedly, we can demonstrate significant corrosion resistance above a critical potential where the passive film breaks down. This is traditionally known as transpassive region with bulk dissolution of metal alloys. However, we find that the EDL forms a transient passivating solution side protective layer in the transpassive region – i.e. we characterize an electric double layer induced corrosion resistance, which solely – and surprisingly – lies in the structure of the solution side. This finding has general important implications for designing degradation resistance in highly corrosive environments.

8:40am **DM+BI+SS-ThM3 Key Issues for the Stability of Protective Surface Oxides**, *Philippe Marcus*, CNRS - Chimie ParisTech, France **INVITED**

This lecture will focus on a surface science approach of corrosion and protection of metals and alloys, with emphasis on the structure and growth of surface oxide layers, a central theme in corrosion science.

Understanding early stage oxidation of metal surfaces at atomic or nanometric scale is a key to a better design and an improved control of engineering metals.

The following topics will be addressed:

- Nanostructure of ultra-thin oxide layers (passive films) on metals,
- Early stage oxidation of stainless steels,
- Local electronic properties of passive films,
- Mechanisms of initiation of localized corrosion, with emphasis on the role of surface defects in localized attack leading to corrosion,

The data that will be presented are obtained by using *in situ* Scanning Tunneling Microscopy (STM), Scanning Tunneling Spectroscopy (STS), X-Ray Photoelectron Spectroscopy (XPS), Time-of-Flight Secondary Ions Mass Spectrometry (ToF-SIMS) combined with electrochemical techniques and DFT calculations.

9:20am **DM+BI+SS-ThM5 Controlling and Observing Localized Dealloying Corrosion and Dissolution via Lateral Modification of Surfactant Inhibitor Layers**, *S. Neupane*, Hasselt University, Belgium; *Frank Uwe Renner*, IMEC vzw. Division IMOMEC, Belgium

Corrosion processes on metals and alloys may result in substantial degradation and loss of functionality. Mitigation strategies include alloy design, to allow for passivation, or the application of inhibitors to protect materials but they are often causing irreversible damage and potential catastrophic failure at more severe corrosion conditions. The ultimate understanding of the involved fundamental processes including the initial stages of corrosion attacks is still lacking, in particular on the important atomic and molecular scale. Surfactant inhibitors protect surfaces from corrosion by forming molecular layers or so-called self-assembled monolayers separating the material from the corrosive environment. Yet, with inhibitors *localized dealloying* takes place at higher electrochemical potentials [1]. To address the fundamental nature of the site of initiation of dealloying corrosion we have recently introduced different strategies for novel surface-science approaches [2]. On the one hand the inhibitor layer can be laterally modified by using a sequential application combining different steps of micro-contact printing and solution backfilling [3]. In consequence an array of artificial defects such as patch boundaries or displacements by overprinting using foreign impurity molecules can be obtained in a well-controlled way. On the other hand the molecular stability may be locally probed by molecular-scale force measurements employing AFM techniques. In the retract force curve molecular fishing events are eventually visible which can be correlated to the inhibition efficiency. We here exemplify both aspects on noble metal model systems such as Cu-Au and more reactive surfaces including Cu-Zn and pure Cu. On Cu-Au surfaces initial dealloying pits are occurring along patch boundaries formed by sequential application of thiol inhibitors [4]. On Cu surfaces we applied different mercapto-benzimidazoles and could indeed link the observed layer stability with the actual corrosion behavior.

[1] A. Pareek et al., *J. Am. Chem. Soc.* 133 (2011) 18264–18271. [2] B. Shrestha et al., *Faraday Discuss.* 180 (2015), 191. [3] S. Neupane et al., *Langmuir*. 34 (2018) 66–72. [4] S. Neupane et al., submitted.

9:40am **DM+BI+SS-ThM6 *In Situ* Characterization of Interactions at Polymer/Metal Oxide Interfaces Under Aqueous Conditions by a Spectro-electrochemical Approach**, *Sven Pletincx*, Vrije Universiteit Brussel, Belgium; *L.-L. Fockaert, J.M.C. Mol*, Delft University of Technology, Netherlands; *H. Terryn, T. Hauffman*, Vrije Universiteit Brussel, Belgium

The mechanisms governing coating/metal oxide delamination are not yet fully understood, although strong and durable adhesive interactions at the interface are considered to be an important prerequisite for good coating durability. Achieving adequate adhesion strengths between an organic and inorganic system in various operating conditions is one of the complex challenges of interface engineering. However, obtaining local chemical information at this solid/solid interface is challenging, since common surface sensitive analysis techniques only operate under vacuum conditions, making it impossible to probe environmental effects *in situ*.¹

The analysis of this so-called buried interfaces is achieved by characterizing ultrathin polymer films onto a metal oxide substrate by ambient-pressure photoelectron spectroscopy (APXPS).² Here, we show that APXPS with a

conventional X-ray source can be used to study the effects of water exposure on the interaction of acrylic coatings with aluminum oxide. This is done by making the polymer layer sufficiently thin to probe the interface non-destructively.

A *spectroelectrochemical* setup of *in situ* ATR-FTIR Kretschmann and Odd Random Phase Electrochemical Impedance Spectroscopy (ORP-EIS) on a complementary model system is used to characterize and monitor the formed bonds at the metal oxide/polymer interface.³ A nanometer thin aluminum layer is sputtered on an IR transparent crystal, such that the IR signal reaches the oxide/polymer interface, obtaining a near-interface spectrum. This way, we have direct access to the interface, and the influence of an above-the-polymer electrolyte (i.e. H₂O) is probed. Simultaneously the protective properties and corrosion processes of the overall hybrid system are monitored by ORP-EIS.

This work shows that by using ultrathin films in combination with a set of recently developed techniques, it is possible to non-destructively and *in situ* probe interfacial changes in hybrid systems.

1. Watts, J. F. The Interfacial Chemistry of Adhesion: Novel Routes to the Holy Grail? *Adhes. Curr. Res. Appl.* 1–16 (2006). doi:10.1002/3527607307.ch1

2. Pletincx, S. *et al.* In Situ Characterization of the Initial Effect of Water on Molecular Interactions at the Interface of Organic/Inorganic Hybrid Systems. *Sci. Rep.* 7, 45123 (2017).

3. Pletincx, S. *et al.* In Situ Methanol Adsorption on Aluminum Oxide Monitored by a Combined ORP-EIS and ATR-FTIR Kretschmann Setup. *J. Phys. Chem. C* 122, 21963–21973 (2018).

11:00am **DM+BI+SS-ThM10 Design of Corrosion Resistant High Entropy Alloys**, *Gerald Frankel*, C.D. Taylor, W. Windl, The Ohio State University; *J.R. Scully*, University of Virginia; *J. Locke*, The Ohio State University; *P. Lu*, Questek Innovations **INVITED**

The corrosion resistance of a metal alloy is dictated by the exposure environment as well as the alloy structure, composition, and details of the surface condition such as the presence of a passive film. The design of new alloys with improved corrosion resistance must take all of these factors into account. As a result, the degrees of freedom in alloy design are so numerous that the standard process of trial and error is extremely lengthy, even using high throughput methods. This is particularly true for emerging materials such as high entropy alloys (HEAs) and bulk metallic glasses. The complexity of the corrosion process makes integrated computational materials engineering (ICME) for corrosion resistance very challenging. In this work we describe an approach for design of corrosion resistant alloys (CRAs) using ICME. The work has focused on HEAs because of the vast, multidimensional compositional and processing space associated with HEAs. The ultimate goal of CRA design is a combination of multiscale, multiphysics models that accurately describe the details of each of the controlling mechanisms and chemical/physical interactions in the degradation process. However, progress can be made using computational approaches coupled with empiricism. Calculation of Phase Diagrams (CalPhaD) methods are extremely useful in this regard. Furthermore, a number of relevant calculable parameters, such as metal-metal and metal-oxygen bond strength or chloride ion adsorption energies, can be used to create correlations with corrosion metrics that enable prediction of corrosion properties of alloys in previously unexplored compositional space. We will present the methodology used for the design of an extremely corrosion resistant HEA as well as a series of HEAs that are less resistant, but allow for the assessment of critical parameters controlling corrosion resistance in HEAs.

11:40am **DM+BI+SS-ThM12 Determination of Hydrogen in High Strength Steels using Scanning Kelvin Probe Force Microscopy**, *Ines Traxler*, G. Schimo-Aichhorn, CEST Competence Centre for Electrochemical Surface Technology, Austria; *A. Muhr, G. Luckeneder, H. Duchaczek, K.-H. Stellnberger*, voestalpine Stahl GmbH, Austria; *D. Rudomilova, T. Prosek*, University of Chemistry and Technology Prague, Czech Republic; *B. Lutzer*, CEST Competence Centre for Electrochemical Surface Technology, Austria; *D. Stifter, S. Hild*, Johannes Kepler University Linz, Austria

High-strength steels are important materials for the automotive industry. Due to their good formability and high strength they are used for the manufacture of light weight and fuel-efficient automotive parts. A disadvantage of high strength steels is their proneness to hydrogen embrittlement. Even small amounts of hydrogen can cause a deterioration of mechanical properties. Therefore, the effect of hydrogen on the steel microstructure is of great interest and it is important to study and visualize

Thursday Morning, October 24, 2019

the effects and mechanisms of hydrogen in steels. For this purpose, Scanning Kelvin Probe Force Microscopy (SKPFM) is a promising technique for the investigation of hydrogen in the steel microstructure with a very good spatial resolution.

Hydrogen diffusion in different high-strength steels was investigated using SKPFM. Hydrogen entry at cut edges and coating defects was studied as well as the influence in the individual steel grains. The measurements were carried out with different salt solutions on the backside of CP1000 (complex phase), DP1000 (dual phase) and zinc coated DP1000 steels to induce corrosion and promote hydrogen entry into the steel. The permeating hydrogen was measured on the upper side of the sample by repeated surface scans and the effect on the contact potential difference (CPD) was studied. Furthermore, SKPFM measurements with different relative humidity were carried out, monitoring the effects of corrosion. Additionally, Scanning Kelvin Probe (SKP) measurements were done for comparison.

With SKPFM, the preferred diffusion pathways of hydrogen through the steel microstructure could be visualized as well as the effect of zinc coatings on hydrogen permeation.

12:00pm **DM+BI+SS-ThM13 Reflection Mode Interferometry for studying interfacial processes**, *Kai Schwenzfeier, P. Bilotto, M. Lengauer, C. Merola, H.-W. Cheng, M. Valtiner*, TU Wien, Austria

Molecular level processes at electrified solid|liquid interfaces play a critical role in corrosion and degradation processes. These include adsorption of ions, evolution of electrochemical double layers, oxidation/dissolution of metals, screening effects as well as liquid properties at an interface. However those processes/effects are notoriously hard to measure due to long integration times or too small probe with many available analysis techniques.

We refined Multiple Beam Interferometry (MBI) to enable time resolved in-situ and operando measurement of processes at solid|liquid interfaces in both transmission and reflection geometry. In this presentation dynamic interfacial processes such as changes of refractive indices in small (nanometer sized gaps), a micro-to-angstrom scale view into corrosion processes and surface oxidation, as well as specific and non-specific potential driven ion adsorption in aqueous solutions will be discussed in detail. We will relate these measurements to molecular resolution AFM imaging and force spectroscopy at solid|liquid interfaces.

Fundamental Discoveries in Heterogeneous Catalysis Focus Topic

Room A213 - Session HC+2D+SS-ThM

Nanoscale Surface Structure in Heterogeneously-Catalyzed Reactions

Moderators: Rebecca Fushimi, Idaho National Laboratory, Eric High, Tufts University

8:20am **HC+2D+SS-ThM2 Low-temperature Investigation of Propylene on TiO₂/Au(111)**, *M. Gillum, M. DePonte, J. Wilke, E. Maxwell, V. Lam, D. Schlosser, Ashleigh Baber*, James Madison University

The partial oxidation of propylene creates industrially important feedstocks that are used in a multitude of chemical fields ranging from textiles to cosmetics to air sanitation. One avenue of research on propylene oxidation is being conducted using metal/oxide model catalysts, as they have shown an affinity for high selectivity oxidation reactions. To gain a comprehensive understanding of olefin intermolecular and surface interactions, temperature programmed desorption (TPD) studies were conducted using Au(111)-based model catalysts with different surface preparations. Using TPD, we were able to identify the specific adsorption sites of propylene on a TiO₂/Au(111) model catalyst, differentiating between the TiO₂ nanoparticles, the Au-TiO₂ interface, and the gold surface. Desorption kinetics propylene were studied on pristine and titania-modified Au(111) surfaces. Desorption products were monitored using quadrupole mass spectrometry and the surface morphology was analyzed using ex-situ atomic force microscopy. The presence of titania was confirmed via X-ray photoelectron spectroscopy. By understanding the characteristic behaviors with combined experimental techniques, active sites and reaction pathways for partial olefin oxidation over Au-based catalysts may be identified.

8:40am **HC+2D+SS-ThM3 Structure and Reactivity of Supported Oxide and Metal Nanoparticles**, *Geoff Thornton*, University College London, UK
INVITED

Heterogeneous catalysts typically consist of metal nanoparticles on an oxide support. Model experiments involving nanoparticle growth on single crystalline oxide have been successfully employed to understand aspects of the nucleation, structure and reactivity. This contributes to catalysis design programs. Many subtleties continue to emerge, some of which will be discussed in this talk. For instance, low temperature STM experiments have allowed direct imaging of CO overlayers formed on the Pd nanoparticles themselves supported on TiO₂. The results show that the nanoparticles grow like a carpet over substrate step-edges, giving rise to a curved top facet that changes the adsorption behavior. Au nanoparticles supported by TiO₂ have been the subject of much work since the discovery by Haruta that Au is a low temperature oxidation catalyst. Despite this earlier work there has been no definitive evidence for the binding site or the direction of charge transfer associated with gold atoms and nanoparticles on the model substrate TiO₂(110). We show with STM that single Au atoms are in indeed bound to oxygen vacancies on the substrate, with dimers similarly anchored. Associated DFT calculations suggest electron transfer from bridging O vacancies to Au. XPEEM in conjunction with STM have also been used to probe the electronic character of Au nanoparticles as a function of particle size and coverage. Pt and related metals on CeO₂/ZrO₂ are used for CO oxidation in autocats. The accepted mechanism is that the oxide supplies oxygen to the metal to react with CO, with the oxide being directly reoxidized. In XPEEM studies of a model inverse catalyst we show that the reoxidation can also involve the metal.

9:40am **HC+2D+SS-ThM6 Structural and Chemical Effects of Cesium on the Cu(111) and Cu₂O/Cu(111) Surface**, *Rebecca Hamlyn¹*, Stony Brook University; *M. Mahapatra*, Brookhaven National Laboratory; *I. Orozco*, Stony Brook University; *M.G. White, S. Senanayake, J.A. Rodriguez*, Brookhaven National Laboratory

Surface additives, particularly those of alkali metals, are commonly used for promotion of catalytic processes. These processes include carbon oxide reactions such as the water-gas shift and methanol synthesis over Cu-based catalysts. Both reactions are known to be promoted by Cs doping. Partially oxidized Cu is also understood to have a critical role in the activity of the aforementioned processes, as strictly metallic copper will not survive under redox conditions. In an effort to better understand how small additions of alkalis such as Cs act as promoters, we have carried out model studies of cesium over a metallic and oxidized copper surface using scanning tunneling microscopy and x-ray photoelectron spectroscopy. We find that the oxide structure assists in anchoring Cs over the weaker electrostatic interactions with the bare copper surface, allowing for room temperature imaging. Furthermore, with higher coverages or elevated temperature, cesium induces formation of a new ordered structure. This work provides a molecular-scale understanding of the cesiated surface, and serves as a basis for insight toward its mechanism of action in conversion of relevant gases (H₂O, CO, CO₂).

11:00am **HC+2D+SS-ThM10 Mythbusting: From Single Crystals in UHV to Catalytic Reactors**, *R.J. Madix, Christian Reece*, Harvard University **INVITED**

For decades it has been an objective of surface science studies of chemical reactivity to make a direct connection to heterogeneous catalysis. Over these years the difficulties encountered in connecting these two areas of research gave rise to the dismissal of this possibility by the catalysis community and the invention of such shorthand terms as “pressure gap” and “materials gap” to express this view. Usually overlooked is also the fact that catalytic reactions are conducted at much higher temperatures than the related studies on single crystal surfaces, so a “temperature gap” also exists. In fact, these regimes of reactivity are directly linked by fundamental knowledge of the identity and rate constants for the operative elementary steps comprising the catalytic cycle under catalytic conditions. Further, for many catalytic materials, its state can be defined by the reaction conditions themselves in quasi-thermodynamic terms. Connection between the reactivity observed on the single crystals with that on the catalyst surface is possible by the use of a transient pressure method which is conducted over the actual catalyst material under Knudsen flow conditions. Recently we have demonstrated this historically elusive connection between UHV-based studies and catalytic performance for the catalytic oxygen-assisted synthesis of methyl formate from methanol over a nanoporous gold catalyst. The connection is entirely based on the kinetics and mechanism determined on single crystal gold surfaces. A brief history of this

¹ Heterogeneous Catalysis Graduate Student Presentation Award Finalist

development will be discussed and the specifics of how this bridge was built examined.

11:40am **HC+2D+SS-ThM12 Cooperativity Between Pd and AgO_x Phases on Ag(111)**, *V. Mehar, M. Yu, Jason Weaver*, University of Florida

Metals dispersed on a reactive metal-oxide have potential to effect selective catalysis through cooperative interactions between the co-existing metal and metal-oxide phases. In this talk, I will discuss our recent investigations of the structure and reactivity of oxidized Ag(111) as well as Pd/AgO_x surfaces that are generated by depositing metallic Pd onto a single-layer AgO_x structure in ultrahigh vacuum (UHV). Scanning tunneling microscopy (STM) and low energy electron diffraction (LEED) show that the oxidation of Ag(111) with atomic oxygen mainly produces a single-layer AgO_x phase with a p(4 x 5r3) structure as well as smaller amounts of p(4 x 4) and c(3 x 5r3) structures during the initial stages of oxidation. Surface infrared spectroscopy and temperature programmed reaction spectroscopy (TPRS) demonstrate that the single-layer AgO_x structures are nearly unreactive and bind CO negligibly at temperatures down to ~100 K. In contrast, we find that CO adsorbs and oxidizes efficiently on Pd islands during TPRS, even when the AgO_x phase is the only oxidant source. STM further demonstrates that the metallic Pd islands induce partial reduction of the AgO_x support structure at 300 K. We find that the Pd/AgO_x surfaces continue to exhibit high CO oxidation activity with increasing Pd coverage up to nearly 2 ML (monolayer), suggesting that oxygen transfer from the AgO_x phase occurs at both the interior and perimeter of Pd islands. Our results reveal a cooperative mechanism for CO oxidation on Pd/AgO_x surfaces wherein O-atoms from the AgO_x support phase migrate onto metallic Pd islands and react with adsorbed CO to produce CO₂. These findings illustrate that oxygen transport across metal/metal-oxide interfaces can be highly efficient when the oxygen chemical potential is lower on the initial metal phase (Pd) compared with the metal-oxide (AgO_x) support.

12:00pm **HC+2D+SS-ThM13 Migration Across Metal/Metal Oxide Interfaces: Enhancing the Reactivity of Ag Oxide with H₂ by the Presence of Pd/Pd Oxide**, *Christopher O'Connor¹, M.A. van Spronsen, E. Muramoto, T. Egle, R.J. Madix, C.M. Friend*, Harvard University

An important factor in exploiting bifunctionality in dilute alloy catalysts is surface migration across interfaces separating the dissimilar materials. Herein, we demonstrate the transfer of hydrogen atoms from islands of Pd oxide onto a surrounding O/Ag(111) surface using ambient pressure X-ray photoelectron spectroscopy (APXPS) and scanning tunneling microscopy (STM). These Pd oxide islands enhance the rate of reduction of Ag oxide by more than four orders of magnitude compared to pure oxidized Ag(111). The increase in the rate of reduction of Ag oxide by H₂ is attributed to H₂ activation on Pd/Pd oxide followed by migration (spillover) to Ag/Ag oxide and rapid reaction thereafter. The oxidation and subsequent reduction processes induce significant structural changes of the catalyst surface. We further establish that the transfer of hydrogen atoms occurs from islands of metallic Pd onto a surrounding Ag(111) surface using high resolution electron energy loss spectroscopy (HREELS) and temperature programmed reaction spectroscopy (TPRS). For the metallic PdAg system, hydrogen spillover is shown to be a kinetically limited process that can be controlled by temperature, pressure of H₂ and surface concentration of Pd. The highest efficiency for the amount of hydrogen spillover per surface Pd occurs for a dilute concentration of Pd in Ag. This study establishes that the migration of intermediates across interfaces can occur for oxidized PdAg alloy surfaces and specifically that hydrogen atom migration has a significant effect on the catalytic activity of this type of binary material.

Frontiers of New Light Sources Applied to Materials, Interfaces, and Processing Focus Topic
Room A124-125 - Session LS+AS+SS-ThM

Operando Methods for Unraveling Fundamental Mechanisms in Devices Towards Renewable Energies

Moderator: Olivier Renault, CEA-LETI, France

8:00am **LS+AS+SS-ThM1 X-Ray Insight into Fuel Cell Catalysis: Operando Studies of Model Surfaces and Working Devices**, *Jakub Drnec, I. Martens*, European Synchrotron Radiation Facility, France; *T. Fuchs*, University of Kiel, Germany; *T. Wiegmann*, European Synchrotron Radiation Facility, Germany; *A. Vamvakeros*, Finden Ltd., UK; *R. Chattot*, European Synchrotron Radiation Facility, France; *O.M. Magnussen*, University of Kiel, Germany

INVITED

Complete physico-chemical operando characterization of electrochemical devices in whole, or its constituent materials separately, is necessary to guide the development and to improve the performance. High brilliance synchrotron X-ray sources play a crucial role in this respect as they act as a probe with relatively high penetration power and low damage potential. In this contribution the new possibilities of using using high energy, high intensity X-rays to probe model fuel cell catalysts and energy conversion devices will be presented.

HESXRD (High Energy Surface X-ray Diffraction) [1] and TDS (Transmission Surface Diffraction) [2] provide ideal tools to study structural changes during reaction conditions on single crystal model electrodes. The main advantage of both techniques is the possibility to follow the structural changes precisely with atomic resolution. While HESXRD is ideally used to determine exact atomic position, the TSD is easier to use and allows studies with high spatial resolution. For example, HESXRD can be used to follow the atomic movement of Pt atoms during electrochemical oxidation and dissolution with very high precision, explaining the different catalyst degradation behaviors and suggesting possible routes to improve its durability [3-4]. The TSD is an excellent tool to study advanced 2D catalysts.

To study fuel cells or batteries as a whole, elastic scattering techniques, such as WAXS and SAXS, can be employed as they can provide important complementary information to more standard X-ray imaging and tomography. The advantage is that the chemical contrast and sensitivity at atomic and nm scales is superior. Coupling these technique with the tomographic reconstruction (XRD-CT and SAXS-CT) is much less common as it requires bright synchrotron sources and advanced instrumentation, but allows 3D imaging of operational devices with unprecedented chemical sensitivity. This can be demonstrated on imaging of standard 5 cm² fuel cells during operation. The change in morphology and atomic arrangement of the catalysts, PEM hydration and water distribution can be followed in one experiment as a function of operating conditions. Furthermore, the fundamental processes leading to the catalyst aging can be assessed with high temporal and spatial resolution. These advanced scattering techniques open a door to holistic investigations of operational devices, which are needed to successfully incorporate new materials at the device level.

[1] J. Gustafson et al., *Science* 343, 758 (2014)

[2] F. Reikowski et al., *J. Phys. Chem. Lett.*, 5, 1067-1071 (2017)

[3] J. Drnec et al, *Electrochim. Acta*, 224 (2017),

[4] Chattot et al., *Nature Materials*, 17(2018)

8:40am **LS+AS+SS-ThM3 Multi-scale Operando X-ray Tomography of Solid-state Li Battery Electrolytes at Elevated Temperatures and Pressures**, *Natalie Seitzman*, Colorado School of Mines; *J. Nelson Weker*, SLAC National Accelerator Laboratory; *M. Al-Jassim*, National Renewable Energy Laboratory; *S. Pylypenko*, Colorado School of Mines

Solid state Li ion conductors are next-generation battery technologies that reap the capacitive benefits of Li metal anodes while mechanically resisting the Li interface evolution and thus prolonging lifetime. Additionally, they are not flammable, offering greater safety than liquid counterparts. However, interface evolution and Li protrusions are observed in solid state batteries despite the mechanical resistance.^{1,2} There is debate as to whether these protrusions nucleate at the Li anode or within the ceramic electrolyte, and there are several factors that affect these protrusions including electrolyte density, pre-existing defects, anode/electrolyte interfacial contact, and imperfect electronic insulation within the electrolyte.³ Understanding the influence of these variables is greatly enhanced by directly imaging the interior of the ceramic at multiple scales in conjunction with electrochemical experiments.

¹ Heterogeneous Catalysis Graduate Student Presentation Award Finalist

Thursday Morning, October 24, 2019

This talk addresses the contribution of electrolyte density and defects, interfacial contact, and conductivity to structural changes in β -Li₃PS₄ (LPS) ceramic electrolyte in operating cells via 3D X-ray imaging with sub-micron resolution. Cells of Li, LPS, and a blocking contact are constructed and studied *in operando* at 200 psi and 70°C. Because electrolyte density and initial defects depend on the composition and synthesis of the ceramic conductor, two syntheses of LPS with different particle sizes are compared. Also, pressure is a key parameter in the quality and stability of interfacial contact while temperature affects both the ionic and electronic conductivity of the ceramic.

Synchrotron micro-tomography is combined with synchrotron transmission x-ray microscopy to study the cells with spatial resolution in the hundreds of nanometers and tens of nanometers. Image analysis of these data has identified sites of Li microstructure growth⁴ and now isolates variable-dependent trends such as pressure-dependent void formation in the Li anode. Linking structural changes observed *in operando* to these factors that contribute to Li evolution will guide the design of robust ceramic electrolytes with improved performance and safety.

1. L. Porz, T. Swamy, B. W. Sheldon, D. Rettenwander, T. Frömling, H. L. Thaman, S. Berendts, R. Uecker, W. C. Carter, and Y.-M. Chiang, *Adv. Energy Mater.*, **7**, 1701003 (2017).
2. E. J. Cheng, A. Sharafi, and J. Sakamoto, *Electrochim. Acta*, **223**, 85–91 (2017).
3. F. Han, A. S. Westover, J. Yue, X. Fan, F. Wang, M. Chi, D. N. Leonard, N. J. Dudney, H. Wang, and C. Wang, *Nat. Energy* (2019).
4. N. Seitzman, H. Guthrey, D. B. Sulas, H. A. S. Platt, M. Al-Jassim, and S. Pylypenko, *J. Electrochem. Soc.*, **165**, 3732–3737 (2018).

9:00am **LS+AS+SS-ThM4 Correlating the Atomic and Electronic Structure in the Formation 2DEGs in Complex Oxides**, *Jessica McChesney, X. Yan, F. Wrobel, H. Hong, D.D. Fong*, Argonne National Laboratory

Using a multimodal approach, we investigate the interplay of the atomic and electronic structure of the formation of 2-D electron gas (2DEG) in complex oxide systems. Using hybrid molecular beam epitaxy for synthesis and *in-situ* synchrotron x-ray scattering atomic precision of the growth is obtained. The electronic structure then characterized via a combination of resonant soft x-ray angle-resolved photoemission and core level spectroscopy and compared with transport measurements.

9:20am **LS+AS+SS-ThM5 Uncover the Mystery of Oxygen Chemistry in Batteries through High-Efficiency mRIXS and Theory**, *Wanli Yang*, Lawrence Berkeley National Laboratory **INVITED**

Energy storage through electrochemical devices (batteries) is under pressure to be greatly improved for today's sustainable energy applications, especially the electric vehicles and power grid using renewable energy sources. A battery utilizes transition-metal (TM) oxides as one of the critical electrodes, the positive electrode, which is often the bottleneck of the energy density. In general, the operation of battery cycling is based on reduction and oxidation (Redox) reactions of TMs and a recently proposed oxygen, which involve the changes on the electron occupation numbers in TM-3*d* and O-2*p* states, as well as the evolution of the electronic configuration. However, technical challenges are formidable on probing these states directly, especially for the unconventional oxygen redox states.

This presentation will start with a brief introduction of several needs and grand challenges of battery devices related with oxygen states, which is followed by soft X-ray spectroscopic experiments for providing relevant information. The focus of this presentation is on an active debate of the oxygen states in charged electrodes. We will explain the limitations on conventional soft X-ray absorption spectroscopy (sXAS) for characterizing the important oxygen states, then showcases the power of full energy-range mapping of resonant inelastic X-ray scattering (mRIXS) for clarifying the oxygen redox behaviors in batteries.

We show that mRIXS provides the ultimate probe of the intrinsic oxygen redox reactions in the lattice of battery electrodes [1], which is associated with transition-metal configurations [2]. These spectroscopic results could be quantified to decipher the electrochemical capacity [3], providing both the rationality of the device performance and evidences for understanding the fundamental mechanism of electrochemical materials for energy applications. Furthermore, the mRIXS results indicate a universal driving force of the oxygen redox reactions [4], which could be tackled through combined studies of mRIXS and theoretical calculations [5]. We show that such a spectroscopic and theoretical collaboration could deliver unprecedented information for both fundamental understanding and

practical optimization on grand challenges in developing high-performance battery devices.

- [1] Gent et al., *Nat Comm* **8**, 2091 (2017)
- [2] Xu et al., *Nat Comm* **9**, 947 (2018)
- [3] Dai et al., *Joule* **3**, 518 (2019)
- [4] Yang & Devereaux, *J. Power Sources* **389**, 188 (2018)
- [5] Zhuo et al., *JPC L* **9**, 6378 (2018)

Frontiers of New Light Sources Applied to Materials, Interfaces, and Processing Focus Topic
Room A124-125 - Session LS+HC+SS-ThM

Frontiers of Time-resolved Techniques for Energy & Catalysis Highlight Session

Moderator: Jessica McChesney, Argonne National Laboratory

11:00am **LS+HC+SS-ThM10 How to Probe Solid/Liquid Interfaces using Standing-wave Photoemission?**, *Slavomir Nemsak*, Lawrence Berkeley National Laboratory; *H. Bluhm*, Fritz Haber Institute, Germany; *C.S. Fadley*, University of California, Davis

A great efforts have been made in the development of *in-situ* and *operando* experimental methods in the last two decades, with ambient pressure photoelectron spectroscopy being one of the most profound examples [1]. In combination with advanced techniques, such as standing wave excitation, an unprecedented depth resolution across operating interfaces can be obtained, providing valuable information on processes governing interfacial behavior.

With the excellent depth selectivity and sensitivity to chemistry and electrostatic gradients, standing wave ambient pressure photoelectron spectroscopy is exploited to probe two different solid/liquid interfaces relevant to energy research, electrochemistry, and atmospheric and environmental science [2,3]. Liquid layers are prepared either by water adsorption in a saturated vapor ambiance or using a so-called meniscus method, in which the sample is pulled out of a liquid reservoir leaving a thin liquid film on the sample's surface. The latter experimental configuration allows also for the *operando* electrochemistry [4]. The outlook and future developments of the technique will be also discussed.

- [1] D.E. Starr et al., *Chem. Soc. Rev.* **42**, 5833 (2013).
- [2] S. Nemsák et al., *Nat. Comm.* **5**, 5441 (2014).
- [3] O. Karslioglu et al., *Faraday Discuss.* **180**, 35 (2015).
- [4] S. Axnanda et al., *Sci. Rep.* **5**, 9788 (2015).

11:20am **LS+HC+SS-ThM11 In situ Spectroscopy of Synthesis of Next-Generation Cathodes for Batteries**, *Feng Wang*, Brookhaven National Laboratory

There has been considerable interest in developing low-cost, high-energy electrodes for batteries. However, synthesizing materials with the desired phases and properties has proven difficult due to the complexity of the reactions involved in chemical synthesis. Additional challenge comes from the fact that synthesis is often undertaken under conditions and, hence, the process is hard to be predicted by theoretical computations. Probing of synthesis reactions allows for identification of intermediates and determination of thermodynamic/kinetic parameters governing kinetic reaction pathways, thereby enabling synthetic design of materials with desired structure and properties. In this presentation, we will report our recent results from technique development and application to *in situ* probing and synthetic control of local structural ordering and stoichiometry during synthesis of next-generation cathode materials for lithium-ion batteries. Findings from this study, along with its implication to designing viable cathodes for practical use in batteries, will be discussed.

ACKNOWLEDGMENT. This work was supported by the U.S. Department of Energy (DOE) Office of Energy Efficiency and Renewable Energy, Vehicle Technologies Office, Contract No. DE-SC0012704.

11:40am **LS+HC+SS-ThM12 Structural Heterogeneity and Dynamics of 2D Materials Studied by Full-field X-ray Diffraction Microscopy and Ultrafast Surface X-ray Diffraction**, *Haidan Wen*, Argonne National Laboratory **INVITED**

Transition metal dichalcogenides (TMD) at the two-dimensional (2D) limit have sparked great interests in both fundamental physics and devices applications. Surfaces and interfaces play an important role in the most

common setting, i.e., a monolayer crystal on a substrate, for studying 2D phenomena and device applications. However, the structural characterization with atomic accuracy in this form has been a challenge because the crystal size is usually small and transmission electron microscopy is difficult to apply. In this talk, we show microscopic insights of structural properties can be obtained in the space or time domain using newly developed multimodal full-field x-ray imaging and ultrafast surface x-ray scattering. In the first example, we demonstrate full-field x-ray diffraction imaging of a monolayer 2D material at the Advanced Photon Source. The structural variation across a TMD monolayer or heterostructure is spatially correlated with the electronic properties characterized by the *in-situ* photoluminescence measurements. The correlation reveals mesoscale structure-property relationship in TMDs. In the second example, we report the first femtosecond surface X-ray diffraction using the free-electron laser at Linac Coherent Light Source to quantify the ultrafast structural dynamics of monolayer WSe₂ crystals supported on a substrate. We found the absorbed optical photon energy is preferably coupled to the in-plane lattice vibrations within one picosecond whereas the out-of-plane lattice vibration amplitude remains unchanged during the first ten picoseconds. The observed nonequilibrium anisotropic structural dynamics agrees with first-principles modeling in both real and momentum space, marking the distinct structural dynamics of monolayer crystals from their bulk counterparts.

Surface Science Division

Room A220-221 - Session SS+AS+HC+TL-ThM

Surface Science of Energy Conversion and Storage

Moderators: Steven L. Tait, Indiana University, Francisco Zaera, University of California, Riverside

8:00am SS+AS+HC+TL-ThM1 Chemical and Electrochemical Stability of Perovskite Oxide Surfaces in Energy Conversion: Mechanisms and Improvements, *Bilge Yildiz*, Massachusetts Institute of Technology INVITED

A broad range of highly active doped ternary oxides, including perovskites, are desirable materials in electrochemical energy conversion, catalysis and information processing applications. At elevated temperatures related to synthesis or operation, however, the structure and chemistry of their surfaces can deviate from the bulk. This can give rise to large variations in the kinetics of reactions taking place at their surfaces, including oxygen reduction, oxygen evolution, and splitting of H₂O and CO₂. In particular, aliovalent dopants introduced for improving the electronic and ionic conductivity enrich and phase separate at the surface perovskite oxides. This gives rise to detrimental effects on surface reaction kinetics in energy conversion devices such as fuel cells, electrolyzers and thermochemical H₂O and CO₂ splitting. This talk will have three parts. First, the mechanisms behind such near-surface chemical evolution will be discussed. Second, the dependence of surface chemistry on environmental conditions, including temperature, gas composition, electrochemical potential and crystal orientation will be described. Third, modifications of the surface chemistry that improve electrochemical stability and activity, designed based on the governing mechanisms, will be presented. Guidelines for enabling high performance perovskite oxides in energy conversion technologies will be presented.

8:40am SS+AS+HC+TL-ThM3 Mechanism of Oxygen Reduction Reaction on Nitrogen-doped Carbon Catalysts, *Junji Nakamura*, University of Tsukuba, Japan

Nitrogen-doped carbon materials are expected to be non-Pt catalysts for oxygen reduction reaction (ORR) in fuel cells. Among several types of nitrogen species in carbon materials, pyridinic nitrogen (nitrogen atom bound to two C atoms) has been found to create ORR active sites in our previous work¹. We then try to prepare catalytically active carbon surfaces covered with pyridinic nitrogen-containing aromatic molecules with high density. Recently we have reported model catalyst studies using HOPG (highly oriented pyrolytic graphite) electrode covered with pyridinic nitrogen-containing aromatic molecules (dibenz[a,c]acridine (DA) molecule and acridine (Ac)molecule)². The DA molecules form a two-dimensional ordered structure along the direction of the HOPG substrate by self-organization. Adsorbed DA on the HOPG surface shows high ORR activity in terms of specific activity per pyridinic nitrogen and is comparable to that of pyridinic-nitrogen-doped carbon catalysts. We study the mechanism of ORR taking place on the DA/HOPG model catalyst. In acidic reaction conditions, pyridinic nitrogen is protonated to pyridinium nitrogen (NH⁺) species. It is suggested that the adsorption of oxygen take place on a

carbon atom in a DA molecule upon reduction of the NH⁺ species. Generally, the reduction of NH⁺ is difficult to proceed thermodynamically at higher potentials above 0 V vs RHE. However, in the presence of oxygen, the reduction of NH⁺ is possible by an energy gain due to simultaneous adsorption of oxygen. The supplied electron goes to pi* system as SOMO electron upon reduction, which is responsible for the adsorption of oxygen. That is, the role of pyridinic nitrogen is to provide SOMO electron upon reduction of NH⁺ species.

References

Guo D, Shibuya R, Akiba C, Saji S, Kondo T, Nakamura J, (2016). Active sites of nitrogen-doped carbon materials for oxygen reduction reaction clarified using model catalysts. *Science*, 351, 361-365.

Shibuya R, Kondo T, Nakamura J, (2018). Bottom-up design of nitrogen-containing carbon catalysts for the oxygen reduction reaction. *ChemCatChem* doi.org/10.1002/cctc.201701928

9:00am SS+AS+HC+TL-ThM4 Copper Corrosion Inhibition Investigated on the Molecular Scale Using APXPS, *Bo-Hong Liu*, Lawrence Berkeley National Laboratory; *O. Karslıoğlu*, Lawrence Berkeley National Laboratory; *M.B. Salmeron*, *S. Nemšák*, Lawrence Berkeley National Laboratory; *H. Bluhm*, Fritz Haber Institute of the Max Planck Society, Germany

Copper has been used in a wide variety of applications. Though relatively inert, it corrodes when in contact with aqueous solutions/water vapor and corroding agents such as chlorine.¹ Benzotriazole (BTA) is a commonly used corrosion inhibitor to protect copper surfaces. A consensus regarding the mechanism of corrosion protection is that BTA complexes with surface copper atoms, resulting in a Cu(I)-BTA protective polymer layer.² UHV-based surface science studies clarified the structure of the BTA layer on copper single crystal surfaces at low dosage, as demonstrated by a very recent study combining DFT and spectroscopic techniques;³ however, the effect of environmental factors could not be well addressed by this approach. Here, we report an Ambient Pressure X-ray Photoelectron Spectroscopy (APXPS) study of the influence of water vapor and chlorine on well-defined Cu surfaces. To capture the material complexity of the corrosion phenomenon, we study copper single crystals as well as polycrystalline foils of metallic copper, cuprous oxide and cupric oxide. In this presentation, we will show that the water uptake of copper surfaces under humid condition is strongly influenced by the presence of a BTA layer. Also, a BTA layer blocks chlorine uptake in some conditions. Based on these experimental results, factors that influence the BTA inhibitory effect on copper corrosion are identified.

1. Atlas, D.; Coombs, J.; Zajicek, O. T., THE CORROSION OF COPPER BY CHLORINATED DRINKING WATERS. *Water Research* **1982**,16 (5), 693-698.

2. Finsgar, M.; Milosev, I., Inhibition of copper corrosion by 1,2,3-benzotriazole: A review. *Corrosion Science* **2010**,52 (9), 2737-2749.

3. Gattinoni, C.; Tsaousis, P.; Euaruksakul, C.; Price, R.; Duncan, D. A.; Pascal, T.; Prendergast, D.; Held, G.; Michaelides, A., Adsorption Behavior of Organic Molecules: A Study of Benzotriazole on Cu(111) with Spectroscopic and Theoretical Methods. *Langmuir* **2019**,35 (4), 882-893.

9:20am SS+AS+HC+TL-ThM5 Analysis and Deliberate Modification of Electrochemical Interfaces, *Esther Takeuchi*, *K. Takeuchi*, *A. Marschilok*, Stony Brook University INVITED

Interfaces in electrochemical energy storage systems are critical in the transport of electrons and ions and are significant factors in electrochemical function, yet remain a challenge to fully understand. In lithium based systems, the interfaces or interphases often form spontaneously due to reactions of the active materials and the electrolytes. The interfaces formed due to these spontaneous reactions may prove beneficial as they provide needed protection inhibiting further and continuous reaction. However, the characteristics of the interface may also contribute to decreased ion transport and the accompanying increased effective resistance.

Conversion-type materials for next generation lithium ion systems are appealing due to the opportunity for multiple electron transfer within one metal center. However, implementation of conversion materials has been hindered by the phase transformations occurring during cycling as well as formation of a resistive solid electrolyte interphase (SEI). This presentation will explore the effective implementation of combinations of characterization techniques including the use of *ex-situ* and *operando* methods to provide insight into the formation, composition and deliberate modification of the SEI.

Thursday Morning, October 24, 2019

11:00am **SS+AS+HC+TL-ThM10 An Investigation on Active Sites of La₂O₃**

Catalyst for OCM Reaction: A Combined Study of *in situ* XRD, XPS and Online MS, **Yong Yang, C. Guan, E.I. Vovk, Z. Liu, X. Zhou, J.P.H. Liu, Y. Pang**, ShanghaiTech University, China
Oxidative coupling of methane (OCM) is a catalytic partial oxidation process that converts methane directly to valuable C₂ products (ethane and ethylene). Previous results suggested that the bulk structure change of the La₂O₃ catalyst was related to the performance of the reaction. In this work, a designed *in situ* XRD-MS coupled characterization setup coupled with online MS instrument are used for measuring both the reaction products and the bulk structure of the catalyst in real time and under simulated industrial conditions. This allows for the more detailed study in order to relate information from of bulk structure change vs. CO₂ related treatment and quantitative analysis of the reaction products, thus for a further connection and understanding of the conversion rate of CH₄ and the selectivity of C₂. The work presented focused on online characterization of the OCM reaction on La₂O₃ catalyst, covering different parameters including: 1. La₂O₃ pretreatment under different CO₂ concentrations, 2. Consecutive OCM reactions, comparing the behavior of a clean surface La₂O₃ catalyst with a La₂O₃ catalyst after OCM, 3. OCM performed after La₂O₃ has undergone pretreatment with pure CO₂. Results indicate that carbonates formation on La₂O₃ is two step, surface carbonates formation at below 500°C and bulk formation at 500-700°C. *In situ* TPD performed in a high pressure gas cell (HPGC) and XPS measurement results confirm the above.

The results showed that bulk CO₃²⁻ formation under CO₂ exposure, results in higher light-off temperature of CO₂ and C₂ than the clean surface during OCM reaction. There is carbonate formation on commercial La₂O₃ during OCM reaction and CO₂ desorption after OCM reaction by *in situ* XRD-MS, and it influences the light-off temperature of CO₂ and C₂ up to 65°C higher than the clean surface. It is proposed that CO₃²⁻ may perform as a catalyst poison in this reaction. This result provides an important insight of the active site for OCM reaction. Based on this result, a brief XPS study of the carbonate free sample surface, which may be only prepared from the HPGC vacuum connected further reveals an oxide feature related with methane activation. Additional DFT calculations based upon the experimental data indicates a carbonation mechanism which occurs in the subsurface, which in turn could be related to La₂O₃ activity.

11:20am **SS+AS+HC+TL-ThM11 Interaction of Amino Acids on Au(111) as Studied with EC-STM: From Islands to Magic Fingers**, J.A. Phillips, K.P. Boyd, I. Baljak, L.K. Harville, **Erin Iski**, University of Tulsa

With growing interest into origin of life studies as well as the advancement of medical research using nanostructured architectures, investigations into amino acid interactions have increased heavily in the field of surface science. Amino acid assembly on metallic surfaces is typically investigated with Scanning Tunneling Microscopy (STM) at low temperatures (LT) and under ultra-high vacuum (UHV), which can achieve the necessary resolution to study detailed molecular interactions and chiral templating. However, in only studying these systems at LT and UHV, results often tend to be uncertain when moving to more relevant temperatures and pressures. This investigation focuses on the Electrochemical STM (EC-STM) study of five simple amino acids (L-Valine, L-threonine, L-Isoleucine, L-Phenylalanine, and L-Tyrosine) as well as two modifications of a single amino acid (L-Isoleucine Ethyl Ester and N-Boc-L-Isoleucine), and the means by which these molecules interact with a Au(111) surface. Using EC-STM under relevant experimental conditions, the amino acids were shown to have a considerable interaction with the underlying surface. In some cases, the amino acids trapped diffusing adatoms to form Au islands and in other cases, they assisted in the formation of magic gold fingers. Importantly, these findings have also been observed under UHV conditions, but this is the first demonstration of the correlation *in situ* and was controlled via an applied external potential. Results indicate that an increase in the molecular weight of the amino acid had a subsequent increase in the area of the islands formed. Furthermore, by shifting from a nonpolar to polar side chain, island area also increased. By analyzing the results gathered via EC-STM at ambient conditions, fundamental insight can be gained into not only the behavior of these amino acids with varied side chains and the underlying surface, but also into the relevance of LT-UHV STM data as it compares to data taken in more realistic scenarios.

11:40am **SS+AS+HC+TL-ThM12 Deposition and Structure of MoO₃ Clusters on Anatase TiO₂ (101)**, **Nassar Doudin, Z. Dohnálek**, Pacific Northwest National Laboratory

Oxide clusters supported on metal oxide substrates are of great interest due to their importance in heterogeneous catalysis [1]. The nature and

strength of the interactions between the metal oxide clusters and the support materials not only govern their structure and stability but also control the energetics of elementary steps that are critical for the overall activity [1]. Understanding the nature of the interactions is therefore important to tailor the supported metal oxide cluster systems to achieve the desired reactivity and selectivity. Here, we present a scanning tunneling microscopy (STM) and X-ray photoelectron spectroscopy (XPS) study of the monodispersed MoO₃ clusters deposited by the sublimation of MoO₃ powder on anatase TiO₂(101) surface at 300 K. After the deposition, the STM images of the lowest concentration of MoO₃ show that the clusters initially migrate over the surface and preferentially anchor at step edges before they start to aggregate on the terraces. Interestingly, the aggregates are mostly composed of three adjacent clusters, with a small concentration of monomers and dimers. Further exposures to MoO₃ increase the cluster coverage until a fully saturated over-layer is created with each clusters being are centered on top of the Ti sites. The adsorbed clusters appear as bright protrusions, with an apparent cluster height of approximately 1.5 Å and diameter of about 8.5 Å. Since the cyclic (MoO₃)₃ trimers are known to be a dominant gas phase species resulting from the sublimation of MoO₃ [1], we propose that each cluster on the surface is a trimer. Annealing to 550 K results in a better-order of the (MoO₃)₃ layer, but further annealing to 650 K leads to three-dimensional clusters. The XPS results indicate that the Mo(3d_{5/2}) binding energy in as-deposited (MoO₃)₃ is characteristic of Mo⁶⁺, and the oxidation state of Mo remains (+6) upon heating to 600 K. As such, this system may offers great promise as an ideal platform for reactivity studies on well-defined supported model transition-metal oxide catalysts.

[1] Zdenek Dohnálek et al. Royal Society of Chemistry 43, 7664-7680 (2014).

Thin Films Division

Room A122-123 - Session TF+EM+NS+SS-ThM

Thin Films for Energy Harvesting and Conversion

Moderators: Siamak Nejati, University of Nebraska-Lincoln, Xinwei Wang, Shenzhen Graduate School, Peking University

8:00am **TF+EM+NS+SS-ThM1 Redesigning Batteries into Efficient Energy Harvesters and Sensors for Wearable Applications**, **Cary Pint**, Vanderbilt University

INVITED

Here I will discuss the research efforts of my team demonstrating how active materials utilized in batteries can be reconfigured into an electrochemical framework to harvest, rather than store, energy. This new functionality of battery materials arises from the fundamental coupling between mechanical stresses and electrochemistry that my group has demonstrated while investigating the “strain-engineering” of battery materials. By exploiting this coupling in a symmetric cell device configuration, we are able to construct devices that convert mechanical energy to electrical energy by mechanical modulation of the electrochemical reaction potential. I will discuss the development of this device platform from proof-of-concept device fabrication using 2D materials to our most recent demonstration of textile-integrated biocompatible fibers integrated into fabrics for harvesting/sensing of human motion. Most notably, I will discuss how the sluggish diffusion kinetics of ions between two electrodes – whereas a challenge for emerging battery applications, enables these devices to measure a continuous response from the whole broad range of frequencies associated with human motion. This allows these wearable harvesters to provide real-time sensing data that can be directly correlated with dynamic human motion models. This new approach leverages the efficient nature of electrochemistry, the wide range of materials selection and chemistries relevant for batteries, and without any of the safety concerns of batteries due to the symmetric electrode configuration.

8:40am **TF+EM+NS+SS-ThM3 Engineering Effective Back Contact Barrier by interfacial MoSe₂ defect states for CZTSe: nanolayer Ge solar cells.**, **Sanghyun Lee**, Indiana State University

The steadily emerging Cu₂ZnSnS₄ (CZTSe) devices are alternative thin film solar cells with abundant elements in earth's crust for the past several years. Despite several advantages such as high absorption coefficient (>10⁴ cm⁻¹) and a tunable direct band gap energy (1 to 1.4 eV), the improvement and understanding have been stagnant in the past several years. Recently, CZTSe: nanolayer Ge solar cells have shown significantly improved pseudo-mono grain toward the depth direction.

Due to the improvement and the similarity between CZTSe and Cu(In,Ga)Se₂ (CIGS) thin film solar cells, the CZTSe/Molybdenum (Mo) back contact interface was often misinterpreted by expecting the similar back contact property to CIGS. However, unlike the stable CIGS (CuInSe₂)/Mo interface, the CZTSe/Mo interface is thermodynamically unstable due to the higher oxidation states of Sn. Although the presence of an interfacial MoSe₂ layer at Mo/absorber is always confirmed, properties of the back contact-interface such as structure and electrical behaviors are convoluted.

Following our empirical results about the back contact barrier of CZTSe: nanolayer Ge devices, we perform analytical and numerical modeling to explain the back contact improvement theoretically. The device modeling are carried out with the simulator, developed at Indiana State University. The tool is run in MATLAB environment, connected to other external tools (Sentaurus TCAD). Based on our result, defects in MoSe₂ interfacial layer dominate the back contact property of CZTSe: nanolayer Ge devices by increasing of the effective back contact barrier, which consists of two different back contact barriers, thereby increasing series resistance as well. The reduction of MoSe₂ defect concentration from 1×10^{17} to 1×10^{15} cm⁻³ decreases the effective barrier height by 51 meV, which results in approximately 34 % decrease in the series resistance (See supporting data). Conversely, as the defect concentration increases, the benefit from the back contact barrier lowering by the valence bands offset between MoSe₂ and CZTSe absorber is reduced and essentially eliminated. However, the back contact barrier between MoSe₂ and Mo metal contact remains the same even with increased MoSe₂ defect concentration. Incorporating thin Ge nanolayer at the interface between the absorber and MoSe₂ positively influences and possibly reduces the defect states, lowering the effective barrier. The exponential fitting of the effective barrier and series resistance agrees well with the experimental results. The improvement of the back contact barrier for CZTSe: nanolayer Ge devices is calculated as 23.8 meV than CZTSe without nanolayer Ge devices.

9:00am TF+EM+NS+SS-ThM4 Development of Low-Cost, Crack-Tolerant Metallization Using Screen Printing for Increased Durability of Silicon Solar Cell Modules, O.K. Abudayyeh, Osazda Energy; A. Chavez, University of New Mexico; J. Chavez, Osazda Energy; Sang M. Han, University of New Mexico; F. Zimbardi, B. Rounsaville, V. Upadhyaya, A. Rohatgi, Georgia Institute of Technology; B. McDanold, T. Silverman, National Renewable Energy Laboratory

One of the ways to reduce the cost of solar electricity to 3¢/kWh, thus reaching parity with fossil-fuel-based generation, is to reduce the degradation rate of solar modules and extend their lifetime well beyond 30 years. The extended module lifetime in turn can positively influence the financial model and the bankability of utility-scale PV projects. Today, the highest-risk-priority solar module degradation mechanism is what is known as hot spots, often induced by cell cracks. In order to address this degradation mechanism, we make use of low-cost, multi-walled carbon nanotubes embedded in commercial screen-printable silver pastes, also known as metal matrix composites. When the carbon nanotubes are properly functionalized and appropriately incorporated into commercial silver pastes, the resulting metal contacts on solar cells, after screen-printing and firing, show exceptional fracture toughness. These composite metal contacts possess increased ductility, electrical gap-bridging capability up to 50 μm, and "self-healing" to regain electrical continuity even after cycles of complete electrical failure under extreme strain [1]. Accelerated thermal cycling tests on mini-modules constructed from aluminum back surface field (Al-BSF) cells show a slower degradation rate for the cells integrated with the composite grid fingers and busbars for the front surface metallization compared to the cells with conventional metallization.

[1] O. K. Abudayyeh, A. Chavez, J. Chavez, S. M. Han, F. Zimbardi, B. Rounsaville, V. Upadhyaya, A. Rohatgi, B. McDanold, T. J. Silverman, and N. Bosco, in "Low-Cost Advanced Metallization to Reduce Cell-Crack-Induced Degradation for Increased Module Reliability," 2019 NREL PV Reliability Workshop, Lakewood, CO, 2019.

9:20am TF+EM+NS+SS-ThM5 Fabrication of Optical Test Structures for Enhanced Absorption in Thin Multi-junction Solar Cells, Erin Cleveland, N.A. Kotulak, S. Tomasulo, P. Jenkins, U.S. Naval Research Laboratory; A. Mellor, P. Pearce, Imperial College London, UK; N.J. Ekins-Daukes, University of New South Wales, Australia; M.K. Yakes, U.S. Naval Research Laboratory

In space applications, a key figure of merit is conversion efficiency at end-of-life, which combines both beginning-of-life efficiency with degradation due to radiation exposure on orbit. In currently used InGaP/GaAs/Ge triple

junctions, the GaAs middle cell has the most pronounced degradation, which limits the total current generation at the end-of-life. Recently, we demonstrated that as the thickness of the GaAs cell decreases, the tolerance to radiation damage increases. [1] However, because the cell absorbs less light as the thickness of the active region is reduced, the beginning-of-life performance suffers as compared to optically thick cells. To realize the benefits of both structures, light trapping architectures may be used to increase absorption within the cell while still maintaining the increased radiation tolerance of the thinner geometry.

Designing a wavelength selective light trapping structure positioned interstitially between two of the subcells of a multi-junction device is a new challenge which prohibits many of the well-known light trapping techniques. Recently, we have proposed a structure which combines a distributed Bragg reflector (DBR) with a textured diffraction grating. [2] Such a structure would provide substantial absorption of light in the middle subcell of a multi-junction device, while still allowing enough low-energy light to pass through the structure so the bottom cell remains well current matched with the other junctions. This structure is proposed to have over an order of magnitude increase in overall radiation tolerance while maintaining comparable beginning of life performance to the current technology.

In this presentation, we present a first experimental demonstration of this structure. The design combines a diffraction grating fabricated via nanosphere natural lithography [3], a low-index transparent spacer layer, and a DBR, which synergistically traps light inside the targeted subcell. This presentation will highlight processing techniques and challenges associated with fabricating a textured ultra-thin solar cell, while illustrating the effectiveness of integrating light trapping structures within an ultra-thin solar cell as an effort towards realizing high efficiency ultra-thin photovoltaic devices.

[1] L. C. Hirst, *et al.*, "Intrinsic radiation tolerance of ultra-thin GaAs solar cells", *APL*, 109 (2016)

[2] A. Mellor, N.P. Hylton, S.A. Maier, N. Ekins-Daukes, "Interstitial light-trapping design for multi-junction solar cells", *Solar Energy Materials & Solar Cells*, 159, (2017)

[3] H.W. Deckman and J.H. Dunsmuir, "Natural lithography", *Applied Physics Letters*, 41(4) (1982)

9:40am TF+EM+NS+SS-ThM6 Phosphorus as a p-Dopant in Pyrite FeS₂, a Potential Low-cost earth-abundant Thin Film Solar Absorber, Bryan Voigt¹, W. Moore, D. Ray, M. Manno, University of Minnesota, Minneapolis; J.D. Jeremiason, Gustavus Adolphus College; L. Gagliardi, E.S. Aydil, C. Leighton, University of Minnesota, Minneapolis

Pyrite FeS₂ has long been considered an ideal absorber material for low-cost and sustainable thin film solar cells because it is composed of earth-abundant, non-toxic, inexpensive elements, has a suitable band gap (0.95 eV), and absorbs light so strongly that a 100-nm-thick film absorbs >90 % of photons with energies above the band gap. Lack of doping control, however, has presented a barrier to realization of the *p-n* pyrite homojunction, *i.e.*, the simplest route to a pyrite solar cell. *Heterojunction* pyrite solar cells have proven to have disappointingly low efficiencies (~3%), surface conduction and leaky surface inversion layers being implicated as the culprit. While mitigation of pyrite surface conduction remains a challenge, doping has begun to yield to understanding, renewing optimism for a *p-n* pyrite homojunction solar cell. In particular, we have shown that rigorously phase-pure pyrite single crystals and thin films are exclusively *n*-type, due to a common dopant. Most recently, we have identified sulfur vacancies as this unintentional *n*-dopant, enabling robust control over *n*-doping levels in single crystals grown by chemical vapor transport (CVT). Progressing towards a *p-n* pyrite homojunction, here we demonstrate effective *p*-type doping in crystals by introducing phosphorus in the vapor phase during CVT growth. Increasing the phosphorus concentration from <0.1 ppm to 30 ppm evolves electronic conduction from *n*-type to *p*-type, with a clear and reproducible majority carrier inversion for concentrations >10 ppm. Typical transport properties of phosphorus-doped, *p*-type pyrite crystals include a hole thermal activation energy, room temperature resistivity, hole density, and mobility of ~170 meV, 3 Ω cm, 2×10^{18} cm⁻³, and $1 \text{ cm}^2 \text{ V}^{-1} \text{ s}^{-1}$, respectively. Density functional theory calculations confirm that phosphorus substituted on the S site is an acceptor, predicting a defect level at 200 meV above the valence band maximum, in good agreement with experiment. With both *n*- and *p*-type

¹ TFD James Harper Award Finalist

doping control achieved, attempts at *p-n* pyrite homojunction solar cells become possible.

This work was supported by the customers of Xcel Energy through a grant from the Renewables Development Fund and in part by the National Science Foundation through the University of Minnesota MRSEC under DMR-1420013.

11:00am TF+EM+NS+SS-ThM10 Relaxor-ferroelectric Thin Films for Energy Harvesting from Low-grade Waste-heat, *Amrit Sharma, B. Xiao, S.K. Pradhan, M.J. Bahoura*, Norfolk State University

The need for efficient energy utilization is driving research into ways to harvest waste-heat which is ubiquitous, abundant and free. Thermal harvesting is a promising method for capturing freely available heat and converting it to a more usable form, such as electrical energy. Thermal harvesting for low power electronic devices using ferroelectric materials is one of the emerging areas of research because they possess spontaneous polarization and exhibit excellent piezoelectric as well as excellent pyroelectric coefficients. These materials are unique as they only sense time-dependent temperature change to generate electric power. We have grown lead-free $\text{BaZr}_{0.2}\text{Ti}_{0.8}\text{O}_3$ (BZT)/ $\text{Ba}_{0.7}\text{Ca}_{0.3}\text{TiO}_3$ (BCT) multilayer heterostructures and studied the structural, dielectric, ferroelectric, pyroelectric and energy density characteristics. The BZT/BCT multilayer epitaxial heterostructures were grown on SrRuO (SRO) buffered SrTiO (STO) single crystal substrate by optimized pulsed laser deposition technique. The large angle x-ray scans showed only diffraction peaks from the substrate and pseudocubic reflections (00 l) from the multilayer heterostructure, confirming that these films are phase pure and epitaxial in nature. The atomic force microscopy (AFM) studies indicate that the surface roughness is low and that film growth is of high quality. The ferroelectric phase transitions have been probed above room temperature with relaxor behavior. The polarization versus electric field (P-E) measurement exhibits well-saturated hysteresis loop with maximum and remnant polarization of 138 and 64 $\mu\text{C}/\text{cm}^2$, respectively. Solid-state, thin-film devices, that convert low-grade heat into electrical energy, are demonstrated using pyroelectric Ericsson cycles, and their performance is optimized by independently enhancing pyroelectric coefficient and suppressing dielectric permittivity in compositionally graded heterostructures. Our findings suggest that pyroelectric devices may be competitive with thermoelectric devices for low-grade thermal harvesting.

11:20am TF+EM+NS+SS-ThM11 Thermal Treatment Effects on the Thermoelectric Devices from Sn/Sn+SnO₂ Thin Films, *Satilmis Budak, E. McGhee, Z. Xiao, E. Barnes, R. Norwood*, Alabama A&M University

Approximately two-thirds of energy is lost as waste heat; the direct harvest of this waste heat using thermoelectric (TE) materials has attracted worldwide interest. TE materials can convert waste heat from industrial processes, furnaces, and engine exhaust streams into useful electricity by the Seebeck effect. The energy conversion efficiency is shown by the dimensionless figure of merit, ZT, and $ZT=S^2\sigma T/K$, where S is the Seebeck coefficient, σ is the electrical conductivity, K is the total thermal conductivity, and T is the absolute temperature. The numerator $S^2\sigma$ defines the power factor (PF), which primarily relates to the electric properties [1]. When operating as an energy-generating device, the TE device is termed a thermoelectric generator (TEG). The source of thermal energy manifests itself as a temperature difference across the TEG. When operating in a cooling or heating mode the TE device is termed a thermoelectric cooler (TEC). Similarly, the TE device produces heating or cooling that takes the form a heat flux which then induces a temperature difference across the TEC. TE devices are solid-state mechanisms that are capable of producing these three effects without any intermediary fluids or processes. For power generation applications TE devices are used in automobiles as exhaust gas waste heat recovery devices where thermal energy is scavenged along the exhaust line of a vehicle and converted into useful electricity [2]. The TE devices from 50 alternating layers of Sn/Sn+SnO₂ thin films were prepared using DC/RF Magnetron Sputtering. They were heat treated at different temperatures to form nanostructures to increase the Seebeck coefficients and electrical conductivity and decrease thermal conductivity. Seebeck coefficient, van der Pauw resistivity, and thermal conductivity were used for the characterization. SEM/EDS was used to characterize the surface morphology of the films.

[1] Hongchao Wang, Wenbin Su, Jian Liu, Chunlei Wang, "Recent development of n-type perovskite thermoelectrics", *J Materiomics* 2 (2016) 225-236

[2] Chetan Jangonda, Ketan Patil, Avinash Kinikar, Raviraj Bhokare, M.D.Gavali, "Review of Various Application of Thermoelectric Module",

International Journal of Innovative Research in Science, Engineering and Technology Vol. 5, Issue 3, (March 2016), 3393-3400.

Acknowledgement

Research was sponsored by NSF with grant numbers NSF-HBCU-RISE-1546965, NSF-EPSCOR-R-II-3-EPS-1158862, NSF-MRI-1337616, DOD with grant numbers W911 NF-08-1-0425, and W911NF-12-1-0063, U.S. Department of Energy National Nuclear Security Administration (DOE-NNSA) with grant numbers DE-NA0001896 and DE-NA0002687.

11:40am TF+EM+NS+SS-ThM12 Thermoelectric Properties of Efficient Thermoelectric Devices from Sb/Sb+SnO₂ Thin Films, *Eshirdanya McGhee, S. Budak, Z. Xiao, N. Caver, B. McNeal*, Alabama A&M University

The thermoelectric (TE) concept could be seen as a perfect solution for recovering waste heat from engine exhaust and converts it to electric energy. TE generators are all solid-state devices that convert heat into electricity. Unlike traditional dynamic heat engines, TE generators contain no moving parts and are completely silent. Such generators have been used reliably for over 30 years of maintenance-free operation in deep space probes such as the Voyager missions of NASA. TE systems can be easily designed to operate with small heat sources and small temperature differences [1]. An ideal TE material behaves like an electron crystal and phonon glass, allowing a large temperature gradient across it while conducting electricity efficiently to generate a TE voltage. Significant progress in the TE performance of materials has been made by exploring ultra low thermal conductivity at high temperature and reducing thermal conductivity by nano-structuring, as well as by resonant doping and energy-dependent scattering of electrons [2]. The figure of merit ZT describes material performance. ZT depends on the thermoelectric material properties of Seebeck coefficient S, electrical conductivity σ , and thermal conductivity K, and $ZT=S^2\sigma T/K$ where T is the temperature of the material [3]. TE devices from 50 alternating layers of Sb/Sb+SnO₂ thin films were prepared by DC/RF Magnetron Sputtering. TE devices were annealed at different temperatures to form nano-structures to increase the Seebeck coefficients and electrical conductivity and decrease thermal conductivity. For the characterization, Seebeck coefficient, van der Pauw resistivity, and thermal conductivity were used. The surface morphology was characterized using SEM/EDS.

[1] Krishna Purohit, Sheetal Kumar Jain, Dr. P M Meena, Khushaboo Singh, Manish Dadhich,

"Review Paper on Optimizations of Thermoelectric System", *International Journal of Innovative Research in Engineering & Management (IJIREM)*, ISSN: 2350-0557, Volume-3, Issue-4, (July-2016), 259-263.

[2] Kedar Hippalgaonkar, Ying Wang, Yu Ye, Diana Y. Qiu, Hanyu Zhu, Yuan Wang, Joel Moore, Steven G. Louie, and Xiang Zhang, "High thermoelectric power factor in two-dimensional crystals of MoS₂", *PHYSICAL REVIEW B* 95, 115407 (2017) 1-9.

[3] Saniya LeBlanc, *Sustainable Materials and Technologies* 1–2 (2014) 26–35.

Acknowledgement

Research was sponsored by NSF with grant numbers NSF-HBCU-RISE-1546965, NSF-EPSCOR-R-II-3-EPS-1158862, NSF-MRI-1337616, DOD with grant numbers W911 NF-08-1-0425, and W911NF-12-1-0063, U.S. Department of Energy National Nuclear Security Administration (DOE-NNSA) with grant numbers DE-NA0001896 and DE-NA0002687.

12:00pm TF+EM+NS+SS-ThM13 3D Printed Triboelectric Nanogenerator, *I. Fattah, E. Utterback, Naga Srinivas Korivi, V. Rangari*, Tuskegee University

We report on the development of polymer nanocomposite layers made by 3D printing. The nanocomposite is composed of polydimethylsiloxane (PDMS), barium titanate nanoparticles, and multi-walled carbon nanotubes. Flexible layers of this composite have been 3D printed using a commercial 3D printer, and function as triboelectric energy generators. To the best of our knowledge, this is the first report of a PDMS based triboelectric nanogenerator fabricated by 3D printing. The nanogenerators have been evaluated in contact and separation mode and produce a maximum of 2.6 Volts under pressure from a human finger.

The fabrication procedure involves sonicating barium titanate (BaTiO₃, Skyspring Nanomaterials) and multi walled carbon nanotubes (MWCNT, Skyspring Nanomaterials) together in ethyl alcohol. This is followed by removing the excess ethyl alcohol, and manually grinding the nanoparticle powder to break any clusters. This is followed by mechanically blending liquid PDMS pre-polymer and its curing agent (~10:1 ratio by weight) with the nanoparticle powder in one beaker. Finally, the blend is filled into a

Thursday Morning, October 24, 2019

dual plastic syringe, which is loaded onto an extrusion printing head of a commercial 3D printer (Hydra 16A, Hyrel LLC, USA). The printer reads a software file that defines the pattern or shape to be printed and dispenses the material from the syringe accordingly onto a base plate. For printing this composite, the base plate temperature was maintained between 75 – 90 °C, to allow curing within a few minutes. Once cured, the solid composite layers (270 µm thickness) can be peeled off the base plate.

The 3D printed PDMS-BaTiO₃-MWCNT layers have been evaluated as triboelectric energy generation. In one embodiment, the 3D printed functions as the negatively charged layer in a contact-separation scheme. A polyimide sheet is used as positively charged layer. Carbon tapes are used as current collectors on both positive and negative charged layers. When these two layers are brought in contact with some pressure applied by a human finger, and then released, characteristic negative and positive voltage spikes are respectively observed. Peak voltages as high as 2.6 Volts have been obtained with the present 3D printed PDMS-BaTiO₃-MWCNT layers. These observations indicate the applicability of this 3D printed composite in triboelectric energy generation.

Acknowledgments: This research was supported by the National Science Foundation grant #1827690.

2D Materials

Room A216 - Session 2D+AS+BI+HC+MN+NS+PS+SS+TL-ThA

Surface Chemistry, Functionalization, Bio, Energy and Sensor Applications

Moderator: Mark Edmonds, Monash University, Australia

2:20pm **2D+AS+BI+HC+MN+NS+PS+SS+TL-ThA1 Molecular Layers on Nanoporous Gold Electrodes**, *Elizabeth Landis*, College of the Holy Cross
Nanoporous gold presents a surface with high conductivity and surface area, which makes it an interesting platform for surface chemistry. However, the nanoporous gold surface lacks the functionality necessary for many applications including sensing. We have investigated self-assembled thiol-based monolayers and the electroreduction of diazonium-based salts to form aryl molecular layers on nanoporous gold. We use infrared spectroscopy and cyclic voltammetry to show that the molecular layer ordering and density depends on the functionalization method, and the underlying nanoporous surface impacts molecular ordering and electron transfer properties.

2:40pm **2D+AS+BI+HC+MN+NS+PS+SS+TL-ThA2 Thermotropic Liquid Crystal (5CB) on Two-dimensional Materials**, *Paul Brown*, American Society for Engineering Education; *S. Fischer, J. Kotacz, C.M. Spillmann, D. Gunlycke*, U.S. Naval Research Laboratory

Current means of redirecting light often rely on either bulky mechanical gimbals or non-mechanical diffractive elements. The former often suffer from wear and are susceptible to failure, while the latter may have significant optical power confined within side lobes. One promising non-mechanical approach that can overcome present limitations in beam redirection incorporates liquid crystal (LC) for continuous, refractive steering. Nematogens, the molecules comprising the LC in a nematic phase, support inherent anisotropic optical and dielectric properties that result from local ordering of single molecules. Recent research suggests the possibility of including two-dimensional materials to act as both an alignment layer and electrode to LC. This offers the possibility of further reducing device dimensions and device response time. Yet little research has focused on the ground state properties of a nematogen interfacing with the two-dimensional substrate. In this talk, we present density functional theory results of the electronic properties of a well-known nematogen (5CB) interacting with graphene, boron nitride, and phosphorene. We also discuss the influence of an introduced single vacancy on the electronic properties of the composite system. We find that 5CB on phosphorene offers the strongest binding of the considered nanosheets. Moreover, we observe qualitatively different band alignments, and focus in particular on type I, which prohibits free carrier transfer between the substrate and nematic LC. Lastly, we discuss the impact of single vacancies on the performance of two-dimensional materials to operate as both an alignment layer and electrode for LC-based applications.

This work has been supported by the Office of Naval Research, directly and through the U.S. Naval Research Laboratory.

3:00pm **2D+AS+BI+HC+MN+NS+PS+SS+TL-ThA3 Is it Possible to Achieve Intra-molecular Resolution with Ambient AFM?**, *Vladimir Korolkov*, Oxford Instruments-Asylum Research; *S.C. Chulikov, M. Watkins*, University of Lincoln, UK; *P.H. Beton*, The University of Nottingham, UK

Although achieving molecular resolution is now almost a routine across various SPM imaging modes, resolving the actual molecular structure at the atomic level has only been accomplished with NC-AFM in UHV often at low temperatures and with a functionalized probe. Of course, the ultimate goal in SPM is to resolve the chemical structure of a molecule identifying each atom.

In this work we are presenting an approach to achieve intra-molecular resolution on adsorbed molecules in the ambient at room temperatures with a standard AFM cantilever with unmodified tip. We have discovered that using a combination of higher eigenmodes and low oscillation amplitudes (~3-5Å) of a standard Si-cantilever routinely provides ultra-high resolution on adsorbed molecules on surfaces^{1,2} and bulk polymers³.

With this approach we have been able to observe both intra-molecular features and inter-molecular contrast in thin films of coronene and melem molecules on the surface of hexagonal boron nitride (hBN). In case of coronene, all six benzene rings have been resolved as well as underlying atomic lattice of hBN. Unlike coronene, melem forms molecular assemblies with square symmetry stabilized with in-plane strong hydrogen bonds between amino groups. We have observed a strong inter-molecular

contrast where the hydrogen bonds are expected to be. Similar to coronene, the observed intra-molecular contrast was associated with three triazine rings. We have used Probe particle model⁴ to simulate our experimental AFM images and found very good agreement between them. In fact, PPM allowed us a correct interpretation of melem square phase assembly.

Both systems were studied at room and elevated temperatures where we observed phase transitions leading to thermodynamically stable systems. The experimental results are in excellent agreement with density functional theory calculations.

We believe the proposed approach, yet still in its infancy, could potentially provide a pathway to unambiguous identification of molecules on surfaces in the ambient on standard AFM systems.

¹Korolkov et al., Nat. Chem., 2017

²Korolkov et al., Nat. Comm., 2017

³Korolkov et al., Nat. Comm., 2019

⁴Hapala et al., Phys. Rev. B 90, 085421

3:20pm **2D+AS+BI+HC+MN+NS+PS+SS+TL-ThA4 Tailoring Surface Properties via Functionalized Hydrofluorinated Graphene Compounds**, *Jangyup Son*, University of Illinois at Urbana-Champaign; *N. Buzov*, University of California at Santa Barbara; *S. Chen*, University of Illinois at Urbana-Champaign; *D. Sung*, Sejong University, Republic of Korea; *H. Ryu*, Seoul National University, Republic of Korea; *J. Kwon*, Yonsei University, Republic of Korea; *S. Kim, J. Xu*, University of Illinois at Urbana-Champaign; *S. Hong*, Sejong University, Republic of Korea; *W. King*, University of Illinois at Urbana-Champaign; *G.H. Lee*, Seoul National University, Republic of Korea; *A.M. van der Zande*, University of Illinois at Urbana-Champaign

Mixing compounds or alloys is an important process to tailor or enhance the intrinsic properties of materials such as chemical reactivity, mechanical strength, and electronic structure. In nanosystems, such as two-dimensional (2D) materials like graphene, transition metal dichalcogenides (TMDCs), and hexagonal boron nitride (hBN), where there is no distinction between the surface and the bulk, mixing of elements is also an important tool for tailoring the interaction of the material with its environment. A successful strategy for manipulating the chemical structures of 2D materials is the chemical functionalization of graphene with single elements such as H, O, N, and F. Yet, an even wider parameter space is possible by combining these functionalization species to produce ternary functionalized graphene compounds.

Here we present a new strategy for producing functionalized graphene compounds through the systematic control of the ratio between adatoms. We demonstrate tailored hydrofluorinated graphene (HFG) compounds via the sequential exposure of graphene to low-energy hydrogen plasma and xenon difluoride (XeF₂) gas. We demonstrate reversible switching of the surface between completely hydrogenated graphene (HG) and fluorinated graphene (FG) as well as the intermediate ratio between two extremes. Moreover, we demonstrate pattern the surface functionalization on a single chip into chemically distinct materials (graphene, FG, HG, and HFG compounds).

Finally, with these patterned structures, we demonstrated tailoring of the surface and electronic properties of the 2D materials. First, the patterned structures enable direct comparisons of the relative surface properties such as wettability and surface friction. Additionally, the electrical properties of functionalized graphene compounds showed unusual recovery of electrical conductance during the partial transformation of FG to HFG, due to initial removal of existing F adatoms when exposed to hydrogen plasma. This study opens a new class of 2D compound materials and innovative chemical patterning that can lead to atomically thin 2D circuits consisting of chemically/electrically modulated regions.

4:20pm **2D+AS+BI+HC+MN+NS+PS+SS+TL-ThA7 Towards Higher Alcohol Synthesis from Syngas on 2D material-based catalysts: A First-Principles Study***, *Tao Jiang, D. Le, T.S. Rahman*, University of Central Florida

Synthesis of higher alcohol from syngas has been of great interest owing to the limited petroleum resources and environmental concerns. Rational designing of cheap and efficient catalyst material for such synthesis is in great demand because of diminishing supply of the current state-of-the-art catalysts. Two dimensional (2D) materials are emerging with far-reaching potential for technical and industrial applications thanks to their unique properties, recent developments and improvement of production technologies. In this talk, we will discuss our recent work, based on first

Thursday Afternoon, October 24, 2019

principles calculations, towards the unitization of 2D materials as catalysts for higher alcohol synthesis. In particular, defect laden hexagonal boron nitride (*dh*-BN) with N vacancies is excellent catalyst for hydrogenation of CO₂ towards ethanol formation, in the reaction pathway of which the crucial step for forming C₂ bond, i.e. reaction of adsorbed species CH₃* and CO* to form CH₃CO*, is exothermic with reasonably low activation barrier (0.68 eV). On the other hand, we also find single layer of MoS₂ functionalized with small Au nanoparticle to catalyze CO hydrogenation reaction towards ethanol formation. Among all the elementary reactions, the important steps are the reaction of an adsorbed CH₃* and a CO* molecule and the hydrogenation of acetyl to acetaldehyde (both are exothermic with activation barriers of 0.69 and 0.47 eV, respectively) to form C₂ species.[1] The results suggest that 2D materials are suitable candidates for higher alcohol synthesis. Full reaction pathways will be discussed together with results of Kinetic Monte Carlo simulations to shed light on the selectivity of the catalysts. Contact will be made with experimental data that validate our theoretical predictions.

[1] K. Almeida, K. Chagoya, A. Felix, T. Jiang et al, "Towards Higher Alcohol Formation using a single-layer MoS₂ activated Au on Silica: Methanol Carbonylation to Acetaldehyde", submitted

*Work supported in part by DOE Grant DE-FG02-07ER15842

4:40pm **2D+AS+BI+HC+MN+NS+PS+SS+TL-ThA8 Proton Conductivity Properties of Electrospun Chitosan Nanofibers, Woo-Kyung Lee, J.J. Pietron, D.A. Kidwell, J.T. Robinson, C.L. McGann, S.P. Mulvaney, U.S. Naval Research Laboratory**

A major challenge of the 21st century will be to establish meaningful two-way communication between biology and electronics. The study of protonics, devices that mimic electronics but pass protons instead of electrons, seeks to bridge this gap. Protonic conductive materials (PCMs) are essential elements of these devices and we have demonstrated significant improvement in conductivity for chitosan PCMs when deposited as electrospun nanofibers. The observed improvements stem from both enhanced molecular alignment and from chemical doping due to the electrospinning carrier fluid, trifluoroacetic acid (TFA). We deposited electrospun chitosan nanofibers over palladium protodes and then used the helium ion microscope to isolate single nanofibers for detailed study. We observed that single chitosan nanofibers are strongly doped by TFA with x-ray photoelectron spectroscopy demonstrating extensively protonated nitrogen functionality. With the isolated, single chitosan nanofibers we observed that water uptake, fiber/electrode contact area, and doping concentration are critical parameters of protonic device performance and lead to increased conductivity (*i.e.* low resistivity). The average resistivity of single chitosan nanofibers is $6.2 \times 10^4 \Omega\text{-cm}$, approximately two orders of magnitude lower than the resistivity of cast chitosan PCMs (cast from acetic acid solutions not TFA). We have observed excellent agreement between theoretical models and experiment results that explore each of the contributions to the improved conductivity. In addition, the fabrication and measurement of ionic field-effect transistor of single chitosan fiber using conductive atomic force microscope will be discussed.

5:00pm **2D+AS+BI+HC+MN+NS+PS+SS+TL-ThA9 Sensor for Breath and Skin Diagnostics, Pelagia I Gouma, The Ohio State University**
Resistive gas sensors have received a bad reputation of being largely non-selective.

Our work has produced a crystallo-chemical model for selective gas sensing by polymorphic

metal oxides. The reaction-based and ferro-electric poling sensing mechanisms are discussed

in detail. Novel processing methods to produce the respective nano sensors are presented along

with the device fabrication for the non-invasive diagnosis of gaseous biomarkers in human

and animal breath or skin. This sensor technology is expected to revolutionize medical diagnostics.

5:20pm **2D+AS+BI+HC+MN+NS+PS+SS+TL-ThA10 Symmetry Controlled Adsorption of Diodobenzene on MoS₂, Zahra Hooshmand, University of Central Florida; P. Evans, P.A. Dowben, University of Nebraska - Lincoln; T.S. Rahman, University of Central Florida**

In a joint experimental and theoretical study, we have uncovered evidence of the importance of symmetry in the adsorption of the isomers of diiodobenzene on MoS₂(0001). The intensity ratio of iodine to molybdenum

measured, as a function of exposure for different isomers of the diiodobenzene, show that while for ortho (1,2-) and para (1,4-) diiodobenzene the rate of adsorption at 100 K is very low, that for meta (1,3-) diiodobenzene is considerably more facile. We have applied dispersion corrected density functional theory-based calculations to understand the subtleties in the electronic structure and geometry of adsorption of these diiodobenzene isomers on MoS₂(0001). All three isomers are found to weakly chemisorb with the same binding strength as well as adopt similar configurations. The calculated electron affinity of the three molecules also do not show a specific trend that would verify experimental data. However, analysis of the frontier orbitals indicate that those of 1,3-diiodobenzene are strongly affected by interactions with MoS₂, while that of the other two isomers remain unchanged. Our results show that symmetry is the identifying factor in these adsorption characteristics. The results of frontier orbitals analysis confirm that for adsorption of (1,2-) and (1,4-) diiodobenzene a reduction in the symmetry of the adsorbent is needed. To further validate our conclusions, we compare the above results with that of the adsorption of the diiodobenzene isomers on defect-laden MoS₂(0001).

* Work support in part by DOE grant DE-FG02-07ER15842

5:40pm **2D+AS+BI+HC+MN+NS+PS+SS+TL-ThA11 Mechanistic Understanding of the CO Hydrogenation Reaction on Defect Engineered 2D-TaS₂ and 2D-MoS₂ Catalysts, Mihai Vaida, University of Central Florida**

Due to global energy demands, investigation of catalytic reaction mechanisms on novel catalytic materials that can lead to efficient production of storable fuels from sustainable inputs is of central importance. In this contribution the adsorption of CO and H₂ molecules, as well as the CO hydrogenation reaction are investigated on defect engineered two dimensional (2D) TaS₂ and MoS₂. Crystalline 2D-TaS₂ and 2D-MoS₂ with surface area of 1 cm² are synthesized via a multistep process based physical vapor deposition on Cu(111). The surface composition, morphology, and electronic structure are investigated via Auger electron spectroscopy, low energy electron diffraction, scanning tunneling microscopy, scanning tunneling spectroscopy, and photoemission spectroscopy. The interaction of the molecules with the surface and the catalytic reaction mechanisms are investigated via temperature programmed desorption/reaction. No catalytic reactions have been observed on crystalline 2D materials. However, an enhanced catalytic activity is observed after the generation of sulfur vacancies via Ar sputtering. The CO hydrogenation on TaS₂ occurs on low coordinated Ta atoms through the formation of formyl radical (HCO) and formaldehyde (HCOH). On 2D-MoS₂, the CO hydrogenation also occurs on low coordinated Mo atoms. However, in this case the formyl radical splits to form methyldyne radical (CH), which subsequently react with other CH radical to produce acetylene (C₂H₂).

Chemical Analysis and Imaging Interfaces Focus Topic Room A120-121 - Session CA+NS+SS+VT-ThA

Progress in Instrumentation and Methods for Spectro-microscopy of Interfaces

Moderators: Jinghua Guo, Lawrence Berkeley National Laboratory, Andrei Kolmakov, National Institute of Standards and Technology (NIST)

2:20pm **CA+NS+SS+VT-ThA1 Helium and Neon Ion Beams for the Imaging and Analysis of Interfaces, John A. Notte, C. Guillermier, F. Khanom, B. Lewis, Carl Zeiss PCS, Inc.**

INVITED
The recently developed ORION NanoFab instrument provides a single platform with He⁺, Ne⁺, and Ga⁺ focused ion beams. The gallium beam is a conventional FIB and offers high currents and high sputter yields for material removal applications such as sample preparation or exposing sub-surface features. The He and Ne ion beams originate from a sub-nanometer ionization volume of the gas field ion source (GFIS) and because of this, can be focused to remarkable small probe sizes, 0.5 nm and 1.9 nm respectively. The He beam is now well established for high resolution imaging with surface sensitivity, long depth of focus, and the ability to image insulating surfaces without a conductive overcoating. The helium beam has also been used successfully in a variety of nanofabrication tasks such as lithographic exposure of resist, fine sputtering, beam chemistry, and precision modification of materials. The neon beam with its intermediate mass provides a higher sputtering yield, and with that, the ability to perform SIMS analysis with an unprecedented small focused probe size. A newly integrated magnetic spectrometer enables analytical

Thursday Afternoon, October 24, 2019

capabilities on this same platform, with a lateral resolution limited only by the collision cascade. Features smaller than 15 nm have been detected. Together these complementary imaging modes can be combined to provide insights of morphology and composition at the smallest length scales.

In this talk the underlying technology of the NanoFab-SIMS will be introduced, as will the physics of the beam-sample interactions. The bulk of the presentation will provide a survey of results, both published and new, demonstrating how this instrument can serve in a variety of applications related to interfaces.

3:00pm **CA+NS+SS+VT-ThA3 Interfacial Studies using Ambient Pressure XPS**, *Paul Dietrich*, A. Thissen, SPECS Surface Nano Analysis GmbH, Germany

INVITED

Over the last decades XPS under Near Ambient Pressure (NAP) conditions has demonstrated its promising potential in a wide variety of applications. Starting from operando studies of surface reactions in catalysis, the applications soon have been enhanced towards studies of processes at liquid surfaces, mainly using freezing/melting cycles, liquid jets or liquid films on rotation disks or wheels. Since more than 15 years, the need for basic studies of fundamental solid-liquid interface chemistry has attracted growing interest. Dip-and-pull experiments at synchrotron sources finally also demonstrated, that in-situ and operando XPS in electrochemical experiments can be realized, significantly contributing to the basic understanding of modern energy converting or storing devices, like batteries, fuel cells, etc.

The development of pure laboratory NAP-XPS systems with optimized sample environments, like special sample holders, Peltier coolers and operando liquid cells combined with full automation and process control provides possibilities for preparation and analysis of a multitude of liquid samples or solid-liquid interfaces on a reliable daily base.

Interfaces of semiconductors with organic solvents are important for production processes and device operation. The first example presented shows the simplicity of obtaining relevant results on Silicon in different organic solvents without the need of highly sophisticated set-ups or special excitation sources beyond Al K α .

Another example shows an operando study of metal corrosion in acetic acid. Moreover a versatile set-up is presented, allowing for studies of solid-electrolyte interfaces for example in Lithium ion batteries as a simple laboratory experiment.

Finally an outlook is given on the future perspective of applications and scientific contributions of routine operando XPS.

4:00pm **CA+NS+SS+VT-ThA6 Operando Spectroscopy and Microscopy of the Electrode-Electrolyte Interface in Batteries**, *Feng Wang*, Brookhaven National Laboratory

INVITED

Real-time tracking structural/chemical changes of electrodes in batteries is crucial to understanding how they function and why they fail. However, in real battery systems electrochemical/chemical reaction occurs at varying length scales, leading to changes not only in the bulk but often locally at electrolyte/electrode interface. *In situ* X-ray techniques are typically employed for studying structural changes in the bulk electrodes and often limited by their poor spatial resolution in probing local changes at interface. Herein, we present our recent results from developing new operando spectroscopy and microscopy techniques, specialized for studying electrochemical/chemical reaction and structural modification of the solid-electrode surface and interface, *in the presence of the electrolyte and during battery operation*. Examples will be given to show how interfacial reaction during battery operation is visualized directly, allowing gaining insights into electrode/electrolyte design for practical use in batteries. New opportunities for combining *first principles* simulation and deep machine learning to complement and guide experiments will also be discussed.

4:40pm **CA+NS+SS+VT-ThA8 Ultrasensitive Combined Tip- and Antenna-Enhanced Infrared Nanoscopy of Protein Complexes**, *B.T. O'Callahan*, Pacific Northwest National Laboratory; *M. Hentschel*, University of Stuttgart, Germany; *M.B. Raschke*, University of Colorado Boulder; *P.Z. El-Khoury*, Pacific Northwest National Laboratory; *Scott Lea*, Pacific Northwest National Laboratory

Surface enhanced infrared absorption (SEIRA) using resonant plasmonic nanoantennas enables zeptomolar detection sensitivity of (bio)analytes, although with diffraction limited spatial resolution. In contrast, infrared scattering-scanning near-field optical microscopy (IR s-SNOM) allows simultaneous imaging and spectroscopy with nanometer spatial resolution

through vibrational coupling to the antenna mode of a probe tip. In this presentation, we discuss our approach combining these two methods to image both continuous and sparse distributions of ferritin protein complexes adsorbed onto IR-resonant Au nanoantennas. The joint tip- and antenna-enhancement yields single protein complex sensitivity due to coupling with the vibrational modes of the bioanalytes. The coupling is revealed through IR s-SNOM spectra in the form of Fano lineshapes, which can be modelled using coupled harmonic oscillators. Through simulations of the recorded hyperspectral images, we extract the optical signatures of protein complex monolayers. This work paves the way for single protein identification and imaging through a combination of tip and antenna-enhanced IR nanoscopy.

5:00pm **CA+NS+SS+VT-ThA9 Imaging and Processing in Liquid Gel Solutions with Focused Electron and X-ray Beams**, *T. Gupta*, National Institute of Standards and Technology (NIST); *P. Zeller*, *M. Amati*, *L. Gregoratti*, Elettra - Sincrotrone Trieste, Trieste, Italy; *Andrei Kolmakov*, National Institute of Standards and Technology (NIST)

Gels are porous polymeric scaffolds that can retain high volume fraction of liquids, can be easily functionalized for a specific need, can be made biocompatible and therefore, found numerous applications in drugs delivery, tissue engineering, soft robotics, sensorics, energy storage, etc. We have recently proposed a technique for micro-patterning and high-resolution additive fabrication of 3D gel structures in natural liquid solutions using electron and soft X-ray scanning microscopes [1]. The core of the technology is the employment of ultrathin electron (X-ray) transparent molecularly impermeable membranes that separate high vacuum of the microscopes from a high-pressure fluidic sample. In this communication, we report on effects of the beam and exposure conditions on to the degree of crosslinking of pristine and composite PEGDA hydrogels. We found that cross-linking occurs at very low irradiation doses. The size of the crosslinked area saturates with the dose and bond scission occurs at elevated radiation doses what has been supported with O 1s and C 1s XPS spectra evolution and prior research [2]. These chemically modified regions can be selectively etched what enables an additional partnering option for the gelled features with a spatial resolution of ca 20 nm. Finally, we defined the imaging conditions for guest particles in composite hydrogels in its liquid state during the crosslinking process. We were able to observe the electrophoretic migration of sub 100 nm Au nanoparticles inside the gel matrix.

References

[1] T. Gupta *et al.*, "Focused Electron and X-ray Beam Crosslinking in Liquids for Nanoscale Hydrogels 3D Printing and Encapsulation," *arXiv preprint arXiv:1904.01652*, 2019.

[2] N. Meyerbröcker and M. Zharnikov, "Modification and Patterning of Nanometer-Thin Poly (ethylene glycol) Films by Electron Irradiation," *ACS applied materials & interfaces*, vol. 5, no. 11, pp. 5129-5138, 2013.

5:20pm **CA+NS+SS+VT-ThA10 In Situ TEM Visualization of Solution-based Nanofabrication Processes: Chemical Wet-etching and Capillary Forces**, *Utkur Mirsaidov*, National University of Singapore, Singapore

INVITED

Controlled fabrication of 3D nanoscale materials from semiconductors is important for many technologies. For example, scaling up the density of the transistors per chip requires the fabrication of smaller and smaller vertical nanowires as channel materials [1]. Two key processes essential to the fabrication of these devices is a precise etching of the nanostructures and the damage-free solution based cleaning (damage occurs during post-clean drying due to capillary forces). However, very little is known about both of these processes because it is extremely challenging to visualize etching and cleaning with solutions directly at the nanoscale. Here, using *in situ* liquid phase dynamic TEM imaging [2-4], we first describe the detailed mechanisms of etching of vertical Si nanopillars in alkaline solutions [5]. Our design of liquid cells includes a periodic array of patterned nanopillars at a density of $1.2 \times 10^{10} \text{ cm}^{-2}$. We show that the nanoscale chemical wet-etch of Si occurs in three stages: 1) intermediates generated during alkaline wet etching aggregate as nanoclusters on the Si surface, 2) then the intermediates detach from the surface before 3) dissolving in the etchant.

Next, we describe the capillary damage of these high-aspect-ratio Si nanopillars during drying after the solution-phase cleaning. Our results reveal that drying induced damage to nanopillars occurs in three distinct steps. First, as water evaporates from the surface patterned with nanopillars, water film thins down non-uniformly leaving small water nanodroplets trapped between the nanopillars. Second, the capillary forces induced by these droplets bend and bring the nanopillars into contact with each other at which point they bond together. Third, droplets trapped

Thursday Afternoon, October 24, 2019

between the nanopillars evaporate leaving the nanopillars bonded to each other. We show that even after the nanodroplets finally evaporate, interfacial water covering the nanopillars act as a glue and holds the pillars together.

Our findings highlight the importance of being able to visualize the processes relevant to nanofabrication in order to resolve the failure modes that will occur more frequently as the device sizes get even smaller in the future.

- [1] C. Thelander et al, *Mater. Today* 9 (2006), 28–35.
- [2] M. J. Williamson et al, *Nature Materials* 2 (2003), p. 532.
- [3] H. Zheng et al, *Science* 324 (2009), p. 1309.
- [4] U. Mirsaidov et al, *Proc. Natl. Acad. Sci. U.S.A.* 109 (2012), p. 7187.
- [5] Z. Aabdin et al, *Nano Letters* 17 (2017), p.2953.
- [6] This work was supported by Singapore National Research (NRF-CRP16-2015-05).

Fundamental Aspects of Material Degradation Focus Topic Room A212 - Session DM1+BI+SS-ThA

Low Fouling Interfaces and Environmental Degradation

Moderator: Axel Rosenhahn, Ruhr-University Bochum, Germany

2:20pm **DM1+BI+SS-ThA1 Utilizing Experimental and MD Simulation Approaches in the Understanding and Design of Low Fouling Interfaces, Paul Molino**, University of Wollongong, Australia **INVITED**

Biofouling is a ubiquitous problem for a diverse suite of industries, impacting the functionality of materials and devices. Diverse approaches taken in the design of materials and interfaces to prevent microbial fouling often rely on atomic and molecular scale processes, however the fundamental mechanism/s underlying these processes, and their mode of action, in many cases continue to elude researchers. Highly hydrophilic chemistries such as polyethylene glycol and zwitterion-based chemistries, have long been used to generate interfaces that prevent biological interactions at surfaces. Such surface chemistries have been proposed to function through a combination of molecular water organisation and steric repulsion at the interface. Experimental approaches have confirmed the presence of hydration layers associated with hydrophilic polymer-based surfaces, yet the fundamental mechanisms underlying their capacity to inhibit surface fouling, and how such hydration layers differ from equally hydrophilic interfaces that do not prevent surface fouling is still unclear. Molecular dynamic (MD) simulations have gone some way to provide critical insights into their respective mechanism/s of action, however experimental approaches capable of adequately resolving features at a suitable spatial resolution to corroborate and build on these models have been lacking. Herein I will present a highly biofouling resistant coating composed of silica nanoparticles functionalised with a short chain hydrophilic silane. To understand the interfacial environment at the hydrated nanoparticle surface, frequency modulation – atomic force microscopy was used to provide sub-atomic resolution of the water structuring about the nanoparticle interface, which we validate using all-atom molecular dynamic simulations that strikingly predict similar structures of water layers on the original and ultralow fouling surfaces. The convergence of experimental and modelling data reveals that suitably spaced, flexible chains with hydrophilic groups interact with water molecules to produce a connective, *quasi-stable* layer, consisting of dynamic interfacial water, that provides a basis for antifouling performance of ultrathin, hydrophilic surface chemistries. This approach provides a road map for the future development and optimisation of interfacial chemistries and materials designed to combat biofouling and biodegradation.

3:00pm **DM1+BI+SS-ThA3 Study of Environmental Exposure Effects on Pristine and DC Magnetron Sputtering Metallic Coated 3D Printed Polymers, D. Mihut, Arash Afshar, P. Chen**, Mercer University

Three dimensional printing is a promising technique for producing complex geometries and high precision structures from different types of materials. The technique is particularly attractive for polymeric materials due to the cost effectiveness; however when compared to other manufacturing techniques the resulting structures have low mechanical properties and low performance as exposed to harsh environmental conditions. ABS (acrylonitrile butadiene styrene) and PLA (polylactic acid) are common thermoplastic polymers used for many applications (e.g. electrical and electronic assemblies, medical devices, implants, toys). For this research, the ABS and PLA specimens for tensile and flexural testing were 3D

manufactured according to standards and their mechanical properties were tested using hardness tester, and Mark-10 tensile testing equipment. In order to simulate outdoor environmental conditions while avoiding the uncertainties associated with it, specimens were exposed to controlled environmental chamber. Accelerated exposure was performed using a UV radiation/condensation (Q-Lab QUV/basic) accelerated weathering tester. ABS and PLA samples were exposed to UV radiation, high temperature and moisture cycles for different time intervals. Some ABS samples were coated with optically thick metallic materials (silver and copper) using high vacuum DC magnetron sputtering deposition system and were later exposed to UV radiation, high temperature and moisture cycles using same conditions as for un-coated samples. The surface and cross section morphology of samples and the adhesion of metallic layers to the polymer substrates were examined using scanning electron microscopy and laser scanning microscopy. The crystalline structure of the metallic coatings was analyzed using X-ray Diffraction technique. The mechanical properties were characterized using flexural and hardness tests over the exposure time. The metallic thin films improved the surface resistance of the substrate materials and enhanced the mechanical behavior of samples exposed to harsh environmental conditions.

3:20pm **DM1+BI+SS-ThA4 Reaction Mechanism of Chloride-induced Depassivation of Oxide Films: a Density Functional Theory Study, Q. Pang, H. DorMohammadi, K. Oware Sarfo, P.V. Murkute, Y. Zhang, O.B. Isgor, J.D. Tucker, Liney Árnadóttir**, Oregon State University

A protective iron oxide film (passive film) forms on the surface of iron in alkaline environment, such as in reinforced concrete. Chloride and other aggressive ions can cause the breakdown of the passive film (depassivation) in the same environment, leading to active corrosion. The mechanism of the Cl-induced depassivation is studied on flat and stepped $\alpha\text{-Fe}_2\text{O}_3$ (0001) surfaces because $\alpha\text{-Fe}_2\text{O}_3$ has been suggested to be one of the dominant oxides in the outer layer of the passive film.

The oxidation state of the surface metal atoms plays an important role in Cl-surface interactions and depassivation. Cl binds more strongly to metal atoms at lower oxidation state and these adsorption sites can facilitate higher local coverage. Defect sites, such as on a step edge or next to a O vacancy have lower oxidation states, suggesting an important role of defects in the depassivation process. Two main mechanisms of depassivation have been proposed in the literature, the point defect model that proposes a depassivation through Cl enhanced Fe vacancy formation on the surface and void formation at the metal oxide/metal interface, and the ion exchange model, which proposes a depassivation mechanism through subsurface Cl. Our studies of the thermodynamics of Cl ingress into the passive film, Fe vacancy formation, and bulk vacancy stability all support the point defect model for iron oxide. The initial stages of Cl-induced depassivation are proposed through a combination of reactive force field molecular dynamics simulations and DFT calculations.

Fundamental Aspects of Material Degradation Focus Topic Room A212 - Session DM2+BI+SS-ThA

Fundamentals of Catalyst Degradation: Dissolution, Oxidation and Sintering

Moderator: Gareth S. Parkinson, TU Wien, Austria

4:00pm **DM2+BI+SS-ThA6 Stability Challenges in Electrocatalysis, Serhiy Cherevko**, Forschungszentrum Jülich GmbH, Germany **INVITED**

Many industrially important electrochemical energy conversion technologies, such as electrolysis and fuel cells, rely on expensive noble metal electrocatalysts to accelerate reactions, and thus, improve energy conversion efficiency. Despite their relatively high stability, even noble metals are not completely immune. Indeed, the latter fact represents a considerable challenge in the wide-spread commercialization of electrolyzers and fuel cells. Electrocatalyst or support corrosion, particle agglomeration and detachment, Ostwald ripening, structural and morphological changes are just a few examples of possible degradation processes.¹ These processes clearly illustrate the level of complexity one has to deal with in order to understand and circumvent degradation in real devices. Thus, it is difficult to imagine modern electrocatalysis research without advanced analytical tools. In this talk I will demonstrate that the application of on-line inductively coupled plasma mass spectrometry, on-line electrochemical mass spectrometry, and identical location transmission electron microscopy in electrocatalysis research can assist in clarifying the mechanisms leading to degradation. As some representative

Thursday Afternoon, October 24, 2019

examples I will show degradation of the state-of-the-art and advanced platinum based catalysts in fuel cells and iridium based catalyst in water electrolysis.^{2,4} Time will also be devoted to discussing application of alternative non-noble metal catalysts in the energy conversion technologies and their stability. Finally, stability in other electrocatalytic systems, e.g. photo-electrochemical water splitting or carbon dioxide reduction will be touched.

Literature:

1 Cherevko, S. *Current Opinion in Electrochemistry***8**, 118-125 (2018).

2 Cherevko, S. *et al. Nano Energy***29**, 275-298, (2016).

3 Kasian, O. *et al. Angewandte Chemie***57**, 2488-2491 (2018).

4 Geiger, S. *et al. Nature Catalysis***1**, 508-515 (2018).

4:40pm **DM2+BI+SS-ThA8 Self-limited Growth of an Oxyhydroxide Phase at the Fe₃O₄(001) Surface in Liquid and Ambient Pressure Water**, *Florian Kraushofer*, TU Wien, Austria; *F. Mirabella*, TU Wien, Austria, Germany; *J. Xu, J. Pavelec, J. Balajka, M. Müllner, N. Resch, Z. Jakob, J. Hulva, M. Meier, M. Schmid, U. Diebold, G.S. Parkinson*, TU Wien, Austria

Atomic-scale investigations of metal oxide surfaces exposed to aqueous environments are vital to understand degradation phenomena (e.g. dissolution and corrosion) as well as the performance of these materials in applications. Here, we utilize a new experimental setup for the UHV-compatible dosing of liquids to explore the stability of the Fe₃O₄(001)-(√2 × √2)R45° surface following exposure to liquid and ambient pressure water, using low energy electron diffraction (LEED), x-ray photoemission spectroscopy (XPS) and scanning tunnelling microscopy (STM).

Short-time exposure of the surface to clean H₂O results in hydroxylation of the surface, which is not observed in UHV. After longer exposure times, we observe lifting of the (√2 × √2)R45° reconstruction with LEED and stronger hydroxylation of the surface with XPS, in agreement with previous reports. However, scanning tunnelling microscopy (STM) images reveal a more complex situation than simply reverting to a bulk-truncation, with the slow growth of an oxyhydroxide phase, which ultimately saturates at approximately 40% coverage. We conclude that the new material contains OH groups from dissociated water coordinated to Fe cations extracted from subsurface layers, and that the surface passivates once the surface oxygen lattice is saturated with H because no further dissociation can take place.

5:00pm **DM2+BI+SS-ThA9 The Impact of W on the Early Stages of Oxide Evolution for Ni-Cr Alloys**, *C. Volders, V.A. Avincola*, University of Virginia; *I. Waluyo*, Brookhaven National Laboratory; *J. Perepezko*, University of Wisconsin - Madison; *Petra Reinke*, University of Virginia

Ni-Cr alloys are highly coveted as they exhibit superior corrosion resistance due to the formation of a passive chromia film which helps protect the underlying alloy from degradation. The properties of this system are further enhanced through the addition of minor alloying elements such as Mo or W. For example, Mo is known to reduce catastrophic events such as pitting and crevice corrosion, thereby enhancing overall corrosion resistance. The ideal composition for technical Ni-Cr alloys has been optimized over many decades, however, the mechanistic understanding for the role of alloying elements such as Mo and W has not been fully developed. The primary objective of this work is to formulate a better mechanistic understanding of how the addition of W impacts the early stages of oxidation for this system and eventually use this information for further improvement of Ni-Cr alloys.

To achieve our goal, a series of oxidation experiments with the direct comparison between Ni-15Cr and Ni-15Cr-6W (weight percent) samples were performed and analyzed with the use of X-ray photoelectron spectroscopy (XPS). The first set of experiments employed an *in-operando* XPS approach where the modulation of alloy and oxide composition and bonding was observed over an extended period of time delivering a detailed view of the reaction pathways. The key results from this work include the observation of Cr surface segregation in the alloys prior to oxidation, which contributes to a rapid nucleation of Cr oxide species in the first reaction steps. The more intriguing result was the addition of W to the alloy resulted in a near complete suppression in the formation of Ni oxide, while further enhancing the formation of a pure chromia phase, which has been attributed to the addition of W increasing the supply of Cr to the surface and will be discussed.

A second series of XPS experiments focus on oxidation as function of crystallographic orientation of individual, large grains for Ni-15Cr and Ni-15Cr-6W. The differences in atom density and surface energies as a

function of orientation lead us to expect significant differences in reactivity which will impact passivation and oxide performance. This has been demonstrated for aqueous corrosion of NiCr and NiCrMo alloys by Scully *et al. J. Phys. Chem. C*, **2018**, 122 (34), 19499-19513, and our work is complementary for thermal oxidation studies. In this work, Ni-15Cr and Ni-15Cr-6W samples were thermally oxidized and we will present and discuss the difference in oxidation products for various grain orientations for both samples.

5:20pm **DM2+BI+SS-ThA10 The Stability of Platinum in Non-aqueous Media**, *J. Ranninger, S. Wachs, J. Möller, K. Mayrhofer, Balázs Berkes*, Forschungszentrum Jülich GmbH, Germany

Many basic reactions in electrochemistry, like the hydrogen oxidation reaction, oxygen reduction reaction, water oxidation or CO₂ reduction reaction has been thoroughly studied in aqueous electrolytes. To these fundamental studies well defined experimental conditions have been chosen: smooth or single crystal electrodes with known surface structures, ultrapure electrolytes and very clean experimental apparatus. In many respects electrocatalysis in organic solvents is much less advanced than its understanding in aqueous systems.

The example of LIBs shows us, however, clearly how much potential of non-aqueous electrochemistry holds, in this particular example for the development of energy storage devices. Other important and possible technical applications are new type of batteries, electro-organic synthesis including electrochemical reduction of CO₂, electrodeposition, supercapacitors or electrochemiluminescence.

Stability of electrochemical systems is a particularly important question in electrocatalysis. No matter if it is a fuel cell, a battery, a supercapacitor, a construction subject to corrosion or an electrode used for synthesis, economic considerations require a certain lifetime of these systems. Therefore, it is also important to understand electrocatalysis especially the aspect of stability in non-aqueous electrolytes. To this end very sophisticated, often in situ and real-time analysis methods are required. In this work we show a powerful approach to study dissolution phenomena in non-aqueous electrochemical systems on the example of platinum.

Platinum is often considered to be a model electrode and catalyst material. This metal is probably the most thoroughly studied one in electrochemistry, however, it still shows many interesting yet not well understood features. This is also true for the stability of the metal during potential cycling. The electrochemical stability window of organic electrolytes is usually much higher than that of water enabling the simultaneous cycling and downstream analysis of dissolution in a higher potential range. As a result, even the electrochemistry of platinum shows hitherto unveiled phenomena regarding its dissolution mechanism especially when using electrolytes with ultra-low (1 ppm) water content. In this work, we focus on the effect of water, anions, cations and organic solvent molecules on the anodic and cathodic dissolution behavior of platinum. To demonstrate the benefits of this novel method on the field of non-aqueous electrochemistry the stability of other non-aqueous systems will be discussed shortly, too.

5:40pm **DM2+BI+SS-ThA11 Stabilizing Transparent Conductive Oxides as a Route to Long-Lived Thin Film Photovoltaics: A Case Study in CIGS**, *N.C. Kovach*, Colorado School of Mines; *R. Matthews, E.B. Pentzer*, Case Western Reserve University; *L. Mansfield*, National Renewable Energy Laboratory; *T.J. Peshek*, NASA Glenn Research Center; *Ina Martin*, Case Western Reserve University

Degradation of the aluminum-doped zinc oxide (AZO) top contact is a known failure mode in Cu(In,Ga)Se₂ (CIGS) solar cells. The degradation of the AZO can be observed in device and module current-voltage characteristics as an increase in series resistance and decrease in fill factor. Due to its low cost and earth abundance, AZO is a good choice for the TCO in thin-film solar cells. However, it has one of the higher degradation rates of TCOs under damp heat stress. 3-aminopropyltriethoxysilane (APTES) was used to modify the AZO top contacts in CIGS solar cells. Results demonstrate that the application of the nm-scale modifier mitigates AZO degradation in damp-heat exposure, and further, arrests the degradation of the full CIGS device.

APTES modification of thick (~0.8 μm) AZO films significantly impedes the electrical degradation of the material caused by DH exposure, without significantly affecting the initial optical, electrical, or structural properties of the AZO films. Upon 1000 h of DH exposure, resistivity of both systems increased and can be attributed only to decreased mobility, as carrier concentration was consistent. APTES modification slowed the increase in AZO resistivity over 1000 h of DH exposure; however, the protective nature

Thursday Afternoon, October 24, 2019

of APTES modification became critical after 1500 h. At this extended exposure time, macroscopic degradation was observed only for bare AZO including pitting and delamination and was accompanied by an increase in resistivity and decrease in carrier concentration. X-ray photoelectron spectroscopy (XPS) data show that the APTES layer stabilizes the oxygen binding environment of the AZO surface, suggesting that covalent passivation of AZO surface sites by silanization essentially “caps” reactive moieties, thereby improving the stability of the material.

Fundamental Discoveries in Heterogeneous Catalysis Focus Topic

Room A213 - Session HC+SS+TL-ThA

Reaction Pathways and Addressing Challenges for Energy Production in the 21st Century & Heterogeneous Catalysis Graduate Student Award Presentation

Moderators: Sanjaya Senanayake, Brookhaven National Laboratory, Arthur Utz, Tufts University

2:20pm **HC+SS+TL-ThA1 High Resolution XPS to Identify C₂H₂ Surface Species on a Cobalt Model Catalyst: New Experimental Evidence for the Importance of Alkylidyne as Growth Intermediates in Fischer-Tropsch Synthesis**, *Kees-Jan Weststrate*, Syngaschem BV, Netherlands; *D. Sharma, D. Garcia Rodriguez, M.A. Gleeson*, DIFFER, Eindhoven University, The Netherlands, Netherlands; *H.O.A. Fredriksson, H.J.W. Niemantsverdriet*, Syngaschem BV, Netherlands

Supported cobalt catalysts find their most widespread application in low temperature Fischer-Tropsch synthesis (FTS), a process in which C-C bond forming reactions produce long chain saturated hydrocarbon chains from synthesis gas, a mixture of CO and H₂. The versatile FTS process may very well continue to play a role in future energy scenarios: synthesis gas can be derived from any carbon-containing source, e.g. biomass or even CO₂ may be used. These renewable carbon sources offer a sustainable alternative to replace petroleum as the principal feedstock of chemicals and liquid transportation fuels.

The FTS reaction mechanism can be ranked among the most complex in the chemical industry. CO and H₂ are converted into long chain hydrocarbons in a sequence of bond-breaking and bond-making steps that are catalyzed by metals such as cobalt, ruthenium and iron (the latter is active in the carbide form). As the steady state concentration of chain growth intermediates is below the detection limits of in-situ spectroscopies simplified model studies are needed to elucidate the mechanism by which long hydrocarbon chains grow on the cobalt catalyst surface. Since chains grow on a surface that is packed with CO, it is of crucial importance to consider how CO spectators influence the reactivity of hydrocarbon adsorbates. We use a Co(0001) single crystal surface as a model system to study how C₂H_x adsorbates react on a cobalt surface, both in ultrahigh vacuum (~10⁻¹⁰ -10⁻⁷ mbar) as well as at near-ambient pressure (~0.1 mbar). By using the high resolution available of x-ray photoemission spectroscopy at the SuperESCA beamline of ELETTRA (Trieste, Italy), and the unique opportunity to combine these qualities with measurements at near-ambient pressure at the HIPPIE beamline of MAX IV (Lund, Sweden), we were able to elucidate the reaction mechanism by which carbon-carbon bonds form on a cobalt surface. We find that CO's presence is of essential importance: It promotes hydrogenation of acetylene, HC≡CH [the most stable C₂H_{ad} without CO] to ethylidyne, ≡C-CH₃, a facile reaction that occurs around 250 K. Ethylidyne dimerization around 310 K produces 2-butyne (H₃C-C≡C-CH₃), a strongly bound alkyne adsorbate that hydrogenates to 2-butene (g) above 400 K. Extrapolated to FTS, the findings speak in favour of the alkylidyne chain growth mechanism: long chain alkylidynes (≡C-R), stabilized by the presence of CO spectators, react with a methylidyne (≡CH_{ad}) monomer to produce a 1-alkyne (R-C-CH) adsorbate. Partial hydrogenation of the 1-alkyne product is promoted by CO_{ad} and produces the alkylidyne species needed for the next CH insertion step.

2:40pm **HC+SS+TL-ThA2 Beam Reflectivity Measurements of Carbon Dissolution on Nickel Single Crystal Catalysts**, *Eric High, D.G. Tinney, A.L. Utz*, Tufts University

The interaction of carbon with metal catalysts is of significant interest. In methane steam reforming, the build-up of carbon in the nickel subsurface leads to a gradual reduction in reactivity on the surface and ultimately results in deactivation of the metal catalyst. Additionally, the initial dissolution and subsequent reemergence of carbon from the subsurface are key steps in the growth of well-ordered graphene on nickel substrates

via chemical vapor deposition (CVD). Researchers have previously used Auger and X-ray photoelectron spectroscopy to investigate the dynamics of carbon dissolution into nickel surfaces. We instead employ beam reflectivity measurements to monitor the process of carbon diffusion into the nickel subsurface in real-time. We will present data collected via exposure of a Ni(997) single crystal to supersonically expanded CH₄ molecules at surface temperatures above 600 K. We observe significant changes in the reaction profile by increasing surface temperature as the rate of dissolution approaches the reactive flux of the high energy gas molecules. We use these results to further develop kinetic models for methane reactivity as a function of surface coverage as well as carbon diffusion into the stepped nickel crystal. The major parameters from these models include the site-blocking coverage and its subsequent dependence on surface temperature as well as an updated measure of the barrier to diffusion for the C/Ni system.

3:00pm **HC+SS+TL-ThA3 Fundamental Research Opportunities to Advance Energy Technologies**, *Bruce Garrett*, Department of Energy **INVITED**

The U. S. Department of Energy (DOE), Office of Science, Office of Basic Energy Sciences (BES) supports fundamental research in chemical and materials sciences to provide the foundations for new energy technologies and to support DOE missions in energy, environment, and national security. This presentation will discuss opportunities for fundamental research to impact DOE's energy mission “to catalyze the timely, material, and efficient transformation of the nation's energy system and secure U.S. leadership in energy technologies” with a focus on the way we generate, store and use energy nationally. I will provide an overview of BES strategic planning over the past decade that identified priority research directions for advancing energy applications, highlight key scientific advances in these areas, and discuss some future opportunities for modern science, particularly studies of interfacial processes, to accelerate the transformation of the U. S. energy portfolio.

4:00pm **HC+SS+TL-ThA6 Oxidation and Redox-Mediated Transformation of a Tb₂O₃ Thin Film from the Cubic Fluorite to Bixbyite Structure**, *Christopher Lee, J.F. Weaver*, University of Florida

The terbium oxides, a member of the rare earth oxide family, exhibit favorable properties in selective oxidation catalysis due to the high mobility of oxygen stored and released within the lattice. Of particular note is the ease of structural rearrangement into highly stable, well-ordered intermediates between the Tb₂O₃ and TbO₂ stoichiometries in addition to a continuum of nonstoichiometric states. As opposed to ceria, which stabilizes strongly in the CeO₂ stoichiometry, thin film terbium is very stable in the Tb₂O₃ stoichiometry and can exist in an oxygen deficient cubic fluorite arrangement (CF-Tb₂O₃) as well as the bixbyite structure (c-Tb₂O₃).

We discovered a redox-mediated mechanism for the transformation of thin film CF-Tb₂O₃(111)/Pt(111) to c-Tb₂O₃(111)/Pt(111) in ultrahigh vacuum (UHV). Low energy electron diffraction (LEED) and temperature programmed desorption (TPD) shows that repeated oxidation and thermal reduction to 1000 K transforms an oxygen deficient cubic fluorite Tb₂O₃(111) thin film to the well-defined bixbyite, or c-Tb₂O₃(111) structure. In addition, TPD measurements show the development of several distinct O₂ desorption peaks arising from the oxidation of c-Tb₂O₃ domains to the stoichiometrically-invariant ι -Tb₇O₁₂ and δ -Tb₁₁O₂₀ phases and demonstrates the more facile oxidation of c-Tb₂O₃ relative to CF-Tb₂O₃. We present evidence that nucleation and growth of c-Tb₂O₃ domains occurs at the buried TbO_x/CF-Tb₂O₃ interface, and that conversion of the interfacial CF-Tb₂O₃ to bixbyite takes place mainly during thermal reduction of TbO_x above ~900 K and causes newly-formed c-Tb₂O₃ to advance deeper into the film. The avoidance of low Tb oxidation states may facilitate the CF to bixbyite transformation via this redox-mechanism.

Further oxidation of a well-ordered c-Tb₂O₃ film provides evidence of the sequential phase stabilization of ι -Tb₇O₁₂, δ -Tb₁₁O₂₀, and α -TbO_{2-x} stoichiometric structures along with lower temperature peaks corresponding with more weakly-bound surface oxygen. Oxidation at temperatures between 300-500 K reveals an apparent Arrhenius activation barrier of ~7.4 kJ/mol for the initial conversion of c-Tb₂O₃ to ι -Tb₇O₁₂. Furthermore, oxidation at 100 K creates an additional oxygen species stable at lower temperatures that has a much more pronounced effect on oxidation of the film surface over the bulk of the film. The ability to control the surface termination of the TbO_x(111) thin films along with selectively creating surface bound oxygen species provides the structural basis necessary to clarify the partial oxidation mechanisms associated with terbium-based catalysis.

Thursday Afternoon, October 24, 2019

4:20pm **HC+SS+TL-ThA7 Discrimination of Surface Storage and Mechanistic Pathways Using Dynamic Pulse Response Experiments**, Y. Wang, M.R. Kunz, Idaho National Laboratory; G. Yablonsky, Washington University in Saint Louis; **Rebecca Fushimi**, Idaho National Laboratory
Pulse response experiments in a pure diffusion reactor significantly increase the number of gas/solid collisions for probing kinetic interactions but maintain straightforward transport modeling by avoiding gas phase dynamics. Using inverse-diffusion methods [1] the millisecond time-dependence of the reaction rate can be calculated as it responds to the forced concentration dynamic. More importantly, in this experiment the gas and surface concentrations are decoupled and their influence on the transformation rates of reactants and products can be studied.

Vacuum pulse response studies of ammonia decomposition on polycrystalline Fe, Co and a CoFe bimetallic preparation were conducted to investigate the microkinetic features that lead to very distinct global performance [2]. We present dynamic atomic accumulation; a new measure used to characterize the ability of a complex surface to regulate adsorbed species. We find Fe can support hydrogenated species with a longer surface lifetime than either CoFe or Co. From the time-dependence of the rate we find Co can support two mechanistic pathways for H₂ production. The quantitative rate, gas and surface concentration data of microkinetic reaction steps explain why materials with cobalt perform better at a global level.

1. Redekop, E.A., et al., *The Y-Procedure methodology for the interpretation of transient kinetic data: Analysis of irreversible adsorption*. Chem. Eng. Sci., 2011. 66(24): p. 6441-6452.

2. Wang, Y., et al., *Transient Kinetic Experiments within the High Conversion Domain: The Case of Ammonia Decomposition*. Catalysts, 2019. 9(1): p. 104.

4:40pm **HC+SS+TL-ThA8 Nuclearity Effects in Supported Zinc and Gallium Catalysts for Alkane Dehydrogenation**, **Susannah Scott**, University of California at Santa Barbara **INVITED**

The selective dehydrogenation of alkanes to alkenes is an important process in the valorization of shale gas liquids and in the production of on-demand olefins. Ga- and Zn-modified aluminosilicates have been extensively studied as catalysts for these reactions. In the presence of Brønsted acid sites (BAS), the olefins undergo subsequent aromatization to more valuable BTX. The nuclearity of the metal active sites, the proximity between the metal sites and the BAS, and the nature of the support, may influence the catalytic activity but detailed structure-property relationships are difficult to ascertain in conventional catalysts with many types of sites. The reactions of GaMe₃ and ZnMe₂ with the hydroxyl-terminated surfaces of dehydrated silica and alumina, as well as with the internal and external surfaces of H-ZSM-5, are particularly simple. They generate methane and isolated dimethylgallium and methylzinc sites. K-edge X-ray absorption spectra, analyzed via inspection of the wavelet transform EXAFS (WT-EXAFS) and curvefitting of the Fourier transform EXAFS (FT-EXAFS), reveal that the silica and zeolite materials contain dinuclear grafted sites, regardless of the thermal pretreatment of the support, while alumina gives dispersed mononuclear grafted sites. Differences in reactivity and stability appear to originate in these structural variations.

5:20pm **HC+SS+TL-ThA10 Fundamental Insights into Hydrocarbon Conversion Mechanisms in Lewis and Brønsted Acid Zeolites using Temporal Analysis of Products**, **Hari Thirumalai¹**, J.D. Rimer, L.C. Grabow, University of Houston

The surge in natural gas production has incentivized the search for processes that can utilize methane and light olefin derivatives in the manufacture of useful products such as benzene, toluene and xylene (BTX). These are important commodity chemicals that are used as fuel additives and as raw materials in the synthesis of specialty chemicals. Industrial demand is met through processes such as the synthesis of BTX through dehydroaromatization of light olefins or through alkylation of aromatics, typically with the use of zeolites as catalysts. Complex reaction mechanisms determined by the presence of a hydrocarbon pool dominate hydrocarbon chemistry and are challenging to study. These challenges hinder the in-depth understanding of the role of the catalyst and its eventual design for tailored applications.¹

In this work, we use the transient kinetics technique, temporal analysis of products (TAP), to probe hydrocarbon conversion and upgrade in the transient regime of reaction. TAP experiments help probe the intrinsic kinetics of reactant conversion in a well-defined Knudsen transport regime

under high-vacuum conditions. We studied the dehydroaromatization of ethylene and the methylation of toluene as case-studies for hydrocarbon conversion reactions. The precise control of reactant molecules entering the reactor and responses recorded by a high-resolution mass spectrometer at the reactor outlet in the dehydroaromatization of ethylene suggest that a Lewis acid such as Ag⁺ or Ga³⁺ in the zeolite accelerate the retention of long lived carbonaceous species in the zeolite, thus attaining the autocatalytic arene cycle more rapidly. Pulse responses provide qualitative evidence that olefins are strongly bound to the metal-exchanged zeolite samples with delayed desorption, enhancing the rate of hydrocarbon conversion and carbon retention. Finally, experiments investigating the methylation of toluene to xylene provide valuable information on competitive binding of reactants to the zeolite acid sites and the ensuing primary reactions that drive the reaction.

Overall, our experiments under semi-idealized conditions help provide insight into the crucial primary reactions that initiate the hydrocarbon pool mechanism, thus elucidating the role of extra-framework species such as Ag⁺ or Ga³⁺ and their synergy with the Brønsted acid sites in hydrocarbon conversion. The fundamental understanding gained from these experiments will be crucial in deciphering the role of the different zeolitic active sites in model hydrocarbon conversion reactions.

References

1. Hsieh, M. F., Zhou, Y., Thirumalai, H., Grabow, L. C., & Rimer, J. D. ChemCatChem, (2017), 9(9), 1675-1682.

Frontiers of New Light Sources Applied to Materials, Interfaces, and Processing Focus Topic Room A210 - Session LS+AC+HC+SS-ThA

Emerging Methods with New Coherent Light Sources

Moderator: Germán Rafael Castro, Spanish CRG BM25-SpLine Beamline at the ESRF

4:00pm **LS+AC+HC+SS-ThA6 Resolving X-ray Based Spectroscopies in the Sub-nanometer Regime: Enabling Atomic Scale Insights into CO Adsorption on Thin Film Surfaces**, **Heath Kersell**, B. Eren, C.H. Wu, Lawrence Berkeley National Laboratory; I. Waluyo, A. Hunt, Brookhaven National Laboratory; G.A. Somorjai, M.B. Salmeron, Lawrence Berkeley National Laboratory

X-ray based spectroscopies routinely yield detailed elemental, chemical, electronic, and magnetic information on a wide array of physically and chemically diverse samples. However, the spatial resolution of these techniques is limited, frequently by the size of the X-ray spot. Conversely, certain structural probes readily resolve sample topography with nanoscale- or even atomic-resolution. The union of X-ray based spectroscopies with nanoscale structural probes enables the acquisition of spectroscopic information at unprecedented length scales. We will demonstrate the combination of X-ray based spectroscopies (e.g. X-ray photoelectron spectroscopy (XPS)) with scanning tunneling microscopy (STM), and its application to CO adsorption and oxidation on model catalyst surfaces.

CO adsorption on various crystal surfaces plays a critical role in numerous chemical processes, including for example CO oxidation, the water gas shift reaction, and methanol oxidation. CO oxidation is widely used as a prototype reaction for studies of fundamental catalytic phenomena and is crucial in exhaust gas processing for automobiles and stationary CO sources. Recent studies demonstrate strikingly high activity for CO oxidation by Pt nanoparticles supported on cobalt oxide (CoO_x) as compared to either of the constituent materials. In the further development of these catalysts, a deeper understanding of the active sites and their deactivation is crucial. Using a combination of *operando* high pressure STM (HP-STM) and ambient pressure XPS (AP-XPS), we investigate the nature of catalytically active sites for CO oxidation on CoO-Pt catalysts at CO and O₂ pressures up to 130 mTorr. Our experiments showed very different behavior for the lattice oxygen (O_{lat}) in CoO between fully oxidized and sub-stoichiometric cobalt oxides. At RT, fully oxidized Co films adsorbed CO in the form of stable surface carbonate species, poisoning the reaction until reaching higher temperatures where they decomposed. On sub-stoichiometric CoO_x the CO oxidation reaction proceeded at RT, reducing the oxide to the metallic state. We discuss these results in the context of structural transformations observed *in-situ* via HP-STM, and demonstrate the behavior of surface sites under relevant gas mixtures.

¹ Morton S. Traum Award Finalist

Thursday Afternoon, October 24, 2019

As an outlook, we will discuss various *in-situ* multi-modal approaches which enhance the spatial resolution of X-ray based spectroscopies toward the nano- or even single atom scales. Such a union of spectroscopic and structural probes will provide a more accurate and complete picture of operating devices in the near future.

4:20pm LS+AC+HC+SS-ThA7 Imaging with XPS: Advanced Characterization for Advanced Materials and Devices, Tatyana Bendikov, H. Kaslasi, E. Sanders, E. Joselevich, D. Cahen, Weizmann Institute of Science, Israel

X-ray Photoelectron Spectroscopy (XPS), as a surface sensitive technique with the sensitivity down to single atomic layer, provides unique information about elemental composition and chemical and electronic states of elements in the material. For some research goals, however, this knowledge is not sufficient as it does not provide the entire information required for a comprehensive characterization of the investigated system. In addition to the basic functions of standard XPS, our instrument is equipped with advanced capabilities such as XPS imaging, which is particularly valuable in the analysis of patterned or inhomogeneous specimens. Following image acquisition, specific areas can thus be chosen and small spot XP spectra acquired at sites of particular interest. This information is useful in the characterization of patterned surfaces or inhomogeneous samples with surface features between several to hundreds of micrometers.

We present here two examples where XPS imaging is successfully used providing crucial information for understanding the investigated systems.

In the first example bunches of GaN nanowires (50-100 nm each) randomly spread on Si substrate were monitored with XPS imaging. Then, focusing on the GaN bunch itself, small area XP spectra were obtained. This allowed to get precise top surface composition of the bunches significantly consuming the analysis time.

In the second example variations in chemical composition through dimensions of the $Cs_xMa_{1-x}PbBr_3$ ($MA = CH_3NH_3$)

crystal were studied using XPS imaging. Significant changes in the N/Cs ratio, depending on the distance from the crystal edge/center, were observed on the top surface. Variations in the N/Cs and Pb/(N+Cs) ratios were also observed along the crystal bulk.

4:40pm LS+AC+HC+SS-ThA8 Time-Resolved Photoemission with Free-Electron Lasers, Kai Rossnagel, CAU Kiel / DESY, Germany **INVITED**

Photoelectron spectroscopy is an essential analytical tool for learning about the properties and workings of quantum materials and functional interfaces, in which electrons are the main actors. In practice, photoelectron spectroscopy is a toolbox comprising three major techniques, where the momentum selectivity and atomic-site specificity of valence and core electron emissions are exploited, respectively: Angle-resolved photoelectron spectroscopy (ARPES) is the most powerful imaging technique for the energy-momentum space of the active electrons near the Fermi level, while x-ray photoelectron spectroscopy (XPS) is a universal tool for chemical analysis and x-ray photoelectron diffraction (XPD) an established surface structural probe. A dream is to combine all three techniques into a single experiment, make it complete by adding spin and femtosecond time resolution, and thus be able to shoot femtostroboscopic movies of intertwined electronic, magnetic, chemical, and geometric structure dynamics and gain previously unachievable, direct "in operando" insight into dynamic structure-function relationships of materials and interfaces. Here, we aim to realize this dream by combining the soft x-ray SASE3 free-electron-laser (FEL) beam at the European XFEL with the most advanced photoelectron detection scheme currently available: the time-of-flight momentum microscope with efficient 3D energy-momentum detection and 2D spin filtering. The status of the project and of FEL-based photoelectron spectroscopy in general will be presented.

5:20pm LS+AC+HC+SS-ThA10 Ultrafast Magnetization Dynamics on the Nanoscale, Bastian Pfau, Max Born Institute, Germany **INVITED**

Nanometer-scale spin configurations are attractive as information entities for spintronic applications to realize nonvolatile and energy-efficient data storage and processing. In recent years, this research field was stimulated by the discovery that the spin can be effectively manipulated using ultra-short light pulses exciting suitably designed magnetic materials. Scattering and imaging methods based on sources delivering ultra-short x-ray pulses are particularly successful in revealing the magnetization dynamics on the relevant time and length scales. I will present research results on optically induced demagnetization and formation of nanoscale magnetic domains and skyrmions in Co-based multilayer systems. We investigate these

processes using small-angle scattering signals or direct imaging via holography with femtosecond x-ray pulses delivered by free-electron laser sources. These methods additionally allow to address the influence of lateral nanoscale inhomogeneity and to work with laterally localized or structured excitation.

**Plasma Science and Technology Division
Room B130 - Session PS+2D+EM+SS+TF-ThA**

Plasma-Enhanced Atomic Layer Etching

Moderators: Steven Vitale, MIT Lincoln Laboratory, Mingmei Wang, TEL Technology Center, America, LLC

2:20pm PS+2D+EM+SS+TF-ThA1 Atomic Layer Etch: Real World Utilization of an Idealized Solution, Peter Biolsi, TEL Technology Center, America, LLC **INVITED**

Atomic Layer Etch: Real World Utilization of an Idealized Solution

Critical dimensions (CD) continue to shrink driven by the quest for cheaper, faster and less power-consuming devices. If simple shrink was not enough, all of the back end, middle and front end of line (BEOL, MOL and MOL) also have introduced structural complexity and stringent topographic dimension, material property integrity and fundamental integration yield requirements. Atomic layer etching (ALE) has gained favor as an approach to extract more control over the fabrication of small CD complex topographic structures, atomic layer etching. The idea is that alternating steps of self-limiting processes (e.g., passivation layer formation) and desorption (e.g., the removal of a passivation layer) mitigate aspect ratio dependence effects that lead to the aforementioned problems. The problem is that not all passivation processes are self-limiting. For the etching of dielectric materials, a self-limiting precursor step is not available as etch processes relies on cyclic process (fluorocarbon deposition and ion bombardment steps). Fluorocarbon based processes are not self-limiting rendering them quasi-atomic layer etch. Without special consideration, quasi-ALE has the same problems that continuous processes possess with additional burden of throughput.

Even though ALE can be difficult to be utilized in real-world scenarios, the learning from ALE finds its use in many etch applications. An etch chamber which can provide wide range of radical to ion flux ratios and precise ion energy control (using pulsing techniques) is suitable for ALE or utilizing ALE learnings. Currently, new ALE techniques based on surface modification by ions (Hydrogen plasma treatment of Silicon Nitride) followed by removal of modified layer by F radicals (High pressure NF₃ or SF₆ plasma) or surface modification by NH₃/HF (to create a quasi-self-limiting diffusion barrier layer) followed by removal of modified layer by thermal means, are employed to etch critical layers where requirements are stringent. New frontier of etch technology will be the ability to achieve area selective etch without compromising etch rate of the process. Examples of such activities will be presented in this presentation.

3:00pm PS+2D+EM+SS+TF-ThA3 Mechanism of SiN Etching Rate Fluctuation in Atomic Layer Etching, Akiko Hirata, M. Fukasawa, K. Kugimiya, K. Nagaoka, Sony Semiconductor Solutions Corporation, Japan; **K. Karahashi, S. Hamaguchi,** Osaka University, Japan

Atomic layer etching (ALE) enables atomic-precision control of the surface reaction and low damage etching of the underlying layer for device fabrication. In this study, we investigated SiN ALE with process optimization of the surface adsorption and desorption steps, and we clarified the rate fluctuation mechanism.

A dual frequency CCP reactor (60 MHz/2 MHz) was used in this study. A SiN (50 nm) was deposited on the Si substrate by LPCVD. One etching cycle consisted of two steps. CH₃F/Ar plasma was applied to deposit the hydrofluorocarbon (HFC) polymer as the adsorption step. Then, Ar plasma was used in the desorption step. The thicknesses of SiN and the HFC polymer were measured by spectroscopic ellipsometry. The chemical bonding was analyzed by XPS.

A 1.2-nm-thick HFC polymer was deposited on SiN as the adsorption step. Next, we investigated the desorption step by using Ar plasma. The etched amount for 1 cycle was 0.58 nm. However, we found the etch-stop of SiN after 10 cycles of ALE, owing to the deposition (>6 nm) of a protective film on the surface. The etch-stop could be caused by sputtering of the Si upper electrode and/or re-deposition of the HFC film. To investigate the etch rate fluctuation, the SiN surface after ALE was analyzed. C-C and C-N bonds were detected after 1 cycle, and C-C bonds increased after 10 cycles. It was

clear that the excess HFC polymer deposition suppressed the ALE reactions. Ar⁺ ion bombardment during the desorption step selectively eliminated the H and F in the HFC polymer, because the bonding energies of C-H and C-F were low. As the bonding energies of C-C (6.4 eV) and C-N (7.8 eV) are relatively high, these bonds remained after the desorption step. We speculated that excess C-rich polymer deposition after ALE started from the residual C-C bond. Residual Si-C bond is also possible reason, since the MD simulation revealed that the formation of Si-C bond was promoted in the fluorocarbon layer during SiO₂ ALE. [1] These results clearly showed that the initial adsorption kinetics of HFC polymer was strongly affected by the residual carbon on the SiN surface. To suppress the C-rich polymer deposition, we studied stable SiN ALE using the desorption step of Ar/O plasma (0.36 nm/cycle) and the two-step sequential desorption step of Ar and O plasma (0.6 nm/cycle). Although the effect of O adsorption in SiO ALE has been studied previously, [2] few studies have been reported for the case of SiN. Because the surface condition is able to fluctuate with the number of cycles, precise surface control is strongly required to achieve stable ALE.

[1] S. Hamaguchi et al., 2018 AVS, PS-FrM6. [2] T. Tsutsumi et al., JVST A 35 (2017) 01A103.

3:20pm PS+2D+EM+SS+TF-ThA4 Effect of Polymerization on Ar+ Bombardment Modification of SiO₂ and Si₃N₄ Substrates: Molecular Dynamics Simulation Study, Hojin Kim, Y. Shi, Y.-H. Tsai, D. Zhang, Y. Han, TEL Technology Center, America, LLC; K. Taniguchi, TEL Miyagi Limited, Japan; S. Morikita, TEL Miyagi Limited; M. Wang, A. Mosden, A. Metz, P.E. Biolsi, TEL Technology Center, America, LLC

To understand the selective removal of silicon oxide (SiO₂) against silicon nitride (Si₃N₄) with gaseous reactants for advanced etch process, we have studied the surface modification of both SiO₂ and Si₃N₄ substrates with Ar+ bombardment by using molecular dynamics (MD) simulation. The substrate samples were prepared with and without carbon (C) and hydrogen (H) polymerization to investigate the effect of polymerization on surface modification. C and H atoms were deposited with low ion energy not to disrupt the surface much. After preparation of substrate, Ar+ bombardment with various ion energy (IE) were performed. We obtained a damage depth with a wigner-seitz defect analysis as a function of IE and compared the cases with and without polymerization to check the role of the added polymer layer on surface modification. In pristine Si₃N₄ and SiO₂ case, at IE=25eV, both substrates start to show the damage with penetration of Ar+ and follows with an exponential raise as the IE increases. Damage depth at Si₃N₄ is deeper than that at SiO₂. In polymerization, simulations show that H is more deposited than C on Si₃N₄ while on SiO₂, C is more deposited than H. no silicon-hydrogen bonds appear on both substrates and in Si₃N₄, nitrogen-hydrogen bond is dominated while oxygen-carbon bond is popular in SiO₂. For damage analysis, in Si₃N₄ case, CH polymerization helps to lower about 30% in the damage depth with exponential behavior. However, SiO₂ case shows the opposite effect of CH polymerization in the damage depth. Formed polymer layer leads to increase the damage depth by comparing with pristine SiO₂ and helps more clear exponential behavior as a function of IE. Finally, analyzed results using XPS and/or SIMS from blanket SiO₂ and Si₃N₄ films etched in a Capacitively Coupled Plasma (CCP) chamber are compared with the MD simulation results.

4:00pm PS+2D+EM+SS+TF-ThA6 Advanced Cyclic Plasma Etch Approaches for Metal Patterning: Synergy and Surface Modification Effects, Nathan Marchack, IBM T.J. Watson Research Center; K. Hernandez, University of Texas at Dallas; J. Innocent-Dolor, M.J.P. Hopstaken, S.U. Engelmann, IBM T.J. Watson Research Center

INVITED

Atomic layer etching or ALE is a burgeoning research area of plasma processing that offers critical advantages needed for future advancements in semiconductor devices, namely lower damage and enhanced selectivity, through its self-limited reaction cycles separated by purge steps. [1] ALE processes offer a significantly higher degree of tunability over traditional continuous-wave (CW) plasma etching, due to the fact that parameters such as gas flows, pressure, and bias power can be adjusted on a step-specific basis rather than as a global setting for the length of the process.

Our previous work investigated the effect of varying the purge step times in a quasi-ALE process using alternating Cl₂/H₂ exposures on the etched profiles of titanium and tantalum nitride. [2] Titanium and tantalum-based conductive films have been previously evaluated as gate materials for CMOS devices but more recently have been incorporated as top electrodes for novel technologies such as magnetoresistive RAM (MRAM) and hard masks for carbon electrodes utilized in biological sensing. As the trend of

downscaling device size continues, the ability to pattern these films at tight pitches with minimal redeposition becomes highly important.

Sub-surface modification of films such as Si₃N₄ and indium-doped tin oxide (ITO) by low atomic weight (LAW) ions such as H⁺ has been discussed in literature as facilitating self-limited etch behavior. [3,4] We present new data exploring the incorporation of LAW species into cyclic etch processes, namely penetration depth into these metal nitride films and their role in surface oxide formation, the latter of which can contribute to novel pitch multiplication schemes. [5] SIMS measurements reveal that the depth of penetration of H⁺ for TaN films can be >40 nm and can occur through a native oxide layer that inhibits etching by Cl species. Pressure variation is a significant factor in tuning this effect, which can potentially modify the etch resistance of these films and enable novel integration schemes.

[1] K. J. Kanarik, T. Lill, E. A. Hudson, S. Sriraman, S. Tan, J. Marks, V. Vahedi, R. A. Gottscho, J. Vac. Sci. Technol. A. 2015, 33, 020802.

[2] N. Marchack, J. M. Papalia, S. U. Engelmann, E. A. Joseph, J. Vac. Sci. Technol. A. 2017, 35, 05C314.

[3] S. D. Sherpa, A. Ranjan, J. Vac. Sci. Technol. A. 2017, 35, 01A102.

[4] A. Hirata, M. Fukasawa, K. Nagahata, H. Li, K. Karahashi, S. Hamaguchi, T. Tatsumi, Jpn. J. Appl. Phys. 2018, 57, 06JB02.

[5] N. Marchack, K. Hernandez, B. Walusiak, J.-I. Innocent-Dolor, S. U. Engelmann, Plasma Process Polym. 2019, e1900008.

4:40pm PS+2D+EM+SS+TF-ThA8 Surface Modification and Stability of Plasma-assisted Atomic-layer Etching (ALE) of Si based Materials; Analysis by Molecular Dynamics (MD) Simulation, Satoshi Hamaguchi, M. Isobe, E.J.C. Tinacha, S. Shigeno, Y. Okada, T. Ito, K. Karahashi, Osaka University, Japan

A plasma-assisted atomic-layer etching (ALE) process typically consists of alternating application of chemically reactive species (adsorption step) and Ar ion bombardment with low bias energy (desorption step) to the surface to be etched. In the adsorption step, a modified layer is formed on the material surface and, in the desorption step, the modified layer is removed with the original material underneath being intact. In this presentation, using the results of MD simulation of ALE for Si, SiO₂, and SiN, together with experimental observations, physical mechanisms of the formation and removal of surface modified layers in typical ALE processes will be discussed.

Our molecular dynamics (MD) simulation of SiO₂ ALE by fluorocarbon adsorption and Ar⁺ ion bombardment shows that preferential sputtering of oxygen takes place by Ar⁺ ion bombardment and a Si rich layer mixed with fluorine and carbon atoms is formed on the SiO₂ surface. Ideally this modified layer should be removed completely in the subsequent desorption step, but in general it is not. In such a layer, the atomic number ratio of Si to O can be as high as unity and carbon provided in the subsequent adsorption step tends to be deposited rather than removing O atoms from the surface by forming CO molecules. Therefore as the ALE cycles proceed, the adsorbed fluorocarbon layer thickens and eventually an etch stop may occur. With fine tuning of incident Ar⁺ ion energy, an etch stop may be avoided but the process window to achieve both continuous ALE cycles (by sufficiently high Ar⁺ ion energy) and ideal self-limit in each cycle (by sufficiently low Ar⁺ ion energy) may still be small or even nonexistent. The incompleteness of the modified surface removal in each ALE cycle seems universal phenomena for plasma-assisted ALE for most materials. For other plasma-assisted ALE processes that we examined by MD simulation, the surface modified layer formed during the adsorption step could not be removed completely by low-energy Ar⁺ ion bombardment, either. Indeed low-energy Ar⁺ ion bombardment contributes to the formation of a deeper modified layer by pushing down adsorbed species into the bulk, rather than simply removing it.

5:00pm PS+2D+EM+SS+TF-ThA9 Innovative Future Etch Technology by Atomic-order Control, Yoshihide Kihara, T. Katsunuma, S. Kumakura, T. Hisamatsu, M. Honda, Tokyo Electron Miyagi Ltd., Japan

INVITED

In recent years, with the progress of device miniaturization and increased challenges in the scale of integration of semiconductor devices, ultra-high selectivity and atomic layer-level critical dimension (CD) control techniques are required in the fabrication processes.

In the conventional etching, using a fluorocarbon (FC) gas, the high selectivity is obtained by taking advantage of the difference of the FC protective film thickness due to the difference of materials. [1] However, adopting the conventional approach to cutting-edge pattern structure becomes difficult due to the excessive FC film clogging the micro slit facet.

To meet the highly complex requirements, alternative process was developed by using ion modification and chemical dry removal.^[2] We have made several improvements on this new approach and applied it to SiN and SiC etching. The improved new approach achieves ultra-high selectivity without FC protective film and we also confirmed this process has the characteristics of a self-limiting reaction based on ion depth profile as well as ALE.

In the patterning processes, lower pattern densities have a larger CD shrinking due to micro-loading. Hence, we developed the new process flow that combines atomic layer deposition (ALD) technique and etching. With this method, we achieved CD shrinking at atomic-layer level precision for various patterns, without causing CD loading.^[3]

Moreover, Quasi-ALE can etch the pattern while maintaining the mask CD for different pattern density. This is because Quasi-ALE precisely controls the surface reaction by controlling the radical flux and ion flux independently.^[3] Also, it was necessary to control oval CD size between X and Y respectively. We found that X-Y CD control can be easily performed by changing the balance of FC adsorption and Ar desorption in Quasi-ALE. However, there are concerns about mask selectivity and ion damage in this approach. To solve these problems, we introduce the Advanced Quasi-ALE technique which combines mask protection together with Quasi-ALE. The Advanced Quasi-ALE achieves wider X-Y CD control margin.

On the other hand, as aspect ratio is increased in the memory fabrication process, the occurrence of bowing profile is a serious problem. To address the issue, the new improvement technique has been developed that combines the concept of ALD and etching. With this method, we are able to etch profile more vertically in high A/R feature.

Reference

- [1] M. Matsui et al., *J. Vac. Sci. Technol. A* 19 1282 (2001)
- [2] N. Posseme et al., *Applied Physics Letters* 105 051605 (2014)
- [3] M. Honda et al., *J. Phys. D: Appl. Phys.*, Vol.50, No.23 (2017)

Plasma Science and Technology Division

Room B131 - Session PS+SS-ThA

Plasma Conversion and Enhanced Catalysis for Chemical Synthesis

Moderator: R. Mohan Sankaran, Case Western Reserve University

2:20pm **PS+SS-ThA1 Rate Limiting Factors of Low Pressure Plasma-catalytic CO₂ Methanation Process**, *Kazunori Koga, A. Yamamoto, K. Kamataki, N. Itagaki, M. Shiratani*, Kyushu University, Japan

The methanation of CO₂ attracts attention as the ways of CO₂ reduction and energy storage as well as space exploration. It is expected to produce rocket propellant fuels at Mars and CO₂ conversion in space stations. The Sabatier reaction has been employed to generate CH₄ from CO₂ and H₂. Using catalysts realizes a high conversion efficiency. However, the conventional catalytic reaction starts at about 200 °C but thermal runaway occurs above 250 °C. The heat management is an important problem. A method using non-thermal plasma with catalyst allows methanation under low-temperature condition [1, 2]. Here, we studied rate-limiting steps of CO₂ methanation and their important parameters in the plasma-catalytic process. Experiments were carried out using a capacitively coupled plasma reactor. The electrode diameter was 50 mm and the distance between the electrodes was 6.1 mm. The Cu electrodes were employed as catalyst. We set a CO₂ gas flow rate between 1.0 sccm and 5.0 sccm and an H₂ gas flow rate between 1.0 sccm and 30 sccm. The pressure was 750 Pa. The discharge power was set in a range of 10 to 100 W. Gas composition in the discharge plasmas was measured with a quadrupole mass spectrometer. CH₄ yield rapidly increases with time after plasma initiation. It tends to be saturated after 200 s. From time dependence of catalyst temperature, the saturation occurs between 350 K and 370 K. The temperature shows the threshold temperature at which the rate-limiting step change from gas-phase reactions in plasma to surface reactions on the catalyst. The CH₄ yield increases with increasing the gas residence time. From optical emission spectroscopy, emission intensity related with CO angstrom band increase with the gas residence time but hydrogen-related emission is irrelevant to the residence time. It suggests that CO excited by plasma is responsible to the CH₄ yield increase. The results of H₂ gas flow rate dependence suggest that electron temperature is an important factor in the rate-limiting step of the gas phase reaction. I will discuss the detail mechanisms at the conference.

Work supported partly by JAXA and JST.

- [1] S. Toko, et al., *Sci. Adv. Mater.* **10** (2018) 655.
- [2] S. Toko, et al., *Sci. Adv. Mater.* **10** (2018) 1087.

2:40pm **PS+SS-ThA2 Radical Nitriding of Graphene Promoted by Surface Plasmon Resonance of Gold Nanoparticle Catalyst**, *Takeshi Kitajima, T. Nakano*, National Defense Academy, Japan

In recent years, catalyst activity¹ of graphene nitride including fuel cell catalysts has attracted attention. We apply the catalytic property² of gold nanoparticles to the surface reaction of graphene, and investigate a process that can nitride graphene while reducing the damage caused by plasma irradiation.

In this study, we compared the degree of nitridation according to the presence or absence of ion irradiation (I), light irradiation from plasma (L) and the presence or absence of gold nanoparticle catalyst (C), respectively, and discovered the presence of radical nitriding by surface plasmon resonance of gold nanoparticles.

Gold is deposited for 2 minutes by electron beam evaporation on graphite crystals in an ultra-high vacuum chamber.

It was found by AFM measurement that gold nanoparticles with a diameter of about 20 nm were formed on the graphite crystal surface by aggregation.

Next, NH₃-Ar (1: 3) mixed plasma (ICP, 70 MHz, 100 W) at a pressure of 10 Pa was generated in the plasma chamber. The sample was irradiated for 10 minutes with radicals and light that passed directly or through a 30 line/inch SUS304 single mesh.

The atomic composition by XPS was examined for each irradiation condition. It was found that in the condition RLC where gold nanoparticles were generated and irradiated with radicals and light, nitridation was promoted about twice as much as plasma irradiation.

It is speculated that irradiation of gold nanoparticles with light excites plasmons to promote the nitridation reaction.

Next, Raman scattering analysis of graphene nitride was performed. Islands found on graphite were considered as graphene. Among the Raman scattering spectra, the component intensities of 2D (2690 cm⁻¹), G (1580 cm⁻¹) and D (1350 cm⁻¹) were measured to evaluate the intensity ratio.

Under RLC conditions, the I2D / IG ratio has not dropped significantly. It can be seen that the structural change of the graphene island due to ion bombardment is prevented. Furthermore, the ID / IG ratio is higher than in plasma irradiation (RIL), and it can be confirmed that nitrogen doping has progressed more. From the above, it is considered that the catalytic activity of the gold nanoparticles is expressed by the effect of surface plasmon excitation, and the formation of graphene nitride with low damage by radicals becomes possible.

1. Haibo Wang, Thandavarayan Maiyalagan, and Xin Wang, *ACS Catalysis* 2, 781 (2012).
2. Marie-Christine Daniel and Didier Astruc, *Chemical Reviews* 104, 293 (2004).

3:00pm **PS+SS-ThA3 Plasma-assisted Catalysis: Exploring the Effects of Plasma Stimulation on Catalyst Performance**, *Jason C. Hicks*, University of Notre Dame

INVITED

Plasmas create incredibly reactive chemical environments and have a long history in chemical synthesis and removal of volatile organic compounds.[1-2] Plasmas can be generated in the presence of a catalyst (plasma-assisted catalysis) to increase conversions and improve the selectivity to desired products. Our research in the area of plasma-assisted catalysis is focused on the ability to control the catalyst performance by tuning the plasma environment or plasma-catalyst interactions.[3-4] We have been particularly interested in the use of non-thermal plasmas for C-H and N₂ activation via dry reforming of methane and ammonia synthesis reactions, respectively. Specifically, this presentation will focus on 1) the reaction regime where catalyst-plasma interactions are observed for these reactions, 2) the various catalyst-plasma interactions observed, and 3) the role of the plasma in enhancing reaction efficiency. This presentation will highlight our recent progress in controlling plasma-catalyst interactions to enhance reaction efficiency.

- (1) Neyts, E. C.; Ostrikov, K.; Sunkara, M. K.; Bogaerts, A. *Chem. Rev.* **2015**, *115* (24)
- (2) Mehta, P.; Barboun, P.; Go, D. B.; Hicks, J. C.; Schneider, W. F. *ACS Energy Lett.* **2019** 5, (4)

Thursday Afternoon, October 24, 2019

(3) Mehta, P.; Barboun, P.; Herrera, F. A.; Kim, J.; Rumbach, P.; Go, D. B.; Hicks, J. C.; Schneider, W. F. *Nat. Catal.* **2018**, No. 4.

(4) Barboun, P. Mehta, P. Herrera, F.A. Go, D.B. Schneider, W.F. Hicks, J.C. *ACS Sus Chem & Eng*, **2019**, accepted.

4:00pm **PS+SS-ThA6 A Plasma-aerosol Droplet Reactor for the Synthesis of Ammonia from Nitrogen and Water**, *Joseph Toth, D.J. Lacks, J. Renner, R.M. Sankaran*, Case Western Reserve University

Alternative approaches are sought to the high-pressure, high-temperature Haber-Bosch (H-B) process for nitrogen fixation in order to enable distributed synthesis from renewable feedstocks. A potentially promising reactive strategy is plasma excitation which was historically the first method to fix nitrogen by reacting nitrogen and oxygen in air. More recently, plasmas have been combined with solid catalyst materials to synthesize ammonia at atmospheric pressure and lower temperatures than the H-B process. However, most of these reactions still require hydrogen gas which remains linked to fossil fuels and leads to both high cost and environmental consequences.

Here, we present a novel plasma-aerosol droplet reactor to synthesize ammonia from nitrogen and water at atmospheric pressure and near room temperature. Introducing the water as droplets instead of water vapor increases the throughput that can be achieved and also simplifies the system, eliminating the need for heated lines to avoid condensation on the walls. The plasma was formed as a dielectric barrier discharge inside a quartz tube with an outer ring electrode and an inner wire electrode. The water droplets were generated using a commercial nebulizer via a high nitrogen flow rate causing a Venturi effect which siphoned the water into the gas stream. The products were collected by bubbling the gas effluent leaving the reactor through a concentrated sulfuric acid bath and condensing in a second trap chilled to -40 °C. The ammonia was then measured by the o-phthalaldehyde colorimetric assay technique. The ammonia production rate was found to be a function of the power and flow rate with production rates up to 600 µg/hr at 70 W. Controls were run with an argon plasma and with no water droplets to verify that no ammonia was produced without both nitrogen and water. In addition to ammonia, we also tested for nitrites/nitrates (NO_x) and measured up to 3000 µg/hr total production rate. The efficiency, power consumption, and potential reaction mechanisms will also be discussed.

4:20pm **PS+SS-ThA7 Plasma-assisted Nitrogen Fixation by Water: Development and Evaluation of Hybrid Membrane Based Plasma-Electrochemical Reactor**, *R. Sharma, Richard M.C.M. van de Sanden, H. Patel, V. Kyriakou, U. Mushtaq*, Dutch Institute for Fundamental Energy, Netherlands; *A. Pandiyan*, Dutch Institute for Fundamental Energy; *S. Welzel, M.N. Tsampas*, Dutch Institute for Fundamental Energy, Netherlands

The worldwide energy crisis and environmental issues have greatly driven the current research on exploring and efficiently utilizing the environmentally-friendly and sustainable energy sources¹. Most sustainable sources such as solar and wind energy are in principle able to meet the global energy demand. Nevertheless, they are intermittent and require new concepts of conversion and storage of electricity. Storing energy in form of chemical bonds is considered as an effective option for long term storage. Thus there is quest of developing effective processes for converting electrical energy into molecules.

In this context, nitrogen fixation is unquestionably one of the most important chemical conversion process since it converts N₂ into molecules of high energy (e.g. NH₃, NO)². However, contemporary chemical industry for nitrogen fixation imposes great concerns about the environmental sustainability in terms of immense energy consumption and burdened emissions profile. Nevertheless, plasma-technology has been receiving renewed attention as an alternative “green” approach for N₂ activation which is one of the fundamental requirement for nitrogen fixation.

Up to now solutions were mainly sought on material axis, however recent theoretical studies have revealed that there are intrinsic limitations of catalysis (i.e. scaling relationships) which keep the processes far from the optimum performance. In this work, we will present a unique solution to the aforementioned limitations by employing a hybrid type reactor consisting of a plasma reactor and solid state water electrolyzers with oxygen ion³ or proton conducting membranes. Unlike conventional plasma catalysis that requires the co-activation of reactants, in the proposed alternative approach, electrolyzers provide reacting species on catalysts with a controllable manner while a radiofrequency plasma is used to increase the reactivity of N₂. Such spatial separation of N₂ dissociation and catalytic formation of the target molecules provides truly independent

parameters to optimise the nitrogen fixation process. One aided benefit of the proposed approach is that both technologies, i.e. water electrolyser and plasma activation, utilize base molecules (N₂ and H₂O) and can be directly powered by renewable electricity. Such a scheme may be a stepping stone to zero carbon footprint processes. Moreover, the advantages of proposed approach will be also compared to conventional plasma catalysis or pure plasma processes.

References

[1] Chu et al, *Nat. Mater.*, 16 (2017), 16

[2] Patil et al, *Catal. Today*, 256 (2015), 49

[3] Tsampas et al, *Catal. Sci. Technol.*, 5 (2015) 4884

4:40pm **PS+SS-ThA8 Plasma-Assisted Ammonia Synthesis in Hybrid Plasma-Catalysis DBD Reactors**, *Z. Chen, X. Yang, Y. Ju, S. Sundaresan, Bruce E. Koel*, Princeton University

INVITED

Solar and wind power are creating increasingly large amounts of electricity, and an important question is how can we take advantage of the expanding increase of renewable electricity for catalysis? One approach is plasma-assisted catalysis, which utilizes excited gaseous molecules or new reactive species formed in a (non-equilibrium, low temperature) gas discharge plasma, along with a catalyst to enable increases in the activity and selectivity for carrying out desirable chemical reactions. A significant challenge in plasma-catalysis hybrid systems is to achieve the strongest synergistic interactions between the plasma and catalyst to increase performance and overall energy efficiency. We report on two types of dielectric barrier discharge (DBD) reactors (with a coaxial tube and parallel plates) that have been used to screen catalytic effects of different metal surfaces and supported catalysts in plasma-catalysis hybrid systems at near atmospheric pressure, utilizing both AC and nanosecond pulsed discharges. We observed strong synergistic effects between non-equilibrium plasma and catalysts for both NH₃ synthesis and methane coupling reactions. We compared the performance for ammonia synthesis of catalysts using active metals (Pd, Pt, and Fe) or less active metals (Au, Ag, and Cu) or their alloys. We found that the metal-nitrogen (M-N) bond energy was not the only parameter governing the catalytic activity for NH₃ synthesis in plasma. Better catalytic activity could be achieved by bimetallic catalysts that contained catalytic sites for both N₂* dissociation and hydrogenation of M-N bonds, leading to our observations of a highly active PdFe catalyst for NH₃ synthesis in plasma. In addition, we will also report briefly about results in CO₂ reforming of methane in the coaxial reactor, where we found that under thermal only conditions, PtFe/Al₂O₃ catalyzed mainly the formation of CO and H₂, but with the plasma on, the selectivity shifted to methane coupling reactions. Interestingly, an Ag/Al₂O₃ catalyst with an AC discharge demonstrated 100% selectivity to CH₄ coupling reactions at 350 °C. Methane coupling using the plasma-catalysis reactor at low temperatures and pressures mainly produced higher hydrocarbons, suggesting a potential route for converting cheap and abundant methane gas into high value hydrocarbons and fuels.

5:20pm **PS+SS-ThA10 Efforts towards Plasma-assisted Catalysis: Elucidating Gas-phase Energetics, Kinetics, and Surface Interactions**, *Angela Hanna, E.R. Fisher*, Colorado State University

With increasing concern about environmental health and climate change, there is a greater need to investigate fundamental reactivity of pollutant species. Improving the effectiveness of substrates used in vehicular emissions abatement hinges on the ability to discern the contributions of gas-phase species in surface reactions. A fundamental understanding of interactions between plasma species is essential to characterizing complex plasma chemistry phenomena. Inductively-coupled N_xO_y plasma systems were investigated to determine possible synergisms between precursor chemistry and gas-surface interface reactions with a variety of catalytic substrates (i.e., Pt substrates and zeolites). The impact of adding dilute amounts of water vapor to the gas feed was also systematically explored. Precursor chemistry was probed via gas-phase diagnostics; time-resolved optical emission data elucidated NO (g) and N₂(g) production kinetics from N_xO_y source gases, whereas steady-state emission and absorbance data provide information regarding energy partitioning between rotational and vibrational degrees of freedom. The presence of micro-structured catalysts within the plasma significantly decreases excited N₂ vibrational temperature, suggesting these materials promote vibrational relaxation within the discharge. Our unique Imaging of Radicals Interacting with Surfaces (IRIS) allows us to probe the gas-surface interface and provides evidence of how plasma species synergistically interact with catalytic substrates. In addition to evaluating the spectroscopic characteristics of the discharge (N_xO_y), we have assessed material morphology and chemical

Thursday Afternoon, October 24, 2019

composition before and after plasma exposure. The porous network of zeolite substrates was maintained after prolonged plasma exposure, although surface etching of oxygen or N-doping occurred at different plasma operating conditions. This holistic experimental approach, combining gas-phase diagnostics, IRIS, and robust materials characterization will be essential to realizing the potential of plasma assisted catalysis for pollution remediation.

Surface Science Division

Room A220-221 - Session SS+2D+AP+AS+OX+SE-ThA

Dynamics at Surfaces/Reactions and Imaging of Oxide Surfaces

Moderators: Irene Groot, Leiden University, The Netherlands, William E. Kaden, University of Central Florida

2:20pm SS+2D+AP+AS+OX+SE-ThA1 Adsorption, Reaction, and Diffusion of Energetic Reagents on Morphologically Diverse Thin Films, *Rebecca Thompson*^{1,2}, *M.R. Brann, S.J. Sibener*, The University of Chicago

I present work from two studies illustrating the impact of condensed-phase film morphology on reaction kinetics and surface adsorption. To begin, I will discuss the **oxidative reactivity of condensed propene films**. This work is conducted in a state-of-the-art ultra-high vacuum chamber equipped for operation at cryogenic substrate temperatures. Time-resolved reflection absorption infrared spectroscopy (RAIRS) is used to track propene reactivity when films are exposed to a supersonic expansion of ground state oxygen atoms, O(³P). I demonstrate that propene reacts significantly on exposure, producing primarily propylene oxide and propanal. Oxide production is significant; partial oxidation products are rarely observed in gas phase studies and olefin oxides are incredibly important chemical intermediates in a variety of industrial processes. Regardless of initial film thickness, the reaction follows zero order kinetics, with a calculated activation energy of 0.5 kcal mol⁻¹. This low barrier closely matches that reported in gas phase studies, suggesting that the condensed-phase reaction is likely diffusion-limited. I also highlight that the propene deposition temperature has a substantial impact on reactivity. Films deposited below 50 K produce dramatically different RAIR spectra that correspond to a more amorphous film composition. These films are nearly unreactive with O(³P), indicating that oxygen diffusion is directly tied to the density and ordering in the more crystalline film.

This dependence on film structure is also observed in the second study, which explores **embedding in and adsorption on crystalline, non-porous amorphous, and porous-amorphous water ice films**. Using a combination of supersonic molecular beams, RAIRS and King and Wells mass spectrometry techniques, I demonstrate that direct embedding into the bulk is remarkably insensitive to film structure; the momentum barrier is identical between amorphous and porous-amorphous ice films. Below this barrier, however, sticking probabilities differ considerably between the different films, suggesting that the pore structure is more efficient at dissipating incident energy. These discoveries are critical for the accurate quantitative modeling of molecular uptake and reactivity on icy astrophysical bodies such as comets and planetesimals. When taken together, these two studies provide fundamental mechanistic insight into the sticking, diffusion, and reactivity of small molecules on complex films, with a specific emphasis on the impact of film morphology and organization.

2:40pm SS+2D+AP+AS+OX+SE-ThA2 Oxidation of Semiconductors and Semimetals by Supersonic Beams of O₂ with Scanning Tunneling Microscopy Visualization, *Ross Edel*³, *T. Grabnic, B. Wiggins, S.J. Sibener*, The University of Chicago

Our research examines the oxidation of semiconductor and semimetal surfaces using a novel, one-of-a-kind instrument that combines a supersonic molecular beam with an in-line scanning tunneling microscope (STM) in ultra-high vacuum. This new approach to surface reaction dynamics provides spatiotemporal information on surface oxidation over nanoscopic and mesoscopic length scales. We have uncovered the kinetic and morphological effects of oxidation conditions on three technologically relevant surfaces: Si(111)-7×7, highly oriented pyrolytic graphite (HOPG), and GaAs(110). A complete understanding of the oxidation mechanism of

these surfaces is critical due to their technological applications and roles as model systems. Samples were exposed to O₂ with kinetic energies from 0.4-1.2 eV and impingement angles 0-45° from normal, with STM characterization between exposures. In some cases, we were able to monitor the evolution of specific features by revisiting the same nanoscopic locations. Our study of Si(111)-7×7 revealed two oxidation channels, leading to the formation of dark and bright reacted sites. The dark sites dominated the surface and exhibited almost no site selectivity while the bright sites preferred the corner sites of the 7×7 unit cell. Our observations suggest that two adsorption pathways, trapping-mediated and direct chemisorption, occur simultaneously. On HOPG, we found that different oxygen energies, incident angles, and surface temperatures produce morphologically distinct etching features: Anisotropic channels, circular pits, and hexagonal pits. Reaction probability increased with beam energy and demonstrated non-Arrhenius behavior with respect to surface temperature, peaking at around 1375 K. Finally, oxidation of GaAs(110) was found to proceed by two morphologically distinct, competing mechanisms: a homogeneous process leading to layer-by-layer oxide growth, and a heterogeneous process with oxide islands nucleating from surface defects. The rates of both mechanisms change with O₂ kinetic energy, with homogeneous oxidation dominating at lower energies (<0.7 eV) and heterogeneous oxidation with higher energies (≥1.0 eV). The results obtained in this work provide vital information about the morphological evolution and kinetics of semiconductor and semimetals, offering a comprehensive overview of the spatiotemporal correlations that govern oxidation dynamics on surfaces.

3:00pm SS+2D+AP+AS+OX+SE-ThA3 Studying Molecule-Surface Interactions using Rotational Orientation Control of Ground-State Molecular Beams, *Gil Alexandrowicz*, Swansea University, UK INVITED

Performing quantum state selective experiments of molecule-surface collisions provides unique insight into the interaction potential. One particularly tricky molecular property to control and measure is the rotational projection states, i.e. the orientation of the rotational plane of the molecule. Previous data was mostly restricted to photo-excited/paramagnetic species. In this talk, I will describe the molecular beam apparatus which allows to control and measure the rotational orientation of ground state molecules [1], present new experimental results for H₂ colliding with ionic surfaces and discuss the future of this new technique in terms of studying molecule-surface interaction-potentials and modifying the outcome of reactive molecule-surface collisions.

[1] Nature Communications, 8, 15357 (2017).

4:00pm SS+2D+AP+AS+OX+SE-ThA6 Diffusion of (100)-epitaxially Supported 3D fcc Nanoclusters: Complex Size-dependence on the Nanoscale, *King Chun Lai, J.W. Evans*, Iowa State University

Diffusion of supported 3D nanoclusters (NCs) followed by coalescence leads to coarsening of ensembles of supported NCs via Smoluchowski Ripening (SR) which is a key pathway for degradation of supported metal catalysts. The dependence of the NC diffusion coefficient, D_N, on size N (in atoms) is the key factor controlling SR kinetics, and traditional treatments assumed simple monotonic decrease with increasing size. We analyze a stochastic model for diffusion of (100)-epitaxially supported fcc NCs mediated by diffusion of atoms around the surface of the NC. Multiple barriers for surface diffusion across and between facets, along step edges, etc. are chosen to accurately describe Ag [Lai and Evans, *Phy. Rev. Materials* 3 (2019) 026001]. KMC simulations reveal a complex oscillatory variation of D_N with N. Local minima D_N sometimes but not always correspond to N = N_c where the equilibrium Winterbottom NC structure is a closed-shell. Local maximum generally correspond to N = N_c + 3. The oscillatory behavior is expected to disappear for larger N above O(10²). Behavior has similarities to but also basic differences from that for 2D supported NCs [Lai et al *Phys. Rev. B* 96 (2017) 235406]. Through detailed analysis of the energetics of the 3D NC diffusion pathway (which involves dissolving and reforming facets), we can elucidate the above behavior as well as observed trends in effective diffusion barrier.

4:20pm SS+2D+AP+AS+OX+SE-ThA7 Oxide Surface Formation on Rh Nanoparticle during O₂ Exposures Observed by Atom Probe Microscopy, *Sten Lambeets*, Pacific Northwest National Laboratory; *T. Visart de Bocarmé*, Université Libre de Bruxelles, Belgium; *N. Kruse*, Washington State University; *D.E. Perea*, Pacific Northwest National Laboratory

Metallic surfaces may undergo a series of surface and subsurface structural and chemical transformations while exposed to reactive gases that inevitably change the surface properties. Understanding such dynamics from a fundamental science point of view is an important requirement to

¹ Morton S. Traum Award Finalist

² National Student Award Finalist

³ National Student Award Finalist

Thursday Afternoon, October 24, 2019

build rational links between chemical/structural surface properties and design new catalysts with desired performance or new materials with enhanced resistance to corrosion. The research presented here addresses the early oxide formation dynamics on a rhodium (Rh) single nanoparticle during O₂ exposures and reveals the inter-facet cooperation between Rh{012} and Rh{113} facets, as well as the important role that the subsurface plays.

Field Ion and Field Emission Microscopies (FIM and FEM) enable correlative atomic to nanoscale imaging of the surface of a very sharp Rh needle, the apex size and shape of which models that of a Rh nanoparticle. FIM is used to map, with atomic lateral resolution, the Rh surface revealing a complex network of crystallographic facets, while FEM is used to observe and record O₂ dissociative adsorption and subsequent reaction with H₂ over this same surface of Rh in real-time with nano-scale lateral resolution. Since FEM imaging relies on local work function variations, it notably can be used to follow the fate of adsorbed oxygen atoms (O(ads)) on the Rh surface. As a result, we directly observe that the O₂ dissociative adsorption is mainly active on the Rh{012} regions. The application of Atom Probe Tomography (APT) provided a means to map the fate of the adsorbed oxygen leading to bulk oxide formation through Rh{113} facets. Thus the correlative combination of FIM, FEM, and APT provides unique insight into the mechanism of bulk oxide formation starting from the dissociative oxygen absorption occurring at {012} facets and subsurface penetration of the adsorbed oxygen occurring through {113} facets. leading to a preferential accumulation of the oxygen within the bulk along the [111] direction. This work offers a unique methodology to explore the interactions between the different crystal facets of a complex surface, to explore the complex dynamics linking the surface and the bulk, and finally, offers exciting perspectives leading to a better understanding of heterogeneous catalysis and corrosion dynamics.

4:40pm **SS+2D+AP+AS+OX+SE-ThA8 Noncontact AFM on Oxide Surfaces: Challenges and Opportunities**, *Martin Setvin*, TU Wien, Austria **INVITED**
Recent development of the noncontact atomic force microscopy (nc-AFM) has opened new possibilities in different fields – imaging of organic molecules [1], controlling the charge state of adsorbed species [2], or enhanced chemical resolution of surface atoms [3]. I will focus on the emerging possibilities and opportunities in the field of oxide surfaces and their surface chemistry.

The limits of atomic resolution will be illustrated on clean and water-exposed binary oxides like TiO₂, In₂O₃ or iron oxides. The enhanced chemical resolution of nc-AFM offers a unique opportunity for approaching complex materials with ternary chemical composition. This will be demonstrated on bulk-terminated perovskites SrTiO₃ and KTaO₃. A dedicated cleaving procedure [4,5] allows preparing flat regions terminated by domains of SrO/TiO₂ (or KO/TaO₂) with a well-defined atomic structure. The surface stability, point defects, electronic structure, and chemical properties of such surfaces will be discussed and linked to the incipient ferroelectric character of these materials.

[1] Gross, L.; Mohn, F.; Moll, N.; Liljeroth, P.; Meyer, G., *Science* 2009, 325, 1110

[2] Gross, L.; Mohn, F.; Liljeroth, P.; Repp, J.; Giessibl, F. J.; Meyer, G., *Science* 2009, 324, 1428

[3] Sugimoto, Y.; Pou, P.; Abe, M.; Jelinek, P.; Perez, R.; Morita, S.; Custance, O., *Nature* 2007, 446, 64

[4] I. Sokolovic, M. Schmid, U. Diebold, M. Setvin, *Phys. Rev. Materials* 3, 034407 (2019)

[5] M. Setvin, M. Reticioli, F. Poelzeleitner, J. Hulva, M. Schmid, L. A. Boatner, C. Franchini, U. Diebold, *Science* 359, 572-575 (2018)

5:20pm **SS+2D+AP+AS+OX+SE-ThA10 Edge-Enhanced Oxygen Evolution Reactivity at Au-Supported, Ultrathin Fe₂O₃ Electrocatalysts**, *Xingyi Deng, D. Kauffman, D.C. Sorescu*, National Energy Technology Laboratory
Transition metal oxides have been emerging as promising candidates to replace the state-of-the-art IrO₂ electrocatalysts for oxygen evolution reaction (OER) in alkaline electrolyte, but their key structure-property relationships are often shadowed by heterogeneities in the typical catalyst samples. To circumvent this challenge, we have combined ultrahigh vacuum surface science techniques, electrochemical measurements, and density functional theory (DFT) to study the structure-dependent activity of well-defined OER electrocatalysts. We present direct evidence that the population of hydroxylated Fe edge-site atoms correlates with the OER activity of ultrathin Fe₂O₃ nanostructures (~0.5 nm apparent height) grown on Au(111) substrates, and the Fe₂O₃/Au catalysts with a high density of

edge sites can outperform an ultrathin IrO_x/Au OER catalyst at moderate overpotentials. DFT calculations support the experimental results, showing more favorable OER at the edge sites along the Fe₂O₃/Au interface with lower predicted overpotentials resulted from beneficial modification of intermediate binding. Our study demonstrates how the combination of surface science, electrochemistry, and computational modeling can be used to identify key structure-property relationships in a well-defined electrocatalytic system.

Thin Films Division

Room A122-123 - Session TF+SS-ThA

Metal Halide Perovskites, Other Organic/Inorganic Hybrid Thin Films

Moderators: Mark Losego, Georgia Institute of Technology, Greg Szulczewski, University of Alabama

2:20pm **TF+SS-ThA1 Tailoring Electrode-electrolyte Interfaces in Lithium-ion Batteries using Molecularly Engineered Functional Polymers**, *Laisuo Su*, Carnegie Mellon University; *J. Weaver*, National Institute of Standards and Technology (NIST); *M. Groenenboom*, National Institute of Standards and Technology (NIST); *B.R. Jayan*, Carnegie Mellon University **INVITED**
The performance and stability of lithium ion batteries (LIBs) depend on charge transfer and reactions at electrode-electrolyte interfaces (EEI), making interfaces design a key issue. Here we molecularly engineer this interface using conformal, functional polymer nanolayers via a novel vapor-based deposition technique. We demonstrate that poly(3,4-ethylenedioxythiophene) (PEDOT) nanolayer doubles the capacities of LiCoO₂ at high rates and extends its 4.5 V cycling life by 260%. The improved rate performance is enabled by high diffusion coefficient of Li⁺ in PEDOT measured from neutron depth profiling. Such behavior is further understood by density functional theory (DFT) simulation. The extended cycling stability comes from strong interactions between PEDOT and Co atoms, as suggested from X-ray photoelectron spectroscopy and DFT simulations. Additionally, in-situ synchrotron X-ray diffraction reveals that PEDOT uniformizes current distribution and improves LiCoO₂ structural stability during cycling tests. This work adds understanding and provides guidelines for designing the EEI for advanced LIBs.

3:00pm **TF+SS-ThA3 Chemoselective Adsorption of Alkyne-functionalized Cyclooctynes for the Formation of Si/Organic Interfaces**, *C. Laenger, Julian Heep*, Justus-Liebig-University, Giessen, Germany; *P. Nikodemski, T. Bohamud*, Philipps-University, Marburg, Germany; *P. Kirsten*, Justus-Liebig-University, Giessen, Germany; *U. Hofer, U. Koert*, Philipps-University, Marburg, Germany; *M. Duerr*, Justus-Liebig-University, Giessen, Germany
Controlled organic functionalization of the Si(001) surface may play an important role in the efforts towards further miniaturization of silicon based electronic devices. The first step of such an organic functionalization in terms of organic molecular layer deposition on Si(001) would be the chemoselective adsorption of bifunctional molecules on silicon: whereas one functionality binds to the surface, the other stays intact for the attachment of further layers. This task, however, is complicated by the high reactivity of the dangling bonds with respect to almost all organic functional groups. As a consequence, bifunctional organic molecules typically react via both functional groups on the silicon surface. We solved this problem using cyclooctyne as the main building block of our strategy. The strained triple bond of cyclooctyne reacts via a direct reaction channel, in contrast to most other organic functional groups, which react on Si(001) via a metastable intermediate. This makes the latter ones effectively unreactive in competition with the direct pathway of cyclooctyne's strained triple bond [1].

In this work, we focus on the preparation of a functionalized organic layer on Si(001) using an alkyne-functionalized cyclooctyne, i.e., ethynyl-cyclopropyl-cyclooctyne (ECCO). If the ECCO molecule binds chemoselectively to the silicon substrate via cyclooctyne's strained triple bond, the terminal, linear triple bond of the ECCO molecule can be employed for the attachment of the second layer of molecules, e.g., via alkyne-azide coupling. We first show that the linear triple bond follows an indirect reaction pathway via a weakly bound intermediate. XPS and STM results then clearly indicate that ECCO adsorbs selectively on Si(001) via a [2+2] cycloaddition of cyclooctyne's strained triple bond. No indication for a reaction via the ethynyl group was detected. This chemoselectivity was observed for all coverages, starting from the isolated molecules up to saturation coverage of one monolayer [2]. The ECCO molecules can thus

form an organic functionalization of the Si(001) surface which can be used for controlled attachment of further molecular layers.

[1] Reutzell, et al., J. Phys. Chem. C **120** 26284 (2016).

[2] C. Langer, et al., J. Phys.: Condens. Matter **31** 034001 (2019).

3:20pm TF+SS-ThA4 Durability of Property Changes in Polyester Fabrics Infused with Inorganics via Vapor Phase Infiltration, *Kira Pyronneau, E.K. McGuinness, M.D. Losego*, Georgia Institute of Technology

Vapor Phase Infiltration (VPI) is a processing method for transforming polymers into organic-inorganic hybrid materials. During VPI, a polymer is exposed to vapor-phase metalorganic precursors that sorb, diffuse, and react within the bulk of the polymer to create new hybrid materials. VPI has been shown to modify properties such as the mechanical strength of spider silk, the thermal and UV degradation resistance of Kevlar, and the fluorescence of polyester. This study aims to better understand how VPI can change textile properties for industrial applications and the durability of these changes. To this end, polyester fabrics were treated with trimethylaluminum (TMA) and co-reacted with water in a custom-built vacuum chamber. The temperature of the treatment process was varied from 60°C to 140°C to establish a relationship between processing temperature, physiochemical structure, and material properties. Using thermogravimetric analysis (TGA), these infiltrated fabrics were found to have inorganic loadings between 5 and 8 weight percent, with a maximum inorganic loading at 100 °C (Figure 1). These results are consistent with our current understanding of precursor / polymer sorption thermodynamics and indicate that processing temperature can be used to control the loading of inorganics through both the diffusion rate and the sorption equilibrium. To examine the durability of this inorganic loading, wash fastness testing at 100°C for 90 minutes followed by TGA and SEM/EDX was used to determine the effects of high temperature wash cycles. These tests demonstrated that the inorganic loading remains even after intense laundering (Figure 2). To further characterize the durability of VPI treatment, known changes due to the VPI process were compared before and after washing. In particular, mechanical properties, fluorescence, and thermal degradation behavior were investigated. This talk will explore the wash-fastness of VPI treatments of polyester at different processing temperatures and the retention of enhanced properties relevant to the textile industry.

4:00pm TF+SS-ThA6 Materials Synthesis and Device Fabrication for Novel Inorganic Perovskites, *Mingzhen Liu*, UESTC, China **INVITED**

In recent years, organic lead halide perovskite materials have attracted much attention due to their outstanding optoelectric properties and low manufacturing cost. To improve the stability of perovskite solar cells, inorganic CsPbI₃ perovskite has been demonstrated as promising material for solar cells owing to the superb photoelectric property and composition stability. However, the low stability of perovskite phase CsPbI₃ (α -phase) with an appropriate band gap under ambient environment hinders its practical application.

Here, we investigate new ways of synthesizing inorganic perovskite materials and optimizing the device stability through dimensional engineering. We tailor the three-dimensional CsPbI₃ perovskite into quasi-two-dimensional Cs_xPEA_{1-x}PbI₃ perovskite, where an optimal Cs_xPEA_{1-x}PbI₃ film remains stable in α phase up to 250°C. Moreover, we further present an in-depth investigation of the so-called stable ' α -CsPbI₃,' especially the starting material hydrogen lead trihalide (HPbI₃, also known as PbI₂·xHI) that is usually used for synthesizing α -CsPbI₃. We notice that the "mythical" HPbI₃, the often-assumed reaction product of HI and PbI₂, does not actually exist. Instead, adding acid to DMF is known to generate a weak base dimethylamine (DMA) through hydrolysis, and with the presence of PbI₂ the actual final product is believed to be a compound of DMAPbI₃. Our findings offer new insights into producing inorganic perovskite materials, and lead to further understanding in perovskite materials for solar cells with improved efficiency and stability.

4:40pm TF+SS-ThA8 Carrier-Gas Assisted Vapor Deposition of Metal Halide Perovskite Thin Films, *Catherine Clark*, University of Minnesota; *E.S. Aydil*, New York University; *R.J. Holmes*, University of Minnesota

Hybrid organic-inorganic halide perovskites have emerged as an important class of optoelectronic materials with potential applications in photovoltaics and light emitting devices. One of the challenges in forming thin films of halide perovskites is controlling stoichiometry and morphology. We have designed and built a carrier-gas assisted vapor deposition (CGAVD) system capable of depositing halide perovskite thin films (e.g., CH₃NH₃SnI₃Br_{3-x}) with independent control over their

stoichiometry and morphology. In our CGAVD system, an inert carrier gas (N₂) transports sublimed material vapors through a hot-walled chamber to a cooled substrate where they selectively condense and/or react. By separately controlling the precursor sublimation rate, *via* source temperature, and the transport rate to the substrate, *via* carrier gas flow rate, we realize fine control of species flux at the substrate and successfully co-deposit materials with very different vapor pressures (e.g. CH₃NH₃Br, SnBr₂). Four additional independent parameters (dilution gas flow, chamber pressure, gas temperature, and substrate temperature) can be varied to access a wide range of deposition conditions and film morphologies with controlled stoichiometry. To navigate the vast parameter space of CGAVD, we use an experimentally validated transport and reaction model, which informs the deposition parameter selections. We find that repeatable and spatially uniform deposition requires operating in a regime where solid source material is at equilibrium with its vapor and convective transport determines the flux of species arriving at the substrate. Importantly, we find that films grown using CGAVD have a stoichiometric "self-correcting" and robust operation window, wherein excess precursor flux during co-deposition is rejected from the film and a phase-pure perovskite film results. This is practically advantageous as it relaxes the need for balancing precursor fluxes exactly during co-deposition. We demonstrate the growth of CH₃NH₃SnI₃Br_{3-x} thin films with a wide range of stoichiometries and morphologies. Specifically, by tuning the source material temperature (140 °C – 290 °C), the carrier gas flow rate (2 sccm – 100 sccm), the substrate temperature (8 °C – 70 °C), and the chamber pressure (350 mTorr – 10 Torr), we realize corresponding changes in grain orientation and grain size from <100 nm to over 1 μ m. CGAVD is a promising approach to deposition of other halide perovskites and can potentially enable the growth of previously inaccessible morphologies and multi-layer perovskite films.

5:00pm TF+SS-ThA9 Synthesis and Optical Properties of Organo-halide 2D Perovskites, *Misook Min*, A.B. Kaul, University of North Texas

Organic-inorganic halide perovskite materials have attracted interest in recent years due to their excellent optoelectronic properties, such as high absorption coefficient, tunable band gap, small exciton binding energy. These advantages combined with the extremely low fabrication cost make this kind material suitable as a light absorber for solar cells, light emitting diodes, field-effect transistors and photo-detectors [1]. Hybrid organic-inorganic perovskite described by the formula ABX₃ (A = organic ammonium cation, B = inorganic compounds, X = halide anion). Specifically, the iodide and bromide versions of CH₃NH₃PbX₃ have led to a breakthrough in various research field. We report the scalable synthesis and properties of the 2D series of lead iodide (CH₃(CH₂)₃NH₃)₂(CH₃NH₃)_{n-1}PbI_nBr_{n+1} (n = 2, 3, and 4) perovskites [2]. The 2D (CH₃(CH₂)₃NH₃)₂(CH₃NH₃)_{n-1}PbI_nBr_{n+1} were synthesized and materials characterization was conducted using atomic force microscopy (AFM), X-ray diffraction (XRD), and Photoluminescence (PL) spectroscopy. The crystal structure and surface morphology for n = 2, 3, and 4 perovskites was validated using XRD and AFM, and the peak optical absorption was consistent with the composition-tunable bandgap for these formulations occurring at ~ 2.18 eV, 2.06 eV, and 2.03 eV. Our results show that hybrid organic-inorganic perovskites can be easily and efficiently prepared. Also, the hybrid organic-inorganic perovskites define a promising class of stable and efficient light absorbing materials for photo-detectors and other applications.

5:20pm TF+SS-ThA10 Encapsulation of Perovskite Nanocrystal Solids using Metal Oxides - A Closer Look into Optical Properties, *Riya Bose, Y. Zheng, T. Gua, Y. Garstein, A.V. Malko*, University of Texas at Dallas

The performance (i.e., light harvesting, optical gain or emission outputs) of many optoelectronics devices (i.e., lasers, photovoltaics (PVs), light emitting diodes (LEDs), etc.) critically depends on the ability to deposit solution processed nanocrystals (NCs) into well-organized, close-packed solids with high photoluminescence quantum yields (PL QYs) and the long term stability of NC films. However, irrespective of the high quality of NCs or the passivation techniques used in solution, the deposition of NC multilayers as well as the exposure to the environment during solid state device fabrication often require or lead to changes in the NCs chemical environment, such as exchange/loss of ligands, which eventually lead to formation of trap states that decrease the PL QYs of NCs and are often detrimental to device performances. An attractive approach to protect the NCs' integrity is the use of atomic layer deposition (ALD) in which self-limiting surface reactions of the precursors allows conformal growth of the metal oxide layer with precise thickness control to encapsulate NCs. This process, though prevents the deterioration of NCs, is observed to decrease their PLQY significantly. To mitigate this issue, we recently developed an

Thursday Afternoon, October 24, 2019

alternate gas phase deposition technique where a pulsed co-deposition of both metal and oxidant precursors at room temperature (RT) (reminiscent of chemical vapor deposition, CVD) is able to deposit uniform metal oxide (AlO_x) films, originating from gas-phase reactions in the immediate vicinity of the NC layer. Unlike conventional ALD, this method is observed to preserve the optical properties, e.g., PLQY and lifetime of metal chalcogenide NCs film. With this new approach, we investigate the encapsulation of hybrid metal halide perovskite NCs, which have been at the forefront of recent optoelectronic materials research due to their high absorption coefficients, high charge carrier mobilities, balanced ambipolar transport properties, and easy solution processability. However, in spite of the exceptional upsurge in the lab scale device efficiency of perovskites in a remarkably short time frame, the practical application of the same in real world is restricted by their inherent instability. AlO_x deposition on perovskite nanocrystals with our modified approach not only retains the optical properties of the NCs, but also improves them, even at a single particle level, which paves the way for unique optoelectronic opportunities.

5:40pm **TF+SS-ThA11 Self-Limited Surface Reaction between Trimethyl Aluminum and Formamidinium Lead Iodide Perovskite**, *Qing Peng, X. Yu, H. Yan*, University of Alabama

Surface site-limited reaction is critical to modifying hybrid halide perovskites without destroying their bulk properties. However, no surface site-limited reaction on hybrid halide perovskites has been demonstrated and confirmed. Herein, we report one surface-site limited reaction on FA lead iodide with tri-methyl aluminum. The strong coordination between organic cations FA⁺ and trimethyl aluminum, a very strong Lewis acid, is found to be the key for this self-limited reaction behavior. Our results provide a model system to understand the effect of surface species on surface reaction behavior on hybrid halide perovskites.

Chemical Analysis and Imaging Interfaces Focus Topic Room A226 - Session CA+AS+NS+SE+SS-FrM

Novel Applications and Approaches in Interfacial Analysis

Moderators: Paul Dietrich, SPECS Surface Nano Analysis GmbH, Germany, Jeong Young Park, Korea Advanced Institute of Science and Technology (KAIST), Republic of Korea

8:20am **CA+AS+NS+SE+SS-FrM1 Chemical Reactions on Bimetal Surfaces with Operando Surface Techniques, Jeong Young Park**, Korea Advanced Institute of Science and Technology (KAIST), Republic of Korea **INVITED**

The origin of the synergistic catalytic effect between metal catalysts and reducible oxide has been debated for decades. Clarification of this effect, namely the strong metal–support interaction (SMSI), requires an understanding of the geometric and electronic structures of metal–metal oxide interfaces under operando conditions.[1] A bimetallic platinum (Pt) alloy catalyst is an excellent platform to uncover the contentious role of the metal–metal oxide interface because the alloyed transition metal can coexist with the Pt surface layer in the form of an oxidized species on the bimetal surface during catalytic reactions.

In this talk, I present in-situ observation results of structural modulation on Pt-Ni metastable and Ni (111) surfaces at 0.1 Torr pressure of CO, O₂, and CO oxidation conditions with ambient-pressure scanning tunneling microscopy (AP-STM) and ambient-pressure X-ray photoelectron spectroscopy (AP-XPS).[2] We show that the stable Pt-skin covered Pt₃Ni(111) surface is broken by segregation of dissociative oxygen-induced Ni oxides under elevated oxygen pressure environment, which evolved clusters could have a crucial relation with enhanced catalytic activity. We show that NiO_{1-x}/Pt-Ni nanostructures are on the Pt₃Ni(111) surface under CO oxidation and these metal-oxide interfaces provide more efficient reaction path for CO oxidation [2]. Furthermore, I will show the research efforts for understand the catalytic behavior of bimetal PtCo and PtNi nanocatalysts using in-situ surface techniques including catalytic nanodiode and transmission electron microscopy. The catalytic nanodiode that consists of metal catalyst film, semiconductor layers, and Ohmic contact pads revealed the strong correlation between the hot electron flux (chemicurrent) and catalytic activity under CO oxidation and hydrogen oxidation. Using this approach, the catalytic activity and hot electron generation on PtCo bimetal nanoparticles were investigated. In-situ transmission electron microscopy reveals the formation of metal oxide layers on bimetal nanoparticle surfaces under oxygen conditions. We show that formation of interface between Pt and CoO enhances both of catalytic activity and chemicurrent yield [3].

[1] J. Y. Park et al. Chemical Reviews 115, 2781-2817 (2015)

[2] J. Kim et al. Science Advances 4, eaat3151 (2018).

[3] H. Lee et al. Nature Communications 9, 2235 (2018).

9:00am **CA+AS+NS+SE+SS-FrM3 Principal Component Analysis to Reveal Camouflaged Information in Spectromicroscopy of (complex) Oxides, David Mueller, M. Giesen, Forschungszentrum Juelich GmbH, Germany; D. Stadler, University of Cologne, Germany; T. Duchon, F. Gunkel, V. Feyer, Forschungszentrum Juelich GmbH, Germany; S. Mathur, University of Cologne, Germany; C.M. Schneider, Forschungszentrum Juelich GmbH, Germany**

Spectroscopic imaging techniques are becoming more and more accurate and available, which results in an increase of data to handle and analyze. Near Edge X-Ray absorption spectroscopy, especially in the soft X-Ray regime, has the ability to identify inhomogeneities in chemistry and electronic structure, which is mostly done by fingerprinting or using internal standards. In a spectromicroscopic image, each pixel contains such a spectrum, and by the lack of rigorous fitting routines that are for example present in XPS, reduction and preevaluation of data is needed. Principal Component Analysis (PCA) of X-PEEM data affords this in an unambiguous and unbiased way by identifying and highlighting spectroscopic features which contribute to a spectrum.¹

Two cases where PCA revealed information that might have been missed otherwise are presented here: Firstly, iron oxide thin films grown by CVD showed a considerable influence of an external magnetic field on chemistry and crystallinity. Combination of O-K- and Fe-L-Edge X-PEEM unambiguously identified different iron oxide polymorphs (Fe₃O₄ and α -Fe₂O₃) depending on field strength during deposition. The former XAS Edge showed subtle spatial variations in the EXAFS regime that could be

identified as the breakdown of long-range ordering, pointing to incomplete crystallization when films are deposited without magnetic field assistance.²

The second example is the surface decomposition of Pr_{0.5}Ba_{0.5}CoO_{3- δ} (PBCO), a promising material for the use as water splitting catalyst and solid oxide electrochemical cell electrode. Using spatially resolved O-K-, Co-L-, and Ba- and Pr-M-Edge XAS, changes in surface chemical composition upon annealing and its impact on the electronic structure were observed. Laterally resolved by X-PEEM, PCA could reveal that exposing thin films of the material to technologically relevant conditions (1073 K, 20 mbar of O₂) leads to a more complex decomposition pathway than simple spinodal unmixing to the end members BaCoO₃ and PrCoO₃ as the spectromicroscopic dataset could only be described satisfactory by a linear combination of three components.

9:20am **CA+AS+NS+SE+SS-FrM4 In situ Electron Microscopy of Catalysts with Atomic Resolution under Atmospheric Pressure, Xiaoqing Pan**, University of California Irvine **INVITED**

Understanding the atomic structures of catalysts under realistic conditions with atomic precision is crucial to design better materials for challenging transformations. For example, under reducing conditions, certain reducible supports migrate onto supported metallic particles and create strong metal–support states that drastically change the reactivity of the systems. The details of this process are still unclear and preclude its thorough exploitation. In the past decade, most of atomic-scale transmission electron microscopy (TEM) studies involving gas-solid interactions were conducted in an environmental TEM, where the gas pressure is typically limited to less than 1/100 of atmosphere. Recently, it has become possible to overcome this limitation through a MEMS-based, electron-transparent closed cell with a heating stage.

In this talk, I will present our recent results using this device (the Protochips Atmosphere™ system) in selected catalyst systems. In a palladium/titania (Pd/ TiO₂) catalyst, we directly observed the formation of the oxide overlayers on the supported Pd particles with atomic resolution under atmospheric pressure and high temperature. It shows that an amorphous reduced titania layer is formed at low temperatures, and that crystallization of the layer into either mono- or bilayer structures is dictated by the reaction environment. This transition occurs in combination with a dramatic reshaping of the metallic surface facets. *In-situ* TEM observations of a modular Pd-ceria core-shell nanostructured catalyst (Pd@CeO₂) showed that an unexpected structural transformation occurs upon heating at high temperatures. The system reaches to a stable state with the mixture of nanoparticles with two different sizes, which accounts for the exceptional catalytic properties that have been reported. Using the similar techniques, we also studied the core-shell platinum-metal (Pt-M) nanoparticles which show a catalytic performance in the oxygen reduction reaction (ORR) superior to that of pure Pt nanoparticles. To understand the formation mechanism of the Pt shell, we studied thermally activated core-shell formation in Pt₃Co nanoparticles via *in-situ* electron microscopy with the gas cell. The disordered Pt₃Co nanoparticle was found to transform into an ordered intermetallic structure after annealing at high temperature (725°C) in 760 Torr O₂, followed by layer-by-layer Pt shell growth on (100) surfaces at low temperature (300°C). The apparent 'anti-oxidation' phenomenon promoted by the ordered Pt₃Co phase is favorable to the ORR catalyst, which operates in an oxidizing environment.

10:00am **CA+AS+NS+SE+SS-FrM6 Exposing Buried Interfaces in Thin Film Photovoltaics through Thermo-mechanical Cleaving, Deborah McGott**, Colorado School of Mines; C.L. Perkins, W.K. Metzger, National Renewable Energy Laboratory; C.A. Wolden, Colorado School of Mines; M.O. Reese, National Renewable Energy Laboratory

Thin film solar cells, such as cadmium telluride (CdTe) and Cu(In,Ga)Se₂ (CIGS), contain buried interfaces that are critical to carrier transport, recombination, and device performance, yet are poorly understood due to their inaccessibility within the device stack. In particular, accessing the interface in a way that preserves the chemical structure has historically been extremely difficult. Here, we describe an innovative technique to expose buried interfaces through a two-step thermo-mechanical cleaving process. First, a stressor layer (typically an epoxy or commercially available polymeric backsheets) is applied to the solar cell. Then, the stack is submerged in a cold bath (T \leq -30°C) to thermally shock the system. This causes the stressor to contract quickly and pull the polycrystalline film cleanly off of its substrate at an interface that is weakened by a monolayer accumulation of 2-D material (CdCl₂ in CdTe and MoS₂ in CIGS).

Focusing on CdTe solar cells, we then use X-ray photoelectron spectroscopy to probe the oxidation states at the newly exposed SnO₂ interface. We

show that the tin oxide front electrode promotes the formation of nanometer-scale oxides of tellurium and sulfur. Most oxidation occurs during CdCl_2/O_2 activation. Surprisingly, we show that relatively low-temperature anneals (180–260°C) used to diffuse and activate copper acceptors in a doping/back contact process also cause significant changes in oxidation at the front of the cell, providing a heretofore missing aspect of how back contact processes can modify device transport, recombination, and performance. Device performance is shown to correlate with the extent of tellurium and sulfur oxidation within this nanometer-scale region. Mechanisms responsible for these beneficial effects are proposed.

10:20am CA+AS+NS+SE+SS-FrM7 Switchable Dopants on Percolation Networks of 2D Materials for Chemiresistive Sensing Applications in Aqueous Environments, Peter Kruse, McMaster University, Canada

Permanent doping of semiconductors and low-dimensional structures to modulate their electronic properties is a well-established concept. Even in cases where doping of thin films by analytes (e.g. carbon nanotubes by ammonia) is applied in sensors, it is only reversed by physical removal of dopant molecules, e.g. heating. We have introduced the concept of molecular switches as chemical dopants for thin nanocarbon (or other 2D-materials) films. These molecules can be switched between doping and non-doping states in the presence or absence of a particular analyte. They impart selectivity not only due to their change in doping behavior, but also by physically blocking other potential dopants in the analyte solution from interacting with the conductive film. The resulting structures can act as chemiresistive films. Chemiresistive sensors are a well-established technology for gas-phase sensing applications. They are simple and economical to manufacture, and can operate reagent-free and with low or no maintenance. Unlike electrochemical sensors they do not require reference electrodes. While in principle they can be made compatible with aqueous environments, only a few such examples have been demonstrated. Challenges include the need to prevent electrical shorts through the aqueous medium and the need to keep the sensing voltage low enough to avoid electrochemical reactions at the sensor. We have built a chemiresistive sensing platform for aqueous media. The active sensor element consists of a percolation network of low-dimensional materials particles that form a conducting film, e.g. from carbon nanotubes, pencil trace, exfoliated graphene or MoS_2 . The first member of that platform was a free chlorine sensor. We are currently working to expand the applicability of our platform to other relevant species, in particular anions and cations that are commonly present as pollutants in surface and drinking water. Our sensors can be incorporated into a variety of systems and will also be suitable for online monitoring in remote and resource-poor locations.

10:40am CA+AS+NS+SE+SS-FrM8 Analysis Of Radioactive Materials In Liquid Using In Situ Sem And Tof-Sims, Jennifer Yao, X.-Y. Yu, Z.H. Zhu, E.C. Buck, Pacific Northwest National Laboratory

Characterization of nuclear materials in solid particles or particles in liquid slurry, particularly in high level waste, can establish the elemental, organic, and isotopic compositions that effect the properties of the materials during nuclear fuel cycle activities and processes. Techniques to evaluate such detailed information, even at small concentrations, can support nuclear materials and science programs by increasing our ability to manage and control nuclear materials. However, radioactive materials analysis in liquids and slurries can be challenging using bulk approaches. We have developed a vacuum compatible microfluidic interface, system for analysis at the liquid vacuum interface (SALVI), to enable surface analysis of liquids and liquid-solid interactions using scanning electron microscopy (SEM) and time-of-flight secondary ion mass spectrometry (ToF-SIMS). In this work, we illustrate the initial results from the analysis of liquid samples of importance in the geologic disposal of UO_2 spent nuclear fuel in a repository environment using in situ liquid SEM and SIMS. Our results demonstrate that multimodal analysis of UO_2 materials is possible using SALVI. Both in situ liquid SEM and SIMS can be used as new approaches to analyze radioactive materials in liquid and slurry forms of high level nuclear waste.

11:00am CA+AS+NS+SE+SS-FrM9 Interactions between Synthetic Bilgewater Emulsion and Biofilms, Jiyoung Son, Earth and Biological Sciences Directorate; J. Yao, Earth & Biological Sciences Directorate; X.-Y. Yu, Pacific Northwest National Laboratory

Presentation Summary:

This presentation will showcase our latest results of the interaction between biofilms and synthetic bilgewater using a surface chemical imaging technique.

Abstract

Bilgewater, an oil-in-water (O/W) emulsion, is a persistent pollutant released to the ocean from the lowest part of ships. Microbes play an important role in the ocean. It is hypothesized that microbes release organics that can act as surfactants that affect bilgewater formation or weakening. We present the first systematic study of emulsions and biofilms and investigate the effects of biofilms on bilgewater emulsions. Three strains were selected *Pseudomonas*, *Arthrobacter*, and *Cobetia marina*. A Navy O/W emulsion consisting of three oils and a detergent mixture was used as the synthetic bilgewater model [1]. Biofilms were cultured in a microchannel to allow healthy culture [2]. Once a thick layer of biofilms was formed, the medium solution was changed to a mixture consisting of 50 % bilgewater emulsion. Dispersed biofilms were collected at 24 hrs. and 48 hrs. after emulsions were introduced into the channel. Bilgewater emulsions, biofilms, and mixtures of bilgewater emulsions and biofilms were analyzed using multiple *in situ* and *ex situ* techniques including time-of-flight secondary ion mass spectrometry (ToF-SIMS), scanning electron microscopy (SEM), and optical microscopy. Our findings indicate that biofilms change the chemical makeup of the emulsion surface compositions and emulsion droplet size distribution, confirming the hypothesis that extracellular polymeric substance (EPS) related components released from biofilms can function as surfactants and change the oil-in-water interfaces.

Key words: bilgewater emulsion, oil-in-water, microfluidics, biofilm, EPS, surfactant

Reference

1. Church, J., D.M. Paynter, and W.H. Lee, *In Situ Characterization of Oil-in-Water Emulsions Stabilized by Surfactant and Salt Using Microsensors*. Langmuir, 2017. **33**(38): p. 9731-9739.
2. Yao, J., et al., *In Situ Characterization of Boehmite Particles in Water Using Liquid SEM*. J Vis Exp, 2017(127).

11:40am CA+AS+NS+SE+SS-FrM11 Artificial Intelligence—An Autonomous TEM for In-situ Studies, Huolin Xin, University of California Irvine INVITED

Deep learning schemes have already impacted areas such as cognitive game theory (e.g., computer chess and the game of Go), pattern (e.g., facial or fingerprint) recognition, event forecasting, and bioinformatics. They are beginning to make major inroads within materials science and hold considerable promise for materials research and discovery. In this talk, I will introduce deep convolutional neural networks and how they can be applied to the computer vision problems in transmission electron microscopy. I will also discuss the development and application of liquid TEM to the study of solid/liquid interfaces at the nanoscale.

Fundamental Discoveries in Heterogeneous Catalysis Focus Topic

Room A213 - Session HC+SS-FrM

Catalysis at Complex Interfaces

Moderators: Elizabeth Landis, College of the Holy Cross, Fan Yang, Dalian Institute of Chemical Physics, China

8:20am HC+SS-FrM1 Pd Nanoparticles on Alumina Nanofibers by Electrospinning for Heterogeneous Catalysis, Miguel Angel Rodriguez Olguin, M. Enes da Silva, J. Faria, A. Susarrey Arce, H. Gardeniers, University of Twente, Netherlands

The pressing transition from unsustainable fossil fuels to a sustainable economy based on renewables with minimal chemical waste is one of the grand challenges for the twenty-first century. To mitigate these challenges, it is crucial that improved synthetic catalytic methods are developed, that increase conversion and selectivity of existing chemical transformation processes. For example, *alumina* is a widely used catalyst support owing to its excellent thermal stability and inherent chemical acidity. Technologies like three-way catalytic converters rely on well-defined alumina-based structured monoliths of about hundred of micrometers to millimeters dimensions without spatial control on the allocation of the metal catalyst. The latter is considered essential to derive at more stable catalysts, it may prevent sintering for instance. Additive manufacturing of catalyst materials can pave the path to control the distribution of catalytic nanoparticles, and mass transport modulation by optimized 3-dimensional support designs. In this work, we present co-axial electrospinning to control the distribution of Pd nanoparticles (Pd NPs) over synthetic fibrous-like Al_2O_3 structures. First, our approach involved several synthetic routes for the fine tuning of the

Friday Morning, October 25, 2019

Al₂O₃ fibers by varying the formulation of Al(NO₃)₃•9H₂O, Al(OH)₃, C₁₄H₂₇AlO₅ precursors and Al₂O₃ nanoparticles additives. Thermal stability and chemical properties of the nanofibers have been tested. The Al₂O₃ fibers morphology is visualized with Scanning Electron Microscopy (SEM), and the fiber diameter is estimated between 81 nm to 107 nm depending on aluminum precursor. Furthermore, X-ray Diffraction (XRD) is utilized to confirm the crystalline phase of the Al₂O₃ used as support. Second, the Al₂O₃ that performs best in terms of morphology, crystallinity, surface area and acidity is loaded with Pd NPs. The location of Pd NPs is varied by tuning the Pd concentration of the precursor suspension. Finally, the Al₂O₃-Pd fibrous catalyst is tested by chemisorbing CO species. CO chemisorption in liquid phase is performed with *in-situ* Attenuated Total Reflectance Infrared Spectroscopy (ATR-IR). Further, liquid phase catalytic reactions will be explored.

8:40am HC+SS-FrM2 Multi-Layered TiO₂ Nanofibrous Structures Decorated with Catalytic Nanoparticles for Photoelectrocatalytic Applications, Cristian Deenen, C. Eyövgé, A. Susarrey-Arce, H. Gardeniers, University of Twente, Netherlands

Electrospinning is a technique to fabricate nanofibers by applying a high potential between a nozzle and a collector. As a solution is pumped through the nozzle, a jet is ejected from the nozzle that solidifies as it moves towards the collector, resulting in nanofiber deposition on the collector.

A drawback in conventional electrospinning setups consisting of a singular electrified nozzle is the difficulty in depositing multiple material combinations due to the time and labor required to either manually replace the nozzle or to flush the fluidic elements of the electrospinning setup. A novel multi-nozzle approach will be demonstrated to reduce the time required for the switching of precursor materials from minutes to seconds. The proposed concept opens up new possibilities for the fabrication of complex devices with a variety of material formulations, such as alternating functional layers of interest to the fields of catalysis, electrochemistry and photovoltaics.

Mounting multiple nozzles on a rotating disc allows the inactive nozzles to be rotated out-of-plane, away from the electric field between the active nozzle and the collector, which at the same time reduces the risks of dripping from the inactive nozzles. Combining this concept with appropriate control of electrical voltages and fluidic flow through the different nozzles, allows the engineering of a flexible platform for fast and reliable manufacturing of multi-component materials using electrospinning. In this work, we will demonstrate the instrumental concept and apply it to the fabrication of catalytic layers composed of TiO₂, decorated with three different metal catalyst nanoparticles (Au, Pd, Pt) which function in concert for light harvesting and efficient hydrogen production during photoelectrocatalysis.

9:00am HC+SS-FrM3 Water Oxidation Reaction in Natural Photosynthesis, J. Yano, Kyle Sutherlin, Lawrence Berkeley National Laboratory INVITED

Many of the catalytic reactions in inorganic systems and natural enzymes involve multiple electrons, and proceed through several intermediate steps. For example, photosynthetic water oxidation in nature is catalyzed by the metal center that consists of oxo-bridged four Mn and one Ca atoms, which is located in multi-subunit membrane protein, Photosystem II (PSII). This is one of the most important, life-sustaining chemical processes occurring in the biosphere. The oxygen-evolving complex (OEC) in PSII, which contains the heteronuclear Mn₄CaO₅ cluster, catalyzes the reaction

$$2\text{H}_2\text{O} \rightarrow \text{O}_2 + 4\text{e}^- + 4\text{H}^+$$

that couples the four-electron oxidation of water with the one-electron photochemistry occurring at the PSII reaction center. The OEC cycles through five intermediate S-states (S₀ to S₄) that corresponds to the abstraction of four successive electrons from the OEC (Fig. 1). Once four oxidizing equivalents are accumulated (S₄-state), a spontaneous reaction occurs that results in the release of O₂ and the formation of the S₀-state.

Recently, the development of X-ray Free Electron Lasers (XFELs) has opened up opportunities for studying the dynamics of biological systems. Intense XFEL pulses enable us to apply both X-ray diffraction and X-ray spectroscopic techniques to dilute systems or small protein crystals. By taking advantage of ultra-bright femtosecond X-ray pulses, one can also collect the data under functional conditions of temperature and pressure, in a time-resolved manner, after initiating reactions, and follow the chemical dynamics during catalytic reactions and electron transfer. Such an approach is particularly beneficial for biological materials and aqueous solution samples that are susceptible to X-ray radiation damage.

We have developed spectroscopy and diffraction techniques necessary to fully utilize the capability of the XFEL x-rays for a wide-variety of metalloenzymes, like Photosystem II, and to study their chemistry under functional conditions. One of such methods is simultaneous data collection for x-ray crystallography and x-ray spectroscopy, to look at overall structural changes of proteins and chemical changes at metal catalytic sites. We have used the above techniques to study the water oxidation reaction of Photosystem II, in which the Mn₄CaO₅ cluster catalyzes the reaction. The current status of this research and the mechanistic understanding of the water oxidation reaction based on the X-ray techniques is presented.

10:00am HC+SS-FrM6 Nanoscale Spectromicroscopy and Chemical Activity of Bilayer Silicate Films on Pd(100) and Pd(111), Samuel Tenney, C. Eads, Brookhaven National Laboratory; L.O. Mark, University of Colorado at Boulder; V. Lee, University of North Texas; M. Wang, Brookhaven National Laboratory; J.W. Medlin, University of Colorado at Boulder; J.A. Kelber, University of North Texas; D.J. Stacchiola, Brookhaven National Laboratory
In this talk we present the first reported photothermal infrared (PTIR) spectra and hyperspectral images of ultrathin bilayer silicate films with a spatial resolution better than 10nm and compare this with traditional infrared reflection absorption spectroscopy (IRRAS) of the same surface. The growth of the ultrathin bilayer silicates on Pd(100) and Pd(111) surfaces was observed in real-time with an in-situ low energy electron microscope (LEEM) capable of selected area low energy electron diffraction (μ -LEED). The samples were further probed with ambient pressure X-ray photoelectron spectroscopy (AP-XPS), temperature programmed desorption (TPD) and high resolution electron energy loss spectroscopy (HREELS). The chemical activity and enhanced selectivity of these model silicate/Pd catalysts will be discussed.

10:20am HC+SS-FrM7 Formation and Properties of Mirror Twin Grain Boundary Networks in Molybdenum Dichalcogenides, Matthias Batzill, University of South Florida INVITED

Edges, defects, and dopants in 2D transition metal dichalcogenides have been shown to give rise to special chemical, electronic, and magnetic properties in these materials. To utilize the potential of these modifications a detailed understanding of their controlled formation and atomic scale properties is needed. In this talk we present our studies on the controlled formation of metallic mirror twin grain boundaries (MTBs) in MoSe₂ [1] or MoTe₂ [2] by incorporation of excess Mo into the lattice. Very high density of MTB networks can be obtained in MoTe₂ that effectively metallizes the material and thus may act as a metallic contact patch [3]. Such line defects may also increase electrocatalytic properties for hydrogen evolution reactions [4]. On a more fundamental level, we show that these 1D metallic grain boundaries host one dimensional electron gas and we present the first angle resolved photoemission (ARPES) studies of such line defects. These studies show evidence for the presence of Tomonaga-Luttinger Liquid behavior of 1D electron systems [5]. Finally, we show that other transition metals may also be incorporated into MoTe₂ and the incorporation of vanadium induces room temperature ferromagnetic ordering and thus is an example of a 2D dilute ferromagnetic semiconductor [6].

[1] Y Ma, S Kolekar, H Coy Diaz, J Aprozanz, I Miccoli, C Tegenkamp, M Batzill. Metallic Twin Grain Boundaries Embedded in MoSe₂ Monolayers Grown by Molecular Beam Epitaxy. *ACS Nano* 11, 5130-5139 (2017)

[2] HC Diaz, Y Ma, R Chaghi, M Batzill. High density of (pseudo) periodic twin-grain boundaries in molecular beam epitaxy-grown van der Waals heterostructure: MoTe₂/MoS₂. *Appl. Phys. Lett.* 108, 191606 (2016)

[3] PM Coelho, HP Komsa, H Coy Diaz, Y Ma, AV Krashennnikov, M Batzill. Post-Synthesis Modifications of Two-Dimensional MoSe₂ or MoTe₂ by Incorporation of Excess Metal Atoms into the Crystal Structure. *ACS Nano* 12, 3975-3984 (2018).

[4] T Kosmala, H Coy Diaz, HP Komsa, Y Ma, AV Krashennnikov, M Batzill, S Agnoli. Metallic Twin Boundaries Boost the Hydrogen Evolution Reaction on the Basal Plane of Molybdenum Selenotellurides. *Adv. Energy Mat.*, 1800031 (2018).

[5] Y Ma, et al. Angle resolved photoemission spectroscopy reveals spin charge separation in metallic MoSe₂ grain boundary. *Nature Commun.* 8, 14231 (2017).

[6] PM Coelho, et al. Room temperature ferromagnetism in MoTe₂ by post-growth incorporation of vanadium impurities. *Adv. Electr. Mat.* in press.

Friday Morning, October 25, 2019

11:00am **HC+SS-FrM9 Selectable Catalytic Reduction of Carbon Dioxide to Formic Acid or Methanol over Defect Hexagonal Boron Nitride***, *K.L. Chagoya, T. Jiang, D.J. Nash, D. Le, Talat S. Rahman, R.G. Blair*, University of Central Florida

Finding effective heterogeneous catalysts, consisting of abundant elements, for the hydrogenation of waste gas carbon dioxide into value added molecules is a challenging task for global energy and sustainability solutions. In a closely coupled computational and experimental effort, we find that vacancies induced in defect-laden hexagonal boron nitride (*dh*-BN) can effectively activate the CO₂ molecule for hydrogenation. Computationally, we demonstrate that activation occurs through back-donation to the π^* orbitals of CO₂ from frontier orbitals (defect state) of the *h*-BN sheet localized near a nitrogen vacancy (V_N). Subsequent hydrogenation to formic acid (HCOOH) and methanol (CH₃OH) occurs through vacancy facilitated co-adsorption of hydrogen and CO₂. More importantly, we find that *dh*-BN is a temperature-driven switchable catalyst with formic acid formation observable at reaction temperatures above 160 °C and pressures of 583 kPa, while methanol formation was observed at lower temperatures (as low as 20 °C), which are in great agreement with thermodynamics and kinetics of our calculated reaction pathways.

*Work supported in part by DOE grant DE-FG02-07ER15842

Advanced Surface Engineering Division

Room A215 - Session SE+AS+SS-FrM

Tribology: From Nano to Macro-scale

Moderator: Robert Franz, Montanuniversität Leoben, Austria

8:20am **SE+AS+SS-FrM1 The Scaling of Tribological Effects from Nano- to Macro-scale**, *Peter Lee*, Southwest Research Institute **INVITED**

The last few decades has seen the advancement of technologies such as atomic force microscopes (AFM), scanning force microscopes (SFM) and friction force microscopes (FFM) to measure friction, wear and adhesions at the nano- and micro-scale, leading to the study of nano- and micro-tribology. The study of two surfaces at the nano- and micro-meter scale has led to the advancement of small scale engineering devices such as nano- and micro-electromechanical systems (NEMS and MEMES). However, it has also led to the study of materials used in macro-engineering in an attempt to understand the fundamentals of lubrication, friction and wear at the asperity scale in macro-systems.

Macro-tribology involves large apparent areas of contact where only a fraction of the asperity tips are in contact, whereas nano-tribology usually involves studying a single asperity contact where the actual contact is the same as the apparent contact. Consequently, roughness and actual contact shape plays a more significant role in the tribological behavior, which in turn means significant effects on forces such as friction, adhesion and surface tension. Tribology at the macro-scale is governed by complex phenomena such as ploughing, abrasive, and adhesive wear. Friction at the nano-scale is often studied purely in the wearless (interfacial) regime, where adhesion is substantial but wear is minimal.

This presentation will explore current research at the nano-scale and discuss how this has the potential to help in understanding and modeling at the macro-scale.

9:00am **SE+AS+SS-FrM3 Nanotribology of Graphene in Organic Solvents**, *Prathima Nalam, B. Sattari Baboukani*, University at Buffalo, State University of New York; *Z. Ye*, Miami University

Two-dimensional (2D) materials such as graphene, *etc.* are emerging as friction-reducing additives for transmission fluids and lubricating oils to enhance the service life of sliding metallic components. Here in this work, we investigate the dissipative mechanism for a supported (on silica substrate), monolayer of graphene when immersed in organic solvents such as *n*-hexadecane and cyclohexane. Nanoscale friction measurements on graphene conducted using atomic force microscope showed a non-monotonic variation *i.e.* a decrease and then an increase in friction forces as a function of immersion time in organic solvents. This behavior was attributed to the re-arrangement of organic molecules at the 2D confinement formed between the graphene and the underlying substrate. The oscillatory forces measured at the interface showed an increased packing order of the solvent molecules under 2D confinement and with equilibration time lead to a higher dissipative interface. The diffusion of organic molecules to the 2D confinement also results in a partially-suspended graphene layer and the interfacial friction is discussed by

understanding the quality (local pinning states of individual atoms) of the contact made by the AFM probe while sliding on graphene.

9:20am **SE+AS+SS-FrM4 Measuring Atomic-scale Surface Friction of a Molecular Vehicle on Au(111)**, *K.Z. Latt, Sanjoy Sarkar, K. Kottur, M. Raeis*, Ohio University; *A. Ngo*, Argonne National Laboratory; *R. Tumbleson, Y. Zhang, E. Masson, S.-W. Hla*, Ohio University

Designing molecules with technomimetic properties has been actively pursued in the past decade. Among these, molecules specially designed for translational motion, dubbed as nanocars or molecular vehicles, are particularly appealing as they could ultimately be used to transport a molecular cargo or some specific chemical information from a start to an end point on a surface and on demand. Here, we have designed and assembled an electric nanovehicle using four molecular wheels and a molecular chassis as separate modules. An 'H' shape chassis is formed by two benzimidazolium groups linking the front and the rear axles to a terphenyl drive shaft. Final assembly of the nanovehicle is realized by attaching four pumpkin shaped cucurbituril molecular wheels. The chassis of the nanovehicle includes positive charges, which are used for the controlled lateral movement of the vehicle by scanning tunneling microscope tip induced electric field manipulation. The threshold voltage required to drive the nanovehicle is determined from the Vaussian-fit of the data. Moreover, we have determined lateral force to move the nanovehicle on a Au(111) surface at 5K and it is found to be in superlubricity regime.

9:40am **SE+AS+SS-FrM5 The Use of the Nanocomposite Concept in Hard Coatings for Improving the Frictional Performance**, *Albano Cavaleiro*, University of Coimbra, Portugal **INVITED**

Nanocomposite thin films based on a structural arrangement consisting of grains of a transition metal nitride enrobed in a thin layer of silicon nitride, have been developed in last decades with the final aim of maximizing the mechanical strength. This specific arrangement was proved to be efficient regarding the oxidation resistance and the structural stability at high temperatures as well as the wear resistance, reason why these coatings are commercially available in the market. However, their performance in applications requiring low friction, against specific materials, is very inefficient. On the other hand, in last years the addition of elements, able to provide low friction, such as Ag or V, to traditional hard coatings (TiN, TiAlN, TiCrN,...) has been deeply studied. Results were very successful from the lubrication point of view but the wear resistance was clearly reduced, due to either a decrease of the global mechanical strength of the coatings or the rapid depletion of the lubricant element from the coating by out diffusion to the contact zone.

In this talk an overview of the influence of the addition of lubricant elements to Ti-Si-N system will be presented. The coatings were deposited by conventional magnetron sputtering as well as by using HiPIMS power supplies. The importance of the type of the structure of the deposited coatings (nanocomposite or supersaturated solid solution) on their thermal stability, including oxidation resistance, will be discussed based on the diffusion of the lubricant elements. A comparison of the mechanical properties of the coatings deposited by both methods will be performed and the results will be interpreted based on the (micro)structure and residual stresses. Results on the tribological behaviour achieved by tests at room and high temperatures (up to 900 °C) against different balls (steel, alumina and Ti-alloy) will be presented and commented. Generally, results show that a decrease of the mechanical performance of the coatings is obtained with that elements addition. However, in relation to tribological performance, significant improvements could be reached although under specific testing conditions (type of ball, temperature, ...). In many cases, no improvements were observed.

10:20am **SE+AS+SS-FrM7 Development of Ultra-thick CrAlAgN Coatings by HiPIMS for Self-lubrication at Elevated Temperatures**, *Jianliang Lin*, Southwest Research Institute; *X. Zhang*, Southeast University, China

The pursuit of advanced coating systems to provide sufficient oxidation resistance and self-lubrication for high temperature tribological application continues. One of the approaches is to dope traditional hard transition metal nitride coatings with solid lubricants, e.g. Ag, Au, which diffuses towards coating surface to provide lubrication at elevated temperatures. However, the long term performance of these self-lubricating coatings at high temperatures in ambient air is limited by the rapid out diffusion of Ag, which is strongly affected by many factors, e.g. the volume fraction of the dopant and the density of the coating. It is expected that dense coating structure combined with increased coating thickness is helpful for achieving long term lubrication performance. In this paper, ultra-thick

Friday Morning, October 25, 2019

CrAlAgN coatings (50 μm) are deposited on steel and cement carbide substrates using high power impulse magnetron sputtering (HiPIMS) by carefully control the processing parameters. The structure and composition of the coatings were first tailored to achieve a combination of good adhesion, high density and good mechanical strength with HiPIMS deposition. The Ag concentration in the coatings is varied in the range of 3-10 at.%. For the coating performance, the oxidation resistance of the coating were studied in ambient air using isothermal test. The high temperature wear resistance of the coating was measured using a high temperature pin-on-disc tribometer in the ambient air from 500 $^{\circ}\text{C}$ to 900 $^{\circ}\text{C}$. It was found that Ag doping degrades the mechanical strength and oxidation resistance of the CrAlN coatings, but the ultra-thick CrAlAgN coating show robust self-lubricating performance at high temperatures.

Surface Science Division

Room A220-221 - Session SS+HC+PS-FrM

Planetary, Ambient, and Operando Environments

Moderators: Catherine Dukes, University of Virginia, Petra Reinke, University of Virginia

8:20am **SS+HC+PS-FrM1 Seeing is Believing: Atomic-scale Imaging of Catalysts under Reaction Conditions, Irene Groot**, Leiden University, The Netherlands, Netherlands **INVITED**

The atomic-scale structure of a catalyst under reaction conditions determines its activity, selectivity, and stability. Recently it has become clear that essential differences can exist between the behavior of catalysts under industrial conditions (high pressure and temperature) and the (ultra)high vacuum conditions of traditional laboratory experiments. Differences in structure, composition, reaction mechanism, activity, and selectivity have been observed. These observations indicated the presence of the so-called pressure gap, and made it clear that meaningful results can only be obtained at high pressures and temperatures. However, most of the techniques traditionally used to study catalysts and their reactions were designed to operate under (ultra)high vacuum conditions. To bridge the pressure gap, the last years have seen a tremendous effort in designing new instruments and adapting existing ones to be able to investigate catalysts in situ under industrially relevant conditions.

In this talk, I will give an overview of the in situ imaging techniques we use to study the structure of model catalysts under industrial conditions of atmospheric pressures and elevated temperatures. We have developed set-ups that combine an ultrahigh vacuum environment for model catalyst preparation and characterization with a high-pressure flow reactor cell, integrated with either a scanning tunneling microscope or an atomic force microscope. With these set-ups we are able to perform atomic-scale investigations of well-defined model catalysts under industrial conditions. Additionally, we combine the structural information from scanning probe microscopy with time-resolved mass spectrometry measurements on the gas mixture that leaves the reactor. In this way, we can correlate structural changes of the catalyst due to the gas composition with its catalytic performance. Furthermore, we use other in situ imaging techniques such as transmission electron microscopy, surface X-ray diffraction, and optical microscopy, all combined with mass spectrometry.

This talk highlights a short overview of the instruments we developed and illustrates their performance with results obtained for different model catalysts and reactions. Results for reactions such as NO oxidation and hydrodesulfurization will be discussed.

9:00am **SS+HC+PS-FrM3 Operando NAP-XPS and NAP-STM Investigation of CO Oxidation on CoO Nanoislands on Noble Metal Surfaces, Jonathan Rodriguez-Fernández, Z. Sun, E. Rattigan**, Aarhus University, Denmark; *C. Martín, E. Carrasco*, IMDEA Nanoscience, Spain; *E. Pellegrin, C. Escudero*, ALBA Synchrotron Light Source, Spain; *D. Ecija*, IMDEA Nanoscience, Spain; *J.V. Lauritsen*, Aarhus University, Denmark

Nanostructured cobalt oxides (CoOx) have proven to be interesting low temperature oxidation catalysts, for example for preferential oxidation (PROX) of carbon monoxide (CO). CoOx has been identified as one of the most active materials for CO oxidation showing activity down to temperatures as low as -80°C . However, the pure oxide catalyst seems to be strongly poisoned by water. Some studies indicate that combining CoOx with gold synergistically improves the catalytic performance and poisoning resistance²⁻³, but an understanding of this metal-oxide effect is lacking. To obtain an atomic scale understanding of the improved catalytic performance of combined Au-CoOx catalysts we have designed a model

system where cobalt oxide nanoparticles are synthesized on an Au single crystal surface by physical vapor deposition in an oxygen environment⁴⁻⁵.

Here, we significantly advance the mechanistic understanding of cobalt oxide nanocatalysts for CO oxidation by studying the surface chemistry of the model catalyst under *operando* conditions. We use powerful near ambient pressure techniques such as scanning tunneling microscopy (NAP-STM) and synchrotron X-ray photoelectron spectroscopy (NAP-XPS) to study CoO_x nanoislands on Au(111) at mbar pressure in a CO/O₂ gas mixture. From STM results, we find that the structure of the $\sim 20\text{nm}$ wide monolayer cobalt oxide nanoislands is static during exposure to a mixture of CO and O₂ gases at a pressure of 1.5 mbar. Under these conditions at room temperature, the nanoislands seem to exhibit activity towards CO oxidation, and we can detect CO, CO₂ surface species by NAP-STM experiments and by analysis of the corresponding O1s and C1s core level NAP-XPS spectra. In addition, we study the morphological evolution by NAP-STM and the reactivity of the CoO nanoislands from RT to 300 $^{\circ}\text{C}$ under *operando* conditions. At around 200 $^{\circ}\text{C}$, CO₂ is found in gas phase and decreasing at the surface. Furthermore, to observe the influence of the substrate, we repeated the CoO nanoislands on Pt(111), obtaining similar reactivity results.

References:

1. Xie, X., et al., Nature 458 (2009): 746-749.
2. Cunningham, D. A. H., et al., Catal. Lett. 25 (1994): 257-264.
3. Liu, Y., et al., J. Catal. 309 (2014): 408-418.
4. Fester, J., et al., Nature Communications 8 (2017): 14169.
5. Walton, Alex S., et al., ACS Nano 9.3 (2015): 2445-2453.

9:20am **SS+HC+PS-FrM4 Reaction of 2-Propanol on SnO₂(110) Studied with Ambient-Pressure X-ray Photoelectron Spectroscopy, J.T. Diulus, R. Addou, Gregory Herman**, Oregon State University

Tin dioxide (SnO₂) has a wide range of applications, including gas sensors, transparent conductors, and oxidation catalysts. The surface chemistries for each of these applications can be strongly influenced by the surface structure and cation oxidation states. The oxidation of volatile organic compounds (VOC) has recently been demonstrated using SnO₂, where 2-propanol was used as the probe molecule. More recently it was observed that the surface Sn²⁺/Sn⁴⁺ ratio strongly influenced the activity of carbon monoxide oxidation. In this study, we have used ambient pressure X-ray photoelectron spectroscopy (AP-XPS) to characterize the surface chemistry of 2-propanol on well-defined SnO₂(110) surfaces. We have prepared stoichiometric and reduced surfaces which were characterized with both AP-XPS and low energy electron diffraction. AP-XPS was performed on these surfaces for 2-propanol pressures up to 1 mbar, various 2-propanol/O₂ ratios, and a range of temperatures. These studies allowed us to evaluate the chemical states of 2-propanol on the SnO₂(110) surface under a wide range of experimental conditions. The effect of surface preparation, 2-propanol/O₂ ratios, and sample temperature was evaluated using AP-XPS and mass spectrometry. Using valence-band spectra, we have found that the surface was reduced from Sn⁴⁺ to Sn²⁺ when the sample was heated in 2-propanol and that the main reaction product in the gas phase was acetone. This suggests that the reaction occurs through a mechanism where bridging oxygens are hydroxylated upon adsorption of 2-propanol. These bridging hydroxyl groups can react and result in water desorption. This process leads to the reduction of the SnO₂(110) surface. We have found that the low temperature AP-XPS spectra (300-400 K) was nearly identical for 2-propanol and 2-propanol/O₂ mixtures. After running the reactions at higher temperatures we found that the surface remained oxidized. Several oxidation products were also observed in the gas phase. Based on the experimental results we find that the surface was inactive for the oxidation of 2-propanol for temperatures below 500 K. With 2-propanol/O₂ mixtures the reactivity increased substantially at lower temperatures. Furthermore, we propose that in 2-propanol/O₂ mixtures the reaction occurs through a Mars-van Krevelen mechanism.

9:40am **SS+HC+PS-FrM5 Chemical Speciation and Structural Evolution of Rhodium and Silver Surfaces with High Oxygen Coverages, Daniel Killelea, M.E. Turano**, Loyola University Chicago; *R.G. Farber, K.D. Gibson, S.J. Sibener*, The University of Chicago; *W. Walkosz*, Lake Forest College; *R.A. Rosenberg*, Argonne National Laboratory

Understanding the interaction of oxygen with transition metal surfaces is important in many areas including corrosion and catalysis. Of interest to us is the formation and chemistry of subsurface oxygen (O_{sub}); oxygen atoms dissolved in the near-surface region of catalytically active metals. The goal of these studies is to understand how incorporation of O_{sub} into the

Friday Morning, October 25, 2019

solvedge alters the surface structure and chemistry. The oxygen – Ag system, in particular, has been studied extensively both experimentally and theoretically because of its role in two important heterogeneously catalyzed industrial reactions: the epoxidation of ethylene to produce ethylene oxide and the partial oxidation of methanol to produce formaldehyde. In addition, the O/Rh and O/Ag systems serve as models for the dissociative chemisorption of diatomic molecules on close packed metal surfaces. Despite extensive research, there remain questions about the fundamental chemistry of the O/Ag system. Rh is also used in partial oxidation reactions, and its response to adsorbed oxygen provides an interesting complement to Ag. Where Ag extensively reconstructs, Rh does not. In particular, the structure of the catalytically active surface remains poorly understood under conditions of high oxygen coverages or subsurface oxygen. To improve our understanding of this system, we use ultra-high vacuum (UHV) surface science techniques to characterize Ag and Rh surfaces after exposure to atomic oxygen (AO) to obtain O coverages in excess of 1 ML. AO is generated by thermally cracking molecular O₂. We then use low-energy electron diffraction (LEED) and UHV Scanning Tunneling Microscopy (UHV-STM) to further characterize the various oxygenaceous structures produced, and quantify the amount of oxygen with temperature programmed desorption (TPD). We have found that the surface temperature during deposition is an important factor for the formation of O_{sub} and the consequent surface structures. Finally, we have recently found that Rh surfaces are significantly more reactive towards CO oxidation when O_{sub} is present. This enhanced reactivity is located at the interface between the less reactive RhO₂oxide and O-covered metallic Rh. These results reveal the conditions under which O_{sub} is formed and stable, and show that O_{sub} also leads to enhanced reactivity of oxidized metal surfaces.

10:00am **SS+HC+PS-FrM6 Molecular Processes on Icy Surfaces in the Interstellar Medium and the Outer Solar System**, *Edith Fayolle, R. Hodyss, P. Johnson*, Jet Propulsion Laboratory, California Institute of Technology; *K. Oberg*, Harvard University; *J-H. Fillion, M. Bertin*, Sorbonne Université

INVITED

Molecular ices have been observed in various planetary and astrophysical environments: from patches in permanently shadowed regions on Mercury and the Moon, to the ice crust of outer Solar System bodies, and onto dust grains in prestellar cores, protostellar envelopes, and protoplanetary disks. Interstellar and planetary ices are mostly composed of H₂O, and more volatile molecules, e.g. N₂, CO, CH₄, CO₂, H₂S, SO₂, NH₃, held together as a solid through van Der Waals forces and dipole-dipole interactions, such as hydrogen bonding. They are found as mixtures or pure layers and display crystalline or amorphous structures.

Understanding ice formation, sublimation, and composition is crucial to interpret both gas phase and solid state observations, constrain the physical conditions encountered in space, and test for the likely chemical inheritance from star-forming environments to planetary systems. Vacuum and cryogenic techniques are used to reproduce astrophysical conditions and grow ice analogues. Analytical techniques, including IR-UV-spectroscopy, mass spectrometry, and microgravimetry, are employed to measure fundamental parameters such as desorption, diffusion energies, and reactions products & rates in the solid phase.

In this talk, I will show several examples of astrochemical experiments relevant to icy environments. The fundamental parameters derived from these experiments are further used as inputs for astrochemical models simulating the formation and evolution of ices on various bodies. In some cases, these experiments can directly explain recent observations, for e.g., the unexpected variety of molecules detected in lunar cold traps by the Lunar Crater Observation and Sensing Satellite mission or the location of snowlines in protostellar and protoplanetary environments probed by radio-interferometers like the Atacama Large Millimeter Array.

10:40am **SS+HC+PS-FrM8 Bilayer Silicates as Models for Space-weather-mediated Water-cycling Processes at the Interface of Airless Bodies**, *B. Dhar, William E. Kaden*, University of Central Florida

Following recent observations indicating the presence of water and/or hydroxyl groups inhomogeneously distributed across the surface of the moon, many groups have worked to put forward feasible models necessary to rationalize both effects. From those models, there seems to be reasonable agreement that a solar-wind mediated, H⁺ implantation-based mechanism is responsible for initial hydration/hydroxylation at the lunar surface. How and why the OH-group concentration varies with both latitude and longitude, however, remains debated in the literature. A recently reported kinetics model provided a plausible temperature-

dependent recombinative desorption/dissociative readsorption pathway, which accurately predicts observed systematic trends in the concentration of OH groups as a function of latitude when also accounting for daily oscillations in photon and proton flux vs. latitude over long periods of time. Key to the postulated OH-group migration pathway is the presence of mineral surfaces with atypically low barriers to recombinative water desorption; something that varies with both surface composition/structure and OH group concentration. To account for the effects of the average lunar mineralogical surface composition, the author's simply modeled the moon as a homogenous distribution of simple binary oxides present at concentrations corresponding those associated with each of the corresponding metals.

In the work presented in this this talk, we have used recently developed recipes allowing for the growth of extremely well-defined, atomically-planar, and crystalline silicate sheets to serve as tailor-designed analogues of mineralogically relevant structures containing deliberately varied surface sites expected to be present at the surface of the moon and elsewhere. More specifically, we have grown and fully characterized two bilayer films; one consisting of pure silica (SiO₂) and the other present as a two-dimensional alumino-silicate (Al_{0.33}Si_{0.67}O₂). Using temperature programmed desorption, we have then characterized differences in the OH-silicate interactions as a function of one deliberately varied surface-site's coordination, and then link our observations to help provide a more nuanced insight into how and why water may evolve and cycle into and out of the surface of airless bodies in the presence of the solar wind.

11:00am **SS+HC+PS-FrM9 Unraveling the Evolution of the Solid-Electrolyte Interphase Layer at Li-Metal Anodes**, *Venkateshkumar Prabhakaran, S. Roy, G.E. Johnson*, Pacific Northwest National Laboratory, Joint Center for Energy Storage Research; *M.H. Engelhard, V. Shutthanandan, A. Martinez, S. Thevuthasan*, Pacific Northwest National Laboratory; *K.T. Mueller, V. Murugesan*, Pacific Northwest National Laboratory, Joint Center for Energy Storage Research

Chemical transformations of electrolyte constituents (such as solvent and solvated electroactive ions) at the Li-metal electrode determine the evolution of the solid-electrolyte interphase (SEI). The ability to rationally design an SEI layer that will provide efficient charge transfer processes will improve the performance of Li-batteries. The main challenge is to unravel the complex set of interfacial reactions that occur during charge transfer processes and subsequently delineate the pathways of various decomposition reactions and phase formation. Herein, we report progress in understanding such complex interfaces using bottom-up assembly of solvated cations and bare anions of selected composition on Li-metal anodes. Soft landing of mass-selected ions, a versatile approach to surface modification, is ideally suited for building the interface with selected electroactive ions which will help unravel the complexity associated with the multitude of interfacial processes occurring during evolution of the SEI layer.^{1,2} Ion soft landing combined with operando infrared reflection-absorption spectroscopy (IRRAS) and in-situ x-ray photoelectron spectroscopy (XPS) were used to characterize the decomposition of counter anions and solvent molecules on bare Li metal surfaces. Specifically, we soft-landed isolated electrolyte anions (e.g., bis(trifluoromethane)sulfonimide, TFSI⁻, polysulfides, S_x⁻) and solvated Li solvent cluster cations (e.g. Li-(dimethoxyethane)_n⁺) on bare Li metal surfaces without their corresponding counter ions, and monitored their spontaneous decomposition using IRRAS and XPS. Our in-situ multimodal measurements captured the spectroscopic signatures of reaction pathways of the electrolyte anions and solvent molecules on the reactive Li surface. We will discuss the evolution of the SEI layer based on multimodal spectroscopic analysis of electrochemical interfaces prepared using the ion soft landing approach. In particular, the chemical signatures of transient species that evolve during decomposition at well-defined interfaces will be discussed.

References:

1. Johnson, G. E.; Hu, Q.; Laskin, J., Soft landing of complex molecules on surfaces. *Annual Review of Analytical Chemistry* **2011**, *4*, 83-104.
2. Prabhakaran, V.; Johnson, G. E.; Wang, B.; Laskin, J., *In situ* solid-state electrochemistry of mass-selected ions at well-defined electrode-electrolyte interfaces. *Proceedings of the National Academy of Sciences* **2016**, *113*, 13324-13329.

Bold page numbers indicate presenter

— A —

Abdel-Rahman, M.: HC+2D+SS-WeM6, **20**
 Abe, Y.: DM+BI+SS-ThM1, 30
 Abelson, J.R.: TF+2D+AP+EL+SS-MoA5, 8
 Abudayyeh, O.K.: TF+EM+NS+SS-ThM4, 37
 Adamsen, K.C.: OX+EM+HC+MI+NS+SS+TF-TuA10, 15; SS+2D+HC-TuM10, **11**
 Addou, R.: SS+HC+PS-FrM4, 59
 Adel, T.: SS-TuP9, **18**
 Afshar, A.: DM1+BI+SS-ThA3, **43**
 Akay, S.: TL+AS+SS+TF-TuA7, 16
 Aleithan, S.H.: 2D+EM+MI+NS+QS+SS-ThM5, 29
 Alexandrowicz, G.: SS+2D+AP+AS+OX+SE-ThA3, **51**
 Al-Jassim, M.: LS+AS+SS-ThM3, 33
 Allen, H.C.: SS-TuP9, 18
 Amabilino, D.: SS-TuP7, 17
 Amati, M.: CA+NS+SS+VT-ThA9, 42
 Andersen, T.K.: OX+EM+MI+SS-WeM2, 21
 Ando, T.: OX+EM+HC+MI+NS+SS+TF-TuA3, 14
 Angel, D.: AP+EL+MS+PS+SS+TF-TuA12, 14
 Antonelli, G.A.: AP+EL+MS+PS+SS+TF-TuA7, **13**
 Anwar, F.: OX+EM+MI+SS-WeM12, 22
 Arnadottir, L.: HC+SS-MoM2, 1
 Árnadóttir, L.: DM1+BI+SS-ThA4, **43**
 Arora, P.: PS+AS+EM+SS+TF-MoA6, **3**
 Arslan, I.: RA+AS+NS+SS-MoA5, 5
 Arts, K.: PS+AS+EM+SS+TF-MoA10, **4**
 Asakura, K.: HC+OX+SS-WeA2, 25
 Aso, R.: TL+AS+SS+TF-TuA3, 15
 Asthagiri, A.: HC+2D+SS-WeM2, **20**; HC+SS-MoM6, 1; SS+HC-MoA3, 6
 Auras, S.V.: SS-TuP14, 18
 Avincola, V.A.: DM2+BI+SS-ThA9, 44
 Aydil, E.S.: TF+EM+NS+SS-ThM6, 37; TF+SS-ThA8, 53
 — B —
 Baber, A.E.: HC+2D+SS-ThM2, **32**; SS-TuP18, 19
 Baer, D.R.: SS-TuP17, 19
 Bahceci, S.: TL+AS+SS+TF-TuA7, 16
 Bahoura, M.J.: TF+EM+NS+SS-ThM10, 38
 Baker, J.: SS-TuP18, 19
 Balajka, J.: DM2+BI+SS-ThA8, 44
 Baljak, I.: SS+AS+HC+TL-ThM11, 36
 Bang, L.: HC+OX+SS-WeA2, 25
 Barnes, E.: TF+EM+NS+SS-ThM11, 38
 Batzill, M.: HC+SS-FrM7, **57**
 Baumler, S.: SS-TuP9, 18
 belahcen, S.: AP+EL+MS+PS+SS+TF-TuA9, 13
 Bendikov, T.: LS+AC+HC+SS-ThA7, **47**
 Bergersen, H.: CA+NS+SS+VT-WeA10, **24**
 Berkes, B.: DM2+BI+SS-ThA10, **44**
 Bertin, M.: SS+HC+PS-FrM6, 60
 Beton, P.H.: 2D+AS+BI+HC+MN+NS+PS+SS+TL-ThA3, 40; SS-TuP7, 17
 Bhattacharya, A.: OX+EM+MI+SS-WeM2, 21
 Bilotto, P.: DM+BI+SS-ThM13, 32
 Binek, C.: OX+EM+HC+MI+NS+SS+TF-TuA1, 14
 Biolsi, P.E.: PS+2D+EM+SS+TF-ThA1, **47**; PS+2D+EM+SS+TF-ThA4, 48
 Blades, W.H.: SS+AS+HC+OX-WeA10, **27**
 Blair, R.G.: HC+SS-FrM9, 58
 Bluhm, H.: CA+NS+SS+VT-WeA3, **24**; LS+HC+SS-ThM10, 34; SS+AS+HC+TL-ThM4, 35
 Bohamud, T.: TF+SS-ThA3, 52
 Bonvalot, M.: AP+EL+MS+PS+SS+TF-TuA9, 13
 Bormashenko, E.: SS-TuP10, 18

Bose, R.: TF+SS-ThA10, **53**
 Bournel, F.: TF+2D+AP+EL+SS-MoA8, 8
 Bowden, M.E.: OX+EM+MI+SS-WeM1, 21; OX+EM+MI+SS-WeM13, 22
 Boyd, K.P.: SS+AS+HC+TL-ThM11, 36
 Boyle, D.T.: SS-TuP18, 19
 Brandt, A.J.: HC+OX+SS-WeA9, 26
 Brann, M.R.: SS+2D+AP+AS+OX+SE-ThA1, 51
 Brena, B.: TF+2D+AP+EL+SS-MoA8, 8
 Brillson, L.J.: 2D+EM+MI+NS+QS+SS-ThM10, 29
 Broderick, A.: CA+NS+SS+VT-WeA8, 24
 Brown, P.: 2D+AS+BI+HC+MN+NS+PS+SS+TL-ThA2, **40**
 Brown, R.D.: SS+HC-MoA10, 7; SS-TuP11, **18**
 Brunelli, N.A.: HC+OX+SS-WeA8, **25**
 Bruner, P.: AP+EL+MS+PS+SS+TF-TuA9, 13
 Bsiesy, A.: AP+EL+MS+PS+SS+TF-TuA9, 13
 Buck, E.C.: CA+AS+NS+SE+SS-FrM8, 56
 Budak, S.: TF+EM+NS+SS-ThM11, **38**; TF+EM+NS+SS-ThM12, 38
 Buzov, N.: 2D+AS+BI+HC+MN+NS+PS+SS+TL-ThA4, 40
 — C —
 Cahen, D.: LS+AC+HC+SS-ThA7, 47
 Campbell, C.T.: HC+SS-MoM5, 1; SS+2D+HC-TuM5, **11**
 Cargnello, M.: HC+OX+SS-WeA3, **25**
 Carrasco, E.: SS+HC+PS-FrM3, 59
 Cavaleiro, A.: SE+AS+SS-FrM5, **58**
 Caver, N.: TF+EM+NS+SS-ThM12, 38
 Chagoya, K.L.: HC+SS-FrM9, 58
 Chambers, S.A.: OX+EM+MI+SS-WeM1, 21; OX+EM+MI+SS-WeM13, 22; OX+EM+MI+SS-WeM5, **22**
 Chang, J.P.: PS+AS+EM+SS+TF-MoA3, **3**
 Chattot, R.: LS+AS+SS-ThM1, 33
 Chaudhary, S.: TF+2D+AP+EL+SS-MoA8, 8
 Chavez, A.: TF+EM+NS+SS-ThM4, 37
 Chavez, J.: TF+EM+NS+SS-ThM4, 37
 Chen, D.A.: HC+OX+SS-WeA9, **26**
 Chen, J.: 2D+EM+MI+NS+QS+SS-ThM4, 29
 Chen, P.: DM1+BI+SS-ThA3, 43
 Chen, S.: 2D+AS+BI+HC+MN+NS+PS+SS+TL-ThA4, 40
 Chen, Z.: PS+SS-ThA8, 50
 Cheng, H.-W.: DM+BI+SS-ThM13, 32
 Cherevko, S.: DM2+BI+SS-ThA6, **43**
 Cherukara, M.: RA+AS+NS+SS-MoA5, 5
 Chien, T.: 2D+EM+MI+NS+QS+SS-ThM3, 29
 Chiriki, S.: SS+2D+HC-TuM10, 11
 Christopher, P.: SS+AS+HC+OX-WeA7, **26**
 Chukwu, C.: HC+SS-MoM2, 1
 Chulkov, S.C.: 2D+AS+BI+HC+MN+NS+PS+SS+TL-ThA3, 40
 Ciešlik, K.: SS+AS+HC+OX-WeA12, 27
 Clark, C.P.: TF+SS-ThA8, **53**
 Cleveland, E.: TF+EM+NS+SS-ThM5, **37**
 Cook, S.: OX+EM+MI+SS-WeM2, 21
 Crosby, L.D.: HC+2D+SS-WeM13, 21
 Cunniff, A.: OX+EM+HC+MI+NS+SS+TF-TuA12, 15
 — D —
 D'Acunto, G.: TF+2D+AP+EL+SS-MoA8, 8
 Darling, S.B.: TL+AS+SS+TF-TuA1, **15**
 David, S.: AP+EL+MS+PS+SS+TF-TuA9, 13
 Deenen, C.S.: HC+SS-FrM2, **57**
 Demkov, A.A.: OX+EM+MI+SS-WeM3, **21**
 Deng, X.: SS+2D+AP+AS+OX+SE-ThA10, **52**
 DePonte, M.: HC+2D+SS-ThM2, 32; SS-TuP18, 19
 Deshpande, N.: HC+OX+SS-WeA8, 25
 Dhar, B.: SS+HC+PS-FrM8, 60

Diebold, U.: DM2+BI+SS-ThA8, 44; SS+AS+HC+OX-WeA9, 27; TL+2D+HC+SS-MoA5, **9**
 Dietrich, P.: CA+NS+SS+VT-ThA3, **42**
 Diulus, J.T.: SS+HC+PS-FrM4, 59
 Dohnálek, Z.: SS+AS+HC+TL-ThM12, 36
 Donnelly, V.M.: PS+AS+EM+SS+TF-MoA5, 3; PS+AS+EM+SS+TF-MoA6, 3
 DorMohammadi, H.: DM1+BI+SS-ThA4, 43
 Dorward, A.: SS-TuP10, 18
 Doudin, N.: SS+AS+HC+TL-ThM12, **36**
 Dowben, P.A.: 2D+AS+BI+HC+MN+NS+PS+SS+TL-ThA10, 41; OX+EM+HC+MI+NS+SS+TF-TuA1, **14**; OX+EM+MI+SS-WeM12, 22
 Drnec, J.: LS+AS+SS-ThM1, **33**
 Du, L.: PS+AS+EM+SS+TF-MoA5, 3
 Du, Y.: OX+EM+HC+MI+NS+SS+TF-TuA7, **14**; OX+EM+MI+SS-WeM1, 21
 Duchaczek, H.: DM+BI+SS-ThM12, 31
 Duchon, T.: CA+AS+NS+SE+SS-FrM3, 55
 Duerr, M.: TF+SS-ThA3, 52
 Dunlap, D.H.: SS+2D+HC-TuM12, 12
 Dworschak, D.: DM+BI+SS-ThM2, **30**
 — E —
 Eads, C.: HC+SS-FrM6, 57; SS-TuP4, 17
 Easton, C.: SS-TuP17, 19
 Ecija, D.: SS+HC+PS-FrM3, 59
 Economou, D.J.: PS+AS+EM+SS+TF-MoA5, 3
 Eddy, C.R.: TF+2D+AP+EL+SS-MoA6, 8
 Edel, R.: SS+2D+AP+AS+OX+SE-ThA2, **51**
 Egle, T.: HC+2D+SS-ThM13, 33
 Ekanayaka, T.K.: 2D+EM+MI+NS+QS+SS-ThM3, **29**
 Ekins-Daukes, N.J.: TF+EM+NS+SS-ThM5, 37
 Elam, J.W.: AP+EL+MS+PS+SS+TF-TuA3, **13**
 El-Khoury, P.Z.: CA+NS+SS+VT-ThA8, 42
 Elliott, J.: RA+AS+NS+SS-MoA1, 4
 Enes da Silva, M.: HC+SS-FrM1, 56
 Engelhard, M.H.: SS+HC+PS-FrM9, 60
 Engelmann, S.U.: OX+EM+HC+MI+NS+SS+TF-TuA3, **14**; PS+2D+EM+SS+TF-ThA6, 48
 Eren, B.: LS+AC+HC+SS-ThA6, 46
 Eriksson, S.: CA+NS+SS+VT-WeA10, 24
 Esat, B.: TL+AS+SS+TF-TuA7, **16**
 Escudero, C.: CA+NS+SS+VT-WeA7, 24; SS+HC+PS-FrM3, 59
 Evans, J.W.: 2D+EM+MI+NS+QS+SS-ThM13, 30; SS+2D+AP+AS+OX+SE-ThA6, 51
 Evans, P.: 2D+AS+BI+HC+MN+NS+PS+SS+TL-ThA10, 41
 Eyöyge, C.: HC+SS-FrM2, 57
 — F —
 Fadley, C.S.: LS+HC+SS-ThM10, 34
 Fanning, K.: SS-TuP19, **19**
 Farber, R.G.: HC+2D+SS-WeM12, 20; SS+2D+HC-TuM6, **11**; SS+HC+PS-FrM5, 59
 Faria, J.: HC+SS-FrM1, 56
 Farzandh, S.: HC+OX+SS-WeA9, 26
 Fattah, I.: TF+EM+NS+SS-ThM13, 38
 Fayolle, E.: SS+HC+PS-FrM6, **60**
 Ferrer, S.: CA+NS+SS+VT-WeA7, 24
 Feyer, V.: CA+AS+NS+SE+SS-FrM3, 55
 Feygelson, B.: TF+2D+AP+EL+SS-MoA3, 7
 Fillion, J.-H.: SS+HC+PS-FrM6, 60
 Fischer, S.: 2D+AS+BI+HC+MN+NS+PS+SS+TL-ThA2, 40
 Fisher, E.R.: PS+SS-ThA10, 50; SS+HC-MoA4, 6
 Fitzgerald, L.: HC+OX+SS-WeA1, 25
 Fockaert, L.-L.: DM+BI+SS-ThM6, 31
 Fong, D.D.: LS+AS+SS-ThM4, 34; OX+EM+MI+SS-WeM2, 21
 Fontseré, A.: CA+NS+SS+VT-WeA7, 24

Author Index

- Frankel, G.S.: DM+BI+SS-ThM10, **31**
 Fraxedas, J.: CA+NS+SS+VT-WeA7, **24**
 Fredriksson, H.O.A.: HC+SS+TL-ThA1, **45**
 Freeland, J.W.: OX+EM+MI+SS-WeM1, **21**
 Friend, C.M.: HC+2D+SS-ThM13, **33**;
 SS+AS+HC+OX-WeA11, **27**; SS+AS+HC+OX-
 WeA3, **26**
 Fu, M.: SS-TuP20, **19**
 Fuchs, T.: LS+AS+SS-ThM1, **33**
 Fujimoto, M.: SS+2D+HC-TuM11, **12**
 Fukasawa, M.: PS+2D+EM+SS+TF-ThA3, **47**
 Fukutani, K.: SS+2D+HC-TuM11, **12**
 Fushimi, R.: HC+SS+TL-ThA7, **46**
 — G —
 Gage, T.E.: RA+AS+NS+SS-MoA5, **5**
 Gagliardi, L.: TF+EM+NS+SS-ThM6, **37**
 Gai, Z.: SS-TuP20, **19**
 Gallant, B.M.: TL+AS+SS+TF-TuA8, **16**
 Garcia Rodriguez, D.: HC+SS+TL-ThA1, **45**
 Garcia, J.: SS-TuP19, **19**
 Gardeniers, H.: HC+SS-FrM1, **56**; HC+SS-
 FrM2, **57**
 Garrett, B.: HC+SS+TL-ThA3, **45**
 Garstein, Y.: TF+SS-ThA10, **53**
 Gassilloud, R.: AP+EL+MS+PS+SS+TF-TuA9,
13
 Ge, Z.: SS-TuP20, **19**
 Gibson, K.D.: SS+HC+PS-FrM5, **59**
 Giesen, M.: CA+AS+NS+SE+SS-FrM3, **55**
 Gillum, M.: HC+2D+SS-ThM2, **32**; SS-TuP18,
19
 Girolami, G.S.: TF+2D+AP+EL+SS-MoA5, **8**
 Gleeson, M.A.: HC+SS+TL-ThA1, **45**
 Gonzalez, N.: CA+NS+SS+VT-WeA7, **24**
 Goto, T.: PS+AS+EM+SS+TF-MoA2, **3**
 Gouma, P.I.:
 2D+AS+BI+HC+MN+NS+PS+SS+TL-ThA9, **41**
 Grabnic, T.: SS+2D+AP+AS+OX+SE-ThA2, **51**
 Grabow, L.C.: HC+SS+TL-ThA10, **46**
 Grassian, V.: CA+NS+SS+VT-WeA1, **24**
 Greenberg, B.: TF+2D+AP+EL+SS-MoA3, **7**
 Gregoratti, L.: CA+NS+SS+VT-ThA9, **42**
 Grehl, T.: AP+EL+MS+PS+SS+TF-TuA9, **13**
 Groenenboom, M.: TF+SS-ThA1, **52**
 Grönbeck, H.: SS+HC-MoA5, **6**
 Groot, I.M.N.: SS+HC+PS-FrM1, **59**
 Gross, L.: SS+2D+HC-TuM3, **11**
 Guan, C.: SS+AS+HC+TL-ThM10, **36**
 Guillemier, C.: CA+NS+SS+VT-ThA1, **41**
 Gunkel, F.: CA+AS+NS+SE+SS-FrM3, **55**
 Gunlycke, D.:
 2D+AS+BI+HC+MN+NS+PS+SS+TL-ThA2, **40**
 Guo, T.: TF+SS-ThA10, **53**
 Gupta, J.A.: SS+HC-MoA3, **6**
 Gupta, T.: CA+NS+SS+VT-ThA9, **42**
 Gurung, G.: 2D+EM+MI+NS+QS+SS-ThM3, **29**
 Gustafson, J.: SS+HC-MoA5, **6**
 — H —
 Hagman, B.: SS+HC-MoA5, **6**
 Hamaguchi, S.: PS+2D+EM+SS+TF-ThA3, **47**;
 PS+2D+EM+SS+TF-ThA8, **48**
 Hamlyn, R.: HC+2D+SS-ThM6, **32**
 Hammer, B.: SS+2D+HC-TuM10, **11**
 Han, S.M.: TF+EM+NS+SS-ThM4, **37**
 Han, Y.: 2D+EM+MI+NS+QS+SS-ThM13, **30**;
 PS+2D+EM+SS+TF-ThA4, **48**
 Hanisch, R.: RA+AS+NS+SS-MoA1, **4**
 Hanna, A.R.: PS+SS-ThA10, **50**
 Harville, L.K.: SS+AS+HC+TL-ThM11, **36**
 Hauffman, T.: DM+BI+SS-ThM6, **31**
 Haun, T.: SS-TuP10, **18**
 He, C.H.: SS-TuP5, **17**
 Head, A.R.: TF+2D+AP+EL+SS-MoA8, **8**
 Heep, J.: TF+SS-ThA3, **52**
 Hellman, A.: SS+HC-MoA5, **6**
 Henkelman, G.: SS+AS+HC+OX-WeA1, **26**
 Hentschel, M.: CA+NS+SS+VT-ThA8, **42**
 Herman, G.S.: SS+HC+PS-FrM4, **59**
 Hernandez, K.: PS+2D+EM+SS+TF-ThA6, **48**
 Herrera-Gomez, A.: RA+AS+NS+SS-MoA10, **5**
 Hersam, M.C.: 2D+EM+MI+NS+QS+SS-ThM1,
29
 Hicks, J.C.: PS+SS-ThA3, **49**
 High, E.A.: HC+SS+TL-ThA2, **45**; SS+HC-
 MoA8, **7**; SS+HC-MoA9, **7**
 Hild, S.: DM+BI+SS-ThM12, **31**
 Hildebrandt, G.: HC+2D+SS-WeM12, **20**
 Hilfiker, J.N.: AP+EL+MS+PS+SS+TF-TuA1, **13**
 Hilton, H.: SS-TuP10, **18**
 Hirata, A.: PS+2D+EM+SS+TF-ThA3, **47**
 Hirsch, E.: PS+AS+EM+SS+TF-MoA5, **3**
 Hisamatsu, T.: PS+2D+EM+SS+TF-ThA9, **48**
 Hiyoto, K.: SS+HC-MoA4, **6**
 Hla, S.-W.: SE+AS+SS-FrM4, **58**
 Hodyss, R.: SS+HC+PS-FrM6, **60**
 Hoefler, U.: TF+SS-ThA3, **52**
 Holmes, R.J.: TF+SS-ThA8, **53**
 Holt, M.V.: RA+AS+NS+SS-MoA5, **5**
 Honda, M.: PS+2D+EM+SS+TF-ThA9, **48**
 Hong, D.: OX+EM+MI+SS-WeM2, **21**
 Hong, H.: LS+AS+SS-ThM4, **34**;
 OX+EM+MI+SS-WeM2, **21**
 Hong, S.: 2D+AS+BI+HC+MN+NS+PS+SS+TL-
 ThA4, **40**
 Hooshmand, Z.:
 2D+AS+BI+HC+MN+NS+PS+SS+TL-ThA10,
41
 Hopstaken, M.J.P.: PS+2D+EM+SS+TF-ThA6,
48
 Horoz, S.: 2D+EM+MI+NS+QS+SS-ThM3, **29**
 Huhtinen, H.: OX+EM+HC+MI+NS+SS+TF-
 TuA11, **15**
 Huijser, A.: TL+2D+HC+SS-MoA10, **10**
 Hulva, J.: DM2+BI+SS-ThA8, **44**;
 SS+AS+HC+OX-WeA9, **27**
 Hunt, A.: LS+AC+HC+SS-ThA6, **46**
 — I —
 Iddir, H.: SS-TuP19, **19**
 Innocent-Dolor, J.: PS+2D+EM+SS+TF-ThA6,
48
 Isbill, S.B.: HC+2D+SS-WeM13, **21**
 Isgor, O.B.: DM1+BI+SS-ThA4, **43**
 Iski, E.V.: SS+AS+HC+TL-ThM11, **36**
 Isobe, M.: PS+2D+EM+SS+TF-ThA8, **48**
 Itagaki, N.: PS+SS-ThA1, **49**
 Ito, T.: PS+2D+EM+SS+TF-ThA8, **48**
 — J —
 Jaffal, M.: AP+EL+MS+PS+SS+TF-TuA9, **13**
 Jakub, Z.: DM2+BI+SS-ThA8, **44**;
 SS+AS+HC+OX-WeA9, **27**
 Jany, B.R.: SS+AS+HC+OX-WeA12, **27**
 Jayan, B.R.: TF+SS-ThA1, **52**
 Jean-Jacques, J.-J.: TF+2D+AP+EL+SS-MoA8,
8
 Jenkins, P.: TF+EM+NS+SS-ThM5, **37**
 Jensen, G.: 2D+EM+MI+NS+QS+SS-ThM5, **29**
 Jeremiason, J.D.: TF+EM+NS+SS-ThM6, **37**
 Jia, M.: CA+NS+SS+VT-WeA9, **24**
 Jiang, N.: SS+2D+HC-TuM1, **11**
 Jiang, T.: 2D+AS+BI+HC+MN+NS+PS+SS+TL-
 ThA7, **40**; HC+SS-FrM9, **58**
 Jiang, Y.: TL+2D+HC+SS-MoA1, **9**
 Johnson, G.E.: SS+HC+PS-FrM9, **60**
 Johnson, P.: SS+HC+PS-FrM6, **60**
 Johnson, S.D.: TF+2D+AP+EL+SS-MoA6, **8**
 Jónsson, H.: SS+HC-MoA1, **6**
 Joselevich, E.: LS+AC+HC+SS-ThA7, **47**
 Joseph, L.: SS+HC-MoA8, **7**; SS-TuP12, **18**
 Ju, Y.: PS+SS-ThA8, **50**
 Julien, S.: 2D+EM+MI+NS+QS+SS-ThM13, **30**
 Juurink, L.B.F.: SS-TuP13, **18**; SS-TuP14, **18**
 — K —
 Kaden, W.E.: SS+HC+PS-FrM8, **60**
 Kalanyan, B.: TF+2D+AP+EL+SS-MoA10, **8**
 Kaleem, H.: SS-TuP18, **19**
 Kamataki, K.: PS+SS-ThA1, **49**
 Kamiuchi, N.: TL+AS+SS+TF-TuA3, **15**
 Kampf, N.: SS-TuP15, **19**
 Kandel, S.A.: SS+HC-MoA10, **7**
 Karahashi, K.: PS+2D+EM+SS+TF-ThA3, **47**;
 PS+2D+EM+SS+TF-ThA8, **48**
 Karslioglu, O.: SS+AS+HC+TL-ThM4, **35**
 Kaslasi, H.: LS+AC+HC+SS-ThA7, **47**
 Kaspar, T.C.: OX+EM+MI+SS-WeM13, **22**
 Katsunuma, T.: PS+2D+EM+SS+TF-ThA9, **48**
 Kauffman, D.: SS+2D+AP+AS+OX+SE-ThA10,
52
 Kaul, A.B.: TF+SS-ThA9, **53**
 Kawakami, R.: 2D+EM+MI+NS+QS+SS-
 ThM10, **29**
 Kawamura, M.: DM+BI+SS-ThM1, **30**
 Kelber, J.A.: HC+SS-FrM6, **57**;
 OX+EM+MI+SS-WeM12, **22**
 Keller, N.: AP+EL+MS+PS+SS+TF-TuA7, **13**
 Kersell, H.: LS+AC+HC+SS-ThA6, **46**
 Kessels, W.M.M.: PS+AS+EM+SS+TF-MoA10,
4
 Khadka, S.: 2D+EM+MI+NS+QS+SS-ThM5, **29**
 Khalifa, Y.: CA+NS+SS+VT-WeA8, **24**
 Khanom, F.: CA+NS+SS+VT-ThA1, **41**
 Kiba, T.: DM+BI+SS-ThM1, **30**
 Kido, D.: HC+OX+SS-WeA2, **25**
 Kidwell, D.A.:
 2D+AS+BI+HC+MN+NS+PS+SS+TL-ThA8, **41**
 Kihara, Y.: PS+2D+EM+SS+TF-ThA9, **48**
 Killelea, D.R.: HC+2D+SS-WeM12, **20**;
 SS+HC+PS-FrM5, **59**; SS-TuP19, **19**
 Kim, H.: PS+2D+EM+SS+TF-ThA4, **48**
 Kim, K.H.: DM+BI+SS-ThM1, **30**
 Kim, M.: HC+2D+SS-WeM2, **20**; HC+SS-
 MoM6, **1**
 Kim, S.: 2D+AS+BI+HC+MN+NS+PS+SS+TL-
 ThA4, **40**
 Kimoto, K.: RA+AS+NS+SS-MoA11, **5**
 King, W.: 2D+AS+BI+HC+MN+NS+PS+SS+TL-
 ThA4, **40**
 Kirsten, P.: TF+SS-ThA3, **52**
 Kishi, Y.: PS+AS+EM+SS+TF-MoA2, **3**
 Kitajima, T.: PS+SS-ThA2, **49**
 Klein, J.: SS-TuP15, **19**
 Knoops, H.C.M.: PS+AS+EM+SS+TF-MoA10, **4**
 Knudsen, J.: TF+2D+AP+EL+SS-MoA8, **8**
 Kocun, M.: SS-TuP7, **17**
 Koel, B.E.: PS+SS-ThA8, **50**
 Koert, U.: TF+SS-ThA3, **52**
 Koga, K.: PS+SS-ThA1, **49**
 Kotacz, J.: 2D+AS+BI+HC+MN+NS+PS+SS+TL-
 ThA2, **40**
 Kolmakov, A.: CA+NS+SS+VT-ThA9, **42**
 Konh, M.: SS-TuP1, **17**
 Koppa, M.A.: SS+2D+HC-TuM12, **12**
 Kordesch, E.: SS-TuP4, **17**
 Korivi, N.S.: TF+EM+NS+SS-ThM13, **38**
 Korolkov, V.V.:
 2D+AS+BI+HC+MN+NS+PS+SS+TL-ThA3, **40**;
 SS-TuP7, **17**
 Kotsonis, G.N.: OX+EM+MI+SS-WeM11, **22**
 Kottur, K.: SE+AS+SS-FrM4, **58**
 Kotulak, N.A.: TF+EM+NS+SS-ThM5, **37**
 Kovach, N.C.: DM2+BI+SS-ThA11, **44**
 Kraushofer, F.: DM2+BI+SS-ThA8, **44**
 Kroes, G.-J.: HC+SS-MoM3, **1**
 Krok, F.: SS+AS+HC+OX-WeA12, **27**
 Kruse, N.: SS+2D+AP+AS+OX+SE-ThA7, **51**
 Kruse, P.: CA+AS+NS+SE+SS-FrM7, **56**

Author Index

- Kudo, E.: DM+BI+SS-ThM1, 30
 Kugimiya, K.: PS+2D+EM+SS+TF-ThA3, 47
 Kumakura, S.: PS+2D+EM+SS+TF-ThA9, 48
 Kunz, M.R.: HC+SS+TL-ThA7, 46
 Kwon, J.: 2D+AS+BI+HC+MN+NS+PS+SS+TL-ThA4, 40
 Kyriakou, V.: PS+SS-ThA7, 50
 — L —
 Lacks, D.J.: PS+SS-ThA6, 50
 Ladewig, C.: OX+EM+MI+SS-WeM12, 22
 Laenger, C.: TF+SS-ThA3, 52
 Lai, K.C.: 2D+EM+MI+NS+QS+SS-ThM13, 30; SS+2D+AP+AS+OX+SE-ThA6, 51
 Lam, V.: HC+2D+SS-ThM2, 32
 Lambeets, S.V.: SS+2D+AP+AS+OX+SE-ThA7, 51
 Landis, E.C.: 2D+AS+BI+HC+MN+NS+PS+SS+TL-ThA1, 40
 Latt, K.Z.: SE+AS+SS-FrM4, 58
 Lauritsen, J.V.: OX+EM+HC+MI+NS+SS+TF-TuA10, 15; SS+2D+HC-TuM10, 11; SS+HC+PS-FrM3, 59
 Le, D.: 2D+AS+BI+HC+MN+NS+PS+SS+TL-ThA7, 40; HC+SS-FrM9, 58
 Lea, A.S.: CA+NS+SS+VT-ThA8, 42
 Lee, C.L.: HC+SS+TL-ThA6, 45
 Lee, G.H.: 2D+AS+BI+HC+MN+NS+PS+SS+TL-ThA4, 40
 Lee, P.M.: SE+AS+SS-FrM1, 58
 Lee, S.: TF+EM+NS+SS-ThM3, 36
 Lee, V.: HC+SS-FrM6, 57
 Lee, W.-K.: 2D+AS+BI+HC+MN+NS+PS+SS+TL-ThA8, 41
 Leighton, C.: TF+EM+NS+SS-ThM6, 37
 Lengauer, M.: DM+BI+SS-ThM13, 32
 Lewis, B.: CA+NS+SS+VT-ThA1, 41
 Li, L.: SS+2D+HC-TuM1, 11
 Libuda, J.: TL+2D+HC+SS-MoA8, 9
 Lii-Rosales, A.: 2D+EM+MI+NS+QS+SS-ThM13, 30
 Lin, J.: SE+AS+SS-FrM7, 58
 Lin, K.-Y.: PS+AS+EM+SS+TF-MoA11, 4
 Lin, W.: SS-TuP15, 19
 Linford, M.R.: SS-TuP17, 19
 Liu, B.H.: SS+AS+HC+TL-ThM4, 35
 Liu, C.: OX+EM+MI+SS-WeM2, 21
 Liu, H.: RA+AS+NS+SS-MoA5, 5
 Liu, J.P.H.: SS+AS+HC+TL-ThM10, 36
 Liu, M.: TF+SS-ThA6, 53
 Liu, Y.: OX+EM+HC+MI+NS+SS+TF-TuA12, 15; RA+AS+NS+SS-MoA5, 5
 Liu, Z.: SS+AS+HC+TL-ThM10, 36
 Livingston, S.: HC+OX+SS-WeA1, 25
 Locke, J.: DM+BI+SS-ThM10, 31
 Losego, M.D.: TF+SS-ThA4, 53
 Lu, P.: DM+BI+SS-ThM10, 31
 Luckeneder, G.: DM+BI+SS-ThM12, 31
 Ludwig, K.F.: TF+2D+AP+EL+SS-MoA6, 8
 Luican-Mayer, A.: 2D+EM+MI+NS+QS+SS-ThM11, 30
 Lundgren, E.: SS+HC-MoA5, 6
 Luo, B.: SS-TuP6, 17
 Lutzer, B.: DM+BI+SS-ThM12, 31
 — M —
 Ma, Y.: HC+OX+SS-WeA7, 25
 Maddumapatabandi, T.D.: HC+OX+SS-WeA9, 26
 Madix, R.J.: HC+2D+SS-ThM10, 32; HC+2D+SS-ThM13, 33; SS+AS+HC+OX-WeA3, 26
 Maginn, E.: CA+NS+SS+VT-WeA8, 24
 Magnussen, O.M.: LS+AS+SS-ThM1, 33
 Mahapatra, M.: HC+2D+SS-ThM6, 32
 Mahapatra, S.: SS+2D+HC-TuM1, 11
 Major, G.H.: SS-TuP17, 19
 Malko, A.V.: TF+SS-ThA10, 53
 Manno, M.: TF+EM+NS+SS-ThM6, 37
 Mansfield, L.: DM2+BI+SS-ThA11, 44
 Mao, Z.: HC+SS-MoM5, 1
 Marchack, N.P.: PS+2D+EM+SS+TF-ThA6, 48
 Marcus, P.R.: DM+BI+SS-ThM3, 31
 Maria, J.-P.: OX+EM+MI+SS-WeM11, 22
 Mark, L.O.: HC+SS-FrM6, 57
 Marschilok, A.: SS+AS+HC+TL-ThM5, 35
 Martens, I.: LS+AS+SS-ThM1, 33
 Martín, C.: SS+HC+PS-FrM3, 59
 Martin, I.T.: DM2+BI+SS-ThA11, 44
 Martinez, A.: SS+HC+PS-FrM9, 60
 Maslar, J.E.: TF+2D+AP+EL+SS-MoA10, 8
 Masson, E.: SE+AS+SS-FrM4, 58
 Mathur, S.: CA+AS+NS+SE+SS-FrM3, 55
 Matsuda, A.: RA+AS+NS+SS-MoA11, 5
 Matsumoto, M.: SS+2D+HC-TuM11, 12
 Matthews, R.: DM2+BI+SS-ThA11, 44
 Maxwell, E.: HC+2D+SS-ThM2, 32; SS-TuP18, 19
 Mayrhofer, K.: DM2+BI+SS-ThA10, 44
 McChesney, J.L.: LS+AS+SS-ThM4, 34
 McClelland, K.: TL+2D+HC+SS-MoA1, 9
 McDaniel, B.: TF+EM+NS+SS-ThM4, 37
 McGann, C.L.: 2D+AS+BI+HC+MN+NS+PS+SS+TL-ThA8, 41
 McGhee, E.: TF+EM+NS+SS-ThM11, 38; TF+EM+NS+SS-ThM12, 38
 McGott, D.L.: CA+AS+NS+SE+SS-FrM6, 55
 McGuinness, E.K.: TF+SS-ThA4, 53
 McNeal, B.: TF+EM+NS+SS-ThM12, 38
 Medlin, J.W.: HC+SS-FrM6, 57
 Mehar, V.: HC+2D+SS-ThM12, 33
 Meier, M.: DM2+BI+SS-ThA8, 44; SS+AS+HC+OX-WeA9, 27
 Mellor, A.: TF+EM+NS+SS-ThM5, 37
 Melton, O.: AP+EL+MS+PS+SS+TF-TuA12, 14
 Merola, C.: DM+BI+SS-ThM13, 32
 Merte, L.R.: SS+HC-MoA5, 6
 Metz, A.: PS+2D+EM+SS+TF-ThA4, 48
 Metzger, W.K.: CA+AS+NS+SE+SS-FrM6, 55
 Mihut, D.: DM1+BI+SS-ThA3, 43
 Mikkelsen, A.: TF+2D+AP+EL+SS-MoA8, 8
 Min, M.: TF+SS-ThA9, 53
 Mirabella, F.: DM2+BI+SS-ThA8, 44
 Mirsaidov, U.: CA+NS+SS+VT-ThA10, 42
 Mize, C.J.: HC+2D+SS-WeM13, 21
 Mol, J.M.C.: DM+BI+SS-ThM6, 31
 Molino, P.J.: DM1+BI+SS-ThA1, 43
 Möller, J.: DM2+BI+SS-ThA10, 44
 Momchilov, A.: TL+AS+SS+TF-TuA7, 16
 Moore, W.: TF+EM+NS+SS-ThM6, 37
 Morikita, S.: PS+2D+EM+SS+TF-ThA4, 48
 Mosden, A.: PS+2D+EM+SS+TF-ThA4, 48
 Mroz, V.: SS-TuP4, 17
 Mueller, D.N.: CA+AS+NS+SE+SS-FrM3, 55
 Mueller, K.T.: SS+HC+PS-FrM9, 60
 Muhr, A.: DM+BI+SS-ThM12, 31
 Muir, M.: HC+2D+SS-WeM5, 20
 Müllner, M.: DM2+BI+SS-ThA8, 44
 Mulvaney, S.P.: 2D+AS+BI+HC+MN+NS+PS+SS+TL-ThA8, 41
 Muramoto, E.: HC+2D+SS-ThM13, 33
 Murkute, P.V.: DM1+BI+SS-ThA4, 43
 Murotani, H.: DM+BI+SS-ThM1, 30
 Murphy, A.: SS-TuP7, 17
 Murgesan, V.: SS+HC+PS-FrM9, 60
 Mushtaq, U.: PS+SS-ThA7, 50
 — N —
 Nagao, H.: RA+AS+NS+SS-MoA11, 5
 Nagaoka, K.: PS+2D+EM+SS+TF-ThA3, 47
 Nagatsuka, N.: SS+2D+HC-TuM11, 12
 Nakamura, J.: SS+AS+HC+TL-ThM3, 35
 Nakano, T.: PS+SS-ThA2, 49
 Nalam, P.: SE+AS+SS-FrM3, 58
 Nam, S.: PS+AS+EM+SS+TF-MoA6, 3
 Narayanan, V.: OX+EM+HC+MI+NS+SS+TF-TuA3, 14
 Nash, D.J.: HC+SS-FrM9, 58
 Nelson Weker, J.: LS+AS+SS-ThM3, 33
 Nemsak, S.: LS+HC+SS-ThM10, 34
 Nemšák, S.: SS+AS+HC+TL-ThM4, 35
 Nepal, N.: TF+2D+AP+EL+SS-MoA6, 8
 Neupane, S.: DM+BI+SS-ThM5, 31
 Newberg, J.T.: CA+NS+SS+VT-WeA8, 24; CA+NS+SS+VT-WeA9, 24
 Ngo, A.: SE+AS+SS-FrM4, 58
 Nguyen, T.: PS+AS+EM+SS+TF-MoA6, 3
 Nie, X.: SS+HC-MoA3, 6
 Niemantsverdriet, H.J.W.: HC+SS+TL-ThA1, 45
 Nikodemski, P.: TF+SS-ThA3, 52
 Noesges, B.A.: 2D+EM+MI+NS+QS+SS-ThM10, 29
 Norwood, R.: TF+EM+NS+SS-ThM11, 38
 Notte, J.A.: CA+NS+SS+VT-ThA1, 41
 — O —
 Oberg, K.: SS+HC+PS-FrM6, 60
 O'Callahan, B.T.: CA+NS+SS+VT-ThA8, 42
 O'Connor, C.R.: HC+2D+SS-ThM13, 33; SS+AS+HC+OX-WeA3, 26
 Oehrlin, G.S.: PS+AS+EM+SS+TF-MoA11, 4; PS+AS+EM+SS+TF-MoA8, 3
 O'Hara, D.: 2D+EM+MI+NS+QS+SS-ThM10, 29
 Ohashi, Y.: SS+2D+HC-TuM11, 12
 Okada, Y.: PS+2D+EM+SS+TF-ThA8, 48
 Opila, R.L.: AP+EL+MS+PS+SS+TF-TuA12, 14
 Orozco, I.: HC+2D+SS-ThM6, 32
 Orvis, T.: OX+EM+HC+MI+NS+SS+TF-TuA12, 15
 Oware Sarfo, K.: DM1+BI+SS-ThA4, 43
 — P —
 Palai, R.: OX+EM+HC+MI+NS+SS+TF-TuA11, 15
 Pan, X.: CA+AS+NS+SE+SS-FrM4, 55
 Pandiyan, A.: PS+SS-ThA7, 50
 Pang, Q.: DM1+BI+SS-ThA4, 43
 Pang, Y.: SS+AS+HC+TL-ThM10, 36
 Park, J.Y.: CA+AS+NS+SE+SS-FrM1, 55
 Parkinson, G.S.: DM2+BI+SS-ThA8, 44; HC+2D+SS-WeM10, 20; SS+AS+HC+OX-WeA9, 27
 Parulkar, A.: HC+OX+SS-WeA8, 25
 Patel, D.A.: SS+AS+HC+OX-WeA3, 26
 Patel, H.: PS+SS-ThA7, 50
 Paudel, T.: 2D+EM+MI+NS+QS+SS-ThM3, 29
 Pavelec, J.: DM2+BI+SS-ThA8, 44
 Pearce, P.: TF+EM+NS+SS-ThM5, 37
 Pellissier, B.: AP+EL+MS+PS+SS+TF-TuA9, 13
 Pellegrin, E.: CA+NS+SS+VT-WeA7, 24; SS+HC+PS-FrM3, 59
 Peng, Q.: TF+SS-ThA11, 54
 Pentzer, E.B.: DM2+BI+SS-ThA11, 44
 Perea, D.E.: SS+2D+AP+AS+OX+SE-ThA7, 51
 Perepezko, J.: DM2+BI+SS-ThA9, 44
 Perez-Dieste, V.: CA+NS+SS+VT-WeA7, 24
 Perkins, C.L.: CA+AS+NS+SE+SS-FrM6, 55
 Pesce, V.: AP+EL+MS+PS+SS+TF-TuA9, 13
 Peshek, T.J.: DM2+BI+SS-ThA11, 44
 Petersen, J.: SS+HC-MoA10, 7
 Pfau, B.: LS+AC+HC+SS-ThA10, 47
 Phillips, J.A.: SS+AS+HC+TL-ThM11, 36
 Pietron, J.J.: 2D+AS+BI+HC+MN+NS+PS+SS+TL-ThA8, 41
 Pint, C.: TF+EM+NS+SS-ThM1, 36
 Plant, A.: RA+AS+NS+SS-MoA1, 4
 Pletincx, S.: DM+BI+SS-ThM6, 31
 Posada-Borbón, A.: SS+HC-MoA5, 6

Author Index

- Posinski, N.: SS-TuP10, 18
 Possesme, N.: AP+EL+MS+PS+SS+TF-TuA9, 13
 Prabhakaran, V.: SS+HC+PS-FrM9, **60**
 Pradhan, S.K.: TF+EM+NS+SS-ThM10, 38
 Pranda, A.: PS+AS+EM+SS+TF-MoA11, **4**
 Prat, J.: CA+NS+SS+VT-WeA7, 24
 Pribil, G.K.: AP+EL+MS+PS+SS+TF-TuA1, 13
 Proksch, R.: SS-TuP7, 17
 Prosek, T.: DM+BI+SS-ThM12, 31
 Puurunen, R.L.: AP+EL+MS+PS+SS+TF-TuA10, **13**; PS+AS+EM+SS+TF-MoA10, 4
 Pylypenko, S.: LS+AS+SS-ThM3, 33
 Pyronneau, K.: TF+SS-ThA4, **53**
- R —
- Raeis, M.: SE+AS+SS-FrM4, 58
 Rahman, T.S.:
 2D+AS+BI+HC+MN+NS+PS+SS+TL-ThA10,
 41; 2D+AS+BI+HC+MN+NS+PS+SS+TL-ThA7,
 40; HC+SS-FrM9, **58**
 Rangari, V.: TF+EM+NS+SS-ThM13, 38
 Ranninger, J.: DM2+BI+SS-ThA10, 44
 Raschke, M.B.: CA+NS+SS+VT-ThA8, 42
 Rattigan, E.: SS+HC+PS-FrM3, 59
 Ravichandran, J.: OX+EM+HC+MI+NS+SS+TF-TuA12, 15
 Ray, D.: TF+EM+NS+SS-ThM6, 37
 Reece, C.: HC+2D+SS-ThM10, **32**
 Reeks, J.M.: SS-TuP10, **18**
 Reese, M.O.: CA+AS+NS+SE+SS-FrM6, 55
 Rehman, F.: TF+2D+AP+EL+SS-MoA8, 8
 Reinke, P.: DM2+BI+SS-ThA9, **44**;
 SS+AS+HC+OX-WeA10, 27
 Rejmak, P.: CA+NS+SS+VT-WeA7, 24
 Renner, F.U.: DM+BI+SS-ThM5, **31**
 Renner, J.: PS+SS-ThA6, 50
 Repicky, J.J.: SS+HC-MoA3, 6
 Resch, N.: DM2+BI+SS-ThA8, 44
 Reuter, K.: HC+SS-MoM10, **2**
 Rimal, G.: 2D+EM+MI+NS+QS+SS-ThM3, 29
 Rimer, J.D.: HC+SS+TL-ThA10, 46
 Robinson, J.T.:
 2D+AS+BI+HC+MN+NS+PS+SS+TL-ThA8, 41
 Robinson, Z.R.: TF+2D+AP+EL+SS-MoA6, 8
 Rochet, F.: TF+2D+AP+EL+SS-MoA8, 8
 Rodenbücher, C.: SS+AS+HC+OX-WeA12, 27
 Rodriguez Olguin, M.A.: HC+SS-FrM1, **56**
 Rodriguez, J.A.: HC+2D+SS-ThM6, 32
 Rodríguez-Fernández, J.: SS+HC+PS-FrM3, **59**
 Rogers, C.: TL+2D+HC+SS-MoA1, 9
 Rohatgi, A.: TF+EM+NS+SS-ThM4, 37
 Rosenberg, R.A.: SS+HC+PS-FrM5, 59
 Rosenberg, S.G.: TF+2D+AP+EL+SS-MoA6, 8
 Rosenhek-Goldian, I.: SS-TuP15, 19
 Rossnagel, K.: LS+AC+HC+SS-ThA8, **47**
 Rounsaville, B.: TF+EM+NS+SS-ThM4, 37
 Roy, S.: HC+2D+SS-WeM13, **21**; SS+HC+PS-FrM9, 60
 Rudomilova, D.: DM+BI+SS-ThM12, 31
 Rumpitz, J.R.: SS+2D+HC-TuM5, 11
 Ryu, H.: 2D+AS+BI+HC+MN+NS+PS+SS+TL-ThA4, 40
- S —
- Salmeron, M.B.: LS+AC+HC+SS-ThA6, 46;
 SS+AS+HC+OX-WeA11, 27; SS+AS+HC+TL-ThM4, 35
 Sánchez-de-Armas, R.: TF+2D+AP+EL+SS-MoA8, 8
 Sanders, E.: LS+AC+HC+SS-ThA7, 47
 Sanjeewa, L.: SS-TuP20, 19
 Sankaran, R.M.: PS+SS-ThA6, 50
 Santagata, N.: SS+HC-MoA3, 6
 Sarkar, S.: SE+AS+SS-FrM4, **58**
 Sasaki, A.: RA+AS+NS+SS-MoA11, 5
 Sasaki, Y.: DM+BI+SS-ThM1, 30
 Sato, Y.: HC+OX+SS-WeA2, 25
 Sattari Baboukani, B.: SE+AS+SS-FrM3, 58
 Schaefer, A.: SS+HC-MoA5, 6
 Schimo-Aichhorn, G.: DM+BI+SS-ThM12, 31
 Schlosser, D.: HC+2D+SS-ThM2, 32
 Schmid, M.: DM2+BI+SS-ThA8, 44
 Schnadt, J.: TF+2D+AP+EL+SS-MoA8, **8**
 Schneider, C.M.: CA+AS+NS+SE+SS-FrM3, 55
 Schreiber, D.K.: OX+EM+MI+SS-WeM13, 22
 Schultz, J.: SS+2D+HC-TuM1, 11
 Schwenzfeier, K.A.: DM+BI+SS-ThM13, **32**
 Schwoebel, P.R.: SS+2D+HC-TuM12, 12
 Scott, S.L.: HC+SS+TL-ThA8, **46**
 Scully, J.R.: DM+BI+SS-ThM10, 31
 Sefat, A.: SS-TuP20, 19
 Seitzman, N.: LS+AS+SS-ThM3, **33**
 Senanayake, S.: HC+2D+SS-ThM6, 32
 Setvin, M.: SS+2D+AP+AS+OX+SE-ThA8, **52**
 Shah, S.Q.A.: OX+EM+MI+SS-WeM12, 22
 Shakya, D.M.: HC+OX+SS-WeA9, 26
 Sharma, A.: TF+EM+NS+SS-ThM10, **38**
 Sharma, D.: HC+SS+TL-ThA1, 45
 Sharma, R.: PS+SS-ThA7, 50
 Shayesteh, P.: TF+2D+AP+EL+SS-MoA8, 8
 Shepardon-Fungairino, S.: SS-TuP12, 18
 Shi, Y.: PS+2D+EM+SS+TF-ThA4, 48
 Shiba, Y.: PS+AS+EM+SS+TF-MoA2, 3
 Shields, S.: SS+HC-MoA3, 6
 Shigeno, S.: PS+2D+EM+SS+TF-ThA8, 48
 Shinotsuka, H.: RA+AS+NS+SS-MoA11, 5
 Shipilin, M.: SS+HC-MoA5, 6
 Shiratani, M.: PS+SS-ThA1, 49
 Shutthanandan, V.: SS+HC+PS-FrM9, 60
 Sibener, S.J.: SS+2D+AP+AS+OX+SE-ThA1, 51;
 SS+2D+AP+AS+OX+SE-ThA2, 51; SS+2D+HC-TuM6, 11; SS+HC+PS-FrM5, 59
 Silski, A.: SS+HC-MoA10, **7**
 Silva-Quinones, D.: SS-TuP2, **17**
 Silverman, T.: TF+EM+NS+SS-ThM4, 37
 Singh, N.: SS+2D+HC-TuM5, 11
 Skinner, W.: SS-TuP17, 19
 Smith, S.: 2D+EM+MI+NS+QS+SS-ThM6, **29**
 Somorjai, G.A.: LS+AC+HC+SS-ThA6, 46
 Son, J.: 2D+AS+BI+HC+MN+NS+PS+SS+TL-ThA4, **40**
 Son, J.Y.: CA+AS+NS+SE+SS-FrM9, **56**
 Sorescu, D.C.: SS+2D+AP+AS+OX+SE-ThA10, 52
 Spanos, A.P.: HC+OX+SS-WeA8, 25
 Sperling, B.A.: TF+2D+AP+EL+SS-MoA10, **8**
 Spillmann, C.M.:
 2D+AS+BI+HC+MN+NS+PS+SS+TL-ThA2, 40
 Spurgeon, S.R.: OX+EM+MI+SS-WeM13, 22
 Stacchiola, D.J.: HC+SS-FrM6, 57
 Stadler, D.: CA+AS+NS+SE+SS-FrM3, 55
 Stellnberger, K.-H.: DM+BI+SS-ThM12, 31
 Stifter, D.: DM+BI+SS-ThM12, 31
 Stinaff, E.: 2D+EM+MI+NS+QS+SS-ThM5, 29
 Strzhemechny, Y.M.: SS-TuP10, 18
 Su, L.: TF+SS-ThA1, **52**
 Sugawa, S.: PS+AS+EM+SS+TF-MoA2, 3
 Summerfield, A.: SS-TuP7, 17
 Sun, Z.: SS+HC+PS-FrM3, 59
 Sundaresan, S.: PS+SS-ThA8, 50
 Sung, D.: 2D+AS+BI+HC+MN+NS+PS+SS+TL-ThA4, 40
 Surendran, M.: OX+EM+HC+MI+NS+SS+TF-TuA12, 15
 Susarrey Arce, A.: HC+SS-FrM1, 56
 Susarrey-Arce, A.: HC+SS-FrM2, 57
 Sutherlin, K.: HC+SS-FrM3, **57**
 Suzuki, M.: RA+AS+NS+SS-MoA11, 5
 Sykes, E.C.: TL+2D+HC+SS-MoA3, **9**
 Sykes, E.C.H.: SS+AS+HC+OX-WeA3, 26
 Szot, K.: SS+AS+HC+OX-WeA12, 27
- T —
- Tait, S.L.: SS+AS+HC+OX-WeA4, **26**
 Takakusagi, S.: HC+OX+SS-WeA2, **25**
 Takeda, S.: TL+AS+SS+TF-TuA3, **15**
 Takeuchi, E.: SS+AS+HC+TL-ThM5, **35**
 Takeuchi, K.: SS+AS+HC+TL-ThM5, 35
 Tamaoka, T.: TL+AS+SS+TF-TuA3, 15
 Tang, J.: 2D+EM+MI+NS+QS+SS-ThM3, 29
 Taniguchi, K.: PS+2D+EM+SS+TF-ThA4, 48
 Taylor, C.D.: DM+BI+SS-ThM10, 31
 Taylor, S.D.: OX+EM+MI+SS-WeM13, 22
 Tenney, S.A.: HC+SS-FrM6, **57**; SS-TuP4, 17
 Teplyakov, A.V.: SS-TuP1, 17; SS-TuP2, 17; SS-TuP5, 17
 Teramoto, A.: PS+AS+EM+SS+TF-MoA2, 3
 Terryn, H.: DM+BI+SS-ThM6, 31
 Thevuthasan, S.: SS+HC+PS-FrM9, 60
 Thiel, P.A.: 2D+EM+MI+NS+QS+SS-ThM13, **30**
 Thirumalai, H.: HC+SS+TL-ThA10, **46**
 Thissen, A.: CA+NS+SS+VT-ThA3, 42
 Thompson, R.S.: SS+2D+AP+AS+OX+SE-ThA1, **51**
 Thorat, R.: 2D+EM+MI+NS+QS+SS-ThM5, 29
 Thornton, G.: HC+2D+SS-ThM3, **32**
 Timm, R.: TF+2D+AP+EL+SS-MoA8, 8
 Tinacba, E.J.C.: PS+2D+EM+SS+TF-ThA8, 48
 Tinney, D.G.: HC+SS+TL-ThA2, 45; SS+HC-MoA8, 7; SS+HC-MoA9, 7
 Tjung, S.J.: SS+HC-MoA3, 6
 Tomasulo, S.: TF+EM+NS+SS-ThM5, 37
 Tortai, J.-H.: AP+EL+MS+PS+SS+TF-TuA9, 13
 Toth, J.R.: PS+SS-ThA6, **50**
 Traxler, I.: DM+BI+SS-ThM12, **31**
 Trenary, M.: HC+2D+SS-WeM5, 20;
 HC+2D+SS-WeM6, 20
 Tringides, M.C.: 2D+EM+MI+NS+QS+SS-ThM13, 30
 Troian, A.: TF+2D+AP+EL+SS-MoA8, 8
 Tsai, Y.-H.: PS+2D+EM+SS+TF-ThA4, 48
 Tsampas, M.N.: PS+SS-ThA7, 50
 Tsyshevskiy, R.: TF+2D+AP+EL+SS-MoA8, 8
 Tucker, J.D.: DM1+BI+SS-ThA4, 43
 Tumbleson, R.: SE+AS+SS-FrM4, 58
 Turano, M.E.: HC+2D+SS-WeM12, **20**;
 SS+HC+PS-FrM5, 59
- U —
- Uedono, A.: AP+EL+MS+PS+SS+TF-TuA9, 13
 Upadhyaya, V.: TF+EM+NS+SS-ThM4, 37
 Urpelainen, S.: TF+2D+AP+EL+SS-MoA8, 8
 Utraiainen, M.: PS+AS+EM+SS+TF-MoA10, 4
 Utterback, E.: TF+EM+NS+SS-ThM13, 38
 Utz, A.L.: HC+SS+TL-ThA2, 45; SS+HC-MoA8, 7; SS+HC-MoA9, 7; SS-TuP12, 18
- V —
- Vaida, M.E.:
 2D+AS+BI+HC+MN+NS+PS+SS+TL-ThA11, **41**
 Vallee, C.: AP+EL+MS+PS+SS+TF-TuA9, **13**
 Valtiner, M.: DM+BI+SS-ThM13, 32;
 DM+BI+SS-ThM2, 30
 Vamvakeros, A.: LS+AS+SS-ThM1, 33
 van de Sanden, M.C.M.: PS+SS-ThA7, **50**
 van der Zande, A.M.:
 2D+AS+BI+HC+MN+NS+PS+SS+TL-ThA4, 40
 van Lent, R.: SS-TuP13, **18**
 van Ommen, J.R.: TF+2D+AP+EL+SS-MoA1, **7**
 van Spronsen, M.A.: HC+2D+SS-ThM13, 33;
 SS+AS+HC+OX-WeA11, **27**
 VanDerslice, J.: AP+EL+MS+PS+SS+TF-TuA1, 13
 Veit, D.R.: SS+2D+HC-TuM6, 11
 Vicente, J.: 2D+EM+MI+NS+QS+SS-ThM4, **29**
 Visart de Bocarmé, T.: SS+2D+AP+AS+OX+SE-ThA7, 51

Author Index

- Voigt, B.: TF+EM+NS+SS-ThM6, **37**
- Volders, C.: DM2+BI+SS-ThA9, 44
- Vovk, E.I.: SS+AS+HC+TL-ThM10, 36
- **W** —
- Wachs, S.: DM2+BI+SS-ThA10, 44
- Walkosz, W.: SS+HC+PS-FrM5, 59; SS-TuP19, 19
- Waluyo, I.: DM2+BI+SS-ThA9, 44; LS+AC+HC+SS-ThA6, 46
- Wan, K.-T.: 2D+EM+MI+NS+QS+SS-ThM13, 30
- Wang, F.: CA+NS+SS+VT-ThA6, **42**; LS+HC+SS-ThM11, **34**
- Wang, L.: OX+EM+MI+SS-WeM1, **21**
- Wang, M.: HC+SS-FrM6, 57; PS+2D+EM+SS+TF-ThA4, 48
- Wang, X.: TF+2D+AP+EL+SS-MoA11, **9**
- Wang, Y.: HC+SS+TL-ThA7, 46
- Wang, Z.: AP+EL+MS+PS+SS+TF-TuA12, **14**
- Watanabe, K.: RA+AS+NS+SS-MoA11, 5
- Watkins, M.: 2D+AS+BI+HC+MN+NS+PS+SS+TL-ThA3, 40
- Way, J.D.: HC+OX+SS-WeA1, 25
- Weaver, J.: TF+SS-ThA1, 52
- Weaver, J.F.: HC+2D+SS-ThM12, **33**; HC+2D+SS-WeM2, 20; HC+SS+TL-ThA6, 45
- Weiss, E.: TL+2D+HC+SS-MoA1, **9**
- Weitering, H.: 2D+EM+MI+NS+QS+SS-ThM6, 29
- Welzel, S.: PS+SS-ThA7, 50
- Wen, H.: LS+HC+SS-ThM12, **34**
- Wen, J.G.: RA+AS+NS+SS-MoA5, 5
- Wendt, S.: OX+EM+HC+MI+NS+SS+TF-TuA10, 15
- Werner, W.S.M.: RA+AS+NS+SS-MoA8, 5
- Weststrate, K.-J.: HC+SS+TL-ThA1, **45**
- White, M.G.: HC+2D+SS-ThM6, 32; HC+OX+SS-WeA7, 25
- Wickramasinghe, T.E.: 2D+EM+MI+NS+QS+SS-ThM5, 29
- Wiegmann, T.: LS+AS+SS-ThM1, 33
- Wiggins, B.: SS+2D+AP+AS+OX+SE-ThA2, 51
- Wiley, H.S.: RA+AS+NS+SS-MoA3, **4**
- Wilke, J.: HC+2D+SS-ThM2, 32
- Windl, W.: DM+BI+SS-ThM10, 31
- Wolden, C.A.: CA+AS+NS+SE+SS-FrM6, 55; HC+OX+SS-WeA1, **25**
- Wollmershauser, J.A.: TF+2D+AP+EL+SS-MoA3, 7
- Woodward, J.M.: TF+2D+AP+EL+SS-MoA6, **8**
- Wrana, D.: SS+AS+HC+OX-WeA12, **27**
- Wrobel, F.: LS+AS+SS-ThM4, 34; OX+EM+MI+SS-WeM2, **21**
- Wu, C.H.: LS+AC+HC+SS-ThA6, 46
- **X** —
- Xiao, B.: TF+EM+NS+SS-ThM10, 38
- Xiao, Z.: TF+EM+NS+SS-ThM11, 38; TF+EM+NS+SS-ThM12, 38
- Xin, H.L.: CA+AS+NS+SE+SS-FrM11, **56**
- Xu, J.: 2D+AS+BI+HC+MN+NS+PS+SS+TL-ThA4, 40; DM2+BI+SS-ThA8, 44
- Xu, T.: OX+EM+HC+MI+NS+SS+TF-TuA10, **15**
- Xu, X.: OX+EM+HC+MI+NS+SS+TF-TuA1, 14
- **Y** —
- Yablonsky, G.: HC+SS+TL-ThA7, 46
- Yakes, M.K.: TF+EM+NS+SS-ThM5, 37
- Yamamoto, A.: PS+SS-ThA1, 49
- Yan, H.: TF+SS-ThA11, 54
- Yan, X.: LS+AS+SS-ThM4, 34
- Yang, W.L.: LS+AS+SS-ThM5, **34**
- Yang, X.: PS+SS-ThA8, 50
- Yang, Y.: SS+AS+HC+TL-ThM10, **36**
- Yang, Z.: OX+EM+MI+SS-WeM1, 21
- Yano, J.: HC+SS-FrM3, 57
- Yao, J.: CA+AS+NS+SE+SS-FrM8, **56**; CA+AS+NS+SE+SS-FrM9, 56
- Ye, Z.: SE+AS+SS-FrM3, 58
- Yildiz, B.: SS+AS+HC+TL-ThM1, **35**
- Yngman, S.: TF+2D+AP+EL+SS-MoA8, 8
- Yoshida, H.: TL+AS+SS+TF-TuA3, 15
- Yoshikawa, H.: RA+AS+NS+SS-MoA11, 5
- Yost, A.J.: 2D+EM+MI+NS+QS+SS-ThM3, 29
- Yu, M.: HC+2D+SS-ThM12, 33
- Yu, X.: TF+SS-ThA11, 54
- Yu, X.-Y.: CA+AS+NS+SE+SS-FrM8, 56; CA+AS+NS+SE+SS-FrM9, 56
- Yuan, B.: AP+EL+MS+PS+SS+TF-TuA12, 14
- Yuk, S.: SS+HC-MoA3, 6
- **Z** —
- Zaera, F.: HC+2D+SS-WeM3, **20**
- Zeller, P.: CA+NS+SS+VT-ThA9, 42
- Zhang, C.: SS+HC-MoA5, 6
- Zhang, D.: PS+2D+EM+SS+TF-ThA4, 48
- Zhang, Q.: SS+HC-MoA3, 6
- Zhang, X.: SE+AS+SS-FrM7, 58
- Zhang, Y.: CA+NS+SS+VT-WeA8, 24; DM1+BI+SS-ThA4, 43; SE+AS+SS-FrM4, 58
- Zhang, Z.: HC+OX+SS-WeA1, 25; TF+2D+AP+EL+SS-MoA5, **8**
- Zheng, Y.: TF+SS-ThA10, 53
- Zhou, X.: SS+AS+HC+TL-ThM10, 36
- Zhu, T.: 2D+EM+MI+NS+QS+SS-ThM10, 29
- Zhu, Z.H.: CA+AS+NS+SE+SS-FrM8, 56
- Zimbaridi, F.: TF+EM+NS+SS-ThM4, 37
- Zou, Q.: SS-TuP20, 19
- Zugic, B.: SS+AS+HC+OX-WeA11, 27